AEROSOL DEPOSITION AND CLEARANCE IN THE HUMAN RESPIRATORY TRACT

BY

PETER C. EMMETT

Thesis for the Degree of Doctor of Philosophy

University of Edinburgh

1979

TO

ROBERT MICHAEL EMMETT

1946 - 1967

I declare that this thesis is the

result of my own efforts.

Sept. 1979

ABSTRACT

The deposition and short term clearance characteristics of monodisperse aerosol particles (size range 4·5 – 13 μm diameter) in the human respiratory tract have been investigated in eighteen subjects.

In order to improve on the accuracy of existing experimental techniques, a new type of apparatus has been constructed which accurately samples the aerosol to be inhaled by a subject and at the same time ensures a rigorous control of the physiological conditions of aerosol administration. Besides measuring the total respiratory tract deposition of the particles, their regional distribution has also been estimated, by means of indirect techniques, the accuracy of which partly depends on certain widely held assumptions.

The total aerosol deposition results are lower than those of other workers, with one exception, in a limited region of comparison. The regional aerosol deposition results demonstrate the importance of the laryngeal/pharyngeal region in filtering out the larger particle sizes before they can enter the trachea. While the results of the present work would also ostensibly suggest that the largest particle sizes penetrate far more effectively into the respiratory zone than had hitherto been considered possible by most investigators, the rapid declines observed in some independently obtained laryngeal/tracheal clearance curves are inconsistent with this finding. Moreover, an analysis of the present data using a simple filter model of the

respiratory tract demonstrates that the respiratory zone aerosol deposition results are wholly inconsistent with the expected behaviour of large airborne particles in this zone. It is therefore concluded that the measured values of one-day retention at the largest particle sizes are being caused by an incomplete clearance of particles which initially deposited on the dead space airways.

An interesting secondary phenomenon has also been investigated. The clearance curves exhibit distinct, non-random fluctuations. By means of single and double radiation detectors placed over the throat, it has been established that the fluctuations are not merely an artefact of the primary measuring detector but have their origin from somewhere below the trachea, not solely in the larynx itself. The possible biological and physical factors that may be implicated in the causation of the clearance pulses are discussed.

CONTENTS

Chapter Page

Chapter Page

LIST OF TABLES AND FIGURES

CHAPTER ONE

INTRODUCTION

The definition of a safe or acceptable level of dust exposure requires some knowledge of the amount and site of deposition of dust in the human respiratory tract, under a variety of conditions, and its subsequent rate of clearance. Calculation of these dust filtration characteristics is complicated and consensus has not yet been established (TAULBEE and YU, 1975). If possible, therefore, they are best determined experimentally.

While useful information may be obtained by use of models or hollow casts of the upper respiratory tract, the technique would be difficult to apply to the more intricate lower respiratory tract (SCHLESINGER and LIPPMANN, 1972). The use of artificially ventilated excised lungs is also limited, for reasons of availability and technique (MITCHELL, 1977). Accurate assessment of the degree of a dust hazard therefore requires experimental work involving live subjects, preferably human.

Such experimental work is often concerned with the measurement of the total amount of dust which deposits in the respiratory tract relative to that inhaled, termed total deposition. It is also possible to combine this with the indirect estimation of the relative amount of dust which deposits within specific zones of the respiratory tract, termed regional deposition, by the use of radioactive aerosols (LIPPMANN and ALBERT, 1969).

Although many experiments have been performed to measure total deposition the scatter of observations has been considerable (DAVIES, 1974). Besides individual variations, such scatter may be due in part to poor aerosol sampling techniques and in part to a failure to define or control those factors, such as breathing rate, which determine the rate of aerosol deposition in the subject. Because of these experimental difficulties very few total deposition experiments have been performed at particle diameters greater than several micrometers. Still fewer experiments have been performed to investigate regional deposition (LIPPMANN, 1977; FOORD et al, 1978; STAHLHOFEN et al. 1979).

It is the purpose of the present work to extend reliable knowledge of total and regional aerosol deposition and clearance characteristics in the human respiratory tract,to the highest practical particle diameter. In this chapter essential background knowledge is reviewed.

1.1 Description of human respiratory tract

(i) Morphology and patterns of gas-flow

For the purposes of the present discussion the human respiratory tract will be divided into three zones: 1. the nasopharynx, oral passages and larynx; 2. the dead space airways, extending from the trachea to the terminal bronchioles; 3. the respiratory zone, where the gas exchange units, or alveoli, are situated.

Air which enters the nose encounters a greater resistance to flow than it does in the mouth, passing through the large narrow channels of the nasal cavities. The lateral walls of the cavities

consist of folded turbinates whose role may be to expose the incoming air to the maximum surface area and hence to enhance the nasal aerosol filtration efficiency (PROCTOR and SWIFT, 1971). Air which enters the mouth will tend to encounter less resistance to flow but possesses a potentially more variable cross-section, mainly determined by the position of the tongue and soft palate. Whether inhaled by either route, air is fully warmed and moistened by the time it enters the major bronchi (PROCTOR, 1964).

It is the larynx that mainly determines entry conditions for flow into the trachea. According to MACKLEM and MEAD (1967), the larynx, together with the mouth and trachea, accounts for about half the viscous resistance to breathing. The degree of glottal opening in the larynx varies according to whether the subject is inspiring or expiring, according to lung volume, and according to the level of exercise (STANESCU et al, 1972). Below the larynx there is less variability at given lung volume.

The conducting airways repeatedly branch in a generally dichotomous manner. The most widely used description of this branching system is that of WEIBEL (1963). In Weibel's 'model A' symmetrical branching system, the number of branches, n, at a given generation, q, is given by,

$$n = 2^q \qquad \text{..... equation 1.1.1}$$

The trachea is defined as the zeroth generation (Table 1.1.1).

Table1.1.1: Weibel model 'A'; Regular dichotomy system, lung volume 4·8 l at ~3/4 maximum inflation

generic term	generation number	number per generation	diameter mm.	length mm.	cumulative length *1 mm.	cross-sect. area per generation cm.^{2}	volume per generation cm.^{3}	cumulative volume cm.^{3}	surface area per generation *1 cm.^{2}	cumulative surface area *1 cm.^{2}	Reynolds' Number *1 *2
TRACHEA	0	1	18·0	120·0	120·0	2·54	30·5	30·5	67·8	67·8	1,510
MAIN BRONCHUS	1	2	12·2	47·6	167·6	2·33	11·3	41·8	36·8	104·6	1070
LOBAR BRONCHUS	2	4	8·3	19·0	186·6	2·13	4·0	45·8	19·1	123·7	797
	3	8	5·6	7·6	194·2	2·00	1·5	47·2	10·9	134·6	573
SEGMENTAL BRONCHUS	4	16	4·5	12·7	206·9	2·48	3·5	50·7	30·8	165·4	370
CARTILAGINOUS BRONCHI	5	32	3·5	10·7	217·6	3·11	3·3	54·0	38·0	203·4	230
↓	6	64	2·8	9·0	226·6	3·96	3·5	57·5	50·4	253·8	145
↓	7	128	2·3	7·6	234·2	5·10	3·9	61·4	67·0	320·8	92
↓	8	256	1·86	6·4	240·6	6·95	4·5	65·8	95·7	416·5	55
↓	9	512	1·54	5·4	246·0	9·56	5·2	71·0	134	550·8	33
↓	10	1,024	1·30	4·6	250·6	13·4	6·2	77·2	191	741·9	20
TERMINAL BRONCHUS	11	2,048	1·09	3·9	254·5	19·6	7·6	84·8	277	1,019	11
BRONCHIOLES	12	4,096	0·95	3·3	257·8	28·8	9·8	94·6	413	1,433	7
↓	13	8,192	0·82	2·7	260·5	44·5	12·5	106	607	2,040	3·6
↓	14	16,384	0·74	2·3	362·8	69·4	16·4	123	886	2,927	2·2
↓	15	32,768	0·66	2·0	264·8	113	21·7	145	1,315	4,242	1·2
TERMINAL BRONCHIOLE	16	65,536	0·60	1·65	266·5	180	29·7	175	1,980	6,222	0·7
RESPIRATORY BRONCHIOLES	17	131,072	0·54	1·41	267·9	300	41·8	217	3,096	9,318	0·37
↓	18	262,144	0·50	1·17	269·0	534	61·1	278	4,888	14,206	0·19
↓	19	524,288	0·47	0·99	270·0	944	93·2	371	7,932	22,138	0·10
ALVEOLAR DUCTS	20	1,048,576	0·45	0·83	270·9	1,600	140	510	12,400	34,538	0·06
↓	21	2,097,152	0·43	0·70	271·6	3,220	224	735	20,865	55,403	0·03
↓	22	4,194,304	0·41	0·59	272·1	5,880	350	1,085	34,146	89,549	0·01
ALVEOLAR SAC	23	8,388,608	0·41	0·50	272·6	11,800	591	1,675	57,658	147,208	< 0·01

*1 calculated by present author. *2 at 10 litres minute volume.

However, the high degree of morphological asymmetry in the conducting airways should always be borne in mind. Convenient mathematical descriptions may sometimes obscure certain physical realities, such as the variation of branching angle from generation to generation (HORSFIELD and CUMMING, 1967).

The total cross-sectional area of the conducting airways increases directly with generation number and, consequently, the gas-flow which initially tends to be turbulent in the large airways is almost certainly laminar in the smaller airways. The nature of gas-flow in an airway is normally characterized by the Reynolds' number Re, which expresses the relative magnitudes of the purely inertial and viscous forces in a fluid, and for a cylinder is given by,

$$Re = \frac{\rho . L . Vo}{\eta} \qquad \text{..... equation 1.1.2}$$

Where (in MKS units), ρ is the mass density of fluid in $Kg.m^{-3}$

L is the diameter of the cylinder in metres

Vo is the mean fluid flow rate in metres sec^{-1}

η is the viscosity of the fluid in Nsm^{-2}

Reynolds' numbers in the human respiratory tract vary from about 0·01 in an alveolar sac, to about 1,500 in the trachea, depending on breathing pattern (Table 1.1.1). It is therefore highly likely that the flow which advances into the respiratory

zone is of the Poiseuille type, i.e. the velocity distribution is parabolic, the velocity being a maximum in the centre of each airway. Very little mixing between the advancing tidal and the surrounding sheaths of expiratory reserve and residual 'air' is therefore likely to occur (DAVIES et al, 1972), and the flow tends to be reversible (MUIR et al, 1971). Transfer of aerosol between these volumes, in the small airways, therefore takes place mainly by virtue of the intrinsic particle mobility.

The dead space airways are considered to end at the terminal bronchioles, beyond which lie the alveolated airways or respiratory bronchioles. The terminal bronchioles are termed generation 16 in the Weibel model and beyond this point the airways are virtually free of cilia. Total airway cross-sectional area increases greatly in the respiratory bronchioles and still more quickly on entering the alveolar ducts and alveoli. There are something like 3×10^8 alveolar units in the normal adult lung.

1.1(ii) Clearance mechanisms

Short-term clearance is generally taken to be synonymous with mucociliary clearance, but it is by no means established that there exists no longer term mucociliary phase. CAMNER and PHILIPSON (1978) demonstrated apparent completion of a short-term clearance phase in humans within about one day after aerosol administration, but the work of GORE and PATRICK (1978) has raised the possibility of a much longer term retention of particles in the trachea and first bifurcation of the conscious rat. Similarly, it cannot be stated with certainty that there exists no rapid phase of alveolar

clearance, although this is considered to be unlikely by most investigators (MORROW, 1977). Moreover, **STAHLHOFEN** et al. (1979) have reported the results of the longer-term clearance of 0·6 μm diameter particles which were deposited overwhelmingly in the respiratory zone, observing no rapid phase component in the clearance curve.

VAN AS (1977) has reviewed some of the inconsistencies in the concept embodied by the term 'mucous sheet', first coined by **LUCAS** and **DOUGLAS** (1934). There is conflicting evidence as to whether this 'sheet' is in fact continuous or not (STURGESS, 1977), as has often been assumed (HATCH and GROSS, 1964). Moreover, there is still much controversy concerning the true composition of the 'mucous sheet' and the role of mucus proper, i.e. the secretory product of mucous glands and goblet cells, in it. In the present work the term 'ciliary transport fluid' will be used throughout, in order to avoid confusion.

The ciliary transport fluid is propelled towards the trachea by the combined beating action of the cilia, which line most of the dead space airways from the zeroth to about the sixteenth airway generation. While the structure and function of the individual cilia have been examined in some detail (DALHAM, 1956), the mechanism of their combined behaviour remains poorly understood. The importance of this information lies in its influence on the thickness of the ciliary transport fluid as it 'ascends' the dead space airways (ASSMUNDSSON and KILBURN, 1970).

No description of short-term clearance would be complete without

mentioning cough. Cough is said to be ineffective beyond the sixth airway generation (LEITH, 1977), where gas-flow rates are considerably lower than in the large airways. However, direct experimental confirmation of this is still lacking and, as has recently been suggested (BATEMAN et al, 1979), changes in lung architecture during disease may well extend the effectiveness of cough to smaller airways.

Longer term clearance processes are believed to involve mainly alveolar macrophages and the pulmonary lymphatic system. However, the present work is concerned purely with short-term clearance phenomena, therefore, longer term mechanisms will not be discussed further.

1.2 Behaviour of aerosols in the human respiratory tract

The term aerosol, an imprecise one, may be applied to any small particle which remains airborne for a reasonable time. According to FUCHS and SUTUGIN (1966), an aerosol may be regarded as 'practically monodisperse' when its geometric standard deviation is less than or equal to 1·2.

1.2(i) Aerosol deposition mechanisms

All terrestrial particles experience the gravitational force. A spherical particle settling in air under the influence of gravity attains a terminal velocity, V_F, when the resistive and gravitational forces are just equal. The resistive force Fd, may be calculated using the well-known Stoke's Law, at low values of particle Reynolds' number, Re_P, i.e. $Re_P <\sim 0{\cdot}05$ (GREEN and LANE, 1957).

$$Fd = 3\pi\eta\, d.V_F \qquad \text{..... equation 1.2.1}$$

where, η , is the viscosity of air in $Nsm.^{-2}$

d , is the particle diameter in metres

Neglecting buoyancy forces and equating resistive and gravitational forces, the terminal velocity is given by,

$$V_F = \frac{\rho . d^2 . g}{18 \eta} \qquad \text{..... equation 1.2.2}$$

where, ρ , is the particle density in $Kg.m.^{-3}$

g , is the acceleration due to gravity in metres $sec.^{-2}$

Therefore, in a fluid of given viscosity, particle density as well as optical diameter must be considered in characterizing the dynamic behaviour of a spherical aerosol particle. It is convenient to accomplish this by defining its aerodynamic diameter, which is the diameter of a sphere of density 10^3 $Kg.m^{-3}$ having the same terminal velocity as the particle in an identical medium.

For very large particles when the particle Reynolds' number is high, equation 1.2.2 may be inaccurate. Similarly, for very small particles, those whose diameters are comparable to the mean free path of the surrounding air molecules, 'slip-correction factors' must be applied. However, in the size range of particles in the present study equation 1.2.2 will suffice.

When a particle is non-spherical but of well defined shape, a shape correction factor may be applied (ALLEN, 1974). However, when

the particle is of highly irregular shape, or, of essentially regular shape but possessing an irregular or deformed surface, its aerodynamic diameter is difficult to predict and may be best determined by direct observation of its falling speed.

When a particle is carried by a moving airsteam which changes in speed or direction, it experiences a lag in its motion relative to the airstream by virtue of its own inertia. The nature of the dependence of inertial effects on the particle density and diameter may perhaps be most easily calculated by considering the elementary case of a particle projected into a still air system, at time $t = 0$, with an initial velocity, V_o. The inertial force is at all times opposed by the drag force on the particle, therefore, for a sphere, Newton's 2nd law of motion leads to (writing in scalar notation for simplicity),

$$m.\frac{dV}{dt} = -3\pi\eta V d \qquad \text{..... equation 1.2.3}$$

where, m, is the particle mass in Kg.

V, is the particle's instantaneous velocity in metres sec^{-1}. in the line of projection, the x-direction say, relative to the still air-system $\left[\therefore V = \frac{dx}{dt}\right]$ (other nomenclature as above)

$$\frac{dV}{V} = \frac{-3\pi\eta d}{m}.dt = -\frac{dt}{\tau} \quad \text{where, } \tau = \frac{m}{3\pi\eta d},$$

and is termed the relaxation time of the particle

$$\therefore \int_{V_o}^{V} \frac{1}{V} \cdot dV = -\frac{1}{\tau} \cdot \int_{0}^{t} dt$$

where V , is the particle velocity at time t, in metres sec^{-1}

$$\left[\log_e(V)\right]_{V_o}^{V} = -\frac{t}{\tau}$$

$$\log_e V - \log_e V_o = \log_e\left[\frac{V}{V_o}\right] = \frac{-t}{\tau}$$

since, $\log_e e^x = x$,

$$\therefore V = V_o . \exp\left[\frac{-t}{\tau}\right]$$

After τ seconds the particle has slowed to $\frac{1}{e}$ of its initial value, V_o , possessed at the time of initial projection into the air-system.

The quantity most often used to represent the inertial behaviour of particles in variable flow regimes is the particle stop distance, So, the distance a projected particle travels before coming to rest.

now, $V = \frac{dx}{dt}$

and from equation 1.2.3,

$$m \cdot \frac{dV}{dx} \cdot \frac{dx}{dt} = -3\pi\eta d \cdot \frac{dx}{dt}$$

$$\therefore m \int_{V_o}^{0} dV = -3\pi\eta d \int_{0}^{S_o} dx$$

$$\therefore V_o = \frac{3\pi\eta d.S_o}{m} = \frac{S_o}{\tau}$$

$$\therefore S_o = V_o\tau \qquad \text{..... equation 1.2.4}$$

Now since, $\tau = \frac{m}{3\pi\eta d} = \frac{\rho d^2}{18\eta}$

$$\therefore S_o = \frac{\rho d^2.V_o}{18\eta} \qquad \text{..... equation 1.2.5}$$

Therefore, like the particle terminal velocity, V_F, So depends on particle diameter squared. Indeed equation 1.2.5 may be re-written more simply as,

$$S_o = \frac{V_F.V_o}{g} \qquad \text{..... equation 1.2.6}$$

and equation 1.2.2 may be re-written more simply as,

$$V_F = \tau g \qquad \text{..... equation 1.2.7}$$

Another important force which must be considered for very fine dusts is that induced by the Brownian motion of the gas molecules which surround each particle. However, in the size range of the present study the diffusive force is negligibly small and will not be considered further. In the special case

of fibrous aerosols, where the dimension of the particle may be a significant fraction of that of the containment vessel, the possible effects of interceptive deposition must be considered. In the present work roughly spherical particles having diameters of negligible size in relation to the smallest human airway have been used and interceptive effects may be ignored.

Aerosols formed by the mechanical dispersal of a volatile liquid invariably carry a substantial electric charge (WHITBY and LIU, 1966). Enhanced aerosol deposition may occur through the induction of electrical image forces and by the mutual repulsion of charged particles, the latter being termed the space-charge effect. The space-charge effect is highly dependent on the aerosol number concentration. YU and CHANDRA (1978) have calculated the rate of deposition of 1 μm diameter particles in the human respiratory tract and conclude that the particle number density must be of the order of 10^5 particles per cubic centimetre before space-charge effects need to be considered. This is a far higher particle concentration than occurs in the present work.

For very fine aerosols it is possible that enhanced particle deposition might occur in the respiratory tract as a result of the induction of an electrical image force on the airway walls. Recent evidence for submicron particles may support this view (MELANDRI et al, 1977). Whether or not deposition by image forces is also important for larger particles will depend on the manner in which the average number of charges per particle increases with increasing particle size, since,

$$Fd \propto V_F . d$$

and $$Fi \propto Q \propto d^n \text{ say,}$$

where, Fi, is the magnitude of the electrical image force in in Newtons

Q, is the total charge on the particle in Coulombs

n, is a pure number

(other nomenclature as above).

Equating Fd and Fi and neglecting the gravitational force, when the particle attains its terminal velocity, V_F , this gives,

$$V_F \propto d^{n-1}$$

For n = 2, V_F would increase, while for $n \leq 1$ the drift velocity would decline or stay constant, with increasing particle size. In the case of an aerosol exposed to a bi-polar ion atmosphere of sufficiently high ion number concentration to attain an eventual Boltzmann type equilibrium, the average number of charges, $\bar{q}$, on a particle has been estimated by GUNN (1955) to be (ignoring sign),

$$\bar{q} = 2 \cdot 37 d^{0.5}$$

For an aerosol inhaled under such conditions, bearing in mind the results of MELANDRI et al (1977), it is therefore unlikely

that image forces are very important in the particle size range of the present study (4·5 – 13 μm diameter). Nevertheless, it is desirable to check this by more direct calculation if possible.

According to YU (1977), the image force, Fi, experienced by a spherical particle in a cylindrical vessel is given by,

$$Fi = \frac{Q^2.r^2}{16\pi R^2 \varepsilon_o (R-r)^2} \qquad \text{..... equation 1.2.8}$$

where, Q = total charge on particle in Coulumbs

r = radial distance of particle from the cylinder axis in metres

R = radius of cylinder in metres

ε_o = permittivity of free space in Farads metre^{-1}

Putting Q = y.e, where e is the fundamental unit of electronic charge and y is the number of such charges on each particle, equation 1.2.8 may be written as,

$$Fi = y^2.K$$

where $$K = \frac{e^2.r^2}{16\pi R^2 \varepsilon_o (R - r)^2}$$

As an example, let R be the radius of the smallest airway in the Weibel model, where R $\simeq$ 0·2 mm. Let r = 0·99R = 198 μm, i.e. let the particle be only 2 μm from the airway wall, since if the

image forces are small over this range in such a small airway, they are likely to be small elsewhere in the respiratory tract.

$$\therefore K = \frac{e^2(\cdot 99)^2}{16\pi\varepsilon_o(10^{-2}.R)^2}$$

Putting $e = 1{\cdot}6 \times 10^{-19}$ Coulombs, $\varepsilon_o = 8{\cdot}85 \times 10^{-12}$ Farads metre^{-1}, gives, $K \simeq 1{\cdot}4 \times 10^{-17}$ Newtons.

The magnitude of the gravitational force, F_g, is given by,

$F_g = m.g$ (nomenclature as above)

Which for a particle of density 10^3 Kg.m^{-3} and diameter $4{\cdot}5\,\mu$m, gives a value $F_g \simeq 4{\cdot}7 \times 10^{-13}$ Newtons. Therefore, for Fi to be comparable to F_g, y must have a value of $(F_g/K)^{0.5}$, which in this case is approximately $1{\cdot}8 \times 10^2$ charges per particle. This is about an order of magnitude greater than the number of elementary charges measured elsewhere to reside on identical aerosol particles to those of the present study (FRY, 1970). It is therefore unlikely that electrostatic deposition is of any significance in the present work. Precautionary measures were nevertheless taken to 'neutralize' the test aerosol, described in Chapter 3, part 2(iv).

A number of other forces exist which may act on an airborne particle, but only diffusiophoretic and thermal forces could be of conceivable relevance here. Diffusiophoretic forces act when

there is a diffusional transfer of gases from regions of high to low gas concentration. In the human lung such diffusive transfer does occur, but owing to the simultaneous transfer of nearly equal numbers of O_2 and CO_2 molecules in opposite directions, the resultant magnitude of the diffusiophoretic effect is thought to be small (HIDY and BROCK, 1969).

For thermal forces to act on a particle a temperature gradient must exist. In the human lung the temperature may be regarded as a nearly uniform 37°c throughout. The temperature in the oral cavity may often be several degrees below this figure and it is possible that very small thermal forces act on inhaled particles. However, since the residence time of particles in the oral cavity is always very small, even during quiet breathing, it is unlikely that thermal deposition forces are of any significance.

Overall then, it is the two basic forces of nature, gravity and inertia, that are likely to be of most significance in determining the respiratory tract deposition of the aerosol particles of the present study. Both depend on the square of particle diameter and the importance of each is likely to be considerably influenced by physiological factors.

1.2(ii) Physiological factors in aerosol deposition

In the following discussion the influence of respiratory physiology on aerosol deposition will be considered only insomuch as it affects the contribution of the two primary deposition mechanisms, gravitational settling or sedimentation, and inertial impaction. Inertial deposition of particles may occur in the

respiratory tract wherever there is a change in the magnitude or direction of gas-flow. Such changes occur most frequently in the upper intrathoracic airways and human head. Besides being influenced by the mean inspired or expired flow rates, it is likely that subtle changes in the configuration of upper respiratory tract anatomy are also important. Such anatomical variability has already been mentioned (see part 1(i) above); in particular, the constriction of the glottal opening during expiration is certain to increase peak flow velocities in the larynx and is therefore likely to lead to enhanced inertial deposition in, and possibly beyond, this region. The importance of inertial deposition at the carinal ridge of the bifurcations has frequently been emphazised (SCHLESINGER et al, 1977). However, little attention has been given to the possible inertial deposition of particles arising from the existence of turbulent eddy currents and secondary swirling motions in the respiratory tract, as has been recently pointed out (HAMILL, 1979). Such deposition is often termed, perhaps misleadingly, 'turbulent diffusion'. Variations in the glottal opening during breathing may be of considerable importance in this respect and conceivably be a major source of both inter- and intra-subject variability.

Anatomical variability may also occur in the nasal cavity, but since the present work involved purely mouth-breathing experiments this will not be considered further.

According to the experimental results of SCHLESINGER and LIPPMANN (1972), who measured aerosol deposition in hollow casts of the human tracheo-bronchial tree, inertial impaction is not

important beyond about the first ten airway generations. As was described above, gas-flow rates are slower, and particle residence times longer, in the smaller airways. This lowers the probability of inertial deposition and raises that of gravitational deposition. Therefore, as aerosol losses due to inertial impaction decrease, those due to sedimentation are likely to increase, towards the smaller airways (TAULBEE and YU, 1975).

The amount of aerosol which deposits in the respiratory zone of the lungs, relative to the amount of aerosol inhaled at the mouth, will be determined by two factors, other influences being equal: 1. the amount of aerosol entering the respiratory zone; 2. the deposition efficiency in the respiratory zone. Since with increasing particle size more aerosol is likely to be lost in the dead space airways, aerosol exposure to the respiratory zone decreases. Yet since the deposition efficiency in the respiratory zone increases with particle size there must be a point at which the deposition there is a maximum. The peak alveolar deposition has normally been predicted to lie between 2–4 μm particle diameter, although this has never been confirmed experimentally (TASK GROUP ON LUNG DYNAMICS, 1966). Moreover, it seems not to have always been appreciated that since the amount of aerosol loss in dead space is likely to vary considerably with breathing pattern, the alveolar peak may not always be at a fixed particle size.

Tidal volume and breathing rate rarely change in isolation from one another. A high level of exercise may result in an increase in both (SILVERMAN et al, 1951). At higher breathing rates there will

be increased particle impaction in the dead space airways; since particle residence times are then lower it is likely that there is a simultaneous decrease in sedimentation losses. Therefore, whether or not there is a change in the aerosol exposure level in the respiratory zone will depend on the relative importance of inertial and gravitational deposition in the dead space airways. At higher breathing rates there will also be shorter particle residence times in the respiratory zone and, consequently, a lower aerosol deposition efficiency. However, it is most important to distinguish between a change in respiratory zone deposition efficiency and a change in the absolute amount of aerosol which deposits there per unit time. For example, a doubling of breathing rate may well result in about a halving of the respiratory zone deposition efficiency, but since double the amount of dust enters the respiratory tract, and something probably close to double may enter the respiratory zone in many cases, the change in the absolute amount of dust which deposits in the respiratory zone may be only slight.

The influence of tidal volume on aerosol deposition is not always entirely dependent on the fact that inhaled particles are taken deeper into the lungs (LIPPMANN, 1977). The increase in penetrance of particles which have already entered the respiratory zone, to the level of the alveolar ducts, with even a substantial increase in lung volume, is only of the order of a few millimetres (Table 1.1.1). At a given breathing rate some of the importance of tidal volume may also lie in the relative proportions of the

inhaled aerosol which occupy the dead space airways and the respiratory zone. Since during quiet breathing a typical tidal volume is something like 600 ml (COMROE et al, 1955), the dead space airways may well account for a substantial fraction of this. At higher tidal volumes the dead space airways become a smaller fraction and a higher relative amount of aerosol deposits in the respiratory zone.

The influence of the degree of lung inflation on aerosol deposition is still controversial. HEYDER et al, (1975) claim that it is the functional residual capacity (FRC) which mainly determines the observed differences in total deposition between subjects. However, DAVIES et al (1977) argue that total deposition correlates better with the residual volume (RV), since FRC includes the expiratory reserve volume (ERV), 'which changes more with age'. Such arguments depend on a number of anatomical imponderables, such as relative numbers and size of alveoli between subjects. Other anatomical factors such as variations in upper respiratory tract morphology, both between and within subjects, appear to have been neglected.

In measuring the total and regional deposition of aerosols in the respiratory tract the influence of the amount of aerosol which is transferred from the tidal to the expiratory reserve or the residual air must be considered (HEYDER, 1971). During the steady breathing of an aerosol of uniform inhaled concentration, the concentration of aerosol in the respiratory zone increases until a steady state level is reached. At this point the rate at which

aerosol is transferred into the respiratory zone is just equal to the rate at which it deposits there. This process is termed the 'wash-in'. On cessation of aerosol inhalation, airborne particles may be observed in the expired air in decreasing amounts for several breaths. This process is termed the 'wash-out' (DAVIES et al, 1972). Consequently, for aerosol particles small enough to remain airborne in the breath which follows that in which they were first inhaled, it is necessary to specify whether total deposition is being measured before or after steady-state equilibrium has been established. Because of the relatively high levels of total deposition measured for particles larger than 4·5 μm (LIPPMANN and ALBERT, 1969; FOORD et al, 1978), it is unlikely that steady-state influences are important above this size (see Chapter 3, part 2(i)).

The temperature and humidity of the inspired air must also be considered as a possible factor in aerosol deposition. If the particles are inhaled from air at ambient temperature, normally about 17°c cooler than the lungs and not completely saturated even at this lower temperature, there exists the possibility of the condensation of water vapour on their initially cooler surfaces. Some total deposition experiments have been conducted at room temperature and humidity (LIPPMANN and ALBERT, 1969; FOORD et al, 1978) while others have for technical reasons required the inspired air to be at ~37°c and ~100% realtive humidity (HEYDER et al, 1973). Such influences are discussed further in Chapter 3, part 3.2.(iv).

Finally, attention is drawn to a potentially important means by

which inertial aerosol deposition in the respiratory tract may be enhanced that appears to have been overlooked in the literature. Relative inertially-induced movement between an inhaled airborne particle and its carrier fluid may arise quite independently of changes in the magnitude or direction of the gas-flow relative to the 'fixed' human respiratory tract, if the individual is himself accelerated relative to the Earth's inertial frame of reference. The magnitude of such an effect relative to the gravitational force may be seen crudely by considering the ability of the human being to jump into the air, overcoming gravity, for short periods. Considering that occupational dust exposure must occur against a backcloth of work, and therefore movement, such effects may merit investigation. In particular, the rapid mechanical vibrations induced in an individual by hand-held machine tools should be considered since these may simultaneously give rise to a high local dust concentration. It should therefore be borne in mind that the laboratory derivation of aerosol deposition curves for the stationary subject may not necessarily be readily applied to the work situation, even when differences in aerosol character and breathing conditions have been taken into account.

1.3 Criteria for defining aerosol hazard to the human respiratory tract

The induction of lung disease through the inhalation of airborne matter may be due to a multitude of factors: individual susceptibility; toxicity of dust; solubility of dust; amount of dust deposited in the diseased region; and residence time of dust in the diseased region. In the present work the latter two factors are of most

relevance.

Perhaps the two most notable contemporary examples of aerosol hazard evaluations are those of the mining and atomic energy industries. Of particular concern in both industries is the dust fraction that is able to penetrate to the respiratory zone of the lungs. In a miner's lungs this dust fraction may give rise to silicosis or pneumoconiosis, while for a worker in the atomic energy industry the radiation dose arising from inhaled radionuclides is highly dependent on their pulmonary residence time. In establishing dust hazard criteria it is desirable to determine the dose-response characteristics of each dust. This requires the environmental sampling of the dust in question such that the individual or average dose to the employees may be determined. Dose-response correlation will be greatest when only that fraction of dust which would deposit in the region of the lungs of most interest is included in the sample (JACOBSEN et al, 1971). As the region of most interest and relevance, historically, has been the respiratory zone of the lungs, a size-fraction of dust has been defined which purports to represent that fraction of the total inhaled dust which deposits in the respiratory zone under normal working conditions (ORENSTEIN, 1960). This dust fraction is usually termed, perhaps rather misleadingly, 'respirable dust'. Although definitive respirable dust sampling criteria have been adopted by a number of nations (Figure 1.3.1), it is important to appreciate the historical origin of these criteria, for their basis is only partly empirical. Currently, the possibility of

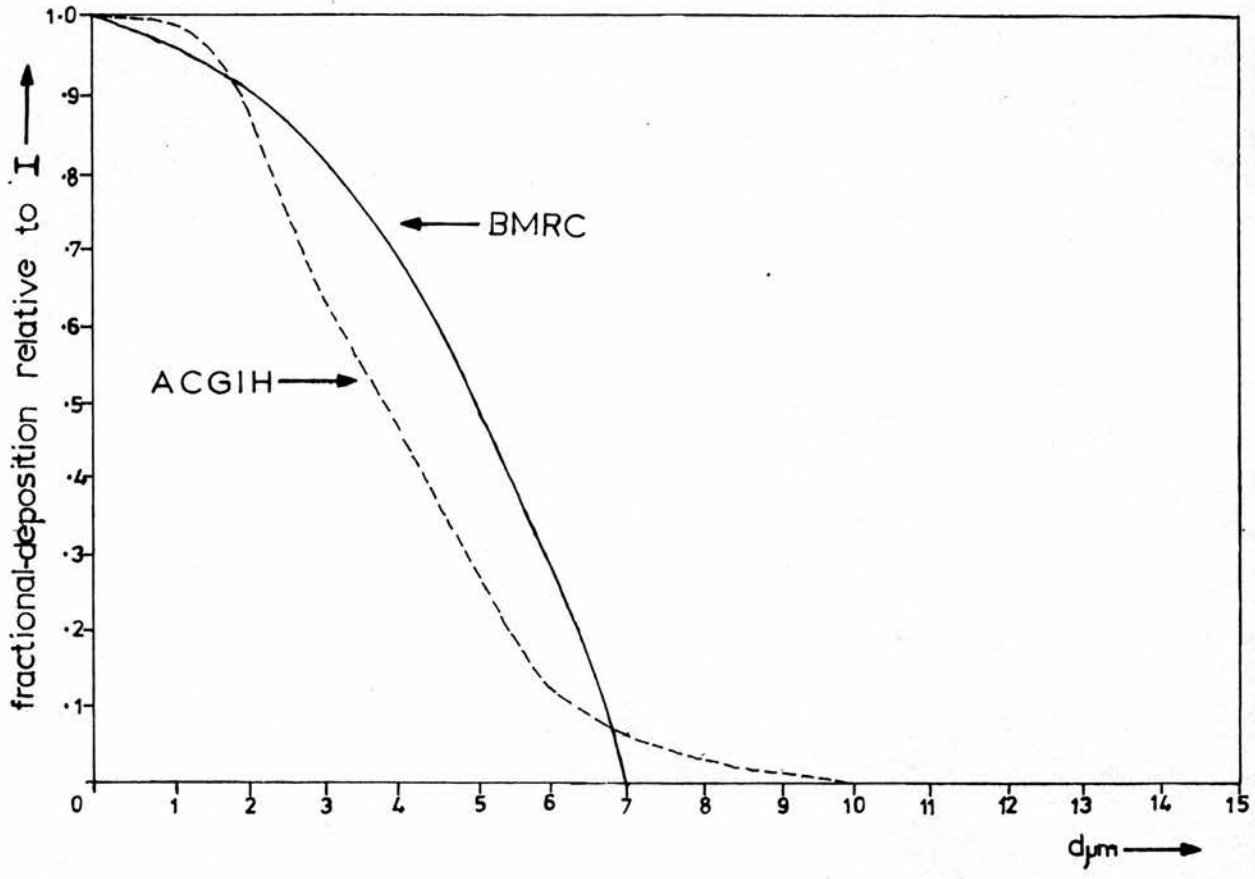

Figure 1.3.1: Respirable dust sampling criteria in U.K. (BMRC)[*1] and U.S.A. (ACGIH).[*2] (I represents inhaled aerosol).

*1 BMRC British Medical Research Council

*2 ACGIH American Conference of Governmental Industrial Hygenists

establishing sampling criteria for 'inhalable dust' is being considered (OGDEN and BIRKETT, 1977). Interest has also been expressed concerning the size fraction of dust which deposits in the dead space airways (ROGAN et al, 1973), which could be implicated in the aetiology of chronic bronchitis. For such new criteria to be established more experimental work is required concerning the fate of the larger inhaled particles in the respiratory tract.

In Chapter 2, the historical origin of existing dust sampling criteria is reviewed from the viewpoint of the experimental work on which they were partly based.

CHAPTER TWO

HISTORICAL AND EXPERIMENTAL BACKGROUND

The possibility of a relationship between the inhalation of airborne matter and lung disease has long been recognised (GALEN, 129-199). However, it was not until late into the industrial revolution, by which time industrially derived aerosols were ubiquitous, that serious attempts were made to quantify the airborne hazard and to investigate the nature of pulmonary defence mechanisms. Although the history of such work has been described many times (HATCH and GROSS, 1964; STUART, 1973) and the experimental findings have often been applied to practical problems of industrial health (TASK GROUP ON LUNG DYNAMICS, 1966), the techniques used to obtain these results have rarely been examined (DAVIES, 1974). The emphasis placed in the present work on experimental accuracy and control may be better understood in this context.

In 1868, LISTER reported that air lost its power to cause putrefaction when mixed with blood by virtue of its having passed into the lungs. The observation was taken as evidence of the air purification properties of the lungs. This was seemingly corroborated by TYNDALL, who in 1870 reported on one of his earlier experiments which he believed had demonstrated the 'deeper portions of expired air' (probably what would now be called the expiratory reserve 'air') to be entirely free of inhaled airborne matter. As described by OWENS (1923), Tyndall's work was widely misinterpreted to mean that

the lungs act as a perfectly efficient filter of all dusts. Although OWENS (1923) clarified the interpretation of these results and had also shown Tyndall's experimental technique to be insufficiently sensitive to detect very fine particles, in the intervening years the belief that the lungs act as a highly efficient dust filter became widesread and this view still persists in many modern textbooks of medicine and physiology:

> 'Particles below 1 μm in size are nearly the only ones to penetrate into the pulmonary depths.... Their deposition rate in alveolar spaces is very high, exceeding 90% of the total number of small particles inhaled, for any respiration rate and depth.' L.DAUTREBANDE in 'Microaerosols', 1962.

2.1 Total deposition

The first attempt to measure total aerosol deposition in man, i.e. the total amount of aerosol which deposits expressed as a fraction or percentage of the total amount of aerosol inhaled, was that of SAITO (1912). The size distribution of dust employed and the breathing pattern of the subjects were not well defined however. Similar comments apply to the works of BAUMBERGER (1923), who attempted to measure differences in the total deposition values of tobacco smoking subjects 'puffing' and 'inhaling'. Baumberger was the first to employ an electrostatic precipitator, which enabled the exhaled aerosol to be collected without the problems that can arise when exhaling through a resistive filter. The electrostatic precipitator was later used in experiments conducted by SAYERS et al, (1924), but the first experiments to measure total deposition

at a well defined breathing pattern were those of DRINKER et al, (1928). Their experiments serve usefully to illustrate the more fundamental experimental problems that may be encountered when attempting to measure total deposition.

Accrding to the simple definition of total deposition mentioned above, other factors being equal, there are only two quantities which need to be measured: the total amounts of aerosol inhaled and exhaled by a subject. Ideally, the aerosol to be inhaled should be sampled as closely as possible to its point of entry into the subject, in order to avoid particle losses in any connecting pipework. The exhaled aerosol must be separately collected, or sampled, and mixing with any dead space aerosol in the apparatus, together with actual losses of exhaled aerosol in this dead space, should be minimized. In the apparatus of DRINKER et al,(1928) the aerosol to be inhaled was sampled remotely from the subject, thus allowing the possibility of high particle losses in the connecting pipework, particularly at large particle sizes. The separation of inhaled and exhaled flows, using flap valves, may have resulted in significant losses of exhaled aerosol before it could be collected. The overall tendency would therefore be for total deposition to be overestimated.

Many later total deposition experiments employed methods possessing similar or equivalent drawbacks (C.E.BROWN, 1931; VAN WIJK and PATTERSON, 1940; WILSON and LA MER, 1948; LANDAHL, 1950; DAUTREBANDE et al, 1957). The scatter of these observations has been considerable (DAVIES, 1964).

ALTSHULER et al, (1957) introduced a new aerosol sampling technique, based on optical scatter from a monodisperse aerosol, which overcame many of the disadvantages mentioned above. The aerosol concentration was measured, as a function of time, close to the point of entry into the subject. By relating this to simultaneous recordings of respiratory flow rates and volumes, the relative amounts of inhaled and exhaled aerosol were calculated. Altshuler's basic apparatus was much improved by MUIR and DAVIES (1967), since no co-operation from the subject was needed for the manipulation of valves. Still further improvements have been made by HEYDER et al, (1973), (1975), particularly with regard to the application of analogue computing techniques in the automatic calculation of results.

Despite these improvements the optical scatter technique still imposes a few limitations. Measurement of the exhaled aerosol is more difficult than measurement of that inhaled, since the concentration of aerosol falls rapidly from the beginning of an expiration and the estimation of the true average is difficult (DAVIES, 1974). This is the converse of the aspiration sampling problem when it is, in general, harder to obtain accurate estimates of the total inhaled aerosol than total exhaled. Large particle sizes are particularly difficult to study using the technique.

2.2 Regional deposition and clearance

Techniques for measuring regional deposition have a more recent history. Two distinct experimental approaches have been adopted. One is based on the fractionation of the expired air into separate volumes and the amounts of aerosol contained within

each are then measured. BROWN et al, (1950) first used the technique for this purpose and their results have probably been applied more extensively than any other in the derivation of international exposure standards (TASK GROUP ON LUNG DYNAMICS, 1966). For this reason their work merits some attention.

The experiments of BROWN et al,(1950) are acknowledged by many to have been misconceived (MERCER, 1973; LIPPMANN and ALTSHULER, 1976). Central to these misconceptions is the assumption that the aerosol concentration measured at a given expired volume can be directly related to the amount of aerosol deposition that has occurred at a given depth, or region, in the lungs. Those who have reviewed their work have usually pointed to the weakness of assuming that aerosol particles follow the same course in the lungs as gases, which neglects the greater diffusibility of gases. In essence, this means there will be an error in the estimation of the amount of aerosol which can be said to have penetrated no further than the dead space airways. More fundamental objections to their methods have sometimes been overlooked. Their basic equations used in the calculation of deposition results from the raw experimental data are mutually inconsistent. A few of the defects in this work were pointed out by ALTSHULER (1959).

The other technique for measuring regional deposition is that first described by ALBERT and ARNETT, (1955). It is based on measurements of the proportion of inhaled radioactive particles cleared from the lungs at about one day after aerosol administration. At an earlier date, WILSON and LA MER, (1948) used radioactive

particles in an attempt to measure regional deposition, but the method was based on the premise that by placing a collimated radiation detector over a section of the lung periphery, a representative measure of relative respiratory zone deposition could be obtained. It is apparent from WILSON and LA MER'S paper (1948), that they well understood the approximate nature of the technique. Nevertheless, their work also merits attention because of its extensive use in the derivation of internationally accepted dust exposure standards (TASK GROUP ON LUNG DYNAMICS, 1966).

WILSON and LA MER'S data (1948) from seven subjects were averaged to obtain a plot of 'relative axillary count' versus optical particle radius. The meaning of 'relative axillary count' must be made clear for it has sometimes been misinterpreted. It represents the number of detector counts per minute per μCi of inhaled radioactivity, averaged over the seven subjects. This is quite distinct from the amount of pulmonary deposition relative to the amount of aerosol inhaled. As was pointed out by Wilson and La Mer, it is quite impossible to obtain any information on total respiratory zone deposition, from this data alone, relative to the inhaled aerosol. In a monograph on pulmonary deposition and retention, HATCH and GROSS, (1964) cite Wilson and La Mer's data and describe their plot of 'relative axillary count' versus particle radius as 'the percentage deposition values in relation to particle size'.

A still earlier misrepresentation of WILSON and LA MER'S data (1948) appears in the paper of BROWN et al, (1950). In this WILSON and LA MER'S 'relative axillary count' also appears as a 'percentage

deposition' ordinate, but the higher deposition peak (there were actually two) is plotted at a level of 55%, not the 87% or so of HATCH and GROSS (1964). The origin of the 55% value may be found in WILSON and LA MER'S paper (1948). As this particular expression of their data has been extensively applied to theoretical and practical problems of industrial health, its origin merits clarification.

As has already been mentioned in the present review, WILSON and LA MER had stated in their paper (1948) that no information could be obtained from their axillary detector results on the amount of respiratory zone deposition relative to the amount of aerosol inhaled. In an attempt, literally, to 'determine this order of magnitude' they adopted two crude calibration schemes: one based on the calibration of their axillary detector in terms of absolute units of radioactivity; the other based on measurements of blood radioactivity concentrations. The former method gave rise to the 55% value, but 27½% would have been equally valid since they had rather arbitrarily decided that their calibration 'pad' represented both lungs rather than the one nearest the detector, the further one being excluded according to their description of the technique. The latter method gave rise to a range of retention values falling between 18% and 63% of the inhaled aerosol. The highly approximate nature of both these methods was clearly stated by WILSON and LA MER (1948).

The interpretation put on WILSON and LA MER'S data (1948) by BROWN et al, (1950) is repeated in many of the reviews of the

literature (DAUTREBANDE et al, 1954; STUART, 1973). Moreover, the same misinterpreted data have been used by Committee 2 of the TASK GROUP ON LUNG DYNAMICS, which sat in 1965 under the auspices of the ICRP* in order to provide a sound basis for inhaled radionuclide dosimetry and setting of international exposure limits. In their report (1966) the WILSON and LA MER data (1948) appear as in the paper of BROWN et al, (1950). As can be seen in Figure 2.2.1, a theoretical curve for percentage respiratory zone deposition (designated 'pulmonary zone deposition' in the report), for mouth breathing, was derived from the Wilson and La Mer data (1948) after making certain adjustments for particle hygroscopicity. Equivalent theoretical curves for nasal breathing were derived from the experimental results of BROWN et al, (1950). This was long after ALTSHULER (1959) had first questioned the basic analytical methods employed by BROWN et al, (1950). The work of the ICRP Task Group forms the basis of current international exposure standards for inhaled radionuclides.

The radioactive aerosol technique described by ALBERT and ARNETT (1955), for the measurement of regional deposition, was later developed by the same principal author and his later co-worker Lippmann (LIPPMANN and ALBERT, 1969). The technique is based on the assumption that the non-respiratory zone of the lung clears more quickly than the respiratory zone, and within about one day, by virtue of its being largely ciliated. The radioactive aerosol technique presents many technical difficulties which are described in later chapters. The results of LIPPMANN and ALBERT

* International Committee on Radiological Protection.

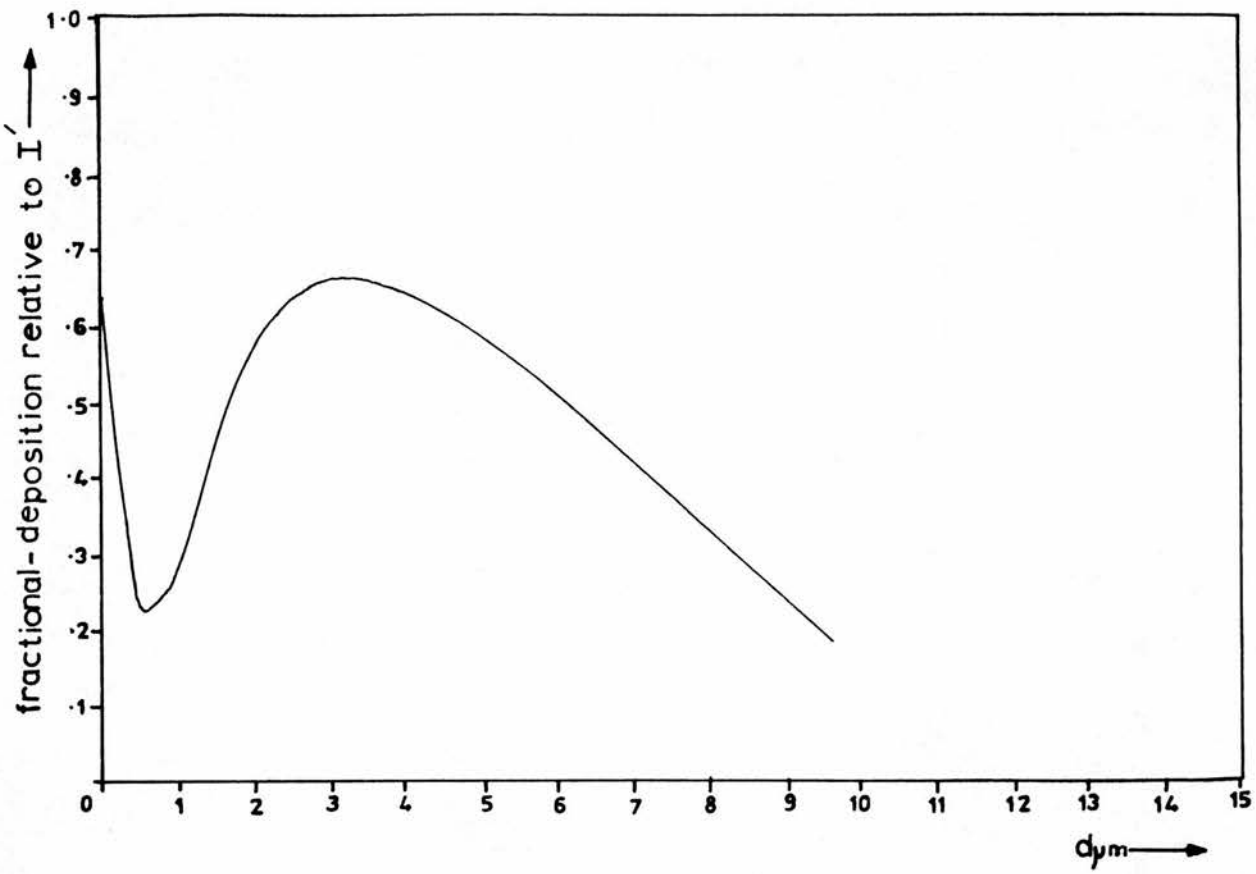

Figure 2.2.1 : Task Group respirable dust curve. Theoretical curve at 15 breaths $min.^{-1}$, 750 cc tidal volume. I' represents aerosol entering trachea.

(1969) and those of the other two groups who have collected data in this field are discussed in Chapter 5.

Besides work on the aggregate clearance of inhaled particles in which the fundamentals of clearance mechanisms are often of only indirect interest, there have been many studies of the basic mechanism of mucociliary clearance and measurements of specific clearance rates in the ciliated airways. These investigations fall broadly into two categories: histological study of tissue excised from animals and man and the study of clearance rates in live subjects. It is beyond the scope of the present review to describe work on long-term clearance or to review the literature which deals with the essentially mechanistic ciliary properties.

From histological study it has been possible to obtain information of limited reliability on clearance rates in airways of various diameters in animals and man (DALHAM, 1956; ASSMUNDSSUN and KILBURN, 1970). This is possible because the cilia beat with a degree of independence from the central nervous system and may continue to beat for some time after death. The limitations to the reliability of this approach arise because of the inevitable experimental interference with the delicate balance of clearance fluids and ciliary beating (SLEIGH, 1977).

In conclusion, this review has considered some of the experimental techniques used to obtain the results of the most important investigations into the deposition and clearance of inhaled particles. The reliability of many of these techniques has been questioned and some errors in the interpretation of certain widely quoted results have been indicated.

CHAPTER THREE

EXPERIMENTAL METHODS

3.1 Particles

This section describes the techniques that were developed to produce a monodisperse test aerosol (coefficient of variation <10%). The particles consisted of polystyrene tagged with a γ-emitting isotope, Technetium^{99m} (Tc^{99m}), whose half-life of radioactive decay is six hours. The latter is a convenient figure for measurements over a period of about one day. Polystyrene particles have been used in many human aerosol inhalation studies conducted elsewhere (BOOKER et al. 1967; PAVIA and THOMPSON, 1976; FOORD et al. 1978). BLACK and WALSH (1970) reported on the work of EVANS (1967), who observed no obvious short-term toxic effects in in vitro cell studies. At an earlier date, SCHOENBERG et al. (1961) studied the phagocytosis of polystyrene particles in the reticulo-endothelial system of the rabbit and concluded they were metabolically inert and non-toxic to the host.

The main advantage of employing monodisperse particles in a human aerosol inhalation study, is that if the mass of aerosol which deposits in a particular region of the respiratory tract is estimable, it is possible to express this value as a fraction of the total inhaled mass, directly. If a polydisperse aerosol is used, the size distribution of each deposition fraction must be measured in order to determine the fractional deposition (in terms of number,

say) of each component size, but this is rarely possible. In the case of a practically monodisperse aerosol differences between mean diameters expressed in terms of mass, area and number, are minimal. Assuming a log-normal distribution, i.e. one in which the relative frequency plotted against $\log_e$ of size is normally distributed, the diameter, $\bar{d}m$, of the particle having a mass equal to the average mass of the sample, is given by (DENNIS, 1976):

$$\log_e . \bar{d}m = \log_e . \bar{d}g + 3{\cdot}5 \log_e^2 . \sigma g \qquad \ldots\ldots\ldots \text{ equation } 3.1.1$$

where, $\bar{d}g$, is the geometric-mean diameter, $= \frac{1}{N} . \sum_i (ni . \log_e di)$

and, N = number of particles in sample

ni = number of particles of diameter di

σg = geometric standard deviation of the sample

For $\sigma g = 1{\cdot}1$, the difference in value between $\bar{d}m$ and $\bar{d}g$ is $0{\cdot}15\ \mu m$ at $\bar{d}g = 4{\cdot}5\ \mu m$ and $0{\cdot}42\ \mu m$ at $\bar{d}g = 13{\cdot}0\ \mu m$, which is the size range used in the present study. The deposition fractions measured at a given value of $\bar{d}g$ for a practically monodisperse aerosol may therefore be assumed to be close to the value of the same deposition fractions that would be measured for a perfectly monodisperse aerosol ($\sigma g = 1$); $\sigma g = 1{\cdot}1$ was therefore adopted as the standard for monodispersity, since differences between mass and number deposition could be ignored, and the average diameter of a sample was expressed in terms of the count-mean diameter, $\bar{d}$, which for an

aerosol of this degree of monodispersity is nearly equal to $\bar{d}g$, above,

and, $\bar{d} = \frac{1}{N} \cdot \sum_i (ni.di)$

(nomenclature as above)

3.1.(i) Aerosol generation principles

Monodisperse polystyrene particles tagged by chemical chelation with Tc^{99m} were produced using a commercially available spinning-top aerosol generator (Research Engineers Ltd.). In this technique the solution to be atomized is fed via a fine needle, at a constant rate, to the centre of an air-driven spinning-top. The feed solution spreads rapidly across the flat surface of the top and is angularly accelerated to the edges at a rate which depends on the rotational frequency (Figure 3.1.1). The solution first forms a ligament as it leaves the edge (i), the ligament then elongates (ii) and finally disintegrates into two or more droplets (iii), (PHILIPSON, 1973). The smaller droplets are termed satellites and the larger droplets termed primaries. By equating the forces on the primary droplet due to angular acceleration and surface tension and determining an empirical constant of proportionality between them, the following relationship has been derived which is useful in estimating the primary droplet diameter, dp, at a particular rotational frequency (MAY, 1949):

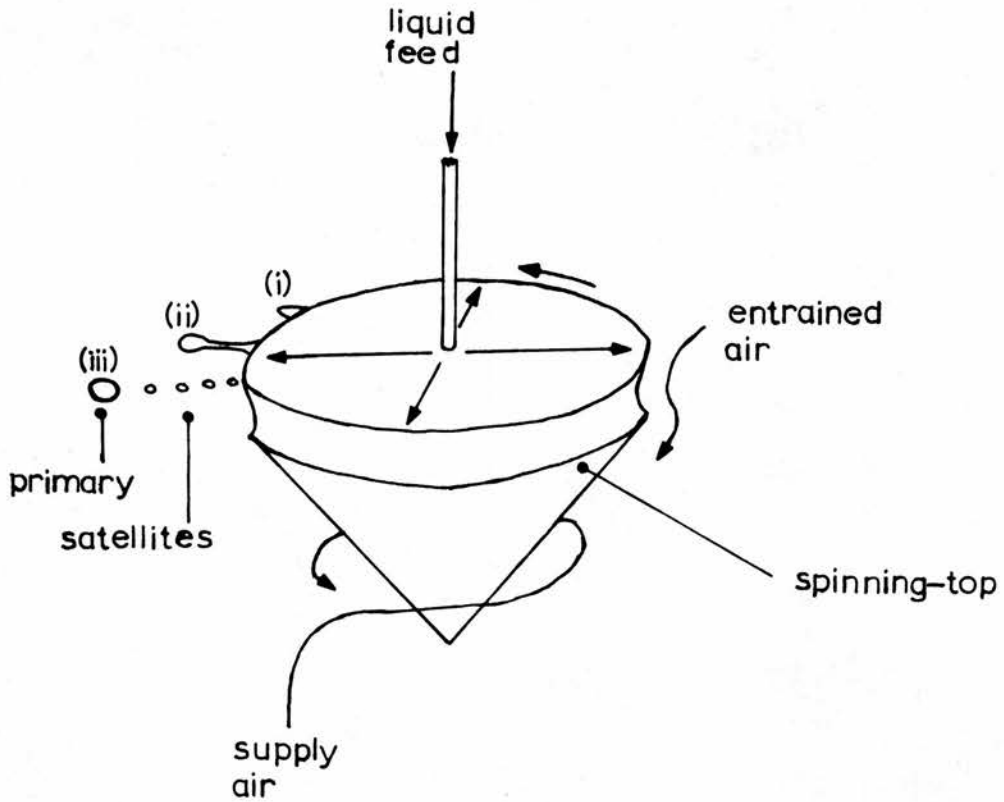

Figure 3.1.1: Spinning - top.

$$dp = \frac{4 \cdot 5}{\omega}\left[\frac{T}{D \cdot \rho}\right]^{\frac{1}{2}} \qquad \text{..... equation 3.1.2}$$

where, ω = angular velocity of spinning-top in radians sec^{-1}

T = surface tension of droplet in $N.m^{-1}$

D = diameter of the top at its surface in metres

ρ = density of feed solution in $Kg.m^{-3}$

dp = primary droplet diameter in metres

There is a practical upper limit to spinning-top speed normally determined by the maximum available air-flow. It is therefore usual practice to produce smaller particles, termed secondaries, by evaporating off the bulk of the primary droplet, leaving behind a smaller, solid, residue. The diameter, ds, of the secondary particle depends on the concentration of solute in the initial solution and is given by:

$$ds = dp\left[\frac{C}{\rho s}\right]^{\frac{1}{3}} \qquad \text{..... equation 3.1.3}$$

where, C = wt.vol.$^{-1}$ concentration of solute in feed solution in $Kg.m^{-3}$

ρs = density of solute in $Kg.m^{-3}$

ds = secondary particle diameter in metres

dp = primary particle diameter in metres.

MAY (1949) stated that the satellite particles are about four times as numerous as the primaries and about one quarter of their

diameter. In the present work a mean size ratio of 0·41 ± ·04 (10 observations ± standard error of the mean) over a size range of 4·5 - 13·0 μm diameter was determined (see part (iii) below for sizing technique).

The monodispersity of the resultant aerosol is dependent on a number of factors (WHITBY et al, 1965). An important one is the separation of the feed needle tip from the spinning-top surface, since if this is too great partial droplet formation may occur at the needle orifice. Accurate centralization of the feed needle tip is also important, otherwise the feed solution tends to spread non-uniformly over the spinning-top surface. Both these problems necessitate some form of fine-control positioning mechanism for the feed needle. Another influence on aerosol monodispersity is the steadiness and rate of feed of solution to the spinning-top (RYLEY, 1959).

The MAY (1949) apparatus (Research Engineers Ltd) incorporates an automatic satellite removal system, which is based on the fact that the satellite particles are projected a lesser distance from the spinning-top edge than the primaries. In practice the system is not always workable because of the poor optimization of suction flow rate with satellite diameter. Moreover, if updraught or downdraught collection of aerosol is employed, the satellite removal system may be ineffective owing to disruption of air-flow in the region of droplet formation.

3.1(ii) Description of aerosol generation and tagging

In attempting to measure the clearance of radioactive particles

from the lungs it is essential to employ a radioactive tag that is stable in the watery fluids that line the dead space airways. For this reason the radioactive tag, Tc^{99m}, was chemically chelated into the polystyrene molecules as tetraphenylarsonium pertechnetate by the method of FEW et al. (1970). In this procedure the tagging is performed while the polystyrene is still in solution, before aerosol production. The radioactive tag is therefore incorporated throughout the volume of each particle, not just on the surface, and the amount of radioactivity per particle varies as the particle mass. The overall process was not very efficient and relatively high amounts of radioactivity ($\sim$1·11GBq or $\sim$ 30mCi) had to be used at the initial stage.

The solution from which the particles were produced consisted of 1% (weight for volume) polystyrene dissolved in a mixture of xylene and methyl iso-butyl ketone of 1:1 volume to volume ratio. The ketone was included to retard the evaporation of xylene over the spinning-top surface which otherwise resulted in the excessive accumulation of polystyrene residue and consequent degradation of particle size uniformity. Production time was always limited to below 20 minutes as impacted polystyrene tended to accumulate on the spinning-top housing, which eventually interfered with its operation (BLACK and WALSH, 1970). Solution feed rate to the spinning-top was optimized at below a nominal value of 0·5 cc $min.^{-1}$, as above this the particle size uniformity was found to be unacceptably poor (>10% coefficient of variation). No more than 10 cc of solution could therefore be sprayed and this necessitated the use

of a feed system in which the volume of liquid dead space was minimal.

As was described in part 1(i) above, there are several important practical requirements for the production of a monodisperse aerosol. To solve the problem of feeding the radioactive solution at a predetermined and steady rate, with minimal liquid dead space losses, the apparatus illustrated in Figure 3.1.2 was devised. It was found that mechanical injector and peristaltic pumps tended to produce spasmodic fluctuations in feed rate. To smooth the liquid feed a simple damping mechanism was used in conjunction with a mechanical injector pump (C.F.Palmer Ltd.). Water was fed at a predetermined rate into a coil of silastic rubber tubing. The coil served both as a reservoir for the incoming water and as a damper of any sudden variations in its feed rate. The silastic coil was connected to a 10 ml. pipette which contained the radioactive solution, thus forming an air-tight system. Owing to the hydrostatic pressure of liquid in the pipette, the air pressure in it was initially negative. This steadily grew more positive as liquid feeding progressed and the hydrostatic pressure of the solution diminished. Water movement in the silastic coil therefore continuously compensated for the pressure changes and, in consequence, the average feed at the needle orifice (internal diameter $\simeq$ 400 μm) was normally a fraction of about 0·6 of the predetermined value. The latter was always set at 0·5 cc $min.^{-1}$, giving a value at the feed needle head always equal to or lower than this and an average rate of about 0·3 cc min^{-1}. As the radioactive solution was completely expelled from the

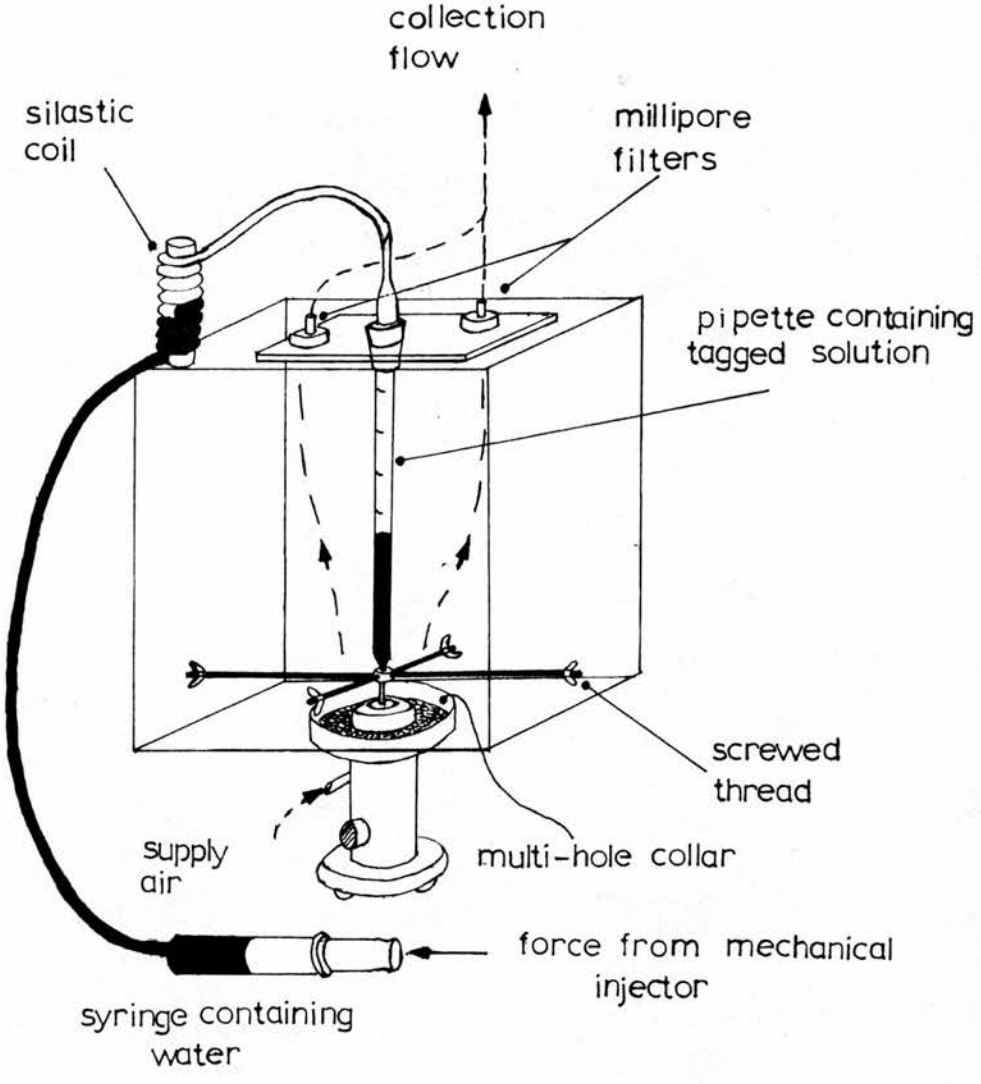

Figure 3.1.2: Aerosol generation apparatus.

pipette there were no liquid dead space losses.

Research Engineers Ltd. supply a device to control the positioning of the feed needle, known as a 'spider', but this is cumbersome and inaccurate in use and has the added disadvantage that aerosol losses tend to occur on it during aerosol production. If radioactive particles are produced it is unsafe to make adjustments during a production run, as is often necessary. Full external fine-positioning control was accomplished in the present work by means of the device illustrated in Figure 3.1.2. In this, four screwed thread rods were mounted crosswise to a central perspex collar, which housed the feed needle. The four free ends of the rods protruded through the walls of a perspex box, which housed the spinning-top unit. Feed needle positioning control was achieved by rotation of butterfly nuts attached to the rod ends. Rotation of opposite pairs of butterfly nuts in concurrent directions resulted in movement of the needle along the axis of the rod in question, with no alteration in the height of the needle or in its position in a direction perpendicular to this axis. Contrawise rotation of any opposite pair of butterfly nuts resulted, owing to a slight central inflection at the crossbar midpoint, in either upward or downward movement of the needle, depending on whether such rotation was an inwards or outwards screwing motion.

The automatic satellite removal system (MAY, 1949), was found to be unsatisfactory in a number of respects, for reasons already mentioned, and was therefore blocked off. This was found not to have any adverse effect on the aerosol monodispersity. Both primary

and satellite particles were collected by means of the updraught collection system illustrated in Figure 3.1.2. The particles were swept upwards in airstreams which converged at two millipore filters (Millipore Filter Corporation) on which they were collected. In order to ensure no external leakage of radioactive particles the updraught collection air-flow rate was always set at a greater value than that of the air supply to the spinning-top stator. The air pressure in the production unit was therefore always negative and the induced air inflow was directed via a multi-hole collar which surrounded the spinning-top housing, in order to provide an additional collection updraught. Millipore filters of nominal pore diameter equal to that of the expected satellite diameter were used. These filters are resistant to xylene vapour and the coefficient of variation in pore diameter is claimed by the manufacturers to be less than $\pm$ 5%. The degree of particle penetration through the millipore filters was checked directly by measuring the radioactivity associated with an additional millipore filter placed in-line with that of a main collection filter (see part 2 (i) of the present chapter). The results indicated a particle collection efficiency close to 100%.

In order to ensure good particle size reproducibility between production runs a calibration curve of air supply flow, in arbitrary units of rotameter scale, versus count-mean particle diameter was derived (Figure 3.1.3). Direct comparison with the theoretical values of particle diameter, predicted using equations 3.1.1 and 3.1.2, is not strictly valid in this case, owing to the possible

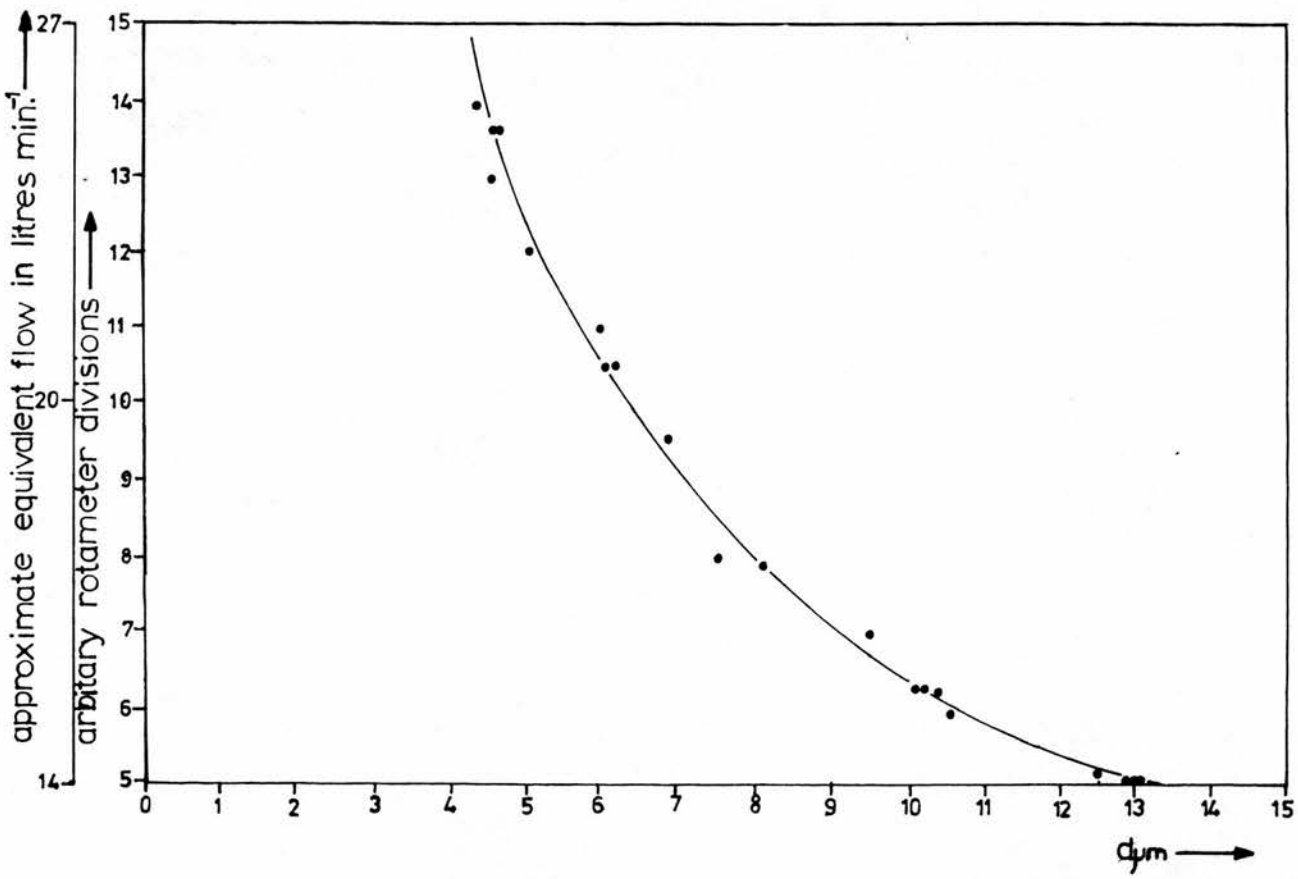

Figure 3.1.3: Particle diameter (μm) vs supply flow (line drawn by eye fit).

effects of blocking the satellite removal port on the spinning-top rotational frequency at a given air supply rate.

Before an aerosol production run the spinning-top and its housing were cleared of excess polystyrene. The spinning-top surface was roughened using medium grade carborundum powder, which facilitated the wetting of its surface by the spraying solution (MAY, 1949). The entire aerosol production unit was housed in a fume cupboard in the interests of radiological safety (Figure 3.1.4).

It was necessary to remove the satellite particles from the sample after a production run. This was accomplished by making use of the fact that primary particles fall more quickly in a fluid than the satellites. Using a centrifuge it was possible to quicken their rates of fall. Ten separate centrifuging operations were performed for each sample and the clear portion of liquid, which contained mostly satellites, was removed after each run. The appropiate levels and durations of centrifuge spin were determined empirically. By such means, the proportion of satellites in the sample was reduced to an average value of $2{\cdot}9 \pm 2{\cdot}5\%$ by mass (mean of 18 observations $\pm$ standard deviation) from the initial value always greater than 27%.

Finally, the required amount of radioactivity was drawn off from the sample and placed in 1·2 ml of ethanol ready for administration to the subject. Aerosol administration techniques are described in section 2 of the present chapter.

3.1.(iii) Particle characterization and in vitro leaching

The count-mean diameter of a sample of 200 particles was

Figure 3.1.4: Photograph of aerosol generation apparatus in fume cupboard.

determined after an experiment using a Timbrell double-image micrometer and particle size analyser (Fleming Instruments Ltd.). The sample was taken from slides placed in the main spraying chamber of the aerosol administration apparatus, which enabled estimates of the proportions of aggregates and satellites in the sample to be determined simultaneously. The calibration accuracy of the sizing instrument was periodically checked using a standard calibration slide.

The count-mean diameters of the particles were found to be log-normally distributed (Figure 3.1.5). It was more convenient to express the particle size uniformity in terms of the coefficient of variation, ν, (ν = standard deviation, σ, ÷ count mean diameter, $\bar{d}$), than geometric standard deviation, σg. According to FUCHS and SUTUGIN (1966), $\nu \simeq \log_e \sigma g$, for small values of ν.

3.1.(iii)(a) Aerodynamic diameter

For purposes of comparison between the aerosol deposition results of the different research groups it is useful to express such results in terms of the aerodynamic diameters of the aerosol particles employed in each case. The aerodynamic diameter of a particle is defined as the diameter of a sphere of density $10^3 Kg.m^{-3}$ having the same falling speed as the particle in an identical fluid. At a given size it is dependent on particle shape and density.

The density of polystyrene has been quoted at $1{\cdot}06 \times 10^3 Kg.m^{-3}$ (BLACK and WALSH, 1970). However, the possibility of the inclusion of some gas or vapour at the moment of particle formation should not be excluded. Particle density was therefore checked directly.

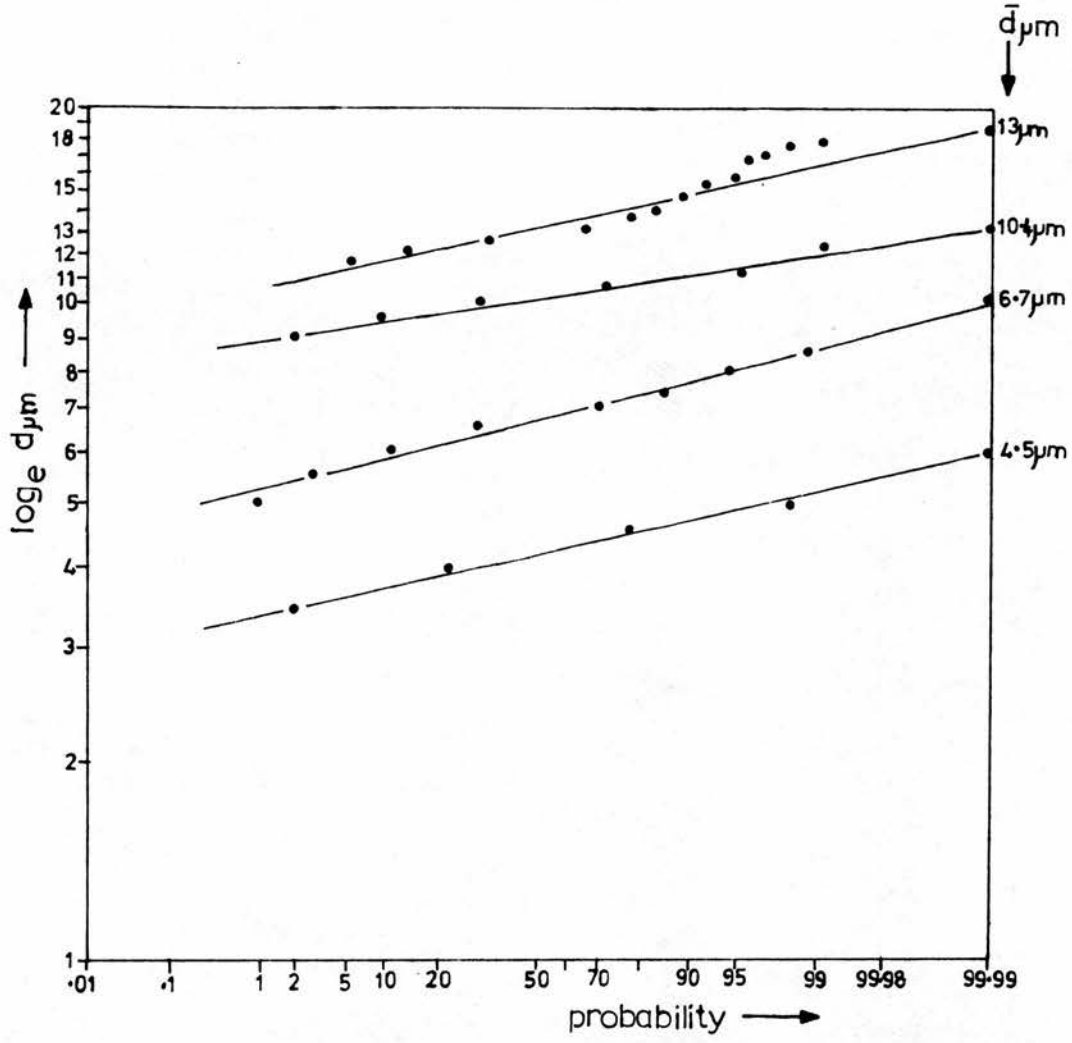

Figure 3.1.5: Particle size distributions; $\log_e$ particle diameter (μm) vs probability.

Polystyrene particles of approximately 10 μm count-mean diameter, which have conveniently short settling times in liquids, were placed in a temperature stabilised ethanol (ρ= 0·789 x 10^3Kg.m^{-3} at 20°c)* based solution whose density could be modified by the addition of known volumes of glycerol triacetate (ρ= 1·156 x 10^3Kg.m^{-3} at 20°c)*. At a solution density of 1·06 x 10^3Kg.m^{-3} and temperature of 20°c, particle buoyancy resulted in slight upwards movement of the particles after several hours. Gravitational settling could just be observed after twenty-four hours at a solution density of 1·03 x 10^3Kg.m^{-3} and steady temperature of 20°c. According to Archimedes' principle, the upthrust on a particle is equal to the weight of an equivalent volume of fluid which is just supported at rest. When the particle is also just supported at rest, in relation to the fluid, the densities of the fluid and particle are equal. It was therefore concluded that at this particle diameter the polystyrene density lay in a range (1·03 - 1·06) x 10^3Kg.m^{-3} at a temperature of 20°c. Particles of 1·5 μm diameter were also checked, using the same procedure, and were found to have densities in the same range.

Figure 3.1.6 shows an electron micrograph of a typical particle sample. Although the overall shape of the particles is shown to be essentially spherical, they are severly indented. Many are 'apple-shaped', having large single indentations. Particles produced from the unlabelled polymer also tended to be 'apple-shaped' but were less severely indented. The possibility was considered that the fluid resistance experienced by such particles would differ from that of spherical particles of identical mass to a degree that

* C.R.C. Handbook of Chemistry and Physics, 1968.

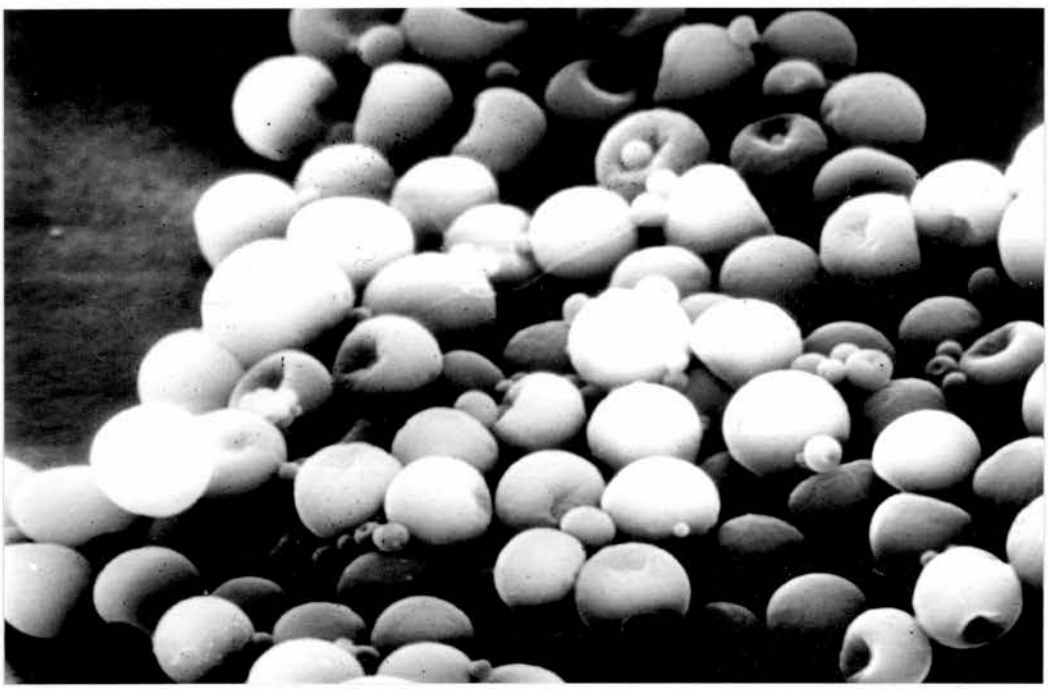

Figure 3.1.6: Electron micrograph of 6·7 μm (dia.) particles showing their non - sphericity.

would significantly influence their falling speeds in air.

The falling speeds of microscopic particles are difficult to measure experimentally and particle shape factors are equally difficult to treat theoretically (ALLEN, 1974). Two experimental approaches were adopted: one based on a macroscopic simulation of the microscopic surface irregularities; the other based on direct measurement of the falling speeds of the microscopic particles in which spherical 'control' particles were used. The purpose of the former approach was to give an indication of whether such surface irregularities were likely to be at all significant; that of the latter was to quantify any such effect as directly as possible, using the actual polystyrene particles.

A plasticine particle of 1·2 cm diameter, having an expanded polystyrene interior for increased buoyancy, was used to determine the effects of three distinct surface characteristics on its falling speed in glycerol (absolute viscosity = 1·45 $Ns.m^{-2}$ @ 20°c)*. The Reynolds' number of the particle in glycerol was below 0·05, which is low enough for Stokes' law to remain valid (see Chapter 1, part 2(i)). The plasticine extension of the particle was moulded into: (i) a sphere; (ii) an 'apple-shape' with smooth exterior; (iii) an 'apple-shape' with severely indented exterior. It was the latter which was considered to most closely approximate to the appearance of the polystyrene particles observed on the electron micrographs. Falling speeds were measured over a distance of 0·205m in a graduated cylinder containing the glycerol, the temperature remaining constant throughout. The respective falling

* C.R.C. Handbook of Chemistry and Physics, 1968.

speeds were: (i)(0·894 $\pm$ 0·018) x 10^{-2} m .sec^{-1}; (ii)(0·805 $\pm$ 0·022) x 10^{-2} m.sec^{-1} ;(iii)(0·695 $\pm$ 0·011) x 10^{-2} m.sec^{-1} , each figure being the mean of eight observations $\pm$ the standard error of the mean. This large ($\sim$22% at the extremes) variation indicated that particle surface irregularities were indeed of some consequence, at least on a macroscopic scale.

To investigate the effects of particle surface irregularity on the microscopic scale an attempt was made to measure the bulk settling rate of particles in olive oil (ρ= 0·918 x 10^{3} $Kg.m^{-3}$@ 15°c, absolute viscosity = 0·084 $Ns.m^{-2}$ @ 20°c)*. The major difficulty of such experiments lies in the near impossibility of eliminating thermal motions in the settling fluid. A further difficulty is the fact that owing to the spread of sizes present, even in samples of good size uniformity (coefficient of variation <10%), the falling edge of the sample in solution, or hydrosol, tends to be more representative of the falling speed of the lower end of the overall particle size distribution than that of the count-mean size. An attempt was made to eliminate these systematic errors by using particles of human serum albumen, which appeared to be smooth and spherical, as controls.

The falling speed of a particle in a fluid may be predicted using Stokes' Law in the form (which takes into account the buoyancy force),

$$V_p = \dot{K}.dp^2.\Delta\rho_p \qquad \text{..... equation 3.1.4}$$

$$V_a = \dot{K}.da^2.\Delta\rho_a \qquad \text{..... equation 3.1.5}$$

* C.R.C. Handbook of Chemistry and Physics, 1968.

where, V_p, V_a = the falling speed of perfectly spherical polystyrene or albumen particles in $m.sec^{-1}$

dp, da = the diameter in metres of the polystyrene or albumen particles.

$\Delta\rho_p$ $\Delta\rho_a$ = the difference in density between the polystyrene or albumen particles and the fluid medium, in $Kg.m^{-3}$, i.e. $\Delta\rho_{p/a} = (\rho_{p/a} - \rho_{fluid})$.

$\dot{K} = \frac{g}{18\eta}$ where g is the acceleration due to gravity in $m.sec^{-2}$ and η is the fluid viscosity in $Ns.m^{-2}$

For particles having surface irregularities falling in a fluid subject to thermally induced fluid motions, the distance of fall of the falling edge of perfectly monodisperse hydrosols of polystyrene or albumen particles may be written as

$$Dp = \dot{K}.dp^2.\Delta\rho_p.t.Sp - \dot{K}' \quad \text{..... equation 3.1.6}$$

$$Da = \dot{K}.da^2.\Delta\rho_a.t.Sa - \dot{K}' \quad \text{..... equation 3.1.7}$$

where, Dp, Da = observed distance of fall of falling edge of the polystyrene or albumen hydrosol in metres

Sp, Sa = the dimension-less drag coefficients which equal unity for a perfect sphere and are less than unity (when the drag is increased) for an imperfect sphere

$\dot{K}'$ = the distance of thermally induced upwards shift in the falling edge of the polystyrene or albumen hydrosol, in metres.

t = period of settlement in seconds.

When $Dp \simeq Da$, over the same period of settlement t,

$$\frac{dp^2 . \Delta\rho_p . Sp}{da^2 . \Delta\rho_a . Sa} \simeq 1 \qquad \text{..... equation 3.1.8}$$

In practice, perfect hydrosol monodispersity is unobtainable. It was therefore necessary to measure the count-mean diameter not of the whole sample, but of those particles which lay at the falling edge of the hydrosol in the fluid medium, dpe and dae, for polystyrene and albumen particles, respectively.

for, $Dp \simeq Da$, and, $Sa = 1$

$$\therefore Sp \simeq \frac{dae^2 . \Delta\rho_a}{dpe^2 . \Delta\rho_p} \qquad \text{..... equation 3.1.9}$$

It is not claimed that experimental error was eliminated using this technique. There would undoubtedly be errors in the estimation of the location of the falling edge of the hydrosol in both cases. However, because the two samples were placed in almost identical geometrical and temperature enviroments the systematic error would tend to be of similar magnitude for each. The purpose of conducting the experiment was to provide what was considered to be a reasonable quantitative indication of the magnitude of the effect on a

microscopic scale.

Using equation 3.1.9 to determine values of Sp eliminated the need for absolute viscosity measurements. Variations in viscosity due to temperature changes did not therefore affect the result.

Polystyrene and albumen particles of various sizes were tried until an approximate match in their falling speeds in olive oil was achieved. The count-mean diameters for the polystyrene and albumen samples were $\bar{d}p = 13{\cdot}1\ \mu m$, (coefficient of variation = 8·9%) and $\bar{d}a = 8{\cdot}6\ \mu m$ (coefficient of variation = 5·2%). The count mean diameters of the polystyrene and albumen particles sampled by means of a syringe at the falling edges of their respective hydrosols after one day of free settling, were, $\bar{d}pe = 12{\cdot}6 \pm {\cdot}002\ \mu m$ (5 observations $\pm$ standard error of the mean), and $\bar{d}ae = 8{\cdot}2 \pm 0{\cdot}008\ \mu m$ (5 observations $\pm$ standard error of the mean).

The hydrosols were left to settle out over a period of about one day, when movement in the falling edges was usually about 8 mm. Both samples were placed in 5 mm bore glass tubing, sealed at one end, and marked with an external scale. The tubes were placed adjacently in a beaker of water in order to ensure their temperatures would be nearly equal at all times. Five separate runs were performed. No aggregation was observed in either sample removed from the falling edges of the hydrosols.

For final determination of Sp, it was necessary to measure the density of the albumen particles, ρa. This was accomplished using a procedure similar to that described above for polystyrene particles, except solutions of acetone and carbon tetrachloride were employed.

It was found that ρ_a lay in the range $1{\cdot}26 - 1{\cdot}27 \times 10^3 Kg.m^{-3}$ and and the mean figure of this range was used in equation 3.1.9 to determine Sp. The result was Sp = $0{\cdot}77 \pm 0{\cdot}02$ (mean of 5 observations $\pm$ standard error of the mean), indicating that particle shape factors were of comparable importance for both the microscopic and macroscopic particles. The aerodynamic diameter of the particles could not therefore be taken as equal to their count-mean diameter. The implications of this result for purposes of comparing the aerosol deposition and clearance data of different research groups are discussed in Chapter 5, part 1 (iii).

3.1 (iii)(b) In vitro leaching

The degree of radioactive leaching from the particles was measured initially in vitro. Particles of $4{\cdot}5\ \mu m$ diameter were produced using the methods described above, including the centrifuging stage. One volume was left to stand for about one day in ethanol solution alone, at ambient temperature ($\sim 20^\circ c$), the other was dried of ethanol and placed in distilled water alone at a temperature of $37^\circ c$, also for about one day.

At the end of the leaching period both solutions were centrifuged and the bulk of clear liquid was removed from each sample for radioassay. Two measurements were performed in each case. The degree of leaching in distilled water was measured to be within 0·03% of the initial activity in the water sample ($\sim 55{\cdot}5$ MBq or $\sim 1{\cdot}5$ mCi), after allowing for isotope decay. For ethanol, the degree of leaching was considerably higher, at 2·6% of the initial activity. For this reason the period for which the particles were stored in

ethanol prior to an experiment was always kept to a minimum (~20 minutes). The possibility of an *in vivo* leaching of the particles is discussed in part 3 (ii) of the present chapter.

3.2 Measurement of total deposition and control of the physiological conditions of aerosol administration

In part (i) below, the origin and purpose of the methods that were devised to measure total deposition are described, and the methods employed to ensure a rigorous control of the physiological conditions of aerosol administration are described in part (ii). The accuracy of a total deposition experiment depends on a multitude of factors. In the methodology of the present work detailed attention has been given to all factors which were considered to exert a possible influence on particle deposition, but since this makes for a rather lengthy description the following introductory paragraphs may serve as a helpful preparatory summary. A briefer description has also been published separately (EMMETT et al, 1979) and is included as an appendix to the present work.

Three major experimental difficulties in measuring total deposition may be identified: (1) measurement of the inhaled aerosol; (2) how to ensure that inhaled and exhaled volumes are very nearly equal in each breath; (3) sampling or collection of the exhaled aerosol.

In order to sample accurately the inhaled aerosol a simple mechanical servomechanism was devised, which consisted essentially of two spirometers in mutual balance operating in conjunction with a precision flow divider (Figure 3.2.1 (iv)). For use in the measurement of total deposition during the steady breathing of an aerosol, it was necessary to incorporate a number of re-setting mechanisms in the apparatus.

The importance of ensuring that inhaled and exhaled volumes are nearly equal in each breath during a total deposition experiment is hard to over-emphasize, yet it is an aspect of such work that has received only scant attention in the literature. In the present work a system of volume limits has been employed to ensure volume equality. The method, although rather complicated, has the added advantage that movement of the main respiratory valve, employed for the separation and subsequent collection of the exhaled aerosol, may be accomplished during the delay introduced by the subject when changing from an inspiration to an expiration, or vice versa. This ensures the efficient collection of the early part of the exhaled aerosol, without which the total deposition might be significantly overestimated. Figure 3.2.4 illustrates the overall operation of the apparatus, in a serialized format.

3.2(i) Total deposition

Total deposition is here defined as

$$f_D(I) = \frac{D}{I} \qquad \text{..... equation 3.2.1}$$

where, $f_D(I)$ is the total respiratory tract deposition, D, expressed as a fraction of the amount of aerosol inhaled by a subject, I, over one or more whole breaths

alternatively $f_D(I)$ may be expressed as

$$f_D(I) = \left[1 - \frac{I}{E}\right] \qquad \text{..... equation 3.2.2}$$

where, E = the amount of aerosol exhaled by a subject over one or more whole breaths

In this context, a whole breath is defined as an inspiration to a volume, V_T litres (37°c, and 100% relative humidity), followed by expiration of the same volume, where V_T is termed the tidal volume of the subject. If inspired and expired volumes are not equal, or nearly equal, in every breath, it is not possible to measure, or closely estimate, $f_D(I)$, by this definition.

The amounts I, D, E, may be expressed in terms of mass, surface area, number, or radioactivity, of an aerosol. For a monodisperse aerosol (coefficient of variation <10%) it is assumed that the values of $f_D(I)$ calculated on each such basis are nearly equal (see section 1 of the present chapter). The distinction between the simple definition of $f_D(I)$ in equations 3.2.1, 3.2.2, and the more complicated steady-state definition of total deposition was discussed in Chapter 1. The difference is not important at that particle size above which no aerosol can be recovered in the expired tidal air of the breath which follows that in which the aerosol was first inhaled. Owing to the small percentage of tidal air known to be involved in the breath-to-breath tidal and reserve air mixing process (HEYDER and DAVIES, 1971), and the relatively high ($\sim$0·7) values of $f_D(I)$ measured in the present work at the smallest particle diameter employed, 4·5 μm, it is unlikely that steady-state influences are of any significance at or above this size.

Accurate measurement of fD(I) requires accurate measurement of I and E. Some of the experimental difficulties likely to be encountered when attempting to measure total deposition were described in Chapter 2. Large particle sizes are particularly difficult to study owing to their greater tendency to deposit by gravitational settling or inertial impaction in the aerosol administration apparatus. Referring to Figure 3.2.1 and considering firstly the problem of estimating the amount of aerosol inhaled by a subject, it may be evident that the sampling configuration illustrated in (i) has certain merits. The sampled aerosol is obtained close to the point of entry into the subject and is therefore likely to be representative. Moreover, if the instantaneous sampling flow rate, fs, could be made at all times equal to the instantaneous inspiratory flow rate, fi, then owing to its inherent symmetry nearly equal aerosol losses would occur in both arms of the Y-piece and the amount of aerosol drawn through the sampling port would be nearly equal to that inspired by the subject.

LANDAHL and his co-workers (1947, 1948, 1950, 1951, 1952) were the first investigators to employ a Y-piece sampling configuration in human aerosol inhalation experiments and, as far as can be ascertained from the literature, were the only ones to have done so. However, in their experiments the onus was always on the subject to maintain an inspiratory flow that was at all times equal to a constant sampling flow. Moreover, the necessity imposed on the subject of having to move to a separate port in order to exhale made this task especially difficult (LANDAHL and HERRMANN, 1948).

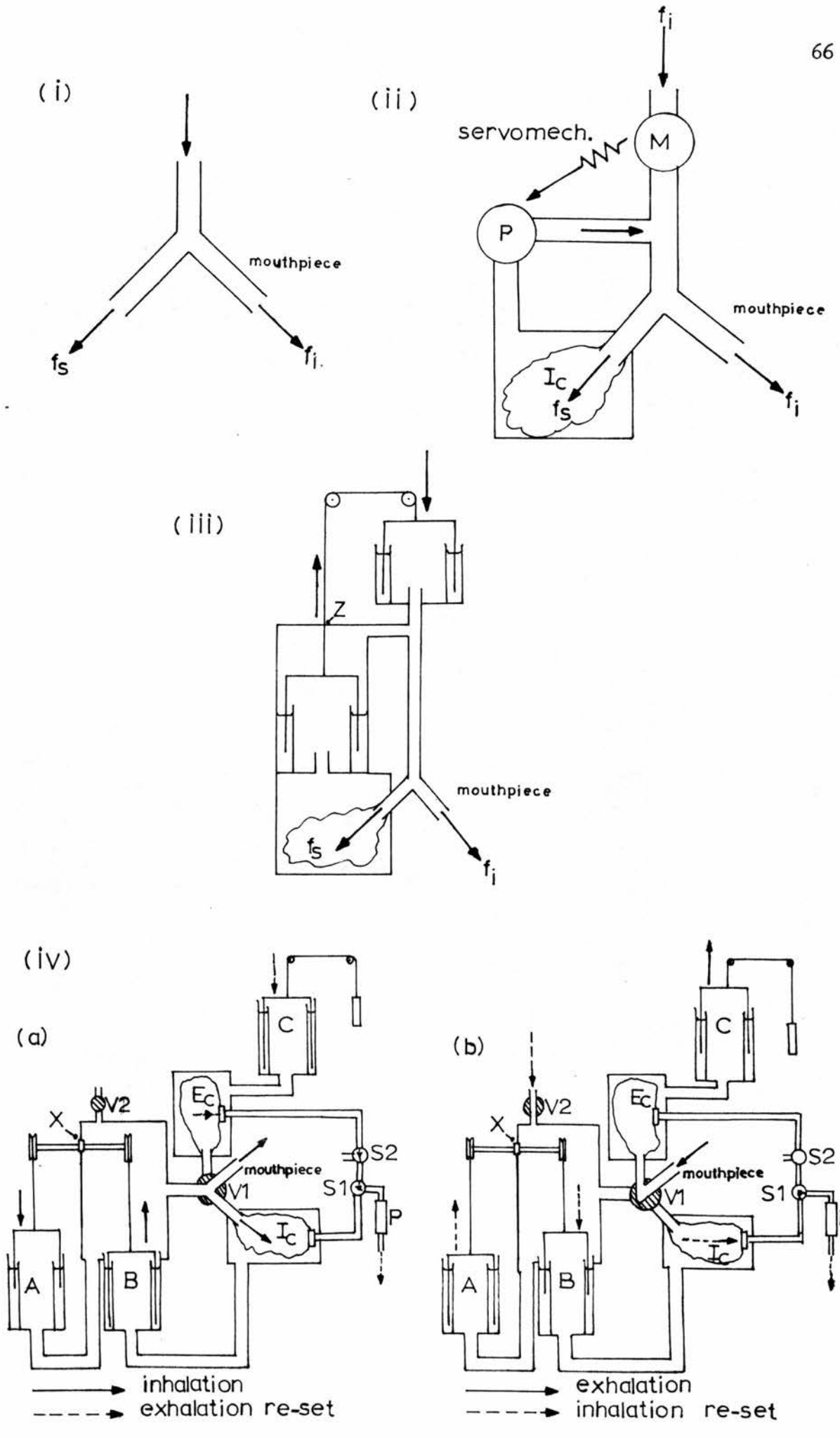

Figure 3.2.1: Aerosol sampling configurations.

An improved approach might be to derive a sampling flow that was somehow made to 'slave' to the inspiratory flow, which was allowed to vary.

Figure 3.2.1 (ii) illustrates how this might be achieved in principle, for radioactive particles. An airflow meter, M, measures total flow into the system which is at all times equal to the total outflow derived by the subject. By some undefined servo-mechanism, the pump, P, derives an equal flow at the sampling port and returns this back into the system in order not to affect the relationship between total inflows and outflows. During this process the radioactive particles are drawn into a collection bag, Ic, for later radioassay. Servomechanisms based on pneumotachographic or other similar measurements of inspired flow were rejected on the grounds that this might seriously diminish the amount of aerosol able to reach the subject, particularly at large particle sizes. Spirometers provide a simple and trouble-free means of measuring gas-flow (MERCER, 1973). By using a pair of nearly identical spirometers in the configuration illustrated in Figure 3.2.1 (iii), these sampling principles are brought closer to practical realization. Several difficulties remain however. Besides the difficulty of sealing at 'Z', on the figure, after a number of inspirations the sampling bag would expand to the limits of its capacity and, similarly, the spirometers would eventually reach the limits of their movement. Also, the exhaled aerosol must somehow be collected. Figure 3.2.1 (iv) illustrates the final design, at least as regards aerosol sampling. In this apparatus movement between the spirometers

was transmitted via pulley wheels attached to a freely rotatable shaft, which could be easily sealed at 'X' on the figure. The expansion of the collection bag, Ic, during an inspiration, was compensated for by an equal volume of contraction during an expiration, by means of pump, P, acting via a filter and solenoid valves, S1 and S2. Rather than separately correct for the inspiratory movement of the spirometers (A and B in the figure), the contraction of the collection bag, Ic, during an expiration, was used to achieve this in a single action. Thin walled neoprene-rubber collection bags were used in order to ensure that attenuation of radiation during radioassay would be neglibly small (see section 3, part (ii)e of the present chapter).

The mode of action was as follows: at the end of an inspiration the valves, V1 and V2, moved to the positions shown in Figure 3.2.1(iv)b. The subject was then free to expire via the expiratory port of V1 into an expiratory collection bag, Ec. Expired volumes were measured by spirometer C, as shown in the figure. The solenoid valves, S1 and S2, re-directed the suction flow of pump P, at the beginning of an expiration (to be distinguished from the end of an inspiration), which resulted in a contraction of the expiratory collection bag, Ec. On commencement of this contraction, the pressure within spirometer B fell below that of atmospheric and its downwards movement was induced. This movement was facilitated by the opening of valve V2, which permitted a compensatory inflow of air into the apparatus. The downwards movement of spirometer B, during expiration, was accompanied by an equal and opposite movement of spirometer A. Contrary to the

situation which existed during an inspiration, spirometer B then led the movement of the spirometer pair and the apparatus was, essentially, in reverse operation.

It was also necessary to re-set the position of spirometer C, following an expiration. This was achieved in a manner similar to that described above for spirometers A and B, except that the process operated only during an inspiration. In this case, valves V1 and V2, moved into the position shown in Figure 3.2.1 (iv)a, at the end of an expiration. Both the inspiratory and expiratory re-setting processes could be halted at a predetermined point by means of the proximity switches, R1 and RE, respectively, illustrated in (ii), Figure 3.2.2. These were magnetically actuated open/close switches (Radiospares Components Ltd.) and the actuating magnet was radially mounted on the spirometer pulleys. The radial arms of the pulleys were slightly weighted in order to counterbalance variations in spirometer flotation weight.

Millipore filters (see part 1 (ii) of the present chapter) were used to collect the radioactive particles within the collection bags during the re-setting processes. Millipore filter holders (Millipore Filter Corporation) incorporating an 'o' ring for effective sealing were also used. A direct check for possible particle penetration was made by placing a filter of a nominal pore diameter (3 μm) equal to that of the collection bag filters in-line with that of the suction feed tube of the expiratory collection bag. An aerosol containing both primary particles ($\sim$6·5 μm diameter) and satellites ($\sim$30% by mass, $\sim$2·6 μm diameter) was sprayed into the main chamber

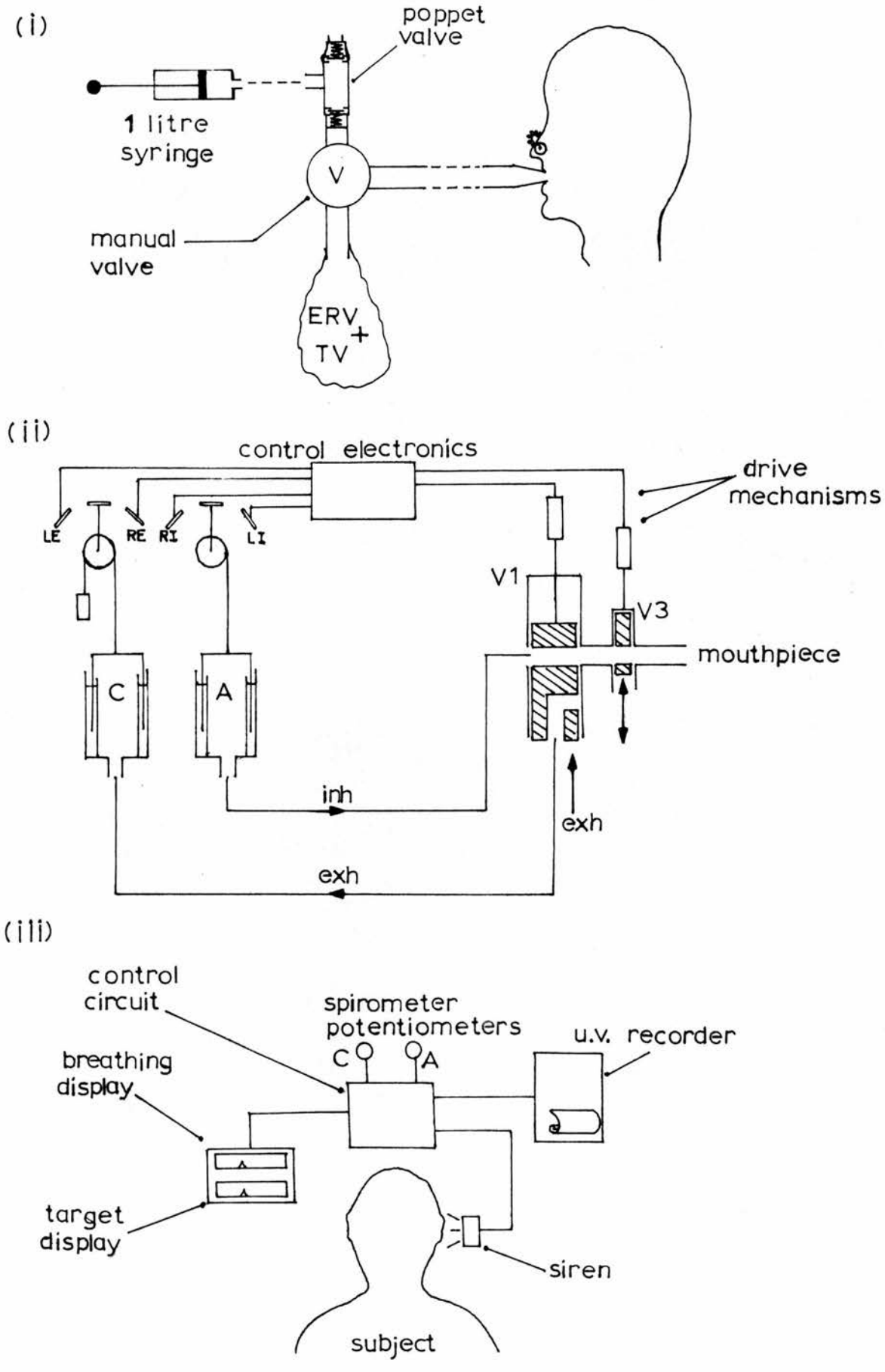

Figure 3.2.2: Breathing control.

of the apparatus and a period of simulated breathing was undertaken (by a method described in part 2(iii)b of the present chapter). The radioactivity measured on the in-line filter (<1·85 KBq or <50 nCi) was 0·13% of that measured on the main collection filter (<1·48 MBq or <40 μCi) indicating a collection efficiency of nearly 100%.

3.2(ii) Breathing control and valve actuation

The apparatus described above does not represent the final system. Neither the mechanism of valve actuation at the end of an inspiration or expiration, nor the method used to control the breathing pattern of the subject during aerosol administration, have yet been described.

3.2(ii)a Breathing Control

The possible influences of breathing pattern on the deposition probability of inhaled particles were discussed in Chapter 1. A symmetrical 'clipped sawtooth' breathing pattern was adopted and aerosol administration was initiated at the subject's functional residual capacity, which had been measured previously (Figure 3.2.3). It should be appreciated that when a subject breathes via an apparatus respiration may become more conscious than it would be normally and some form of artificial control might in any case be required. The reason for adopting a fixed tidal volume and breathing rate was to standardize the residence time of particles in the respiratory tract between different breaths. Specific gas-flow rates and the average particle residence times in different airways must also be considered. In common with the work of HEYDER et al, (1973) and DAVIES et al, (1972), the instantaneous gas-flow was made equal to the mean gas-flow over times $\bar{t}i$ and $\bar{t}e$, (Figure 3.2.3), where

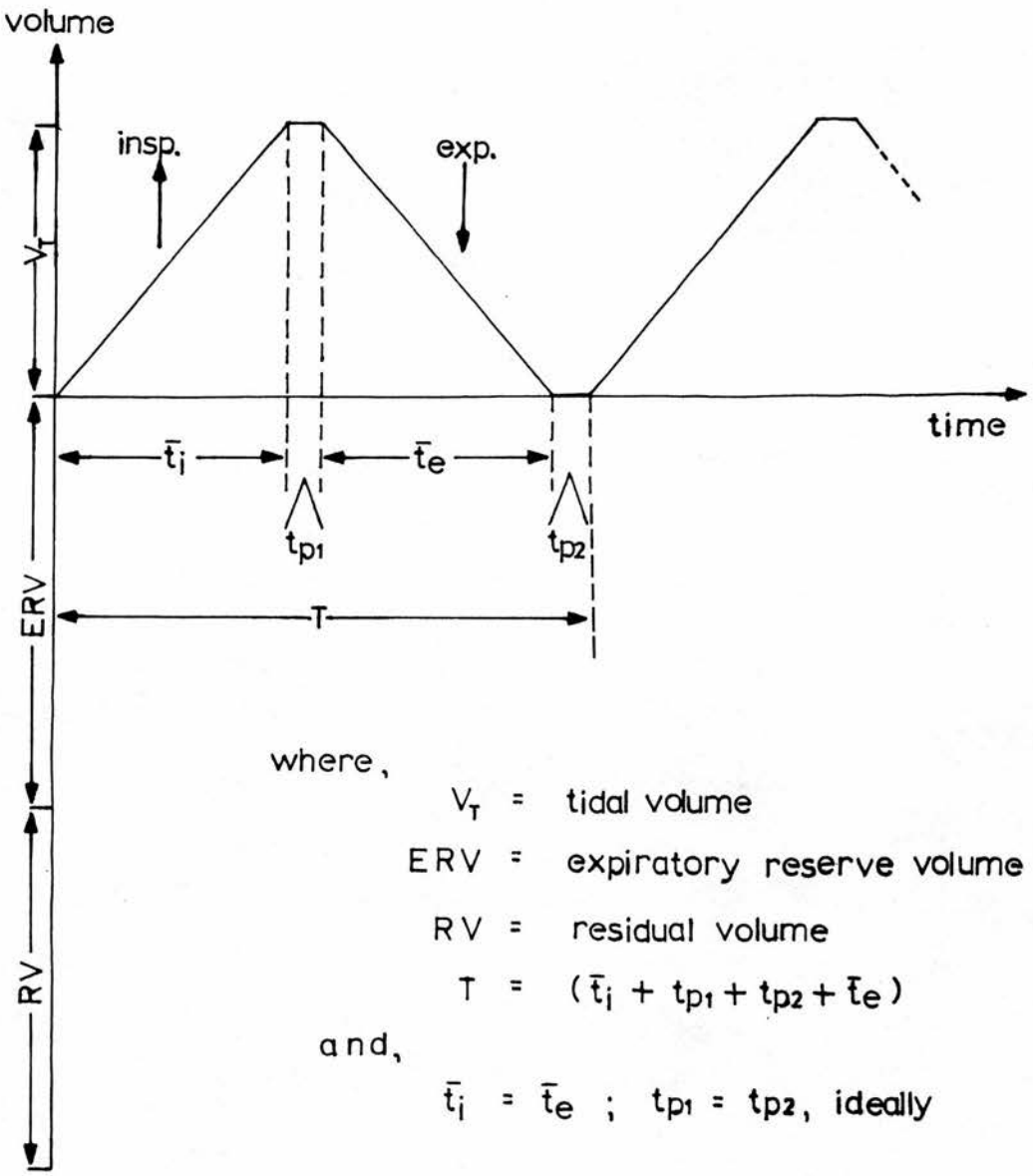

Figure 3.2.3: Standard breathing pattern.

$\bar{t}i = \bar{t}e$, ideally. This greatly simplifies the problem of standardization between different research groups. Aerosol administration was initiated at the functional residual capacity of the subject because this most closely represented the lung volume during normal breathing at rest, or quiet breathing. It may also be the lung volume at which the total deposition between different subjects can be equalized, at least at small particle sizes (HEYDER et al, 1975). The complicated considerations involved in this problem were mentioned in Chapter 1.

The problem of breathing control is particularly acute in experiments involving the inhalation of radioactive particles. Once these have been administered to the subject there can be no opportunity for a second attempt, if at all, until the radioactivity has almost entirely decayed. It is therefore essential to adopt a procedure that is simple and effective in use, even for previously untrained subjects.

The apparatus shown in Figure 3.2.2(i) was used to set lung volumes prior to aerosol administration. The subject first completed a maximal expiration and then inspired a fixed volume of air, equal to expiratory reserve volume plus tidal volume, from a rubber bag. Wearing a noseclip throughout the procedure, the subject then transferred to the mouthpiece of the main apparatus and preceded aerosol inhalation proper with an expiration. The procedure was practiced several times before an experiment to ensure that no gas would be inspired or expired during transferal.

Control of the two main respiratory parameters, tidal volume

and breathing rate, presents a more severe practical problem. As was discussed above, it is particularly important to ensure that inspired and expired volumes are equal in any breath. Yet it has been stated by both DAVIES et al, (1972) and HEYDER et al (1973), that even experienced subjects cannot cannot ensure that this is achieved. If the expired volume is less than that inspired in any breath, then the volume difference may be erroneously measured to have been wholly or partly deposited. Part of the problem of breathing control may be that the subject is often required to attempt simultaneous control and co-ordination of different variables. An improved approach might be to place one of these variables under automatic control, thus allowing the subject to concentrate more on the control of the remaining variable. The obvious candidate for automatic control is tidal volume, since this can be controlled by means of volume limits, whereas automatic flow rate control might necessitate some means of artificial respiration.

Automatic tidal volume control was achieved by means of magnetically actuated volume limit switches operating in conjunction with a mouthpiece blocking-valve, V3 (Figure 3.2.2(ii)). Although this same expedient is closely related to the more complicated problem of respiratory valve actuation, for the sake of clarity, its role in breathing control will first be considered separately.

Referring to Figure 3.2.2(ii), A and C were the spirometers used for the detection of inspired and expired volumes, respectively (nomenclature as in Figure 3.2.1(iv)). Spirometer C was

thermostatically maintained at a temperature of 37°c. LI and LE, were proximity limit switches (crossover type, Radiospares Components Ltd.), whose position was adjusted relative to Rl and RE, (the resetting process limit switches mentioned in 3.2(i)), to obtain the desired tidal volume, defined at 37°c and 100% relative humidity. Inspired and expired volumes were equalized by appropiate adjustment of LI, allowing for gas expansion in the lungs, assumed to be at 37°c and 100% relative humidity, from ambient temperature and humidity. The temperature of the air in the aerosol administration apparatus was measured prior to an experiment by means of a mercury-in-glass thermometer, which was permenently housed within it. The inspired air was always very nearly saturated with water vapour owing to the presence of a water-filled spirometer in the apparatus. Although a small amount of ethanol vapour was also present its partial pressure contribution was negligible. A slight lowering of temperature ($<2^{\circ}c$) occurred because of ethanol evaporation: this needed about 250 Joules of latent heat of vapourisation, compared to the 120 or more Joules of heat required to change the temperature of air within the spraying chamber by 1°c. Correction factors were calculated using the ideal gas equation in the form,

$$Vi = \left[\frac{273 + ti}{273 + te} \cdot \frac{760 - Pe}{760 - Pi}\right] \cdot Ve \quad \text{..... equation 3.2.3}$$

where, ti = temperature of inspired air in degrees centigrade

te = temperature of expired air = 37°c (after warming)

Pe = saturation vapour pressure of water at te°c in mmHg

Pi = saturation vapour pressure of water at ti°c in mmHg

Vi = volume of inspired air at ti°c and 100% RH

Ve volume of expired 'air' at te°c and 100% RH

The expired air was assumed to be at 37°c and 100% relative humidity because of uncertainty in the amount of cooling and condensation that might occur before its exit from the mouth (WALKER et al, 1961). This assumption was of no consequence because of subsequent re-heating and re-saturation of the expired gas in the wetted expiratory collection bag (Figure 3.2.8(i)), which was almost instantaneous (less than 6·8 joules of heat are needed to raise the temperature of 1 litre of air by 5°c). It was possible to check the equality of inspired and expired volumes using a simple bag-in-a-box breathing simulator (see part 2(iii)b of the present chapter). In the resting subject the volume of inspired air, temperature and humidity notwithstanding, exceeds that of the expired gas by less than 1% in any breath, owing to unequal exchange of carbon dioxide and oxygen in the lungs (COMROE et al, 1955). Over ten breaths this could amount to about 10% of the tidal volume or about 100 ml at a tidal volume of 1·0 litre. As this figure was small in comparison with a typical functional residual capacity of about 2 litres, the effect was ignored. It should be appreciated that this volume error is distinct from the error

which results from the misdirection of the early portion of expired gas (see above). Its significance lies not with the calculation of total deposition as such, but with the control of the lung volume of the subject during aerosol administration. It should also be borne in mind that in the absence of automatic volume control a drift of at least this order is to be expected from breath to breath; this would not only result in a change in lung volume throughout aerosol administration, but also cause an error in the measurement of total deposition.

Referring again to Figure 3.2.2(ii), and considering only at this stage the role of the respiratory control valve, V3, and its positions at various stages in one breathing cycle; V3 was a rapid-action blocking valve which prevented air-flow through the mouthpiece by closing at the end of an inspiration or expiration, determined when the magnet actuators on the spirometer pulley arms reached the limit switches, LI or LE, respectively. At the instant that V3 closed, the subject received a signal to change from expiration to inspiration, or vice versa. Referring to Figure 3.2.2(iii), this signal was applied by a miniature siren situated close to the subject's right ear which sounded for as long as the subject took to respond. Its purpose was to minimize the duration of breath-holding. The mean figure for the latter, for all subjects was 0·38 sec. (σ= 0·14 sec., 20 observations).

The respiratory flow control system is shown in Figure 3.2.2(iii). This incorporated a pair of miniature edge-level indicators, one of which, termed the target display, was connected to a sawtooth

wave generator of adjustable wave frequency and amplitude. It could therefore be used for a variety of tidal volumes and flow-rates. Mounted directly above this was an identical indicator, termed the breathing display, whose indicator followed the movements of the inspiratory and expiratory spirometers, A and C, in each half cycle, adjustable for scale. The subject had therefore to match the movement of the two indicators. This proved to be more effective than a metronome in controlling breathing rates. For those subjects in the main study of particle size at constant respiratory pattern (target breathing rate = 10 breaths minute^{-1}, tidal volume = 1·0 litre) the mean figure was 10·03 breaths minute (13 observations, σ = 0·26 breaths min.$^{-1}$). The method was less successful in controlling the relative durations of an inspiration ($\bar{t}i$) and an expiration ($\bar{t}e$) within a single breath. Most subjects consistently inspired more rapidly than they expired, the mean figure being $\bar{t}e$ = 1·28 $\bar{t}i$ (20 observations, σ = 0·4). In some individuals this tendency was particularly pronounced (see Tables 5.1.2 and 5.1.4).

The breathing patterns of each subject were recorded by means of a U.V. light-sensitive paper recorder (S.E. Electronics Ltd.). Only the excursions of the inspiratory spirometer were recorded as this was all that was necessary to derive the times, $\bar{t}i$, tp_1 , and T, from which $\bar{t}e$ could be estimated by assuming $tp_1 = tp_2$ (Figure 3.2.3).

3.2(ii)b Valve actuation

Actuation of the respiratory valve(s) used to separate inhaled and exhaled aerosol flows is one of the most difficult experimental

problems in human aerosol inhalation research (WALSH et al. 1977). Its importance lies mainly in the danger of misdirecting a portion of the exhaled aerosol through the inspiratory port of the apparatus. The concentration of the exhaled aerosol falls rapidly from the beginning of an expiration (MUIR, 1967) and if at this time a small volume of the expired flow were to be misdirected, an error in the estimation of the exhaled aerosol would result, the magnitude of which might be far greater than the actual fraction of the misdirected expired volume would suggest, particularly at large particle sizes.

A number of approaches to the problem of valve actuation have been adopted by other investigators. ALTSHULER et al. (1957) used manually operated valves to separate inspired and expired aerosol flows, with the accompanying danger of subject error and excessive breath-holding. DENNIS (1950, 1971) introduced a valve sensitive to pressure changes at the mouthpiece, but the delay between the application of pressure signal and completion of valve movement was high (~200 milliseconds). A much improved pressure-sensitive valve has recently been developed which uses sensitive pressure sensors and rapid-action solenoid actuators (WALSH et al. 1977). The authors state that the time delay between generation of a signal at the mouthpiece and completion of valve movement was reduced to about 40 milliseconds, which resulted in a measurable volume of misdirected expired gas of less than 5% of tidal volume. This delay is close to that (~50 milliseconds), measured for a compressed-air driven valve, V3 (Figure 3.2.2(ii)), constructed

for use in the present work, which was found to be the best that could be achieved. One of the main objectives of the present work was to measure total deposition at the largest particle sizes able to penetrate below the larynx. At such particle diameters, which turned out to be greater than roughly 13 μm (see Chapter 5), the error due to the misdirection of exhaled aerosol is likely to be far greater than that which obtains when using aerosol particles of about half this diameter (FOORD et al. 1978). Considering the relatively high falling speeds of 13 μm diameter spherical particles of density $10^3 Kg.m^{-3}$ ($V_F \simeq 0{\cdot}54$ cm. sec^{-1} in air), it is possible that the majority of exhaled particles at this size are returned from the trachea, which is almost vertical during aerosol administration, and main bronchi, whose total volume is only about 42 ml (WEIBEL, 1963). This figure is comparable with the expected volume of misdirected expired flow at a tidal volume of one litre. It was therefore considered necessary to adopt a method of valve actuation that would be totally effective in preventing any of the expired flow from being misdirected. For the sake of clarity the method of breathing control was described separately, in part $(ii)_a$ of this section. The overall operation of the apparatus is described below as far as it is relevant to the problem of respiratory valve actuation.

Figure 3.2.4 is an attempt to represent the overall operation of the apparatus, the nomenclature being the same as before. The blocking valve, V3, is again of central importance. Its purpose in this instance, besides that of assisting in the control of the tidal volume of the subject, was to enable the main respiratory

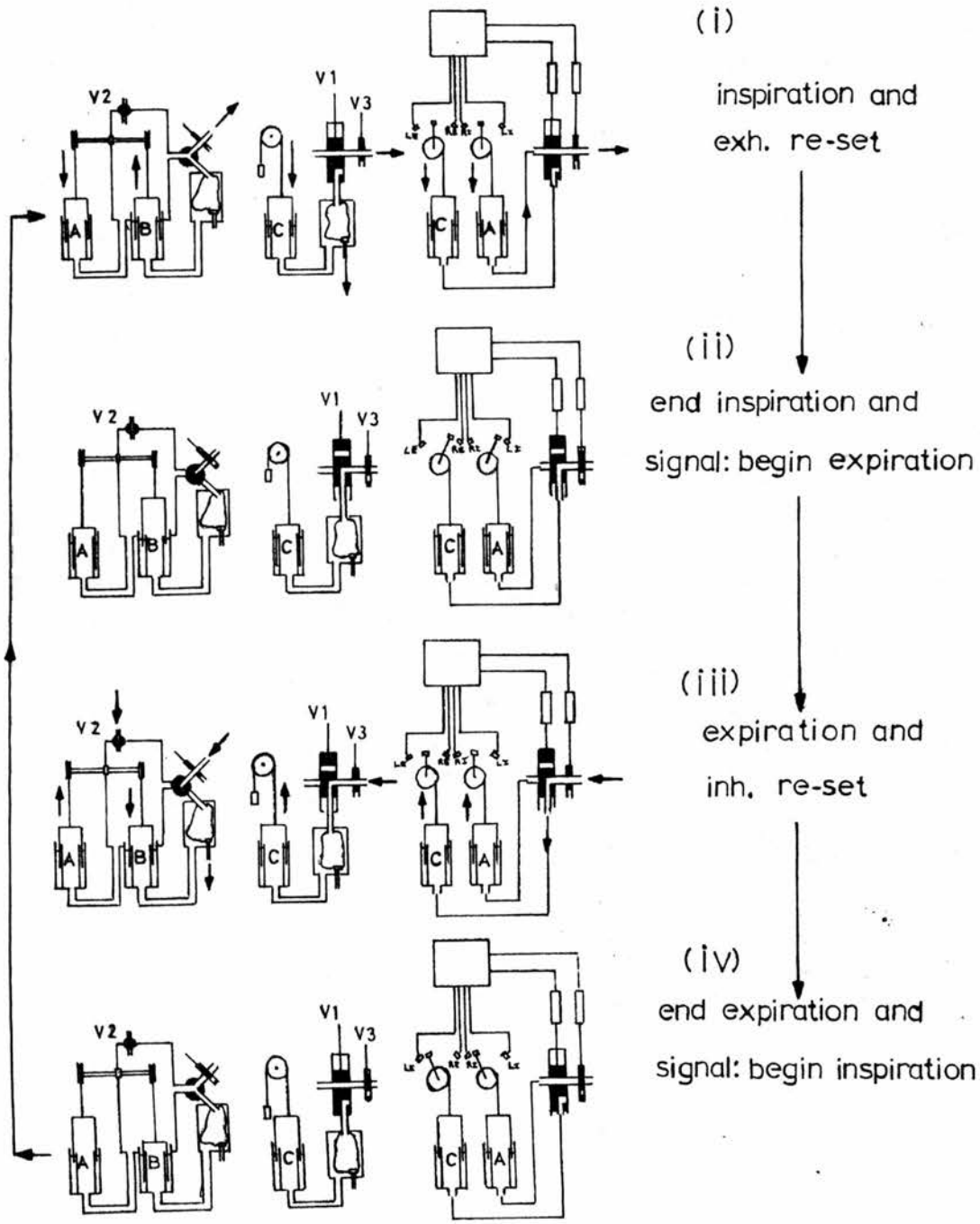

Figure 3.2.4: Overall operation of apparatus.

valve, V1, to change its position when a signal to change from an inspiration to expiration, or vice versa, was indicated to the subject, in anticipation of the subject's response. Since V1 changed position before any changes on the part of the subject, and since after V3 had blocked the mouthpiece it could only be opened again by application of the appropiate pressure signal by the subject, there was no possibility of any misdirection of exhaled aerosol.

It should be noted that while the position of V1 was determined only by the limit switches, LI and LE, V3 was under combined automatic and subject control. Referring as above to Figure 3.2.4, the position of the respiratory valves and spirometers during an inspiration was as shown in (i). During the early period of inspiration the position of the expiratory spirometer, C, was reset in the manner described above. The end of inspiration (ii) occurred when the magnet actuator on the pulley of spirometer A, reached LI. At this point the main respiratory valve, V1, moved into the expiratory position and V3 closed, blocking the mouthpiece. Simultaneously the subject had received a signal to begin an expiration, in the manner described in part 2(ii)a above. At this point, V3 was under subject control and when the subject responded to the applied stimulus by expiring, micromanometer probes detected the resultant pressure change (operational threshold = + 0·2 mm H_2O), which caused V3 to be opened by the electropneumatic control apparatus (Figure 3.2.5). V3 did not open if the subject continued to apply only a negative pressure at the mouthpiece. At the instant that V3 opened, defined as the beginning of

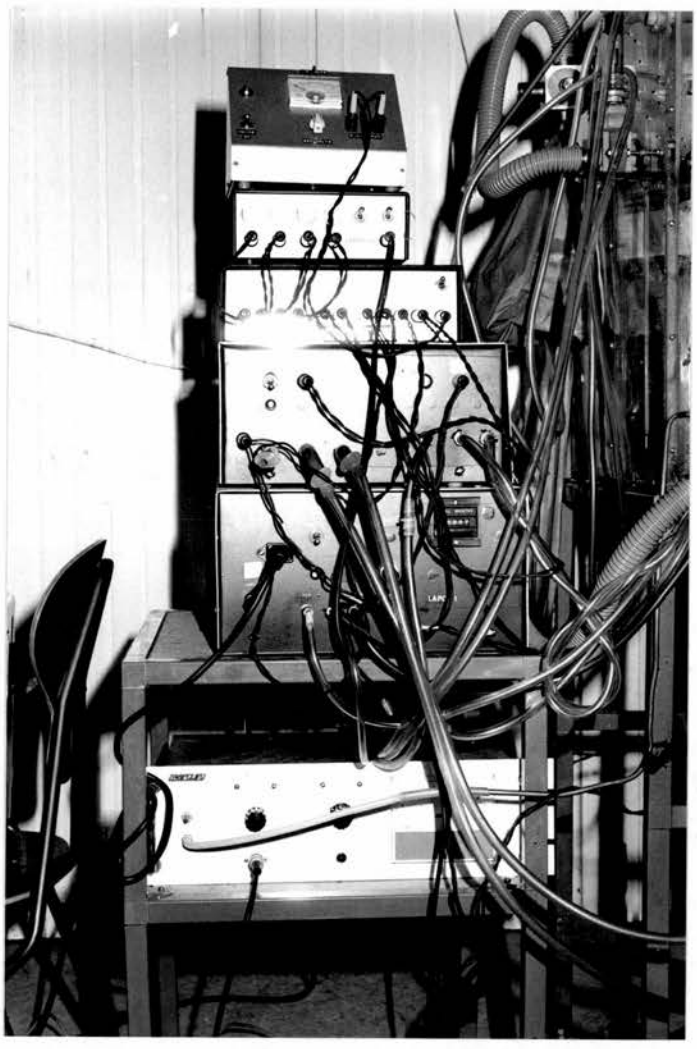

Figure 3.2.5: Photograph of electro-pneumatic control apparatus.

an expiration, the spirometer re-setting process was initiated for spirometers A and B (iii). The end of expiration (iv) occurred when the magnet actuator on the pulley of spirometer C, reached LE. At this point the main respiratory valve, V1, moved into the inspiratory position and V3 closed, blocking the mouthpiece. Simultaneously the subject had received a signal to begin an inspiration. At this point, V3 was once more under subject control and when the subject responded to the applied stimulus by inspiring, micromanometer probes detected the resultant pressure change (operational threshold = $-0{\cdot}2$ mm H_2O) and V3 was opened. V3 did not open if the subject continued to apply only a positive pressure. At the instant that V3 opened, defined as the beginning of an inspiration, the spirometer re-setting process was initiated for spirometer C (i).

As a safety feature it was considered necessary to incorporate some means of preventing a change in the direction of respiratory excursion before the limit switches, LI and LE, had been reached by the magnet actuators; i.e. during modes (i) and (iii), in Figure 3.2.4. To this end, if a small positive pressure change of + $0{\cdot}05$ mm H_2O, in the case of an inspiration, or of - $0{\cdot}05$ mm H_2O, in the case of an expiration, occurred, V3 closed until the correct pressure was re-applied. Inevitably, if such an error was committed by a subject, a small volume of aerosol would be misdirected during the delay (~ 50 milliseconds) between the application of signal and completion of valve movement. In the event, the additional facility was not needed on a single occasion during the study.

The respiratory valves, V1 and V3, and the respiratory flow rate control device, are shown in Figure 3.2.6.

3.2(iii) Treatment of dead space errors and testing of sampling accuracy

(a) Dead space errors

Errors due to dead space losses were important above a particle diameter of about 10 μm and and had therefore to be taken into account (Table 3.2.1). Two types of dead space error were distinguished in the treatment: those due to particle losses in the mouthpiece during expiration; and those due to particles which remained airborne long enough in the dead space to be passed into the inspiratory or expiratory collection bags. The latter quantity was estimated from the known volume of mouthpiece and sampling tube dead space, 25 ml in both cases, and the amount of aerosol known to have penetrated beyond the line b′, shown on Figure 3.2.7(i) (see equation 3.2.6). Aerosol losses in the mouthpiece during expiration were estimated by assuming equal loss efficiencies in both directions of flow; hence the losses in each direction were assumed to depend only on the relative aerosol concentrations and average particle residence times in the mouthpiece during inspiration and expiration. Owing to the smallness of these losses their values could be approximated using equation 3.2.5.

The equation (3.2.2) for the calculation of total deposition, fD(I) becomes,

$$fD(I) = \left(1 - \left[\frac{Ic - Kn + DS' - 1i}{Ec - Kn + 1e}\right]\right) = \left[\frac{Ic - (Ec + DS - DS')}{Ic - Kn + DS' - 1i}\right]$$

..... equation 3.2.4

Figure 3.2.6: Photograph of respiratory control valves and breathing control apparatus.

$\bar{d}\mu m$	$DS' \pm \sigma$% of I	$DS \pm \sigma$% of I
4·5	0·46±·22	0·53±·92
6·7	1·79 ±·46	1·26 ±·88
10·4	5·70 ±·89	4·44 ± 1·41
13	7·00±·93	7·15±·45

Table 3.2.1: Dead space losses in mouthpiece (DS) and sampling tube (DS′) averaged over three subjects at each particle size ($\bar{d}\,\mu m$). (Subjects of variable particle size study only).

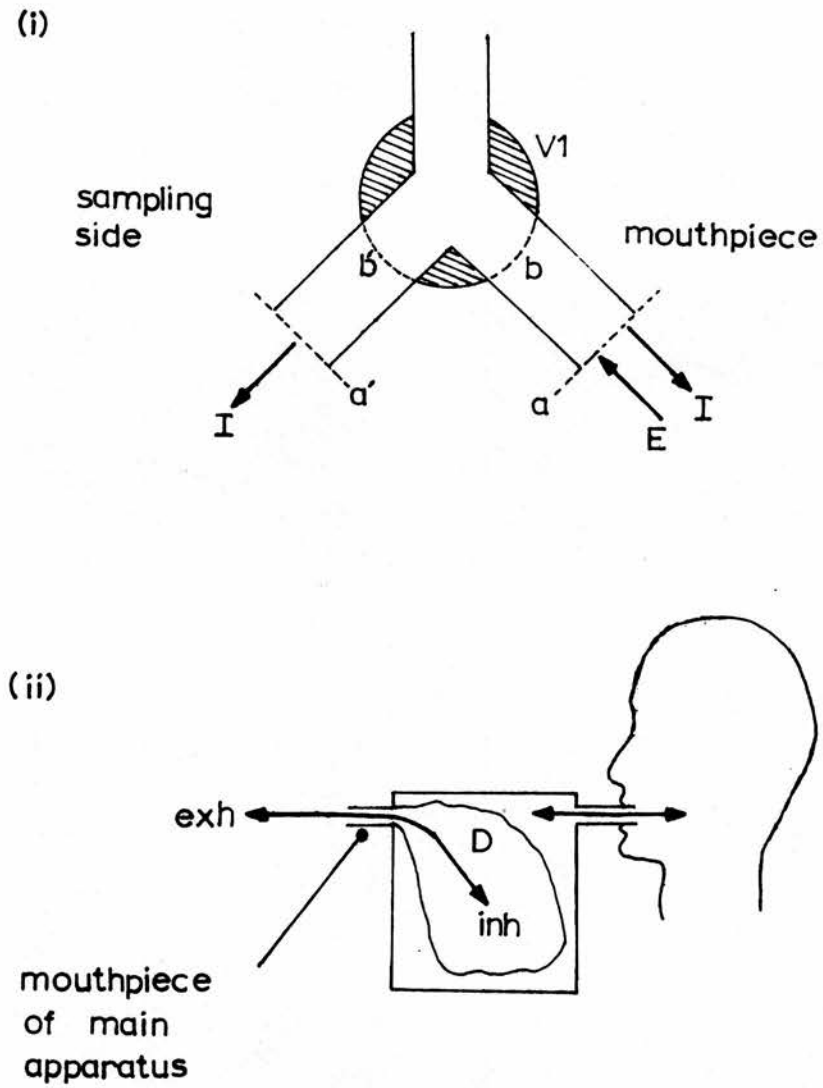

Figure 3.2.7: Dead space and accuracy test.

and, $$li \simeq \left[\frac{Ic}{Ic + Ec}\right] . \left[\frac{ti}{ti + te}\right] DS \quad \text{..... equation 3.2.5}$$

$$Kn \simeq \left[\frac{0{\cdot}025}{V_T}\right] . (Ic + DS') \quad \text{..... equation 3.2.6}$$

where, Ic = amount of aerosol drawn into inspiratory collection bag

Ec = amount of aerosol passed into expiratory collection bag

Kn = average amount of aerosol per breath which occupies the mouthpiece or sampling tube at the end of an inspiration, times the number of breaths, n

li = aerosol losses in the sampling tube or mouthpiece, assumed equal during an inspiration

le = aerosol losses in mouthpiece over allexpirations

DS = total inspiratory and expiratory aerosol losses in the mouthpiece, assumed to equal (li + le)

DS' = total aerosol losses in sampling tube

ti = average duration of inspiration in seconds

te = average duration of expiration in seconds

V_T = tidal volume in litres at 37°c and 100%RH

One type of dead space error was ignored in this treatment. This was the sampling error which arose by virtue of the valve, V3 (which closed shortly before V1) and spirometer B (Figure 3.2.4), occupying

a finite volume. Their combined effect was estimated to lead to an underestimate of less than 0·4% in the amount of aerosol inhaled by the subject.

The amounts of aerosol deposited in the various dead space regions of the apparatus and collection bags were assessed by measuring the relative amounts of radioactivity associated with each. At the end of aerosol administration the mouthpiece, sampling tube, and connecting tubing to the expiratory collection bag, were swapped. The collection bags were removed and folded into geometrically identical containers for radioassay. Attenuation of γ-radiation through the walls of the folded rubber bags was only slight ($<5\%$), using Tc^{99m} (photopeak energy = 140 keV), and in any case about equal in each bag and sample. Radioassay of samples was performed using a whole body monitor, details of which are given in section 3 of the present chapter.

3.2(iii)b Testing of sampling accuracy

Owing to the sensitivity of the aerosol sampling system to minor air leakages the air-tightness of the apparatus was always checked before an experiment by withdrawing a known volume of air from the system and checking this against spirometer deflection, as measured on linear scales fixed parallel to the spirometer-bell attachment strings (Figure 3.2.8(i)). A previously calibrated brass syringe (1·0 litre) was used for this purpose and was always pumped about ten times in order that the cumulative effect of any minor leak would be apparent.

All spirometers were constructed from thin aluminium sheet in order that their mechanical response to pressure changes would be

(i)

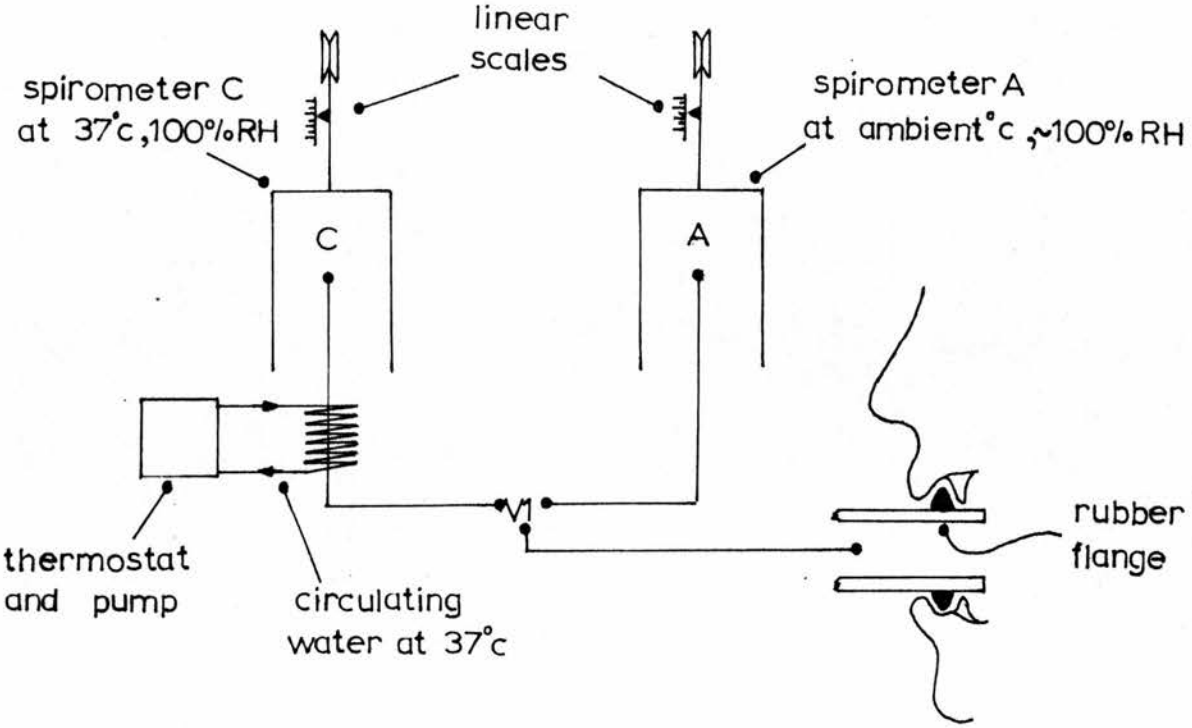

(ii)

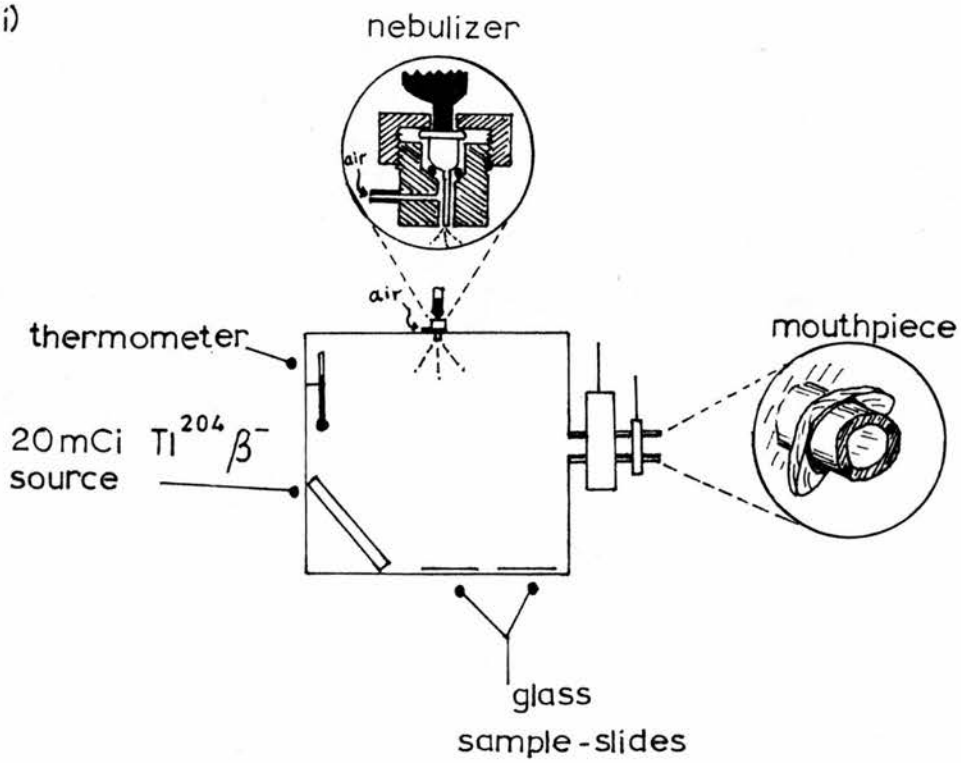

Figure 3.2.8: Constructional aspects of apparatus.

as rapid as possible. This response was measured by means of a pneumotachograph (Fleisch No.4) connected to the mouthpiece. Flow rates at the mouthpiece could then be compared to the volume changes calculated from the movement of the inspiratory spirometer A, measured by means of a potentiometer attached to its pulley wheel. Figure 3.2.9 shows the results for airflow rates of 32 and 41 litres minute^{-1} , which confirmed that spirometer response was satisfactory at air flow rates greater than those likely to be encountered in the experiments (target rates = 13 - 20 litres minute^{-1}).

As the overall accuracy of a total deposition measurement depended on a multitude of factors it was considered necessary to devise a method of checking it as directly as possible.To this end, the apparatus shown in Figure 3.2.7(ii) was used to measure the accuracy of aerosol sampling and collection over a number of breaths. It was also useful in determining the aerosol delivery efficiency at a given particle size and,moreover,served as a direct check on the accuracy of volume control since the volume of air in the collection bag, D, changed considerably over a number of breaths for only a small inspired and expired volume inequality. The aerosol which was 'inhaled' into the collection bag, D, either settled out or was passed into the expiratory collection bag, Ec. The actual quantity of 'inhaled' aerosol could therefore be derived from measurements of the radioactive contents of the expiratory collection bag, Ec, and bag, D, taking into account the dead space losses.

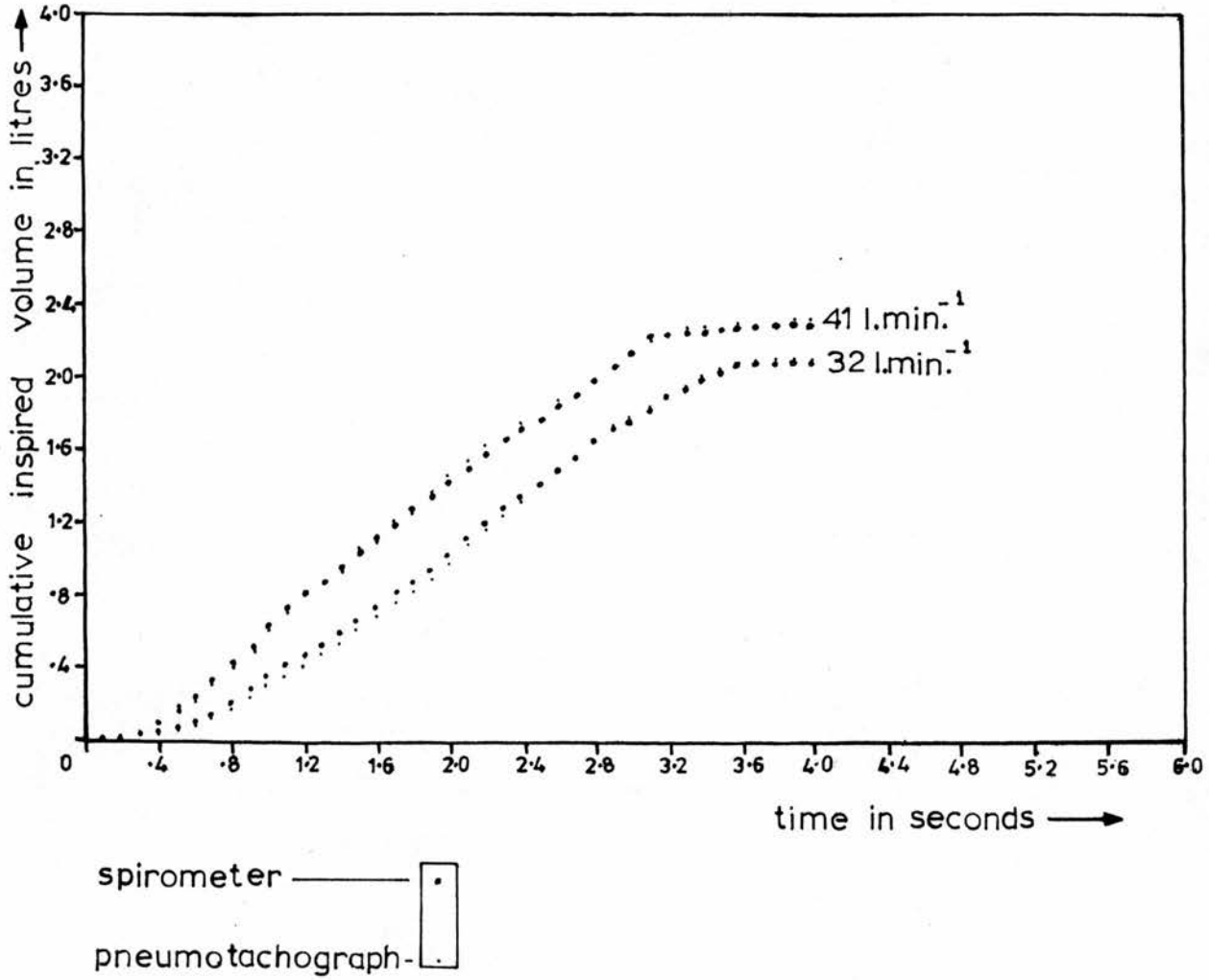

Figure 3.2.9: Spirometer response.

The measured quantity of 'inhaled' aerosol was then compared to that predicted from equation 3.2.8.

$$I \text{ measured} = (Ec - Kn + 1e + Dc) \quad \ldots\ldots\ldots \text{ equation } 3.2.7$$

$$I \text{ predicted} = (Ic - Kn + DS' - 1i) \quad \ldots\ldots\ldots \text{ equation } 3.2.8$$

where, Dc = amount of aerosol deposited in the collection bag, D

and, 1e = (DS - 1i)

(other nomenclature having the same meaning as above)

The results of nine such observations, all at a tidal volume of one litre and mean breathing rate of approximately 10 breaths $minute^{-1}$, are given in Table 3.2.2, having a satisfactory accuracy at all particle sizes. The mean predicted figure, expressed as a percentage of the measured figure, was $100{\cdot}02 \pm 0{\cdot}8\%$, ($\pm$ standard error of the mean, $\sigma = 2{\cdot}4\%$).

3.2(iv) Re-dispersion of particles and aerosol characterization

The techniques employed for the generation and characterization of monodisperse polystyrene particles were described in 3.1. However, as these particles were re-dispersed at a later stage, for aerosol administration, full characterization of the aerosol actually inhaled by the subject required consideration of changes in its bulk aerodynamic properties after secondary dispersal.

(a) Re-dispersion

The particles were re-dispersed in the aerosol administration

nominal particle dia.μm	test no.	Ipredicted as % Imeasured
4·5	1	100·18
6·5	2	102·19
4·5	3	98·96
6·5	4	95·37
4·5	5	97·76
4·5	6	103·80
4·5	7	100·86
9·5	8	101·46
13·0	9	99·57
6·44	means	100·02

Table 3.2.2: Testing of sampling accuracy - results.

apparatus by incorporating them into 1·2 ml of ethanol, which was subsequently dispersed as a fine mist by means of an air-jet nebulizer (Figure 3.2.8(ii)). The nebulizer was operated by a small pump which aspirated from the ambient air at a rate of 12 litres $minute^{-1}$, such that nebulization was normally completed within about ten seconds. The assumption was that the ethanol droplets, most of which would contain one particle, quickly evaporated leaving the dry, airborne polystyrene particles. In such circumstances it was considered inadvisable to rely solely on theoretical predictions of droplet lifetimes. There was the possibility, for example, of water vapour condensation on the particles immediately following dispersion, owing to the lowering of their temperature relative to that of the surrounding air as the ethanol evaporated. However, experimental observation of fine droplet evaporation is a difficult problem (PORSTENDÖRFER et al, 1977). In order to make such observations as directly as possible the apparatus shown in Figure 3.2.10 was used to trap a portion of sprayed particles in a viscous oil (silicone oil, kinematic viscosity = 2×10^{-4} m^2 sec^{-1}), for subsequent microscopic examination.

A sample of polydisperse polystyrene particles in 0·5 ml. of ethanol solution was sprayed into a 28 litre perspex box which was saturated with water vapour. When spraying was completed, after about ten seconds, a tap was turned to allow in a displacement flow of air into the box and force a portion of the aerosol through a narrow orifice. At the orificial exit the particle laden airstream impacted into a fine jet of the oil and those particles that were

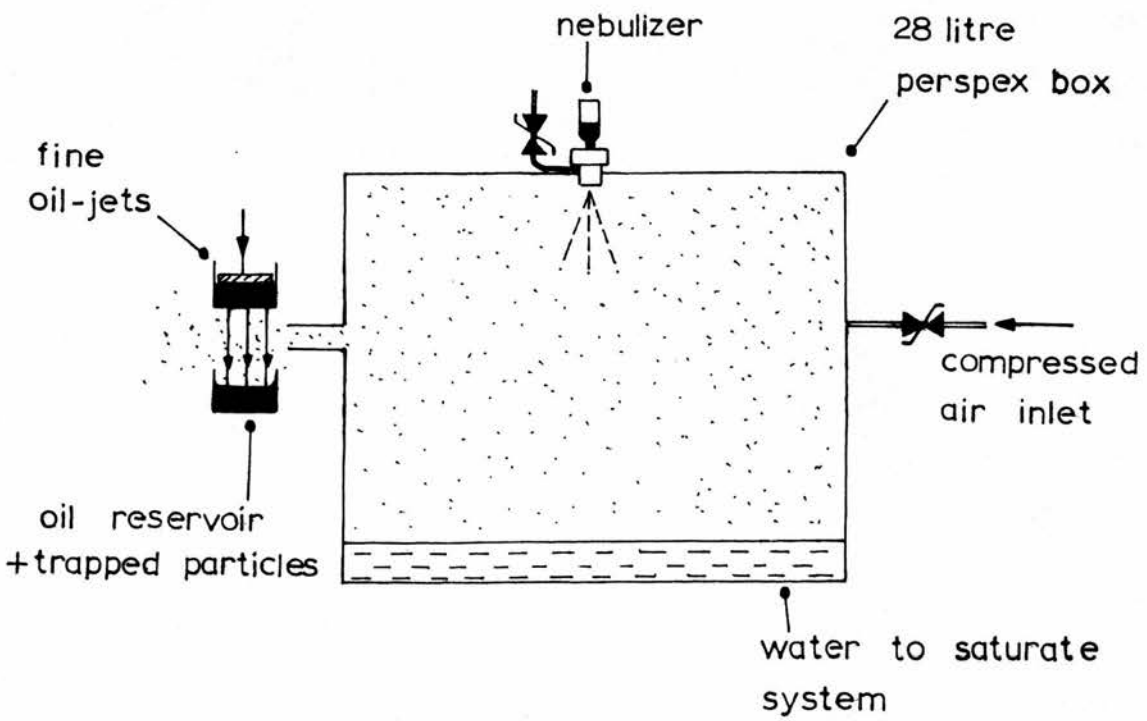

Figure 3.2.10: Testing of particle dryness following dispersion.

captured became trapped in a resevoir directly below. The purpose of using the oil jets was to encapsulate the particles in a fluid as rapidly as possible, thus arresting any evaporation process and facilitating their direct microscopic examination. That the technique was effective in achieving this was confirmed by placing oil-impaction jets at about one centimetre from the nebulizer nozzle, when ethanol was sprayed on its own. Ethanol droplets in a variety of sizes could be observed on microscopic examination of the fluid. On microscopic examination of the particles collected in the manner described above, no liquid residue could be discerned. Liquid droplets were distinguishable from solid particles because of their good sphericity which contrasted sharply with the surface irregularity of the polystyrene particles. As a final check, ethanol was also sprayed on its own into the box. No droplets were observed in the fluid.

The absence of any fluid around the particles also indicated an absence of any significant water vapour condensation on the particles. As the particles must have undergone considerable cooling during ethanol evaporation, this result suggests that condensation of water vapour on the particles on entering the warmer, saturated, respiratory tract, is also of no consequence.

The volume of alcohol sprayed into the apparatus for aerosol administration was determined as that which would not result in any respiratory discomfort for the majority of subjects (ethanol concentration $\sim$13·3 milligrams litre^{-1} or $\sim$1% by volume). HOLMA (1967) reported that the inhalation of ethanol vapour had no

effect on rates of short-term clearance in rabbits at concentrations as high as 5% by volume. In the present work, ethanol was also found to have no obvious bronchial constriction or dilation effects. The maximum expiratory flow at 50% of forced vital capacity (MEF 50%) for two subjects was measured before and after they had inhaled alcohol vapour, at a concentration of~13·3 milligrams litre^{-1}, over ten breaths. The results before and after alcohol inhalation were, respectively, (1) 3·76 $\pm$ 0·014, 3·88 $\pm$ 0·019; (2) 4·26 $\pm$ 0·011, 4·25 $\pm$ 0·002, all results being the mean $\pm$ the standard error of 3 observations, flow rates being expressed, at body temperature and pressure, in litres second^{-1}.

The possibility of airways obstruction being caused through the inhalation of the polystyrene dust itself should also be noted. ANDERSON et al. (1979) studied the effects of the five hour inhalation of an 'inert' polymerized plastic dust, in mass concentrations comparable to those used in the present work ($\sim$10 mgm.m^{-3}), on lung function and nasal mucus flow. No effect was observed on nasal mucus flow, but a slight airways obstruction was found. The degree of respiratory discomfort was proportional to the concentration of dust, but lagged almost two hours behind the changes in dust concentration. Considering that the dust exposure period in the present work was always less than 1·5 minutes (c.f. 5 hours), it is unlikely that any significant bronchial constriction was induced.

Average aerosol delivery efficiency over ten breaths, expressed as the amount of aerosol inhaled by the subject relative to the amount sprayed into the apparatus, ranged from approximately 1% at

at a particle diameter of 13 μm, to nearly 5% at a particle diameter of 4·5 μm. Alternatively expressed as the percentage decrease in aerosol concentration in the actual volume of air inhaled by a subject, the figures were at least 9% and 45% for 13 μm and 4·5 μm particles, respectively. As this decrease normally occured over a period of at least one minute of breathing, the decrease in aerosol concentration over a period of one breath (3 - 4·5 seconds) was small. The mass of aerosol deposited in the subjects was typically in the region of 100 μgm, corresponding to particle numbers of between 10^5 and 2 x 10^6, or an average inhaled concentration of between 10 - 200 particles per cubic centimetre. In the region of 370 kBq (10 μCi) of radioactivity was normally delivered to the subject, although this sometimes varied owing to a degree of unpredictability in the particle labelling efficiency and was set at about twice this figure for some selective applications. Radiation dose was set as low as possible, consistent with reasonable counting statistics. Relevant aspects of radiation counting statistics are discussed in section 3 of the present chapter. Radiation dose given to the lungs varied according to the proportion of clearance. The maximum dose given to the lungs, assuming complete retention, varied from approximately 20 μSv (2 m.rem) to 175 μSv (17·5 m.rem), but 50 μSv (5 m.rem) typically. In many cases, most of the particles deposited in the lungs were rapidly translocated to the abdomen. Assuming complete clearance to the transverse colon (as an example) the radiation dose to this organ again varied from approximately 20 μSv (2 m.rem) to 175 μSv (17·5 m.rem), and 50 μSv (5 m.rem)

typically. Two subjects participated in repeat studies and in their case total radiation dose in each of the above organs was below 150 μSv (15 m.rem). Conversion factors from absolute radioactivity to radiation dose given to specific organs were taken from ICRP report No. 17 'Protection of the Patient in Radionuclide Investigations' (1971).

3.2.(iv)b Aerosol characterization

The possible influence of electrical charges on airborne particle deposition was discussed in Chapter 1. Although it was considered unlikely to be an influence in the particle size range and conditions of the present study (4·5 - 13·0 μm diameter), the electrical neutralization of the test aerosol was attempted by exposing it to a mixture of positive and negative free ions generated by an ionizing radiation source. Owing to a degree of uncertainty in the published literature as to the time taken to achieve a Boltzmann type equilibrium, the strength of source used was set considerably higher than was considered absolutely necessary (TAKAHASHI and KUDO, 1973). It was not possible to measure the charge distribution of the test aerosol directly. The radiation source used consisted of a 5 x 25 cm rectangular metal foil impregnated with approximately 740 MBq (20 m.Ci) of Thallium^{204}, which is a pure β-emitter (energy = 0·77 MeV) and has a conveniently long half-life of radioactive decay ($T_{\frac{1}{2}}$ = 3·9 years). It was housed in a lead-lined box which had a hinged lid to facilitate radiation exposure during an experiment (Figure 3.2.8(ii)).

The time in seconds, tb, taken to achieve a Boltzmann charge

distribution was estimated using the equation of GUNN (1954). i.e.

$$tb = \frac{1}{4\pi e \dot{N} \mu} \qquad \text{..... equation 3.2.9}$$

where, e = fundamental unit of electronic charge in Coulombs

$\dot{N}$ = small ion pair density (number m^{-3}).

μ = small ion mobility in $m.^2 V^{-1} sec.^{-1}$

Values of ion pair density corresponding to a given β-radiation source in a given volume were taken from the empirical data of TAKAHASHI and KUDO (1973). A value of $\mu = 1{\cdot}4 \times 10^{-4} m^2 . V^{-1} sec^{-1}$. was used, which is the average mobility of positive and negative ions quoted by BRICARD and PRADEL (1966), giving a value for tb of 1·6 seconds. This value should only be taken as an order of magnitude estimate as equation 3.2.9 was not intended, strictly, to apply to particle diameters above about 3 μm. It is however within an order of magnitude of the value of tb predicted by FRY (1970), who employed a β-radiation source of similar strength, but with much shorter particle residence times ($\sim$1 second) near it. In the present work, there was normally greater than a 30 second delay between the end of particle dispersal and the first intake of aerosol by the subject.

It should be appreciated that the purpose of such electrical neutralization was not to eliminate such effects entirely, but merely to standardize them between separate experiments.

Besides defining the size, shape, density and electrical

charge characteristics of the particles, it was also necessary to consider the relative proportions of satellite and aggregated particles present in the aerosol inhaled by each subject. Since satellite particles fall more slowly than their corresponding primaries it is likely that their relative concentration would increase with time after initial dispersal, with a more pronounced effect at increasing particle size. The effect was measured at 10·4 μm and 13 μm particle diameters by aspirating for one minute, about 30 seconds after particle dispersal, through a millipore filter attached to the mouthpiece of the aerosol administration apparatus. The relative proportions of satellites to primaries on the filter, Ns_1/Np_1, was then compared to that measured on glass slides, Ns_2/Np_2, placed on the floor of the main spraying chamber. Two such tests were performed for each size and the average result expressed as $\left[\frac{Ns_1}{Np_1} \times \frac{Np_2}{Ns_2}\right]$, which gave average figures of 2·3 and 2·8, for 10·4 μm and 13 μm diameter particles, respectively. The ratio of satellites in any given particle sample at these sizes was calculated as the product of this factor and the proportion of satellites measured on glass slides placed on the floor of the spraying chamber during aerosol administration. In only two cases (subjects KD, TDW), at particle diameters $\geq$ 10·4 μm, did this value exceed 2%. Differential settling of satellites and primaries at the two sizes studied below 10·4 μm, was found to be negligible over a period of two minutes. The relative proportions of satellites and primaries for all experiments are listed in Table 3.2.3.

Aggregation of particles was not generally significant above a

subject	$\bar{d}$ μm	coeficient of variation	primaries % mass	singlets % by no.	doublets + triplets % by no.
DCFM	4·5	9·0	n.d.	n.d.	n.d.
AM	4·6	5·6	92·2	87·5	11·9
AR	4·5	8·8	95·0	82·6	13·0
group av.	4·5	7·8	93·6	85·1	12·5
HG	7·0	10·0	96·4	96 0	4·0
RB	6·3	7·1	97·8	72·8	17·9
PCE	6·9	8·0	n.d.	n.d.	n.d.
group av.	6·7	8·4	97·1	84·4	11·0
PT *	10·4	5·9	98·2	97·3	2·7
PH	10·4	5·1	99·0	100·0	0
KD	10·5	5·3	89·9	94·5	5·5
group av.	10·4	5·4	95·7	97·3	2·7
TDW	12·9	4·7	91·3	98·0	2·0
JH	13·0	8·6	98·9	96·2	3·8
AD	13·2	10·1	98·9	100·0	0
group av.	13·0	7·8	96·4	98·1	1·9
ATM	4·5	6·9	99·5	91·6	8·4
FH	4·5	7·9	98·2	95·0	5·5
RH	4·5	9·0	98·4	95·5	4·5
group av.	4·5	7·9	98·7	94·0	6·1
VC	4·6	7·0	98·7	91·0	9·0
MS *	4·6	7·4	97·9	83·3	12·3
JV	4·6	8·2	96·9	89·7	9·6
group av.	4·6	7·5	97·8	88·0	10·3

* average of two runs
nd = not determined

Table 3.2.3: Particle characterization.

particle diameter of 4·5 μm because of the relatively fewer numbers dispersed from solution. At 4·5 μm particle diameter, the proportion of particles sprayed as singlets fell in a range 72% - 100%, of the total number of entities, the average value being 92%. The majority of those particles not dispersed as singlets were either doublet or triplet entities (Table 3.2.3). The proportions of aggregates were obtained by microscopic analysis of glass slides which had been placed on the floor of the spraying chamber during aerosol administration. The degree of aggregation was reduced as far as possible by minimizing the number concentration of particles in the ethanol spraying solution and by subjecting it to several minutes of vibration in an ultrasonic bath prior to aerosol administration. Owing to a rapid decline in aerosol production efficiency with low polymer concentrations, a lower limit to particle number concentration in the ethanol spraying solution was imposed and a finite degree of particle aggregation was unavoidable, particularly for small particle sizes.

The effects of particle agglomeration may be examined using the semi-empirical relationship of Stöber (1972) which applies to chain-like aggregates of particles:

$$dae = \ddot{K} . \rho^{\frac{1}{2}} . \dot{n}^{\frac{1}{6}} . d \qquad \text{..... equation 3.2.10}$$

where, $\ddot{K}$ = a constant of proportionality

ρ = 'primary' particle density in $Kg.m^{-3}$

$\dot{n}$ = number of 'primary' particles in the agglomerate

d = 'primary' particle diameter in metres

dae = aerodynamic diameter of the agglomerate in metres

Using a value of $\ddot{K} = 1$, which lies closely between the empirical values observed by KOPS et al. (1975) and STOBER (1972), this gives a value of dae = 5·05 μm for doublets and dae = 5·4 μm for triplets, at d = 4·5 μm. The overall effect of particle aggregation in the proportions observed in the present work at 4·5 μm, is therefore likely to be small.

3.2(v) Construction of apparatus and control electronics

Only a brief description of certain constructional aspects, considered relevant, will be attempted here.

It was important that the subject's mouth was effectively sealed over the mouthpiece during aerosol administration. Since the diameter of mouthpiece used was in any case made relatively wide (2·5 cm), in order to minimize air-flow resistance, the resultant stretching of the subject's lips favoured good sealing. As an additional safeguard a rubber flange was incorporated into the mouthpiece (Figure 3.2.8). The right and left edges of the flange were elongated in order to prevent 'side-breathing' by the subject. The flange was fitted about one centimetre along the mouthpiece such that the latter normally penetrated to a distance of about three centimetres into the subject's mouth.

The subject sat in a chair, of variable height, such that his back was slightly off-vertical during arosol administration, as shown in Figure 3.2.11, which also shows the complete aerosol

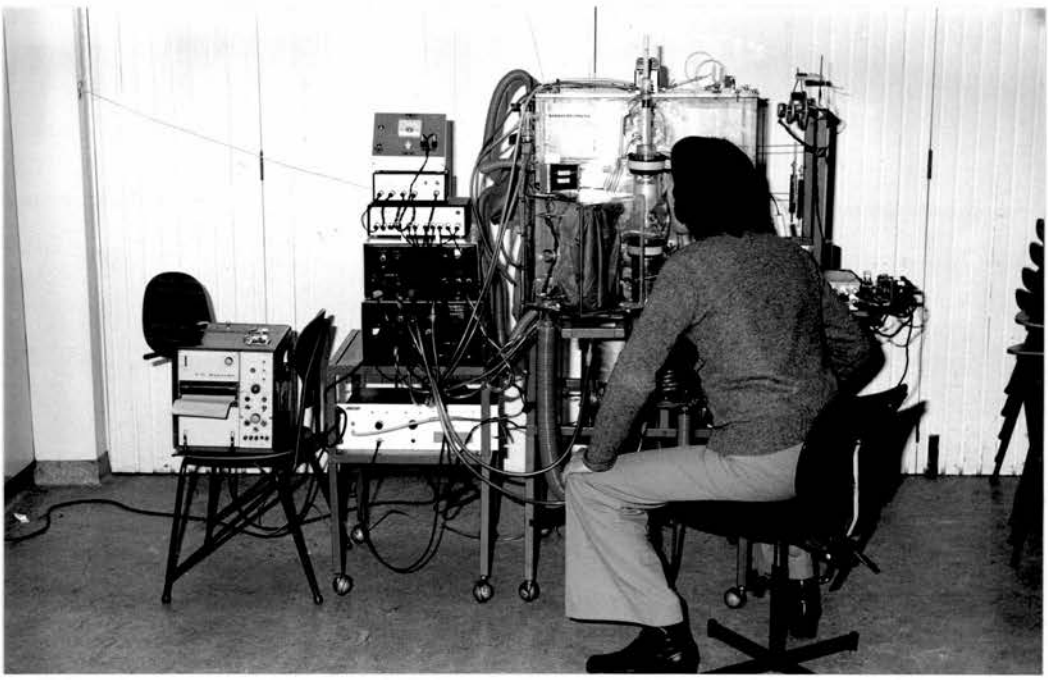

Figure 3.2.11: Photograph of a subject breathing on aerosol administration apparatus.

administration apparatus.

From the description of the breath to breath operating sequences described earlier in this chapter it may be apparent that an electro-pneumatic control system of considerable complexity was required. It was also essential that high reliability was achieved, because of the one-off nature of the experiments. A circuit that employed as few discrete components as possible was used in order to minimize the probability of a failure occurring in the whole system.

Pressure changes were detected using a commercially available micromanometer (Mercury Electronics Ltd.).

3.3 Measurement of regional aerosol deposition and clearance

(i) Definitions

While the total deposition fraction may be measured by direct means, because of its relative inaccessibility, it is necessary to employ indirect techniques in the estimation of the regional distribution of this fraction within the respiratory tract.

In Chapter 1 the essentially continuous nature of the respiratory tract was described. Yet some practical means of distinction must be adopted when it becomes necessary to consider the aerosol filtration characteristics of each region separately. However, if indirect techniques are employed, such distinctions ought not to presume an automatic correspondence between the anatomical region under consideration, however precisely it is defined, and the deposition fraction measured empirically. For these reasons purely functional definitions of regional deposition fractions were employed, which related as closely as possible to the experimental methods used for the derivation of each:

1. fW(I) That fraction of the inhaled aerosol which could be recovered by washing of the mouth shortly after the end of aerosol administration, normally within 1 - 2 minutes.
2. fS(I) That fraction of the inhaled aerosol removed to the stomach, by swallowing, between the first and second radioactive lung burden measurements, the second being performed 9 - 12 minutes after the end of

aerosol administration (The purpose of measuring fS(I) was to estimate aerosol losses in the pharyngeal and laryngeal regions which could not be recovered in fW(I), but neither could be strictly counted as a lung deposit).

3. fC(I) That fraction of the inhaled aerosol cleared from the lungs between the second and final radioactive lung burden measurements, the final measurement normally being performed 20 - 22 hours after the end of aerosol administration. If it is assumed that only that fraction of the inhaled aerosol which initially deposited on the dead space airways was cleared during this period, fC(I) is that fraction.

4. fR(I) That fraction of the inhaled aerosol retained in the lungs at the time of the final radioactive lung burden measurement. If it is assumed that only that fraction of the inhaled aerosol which initially deposited in the respiratory zone was retained at this time, fR(I) is that fraction.

These fractions, and all others relating to aerosol deposition in the present work, have been written in the general form,

$$f_x(y) = \frac{x}{y} \qquad \text{..... equation 3.3.1}$$

where, x is the magnitude of the quantity under consideration

expressed as a fraction of another quantity, y, expressed in the same units as x.

hence,

$$fW(I) = \frac{W}{I} \quad \text{..... equation 3.3.2}$$

$$fS(I) = \frac{S}{I} \quad \text{..... equation 3.3.3}$$

$$fC(I) = \frac{C}{I} \quad \text{..... equation 3.3.4}$$

$$fR(I) = \frac{R}{I} \quad \text{..... equation 3.3.5}$$

and, $fD(I) = fW(I) + fS(I) + fC(I) + fR(I)$ .. equation 3.3.6

where, I represents the inhaled aerosol.

W, was measured in arbitrary detector counts and expressed directly as a fraction of I; S, C and R, were measured firstly as fractions of quantities other than I, and then converted to fractions of I, by means of the following equations,

$$fS(I) = fS(C + R + S).(fD(I) - fW(I)) \quad \text{..... equation 3.3.7}$$

$$fC(I) = fC(C + R).(fD(I) - fW(I) - fS(I)) \quad \text{..... equation 3.3.8}$$

$$fR(I) = fR(C + R).(fD(I) - fW(I) - fS(I)) \quad \text{..... equation 3.3.9}$$

where, $fS(C + R + S)$, $fC(C + R)$ and $fR(C + R)$, were estimated from

measurements of whole body radioactivity.

and, $fC(C + R) + fR(C + R) = 1$ ..... equation 3.3.10

In the determination of the retained and cleared fractions it should be noted that it is also necessary to assume that particles cleared from the lungs do not subsequently return. This is less improbable than it might at first appear since the possibility must be considered of a transfer of particles through the walls of the alimentary canal, subsequently to be re-distributed elsewhere in the body, for example, in the fine pulmonary capilliary structure. However, recent unpublished work using particles smaller than those of the present work has confirmed that such transfer does not occur (BOLTON, 1979). Moreover, an analysis of the urinary secretion, over the full clearance period, of one subject in the present work (see part (ii)e of this section) confirmed the absence of both particles and leached radioactivity.

It should also be noted that it is assumed that particles are not retained indefinately in the oesophagus following removal, but are removed swiftly into the stomach. That such retention did not occur was confirmed in two subjects (PCE and DCFM) who, in a separate experiment conducted for a different purpose (see part 3(ii)c below), had taken a small dose of radioactive particles administered orally (with food), followed by several profile scans, as described later in the text.

3.3(ii) Measurement techniques

(a) Mouth and throat deposits

Radioactive particles deposited in the mouth during aerosol administration were removed by means of the apparatus illustrated in Figure 3.3.1. Several pressurised water-jets were directed upwards into the subject's mouth, from a 50 ml syringe, in order to ensure that any particles removed would be washed downwards into the collection vessel. Mouthwash duration was normally about thirty seconds.Gargling methods were rejected as these were found to be more likely to lead to swallowing, which in this case it was desirable to avoid as far as possible. Moreover, gargling methods would also almost certainly remove a portion of the throat deposit. Therefore,a strict comparison between the mouthwash fractions obtained in the present work and those obtained by some other groups (see Chapter 5, part 1(iii)) cannot be made. During this procedure the subject was requested to swirl his tongue around in order to maximize the particle removal efficiency. The latter was measured in three subjects (PCE, RJA and PT) by administering a small quantity of tagged particles via a teaspoon, with no swallowing, followed by the mouthwash procedure described above. The subjects were then measured for residual radioactivity by means of a profile scanner, used in the manner described later in the text. This test demonstrated that the removal technique was not completely effective, giving an average removal efficiency of $78 \pm 13\%$ (mean $\pm$ standard deviation). It should be appreciated that any residual particles remaining in the mouth after this procedure would not be entirely excluded from the measurements,

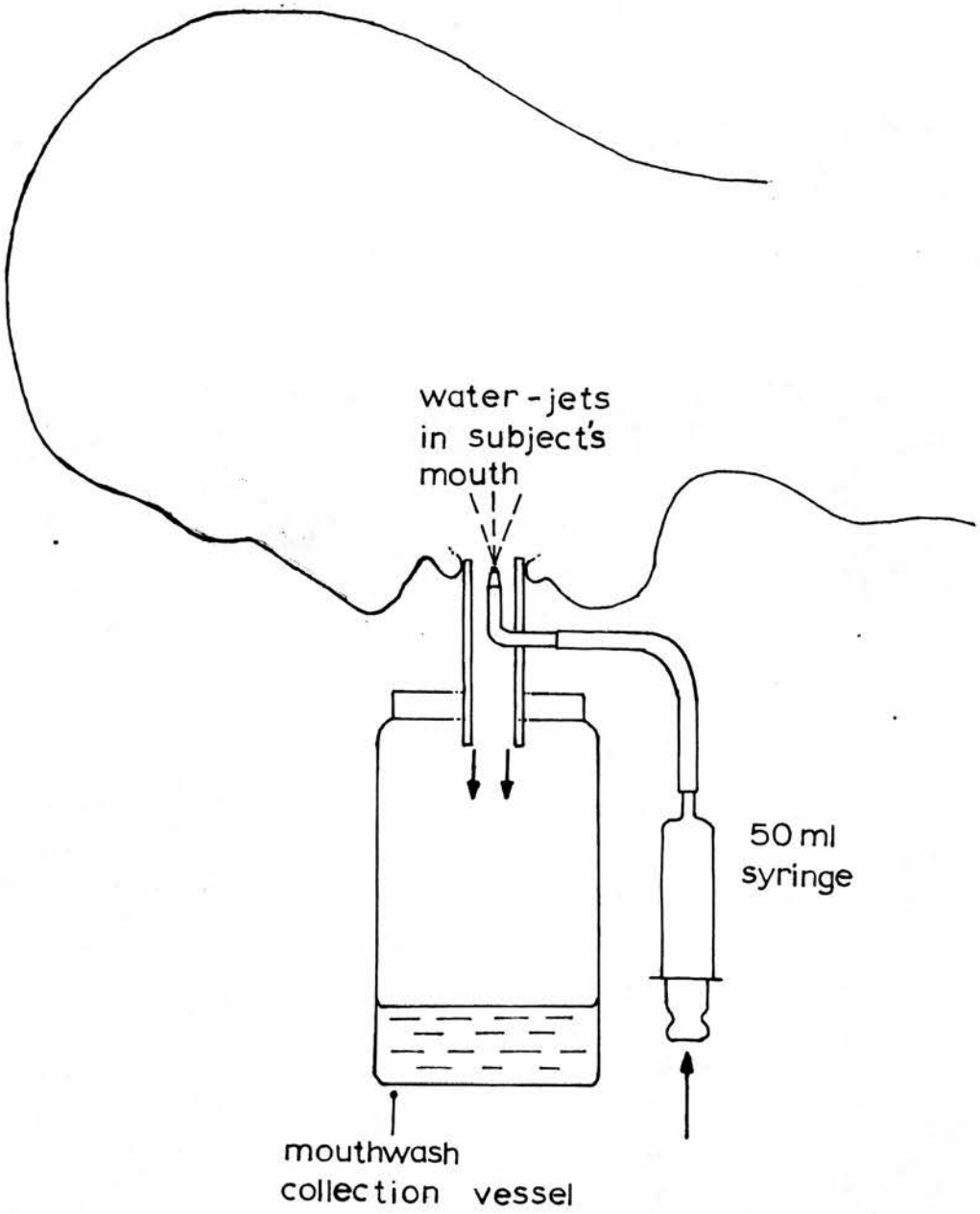

Figure 3.3.1: Mouthwash apparatus.

but would be counted as a part of the throat deposit fS(I). Measurement of the mouth deposit by this means would at least give an indication of how this fraction might vary with particle size.

The radioactive content of the mouthwash collection vessel was measured in arbitrary detector counts. For each radioassay the vessel was placed in a standard position within the detector and the amount of fluid was always made up to a standard level. Further details of radioassay procedures are given below (part 3(ii)e).

In the determination of dust-exposure standards it is desirable to have some knowledge of the proportion of aerosol which is able to penetrate beyond the larynx at a given particle size or breathing pattern. Estimation of the proportion of inhaled aerosol which deposits in the laryngeal region presents severe practical difficulties however. In particular, the subject is able to remove some or all of the initial throat deposit before it can be measured. LIPPMANN and ALBERT (1969) were the first to attempt such measurements. In their technique the throat and lung deposits were measured in sequence, the lung being the first to be measured. In the present work, in order to minimize the time available for swallowing, the measurement of the initial lung and throat deposits was performed in a single manoeuvre (although it was actually considered more desirable to define the initial lung burden at the time of the second lung measurement, in order to allow the initial throat deposit time to clear, as discussed below). This eliminated the need for measurements of absolute radioactivity in the subject's

throat since the throat deposit could be expressed directly as a fraction of the total deposit, in arbitrary detector counts. No conscious or deliberate coughing or swallowing was reported by any subject in this early period after aerosol administration. Moreover, it was possible, by means of the technique, to detect whether a significant amount of radioactivity had actually been swallowed before the first radioactive body-burden measurement. None was observed for any subject. Further details of the method are given in part 3(ii)c below.

3.3(ii)b Retained and cleared fractions

The fraction of the inhaled radioactive particles cleared from or retained in the lungs of a subject at a given time, ought not to automatically be assumed to correspond to the fractions of aerosol which initially deposited in the largely ciliated, non-respiratory, and non-ciliated, respiratory, zones of the lung. The reasons for this were discussed in Chapter 1. The definition of an aerosol deposition fraction in terms of levels of retention at specific times therefore enables the behaviour of particles in the respiratory tract to be described using the minimum number of assumptions.

In order to obtain the levels of lung retention at a given time, ideally, the total radioactive contents of both lungs should be measured. However, owing to an arbitrary degree of anatomical overlap between the lungs and those organs through which swallowed radioactivity must eventually traverse, notably the stomach, duodenum and transverse colon, this would appear to be impossible to achieve in practice even when using detectors of the highest

available resolution. By resolution is meant the ability of a detector to distinguish between regions. If the resolution of an instrument is increased it is normally at the expense of a decrease in sensitivity, which is most often measured in terms of the number of detector counts above background per absolute unit of radioactivity measured. In a clearance study such difficulties are further compounded by the necessity of monitoring the radioactive lung burden for a finite time, since this requires the use of an initial radioactive lung burden that is high enough to leave a detectable magnitude of radioactivity at the end of the clearance period. Detectors of high sensitivity are normally employed in lung clearance studies (LIPPMANN and ALBERT, 1969; CAMNER, 1971; MORSEY et al, 1978; FOORD et al, 1978). These may detect low lung burdens, considered ethically acceptable for administration to healthy volunteer subjects, but only at the cost of a poor detector resolution. A compromise is therefore normally required between detector resolution and sensitivity, such that a reasonably large fraction of the lung burden may be measured while it is at the same time ensured that there is no significant contribution to detector counts from radioactivity that has already been passed down the oesophagus.

With the exception of CAMNER (1971), the other workers mentioned above employed radiation detectors placed in a stationary position relative to the subject's chest. The main disadvantage of such an approach is that the magnitude of the abdominal contribution to detector counts is subject to a degree of uncertainty for any given

measurement, with the attendant consequence that more of the lung radioactive burden may be excluded than was absolutely necessary. FOORD et al. (1977) have demonstrated the large inter-subject differences and rapid temporal variations in the abdominal contribution to fixed detector count rates. CAMNER (1971) employed a linear scanning detector to measure rates of short-term clearance. The advantage of this approach is that a one-dimensional profile of whole body radioactivity is obtained, from which it is possible to estimate the relative radioactive contents of lung and abdomen and their degree of mutual overlap for a given detector resolution. A similar technique was employed in the present work, details of which are given below.

3.3(ii)c Use of profile scanner in the estimation of deposition fractions and clearance rates

The profile scanner used in the present work is illustrated in Figure 3.3.2. The apparatus was essentially that described by TOTHILL and GALT (1971), who conducted a quantitative analysis of its performance. Two diametrical detectors were positioned above and below the subject, which reduced variatons in detector response along any vertical line between them. The detectors consisted of thallium activated sodium-iodide crystals, optically coupled to single photomultiplier tubes. Parallel slit lead collimators were fitted and their width could be varied to give a range of spatial responses and resolutions. The subject lay in a supine position approximately mid-way between the detector-pair and could be moved at a pre-determined rate, in a horizontal plane, such that the full

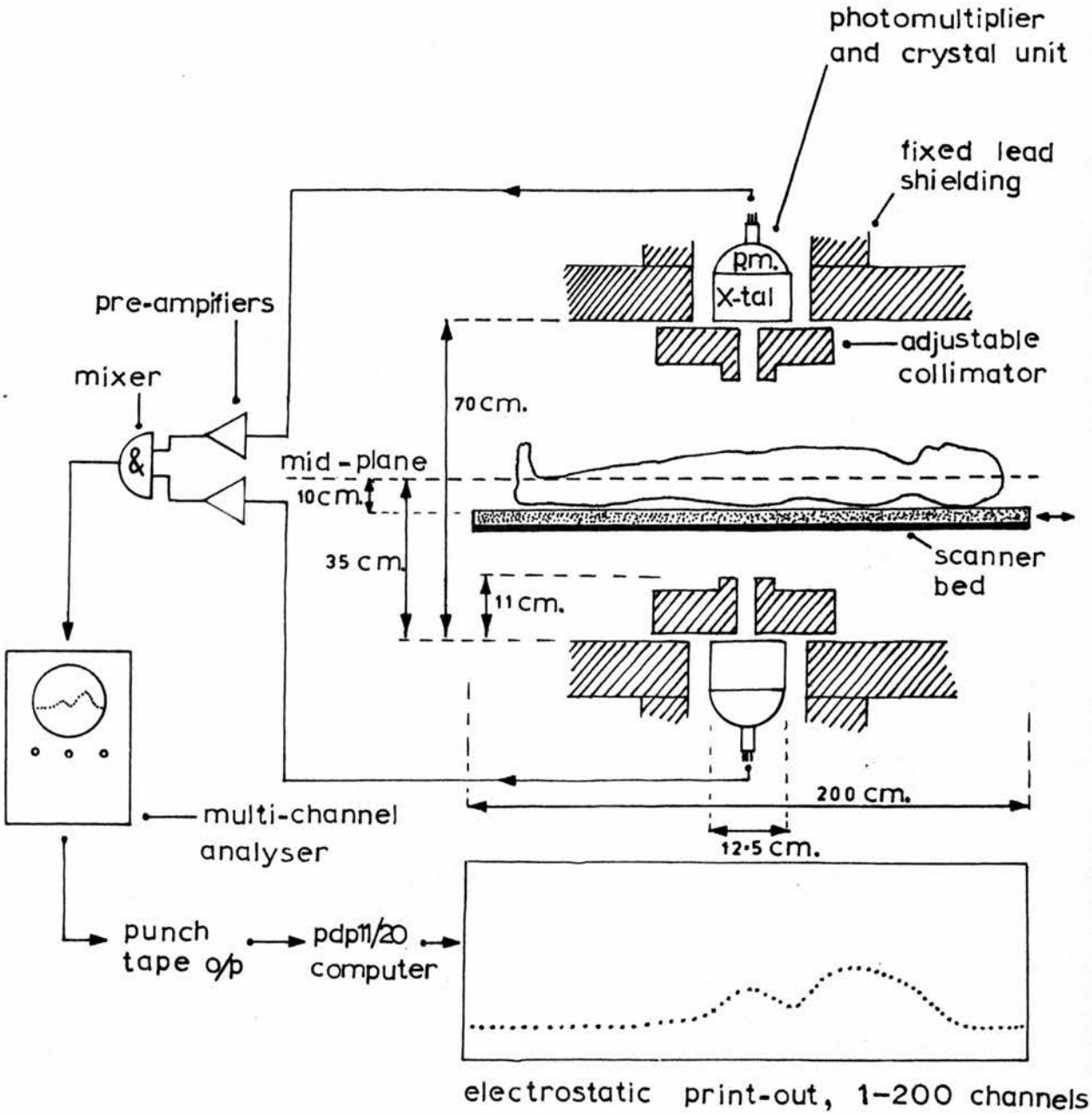

Figure 3.3.2: Profile scanner.

body length was scanned.

The two photomultiplier outputs were first amplified and then passed via a mixer into a multi-channel spectrum analyser operated in the multi-scaling mode. In essence, this mode of operation enabled the detector output for a given period, at a particular time, to be assigned a particular location or channel number in the analyser memory, correspoding to the particular position of the scanner trolley at that time. A whole body profile of the radioactive distribution within the subject could therefore be obtained, an illustrative example of which is shown in Figure 3.3.3. By setting the analyser counting period, or dwell time, to one second, and setting the scanner trolley speed to one centimetre per second, each point on the scan profile, of which there were 200, corresponded to a one centimetre trolley movement. The calibration accuracy of the apparatus was periodically checked, using a stop watch, both with and without a subject on the scanner trolley. Total scan time was 200 seconds which was sufficient to obtain 4,000 - 5,000 scan counts per 37 KBq (1 μCi) of inhaled radioactivity. Only some 50 seconds of this period were spent actually scanning the lungs, in which time only a small degree of clearance would be likely to occur. From a series of such profiles a lung clearance curve for each subject was derived, by a method described below, each point on the curve being derived from one profile scan. From the magnitude of lung retention averaged over the three final scans, normally performed 20 - 22 hours after aerosol administration, values of fC(C + R) and fR(C + R), were derived (equations 3.3.(8 - 10)).

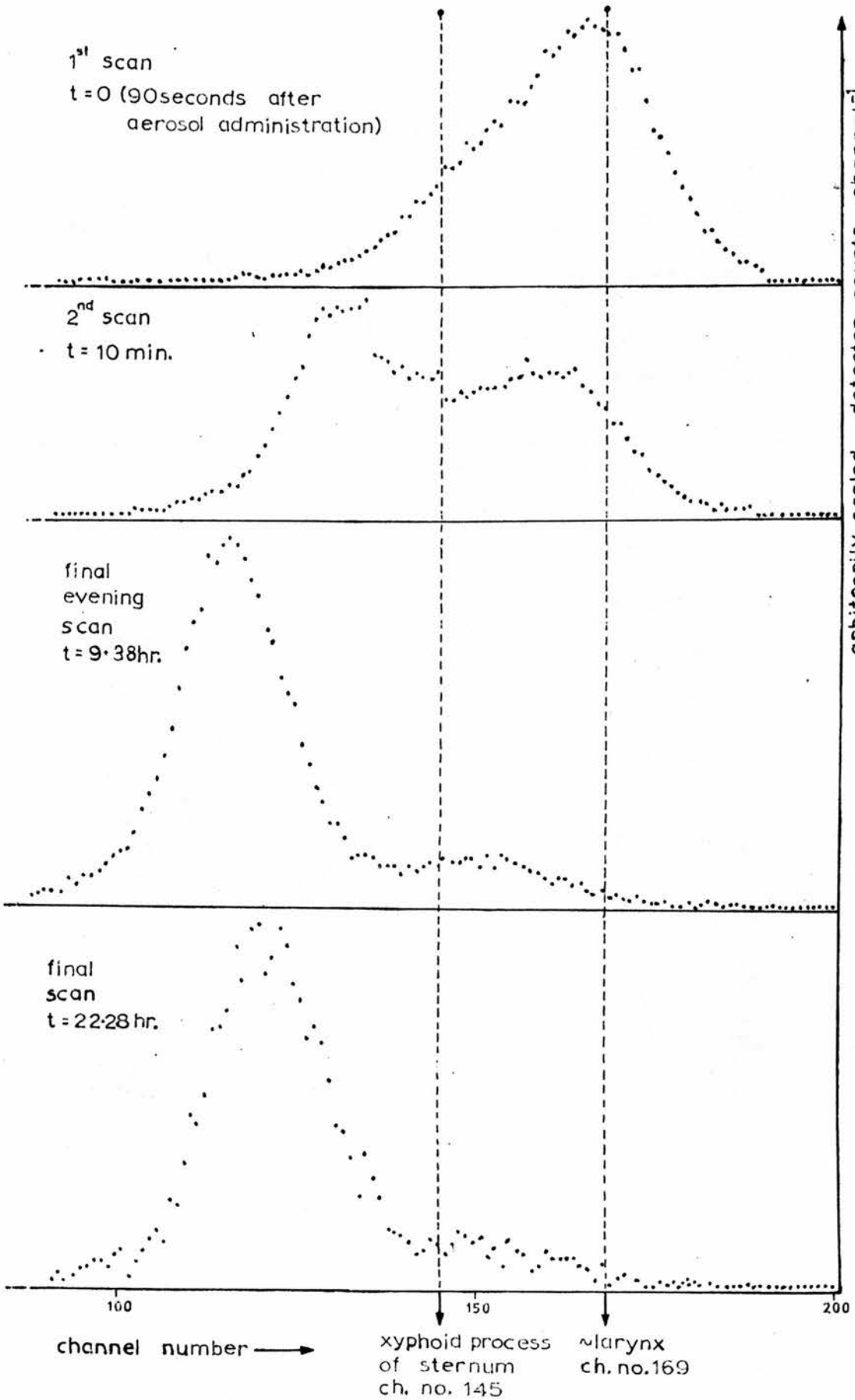

Figure 3.3.3: Example of profile scans obtained at various times (t). Subject PT1, $\bar{d}$ = 10·2 μm.

Owing to the large number of scan profiles obtained for each subject, which varied from 20 - 50, corrections for background radiation and isotope decay were performed on each profile by means of a PDP 11/20 computer (Digital Equipment Corporation). The unprocessed profile scan data were first stored on punched tape and then transferred to a magnetic storage disc. Figures for background radiation and time of scan were fed into the computer, via a teletype, and a computer program (HANNAN, 1978) applied the necessary corrections to each data point of the profile, printing the corrected version on an electrostatic printer. The figure for background radiation, normally between 1,500 - 2,500 detector counts, was derived from the average of five or more scans performed during the clearance period without a subject on the trolley. The coefficient of variation in background detector counts was always within $\pm$ 5% of the average value during the scanning period. Relevant aspects of radiation counting statistics are discussed in part (ii)d of this section.

As the lung clearance measurements were performed in a hospital department where radioisotopes were in frequent use, care was taken to ensure that the subject was not contaminated by this environment, as far as possible. The subject was instructed to wear shoes when it was necessary to venture into the hospital corridor and to remove them before a scan. Scanning of the experimental operatives who had been in the hospital for several hours confirmed that there was normally no pick-up from airborne radioactive contamination detectable above normal background radiation. Before use it was

necessary to set an 'energy-window' on the multi-channel analyser such that only those scintillation photons that had arisen mainly as a result of photoelectric absorption of Tc^{99m} γ-photons (photo-peak energy = 140 KeV) in the scintillator crystal were included in the data output. This ensured greater overall accuracy by preferential exclusion of background radiation, at slight cost in terms of sensitivity due to exclusion of scintillation photons that had arisen mainly as a result of Compton interactions within the scintillation crystal or subject.

As was described above, a compromise is needed between detector resolution and sensitivity such that as large a portion of the lungs is measured with a minimal contribution from swallowed radio-activity. In this, it is essential to have some means of knowing the contribution of the cleared radioactivity, and its distribution within the abdomen at various times after aerosol administration, for a given detector resolution. Such knowledge cannot be obtained by calculation alone but must be determined empirically. In order to determine the optimum collimator slit-width, profile scans were performed using two volunteer subjects who had been intravenously injected with Tc^{99m} labelled human serum albumen microspheres. These subsequently became trapped in the pulmonary fine-capillary structure and their distribution on the whole body profile was compared to that of Tc^{99m} labelled polystyrene particles taken orally (i.e. swallowed). Since the swallowed particles were taken a little earlier than the particles taken intravenously, it was possible to confirm that the swallowed particles did not reside

for any time in the oesophagus but were rapidly translocated to the stomach. Slit-widths from 2 to 20 centimetres were tried. At a slit-width of 2 centimetres the advantage in terms of lung/abdominal overlap appeared minimal in comparison with the results obtained at a slit-width of 5 centimetres, when detector sensitivity was some six times greater. Lung/abdominal profiles were barely distinguishable above a collimator width of 8 centimetres, but appeared satisfactory for both subjects at 5 centimetres (Figure 3.3.4(i) and (ii)). At an isotopic photopeak energy of 140 KeV, the mid-planar resolution, defined as the width of a profile peak at half its maximum height obtained by scanning a point source at the mid-line of the mid-plane, is approximately three times the slit-width (TOTHILL, 1974). For a slit width of 5 centimetres this implies that for radioactivity placed at the boundary of an organ, its contribution to detector counts will not fall below half its peak value until the detectors have moved approximately 7·5 centimetres off a vertical line above the boundary.

This contribution will fall to zero at a distance,

$$do = q\left[\frac{d}{a} - 1\right] \qquad \text{..... equation 3.3.11}$$

Also, the full width half maximum resolution, $R(\frac{1}{2})$, could be approximated by,

$$R(\tfrac{1}{2}) = (do + q) \qquad \text{..... equation 3.3.12}$$

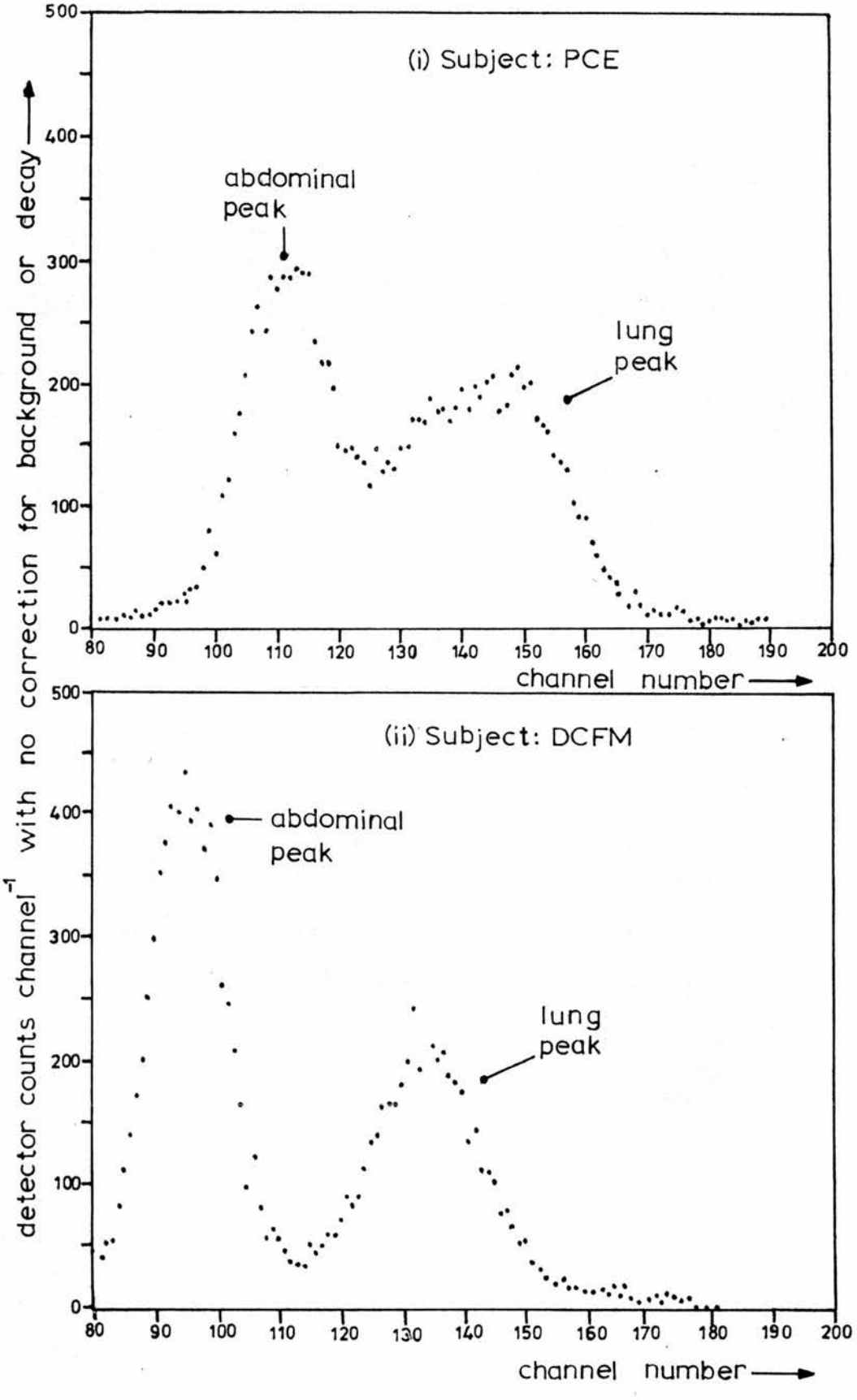

Figure 3.3.4: Slit width optimization - results for two subjects at 5cm. collimator slit width.

where, q = collimator slit width (5 centimetres)

$\dot{d}$ = distance from the crystal to mid-plane

a = collimator length (11 centimetres)

do = distance in a horizontal plane from the slit edge to the point at which the contribution of a point source at the mid-line of the mid-plane is zero.

At the mid-plane ($\dot{d}$ = 35 centimetres), this gives a value, do = 10·9 centimetres. Consequently, even if all swallowed radioactivity remained at the nearest point to the lungs, normally the stomach, the portion of the lungs scanned by the region of maximum detector response could still be between about one half to two thirds of the total and yet still exclude the abdominal contribution. Variation in spatial response in a vertical plane parallel to the collimator slits is discussed in part 3(ii)d below. The relatively small degree of lung/abdominal overlap on the scan profiles at a slit width of 5 centimetres, shown in Figure 3.3.4, is consistent with these predictions. Collimator slit-width was set at 5 centimetres for all measurements.

Figure 3.3.5(i) shows the characteristic shape of a scan profile obtained as soon as possible after aerosol administration, normally within 1 - 2 minutes. The channel number of the small 'hump' on the otherwise smooth larger peak always corresponded, to within approximately 2 centimetres, to the position of the subject's larynx relative to the scanner trolley. After completion of the first scan, the subject was asked to gargle and swallow several

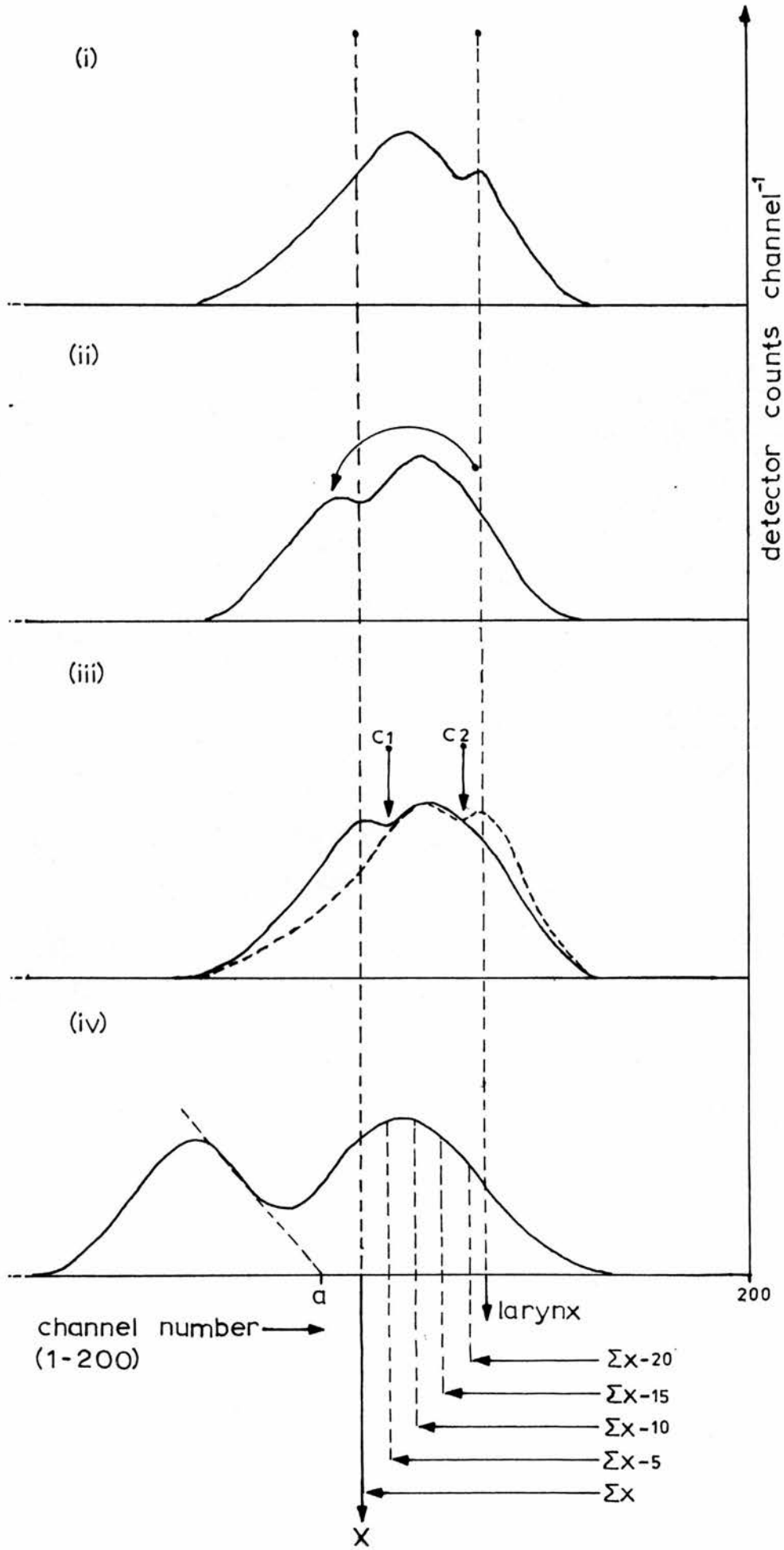

Figure 3.3.5: Profile scan analysis.

times with drinking water. Following this procedure the second profile scan, normally performed within 8 -10 minutes after the first, had the characteristic shape shown in Figure 3.3.5(ii). The laryngeal 'hump' transfered to the abdominal region, with no selective deposit remaining in the laryngeal region discernible on the scan profile. This indicated that the period of time between the first and second scans was sufficient for material deposited in the laryngeal region to have been cleared and passed down the oesophagus.

The magnitude of the laryngeal 'hump' was obtained by subtracting the channel counts of the second profile summed over channels (0 - C1) from the corresponding ones of the first, where C1 was a standard reference point obtained by superimposing the two profiles and determining the point at which they converged (Figure 3.3.5(iii)). There were actually two points of convergence, C1 and C2. Summation and subsequent profile subtraction could therefore have been made either over channels (C2 - 200) or (0 - C1). In practice it was normally found to make no difference on which side the subtraction was executed, indicating an insignificant change in count rate, or sensitivity, due to the changed spatial distribution of the radioactive particles.

In obtaining the laryngeal/pharyngeal deposit, fS(I), by such means, an element of cleared upper-tracheal deposit below the larynx was included. Estimation of this deposit by, for example, planimetric analysis of the first scan profile, would not overcome this difficulty as it could not be assumed that some of the

'hump' was not due to selective tracheal losses immediately below the larynx. Assuming a tracheal ciliary transport rate of one centimetre per minute (GOODMAN et al. 1978), the approximate maximum boundaries of the region thought to be included by adoption of this method may be as shown in Figure 3.3.6. In practice it is unlikely that the material included extended this far below the larynx owing to the additional clearance delay introduced by the larynx itself. While it is technically possible to estimate the laryngeal/pharyngeal initial deposit by means of fixed radiation detectors (LIPPMANN and ALBERT, 1969), the profile scanner has the clear advantage that it may be confirmed directly from the scan profile whether or not a significant amount of radioactivity has been swallowed before the first measurement. However, it should be appreciated that any differences between the estimates for 'throat losses' of different research groups may be due not only to differences in technique, but also to differences in the definition of this fraction.

The initial value of the lung deposit from below or just below the larynx, was derived from the second scan profile performed 9 - 10 minutes after the end of aerosol administration. There may have been a finite fraction of tracheal deposit cleared in this period, most of which would be included in the fraction, fS(I). This magnitude may be estimated from the lung clearance curves averaged over three subjects at each particle size (Figures 5.2.1 - 5.2.4, Chapter 5). In the particle size range studied (1·5 - 13·0 μm diameter), this magnitude was between 2 - 4% of the

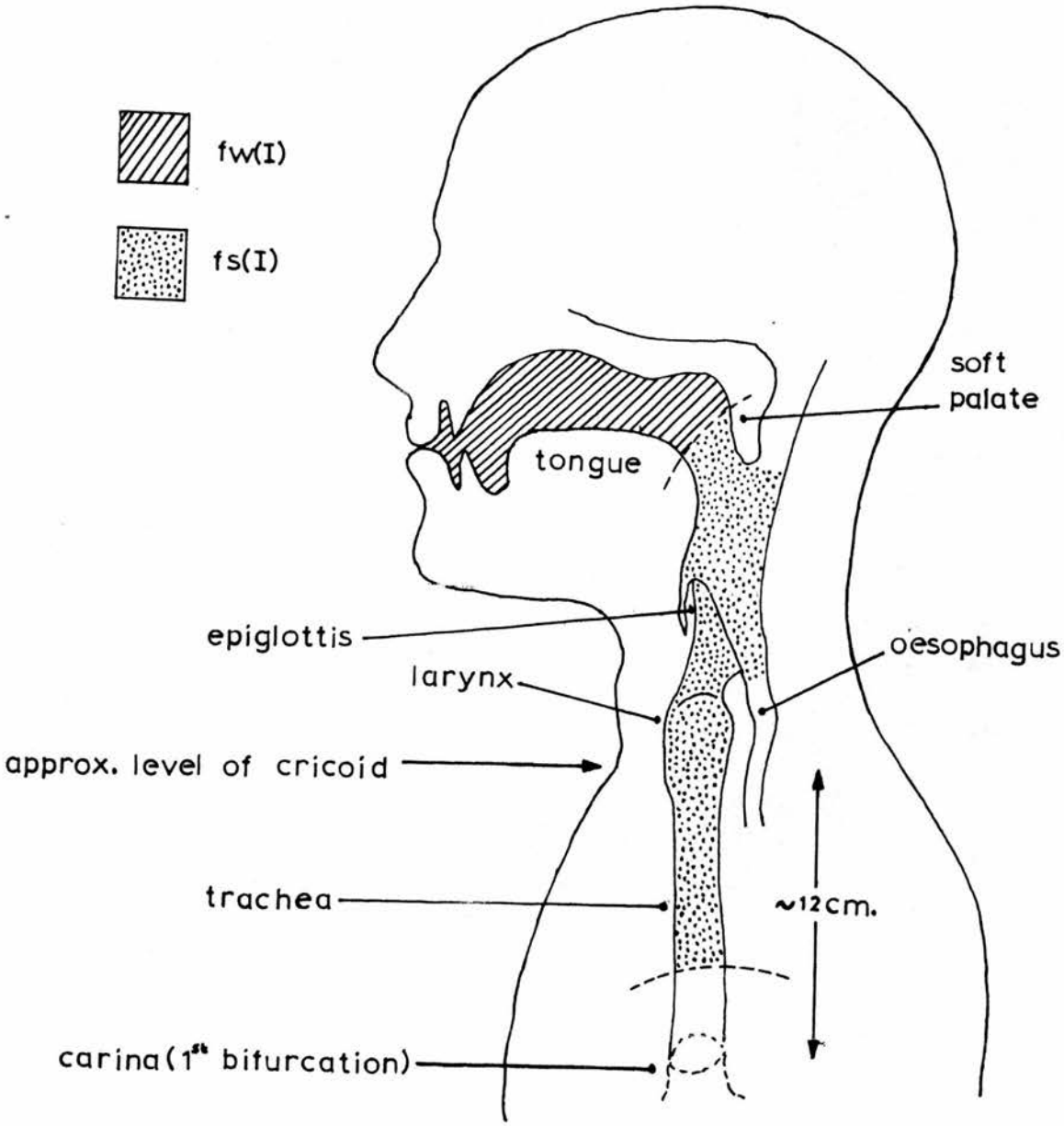

Figure 3.3.6: Regional deposition fractions fW(I) (mouth deposit), fS(I) (throat deposit) - approximate maximum boundaries of inclusion.

initial deposit over the first ten minutes of clearance after aerosol administration, the largest particle size exhibiting the most rapid clearance, as might be expected. In terms of the amount of aerosol inhaled by a subject these magnitudes reduce to, $(fC(I) + fR(I)) \times (2 - 4\%)$, which gives values in the range 1·5 - 2·0% in the particle size range studied. In addition to the two profile scans performed 1 - 2 and 9 - 12 minutes after aerosol administration, between these times, approximately 4 - 5 minutes after aerosol administration, measurements of tracheal radioactivity immediately below the larynx were conducted, using a fixed radiation detector system. A second such measurement was performed immediately following the second profile scan, about 11 - 14 minutes after aerosol administration. These measurements were actually initiated for a quite different purpose, explained below, and not all subjects were measured. Details of the method are given in part (iii) of this section. By estimating the area of the tracheal clearance curve bounded by these times, the magnitude of the deposit which had passed through the trachea in that interval could be estimated in relation to the magnitude of the deposit subequently cleared through the trachea, i.e. to fC(I). These estimates confirmed those obtained from the averaged profile scan clearance curves, giving average values at each particle size in the range 0·3 - 1·6% for the deposit cleared between the first and second tracheal measurements, expressed as a percentage of the amount of aerosol inhaled by the subject (Table 3.3.1). These percentages amounted to only a small fraction of fS(I) at any

$\bar{d}$ µm	subject	% of I	average % of I
13·0	A D	1·9	1·52
	J H	1·1	
4·5	ATM	0·4	0·31
	F H	0·1	
	R H	0·5	
10·4	P T 2	1·0	0·85
	K D	0·7	
4·6	MS 1	0·2	0·44
	MS 2	0·6	
	J V	0·5	

Table: 3.3.1: Estimation of amount cleared between first two throat measurements. Particle size range 4·5 – 13 µm.

particle size (see Chapter 5). It is not possible to reach conclusions as to the proportions of aerosol which initially deposited in the pharynx or larynx separately, owing to uncertainty concerning the amount of clearance from the larynx before the first, fixed detector, throat clearance measurement. However, it may be observed that owing to the small proportion of radioactive particles estimated to have been cleared in the first 9 - 12 minutes after the end of aerosol administration, the striking differences between these results and those reported by ALBERT et al. (1967), LIPPMANN and ALBERT (1969) and ALBERT and LIPPMANN (1973), cannot be explained in terms of differences in the definition of deposition and clearance fractions. Differences in technique must therefore be considered. This is discussed further in Chapter 5.

Figure 3.3.3 shows scan profiles for one subject*1 at successively greater times after aerosol administration. The regions containing cleared and retained radioactivity are readily discernible on the later scan profiles.

Planimetric analysis of the scan profiles (CAMNER, 1971) was rejected on the grounds that assumptions would be required concerning the shape of the purely abdominal or lung profiles in the region of overlap. Instead, the lung contribution was obtained by summation of all counts to the right of an anatomical reference point, marked 'X' on Figure 3.3.5, a certain number of channels beyond which it was considered that the abdominal contribution would be neglible. Before each experiment the subject's chest was marked close to the xyphoid process of the sternum bone, such that the position of the mark relative to the scanner trolley, and

*1 Using this same example, the analytical procedure by which the deposition fractions and clearance curves were derived from the scan profiles is demonstrated in Appendix 4 of the thesis.

hence to the scan profile, could be conveniently determined. Five separate clearance curves were initially derived from the whole series of scan profiles for each subject: Σx, $\Sigma x - 5$, $\Sigma x - 10$, $\Sigma x - 15$, $\Sigma x - 20$; each of which, except for Σx, were derived by summation of five fewer channels than the preceding clearance curve (Figure 3.3.5(iv)). The same section of the lung profile would therefore be included in the determination of each point on the curves, provided the anatomical reference point had been accurately measured. It should be noted that by adopting this method of analysis, the derived levels of retention could exceed unity, for certain periods, since material was cleared upwards into the selected summation region of the profile scan prior to removal into the abdominal region. The effect was likely to be most pronounced over the smallest summation sections (e.g. $\Sigma x - 20$, Figure 3.3.7).

As might be expected the clearance curve based on the highest number of detector counts, i.e. Σx, exhibited the least scatter of points, and that based on the smallest, i.e. $\Sigma x - 20$, exhibited the largest. An example is shown in Figure 3.3.7. However, the scatter was greater than anticipated on a purely statistical basis (discussed in part (ii)d of this section). Moreover it appeared not to be entirely random but often formed distinct peaks along the curves when several successive points were close, which became more pronounced on those curves derived from scan profile sections at successively greater distances from the referance point, 'X', implying an association with the upper reaches of the lungs,

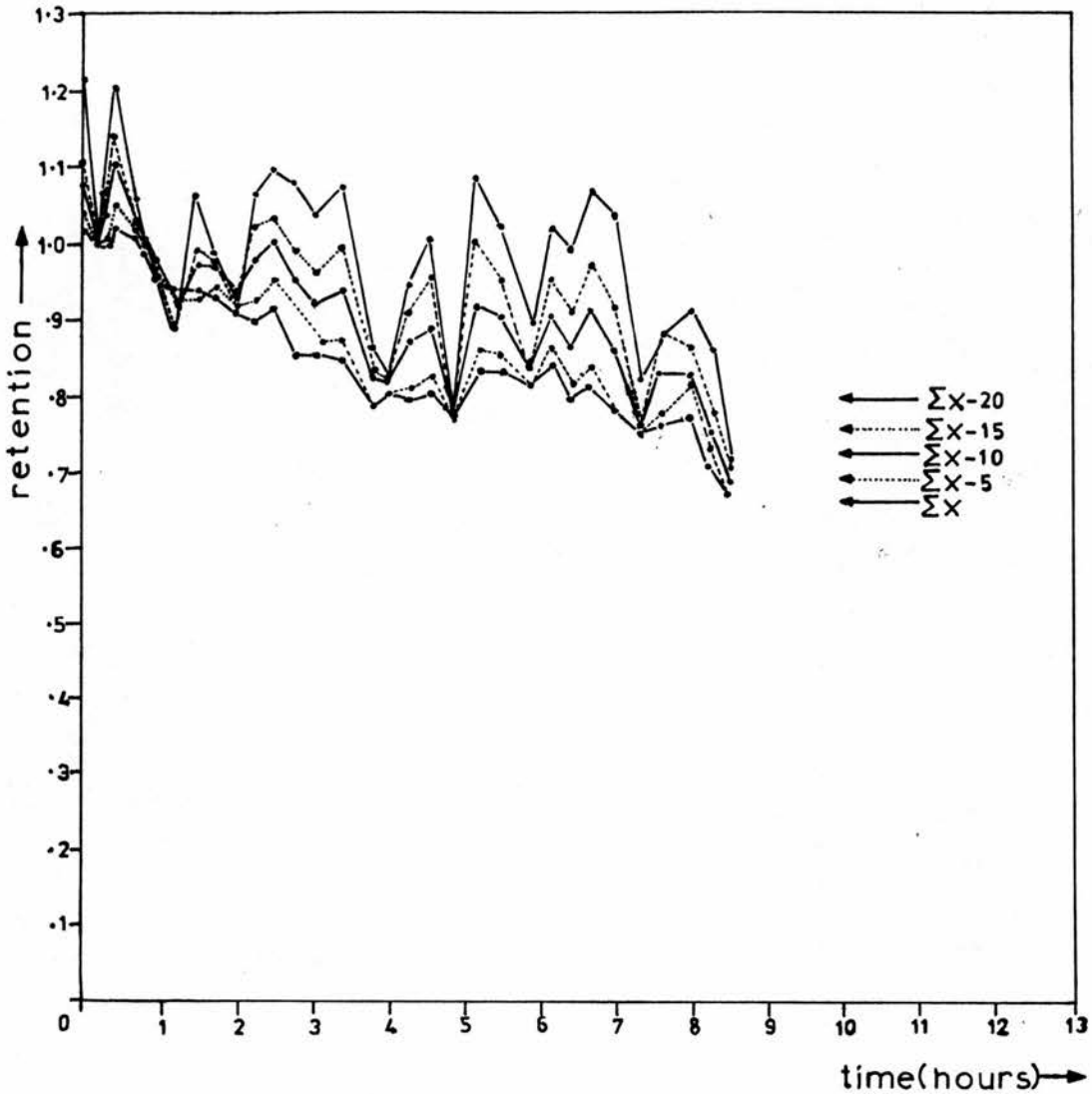

Figure 3.3.7: Example of family of clearance curves obtained for one subject (AM), $\bar{d} = 4{\cdot}6\ \mu m$.

towards the trachea. The possible origin of this phenomenon is discussed below and in Chapter 5. This scatter reduced considerably for the final profile scans, 20 - 22 hours after aerosol administration, although by this time purely statistical scatter was more important. A small range of values for fC(C + R), fR(C + R), was therefore possible and it was considered necessary to adopt a standard criterion for the selection of the summation section to be employed in the derivation of these values, in each case. As the position of the abdominal peak on the scan profile was of most importance in determining the degree of lung/abdominal overlap, the criterion adopted was derived by projecting the right - hand side of the abdominal peak, which was in all cases discernible, to the channel number scale baseline at 'a', Figure 3.3.5(iv). In the event of a small quantity of abdominal radioactivity residing at 'a', in the subject, it would be approximately ten channels further along the profile before its contribution to detector counts fell to nought. The summation point was therefore selected as that which was greater than ten channels from 'a'. This was normally either $\Sigma x - 5$ or $\Sigma x - 10$, and in a few cases, $\Sigma x - 15$. The proportion of total initial lung counts included in the derivation of the selected clearance curves averaged $52 \pm 24\%$ (mean $\pm$ standard deviation).

A comparison between the methods used to obtain the lung clearance curve from the scan profiles was made in one subject (Figure 3.3.8(i)). One clearance curve was derived using a planimetric method, based essentially on the assumption of

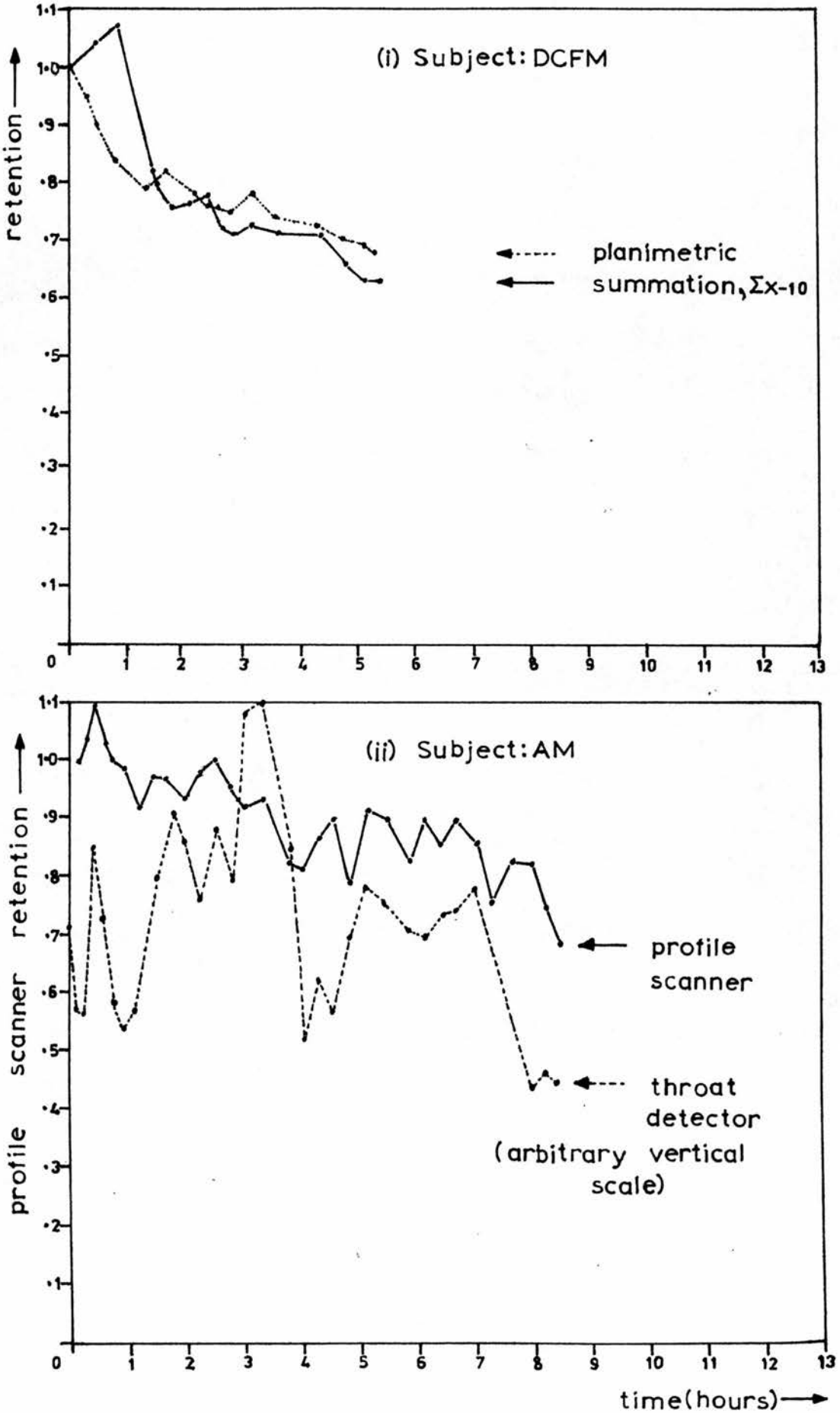

Figure 3.3.8: Comparison of methods of profile analysis (i) and observation of clearance fluctuations (ii).

symmetry between the right and left halves of the abdominal and lung sections of the scan profiles. The other clearance curve was derived from the same profiles using the summation method described above. As shown in the figure, the scatter of points is far less for the curve derived by the planimetric method and is similar to those reported by CAMNER (1971). A larger scatter of points was observed whenever the summation method was employed. Individual and group average clearance curves are presented and discussed in Chapter 5, section 2.

It was considered that the clearance pulses may have arisen as a result of an experimental artefact, although none was known that could satisfactorily explain such non-random behaviour. To investigate the possibility that the phenomenon was due to genuine variations in the radioactive content of the lung section being scanned, for one subject, a single fixed radiation detector was placed vertically over the throat at regular intervals during the clearance period. The detector consisted of a scintillation crystal (Nuclear Enterprises Ltd), optically coupled to a photomultiplier tube, which was mounted in a cylindrical brass collimator (bore = 6·5 centimetres) at a depth of 8 centimetres. The photomultiplier output was fed into a counter-ratemeter and single channel analyser (J and P Engineering Ltd., type MS310) and the number of detector counts obtained over a two-minute counting period was recorded manually. Figure 3.3.8(ii) shows the result obtained after application of the appropiate corrections for radiation background and isotope decay. The reasonable degree of temporal matching

between the scanning and fixed detector clearance pulses indicated that the clearance pulses were indeed associated with the distribution of radioactivity in the subject. The phenomenon was further investigated in other subjects and more refined methods of measuring the clearance of radioactive particles in the throat were developed. These are described in part (iii) of the present section.

3.3(ii)d Limitations of profile scanning

The use of a profile scanner in the estimation of the deposition and retention of radioactive particles in the respiratory tract has been described above, but not its limitations. These are difficult to quantify and involve complex considerations.

An important limitation was that the spatial response of the scanner was not entirely uniform but varied in a complicated way according to the photopeak energy of isotope used, the mode of combining detector counts from each detector output, and the degree of variation in tissue scatter from point to point (TOTHILL and GALT, 1971). Spatial response was measured using a hardboard phantom, having a density of approximately 10^{3} $Kg.m^{-3}$. to simulate tissue scatter. A Tc^{99m} point source was placed at various points within the phantom and a profile scan was performed for each source position, the settings being the same as they would for a profile scan of an actual subject. The total detector counts for each scan were corrected for background and isotope decay and expressed as percentages of the counts obtained after scanning the point source at the mid-line of the mid-plane between the detectors (Figure 3.3.9). Point to point variations of about $\pm$ 30% were

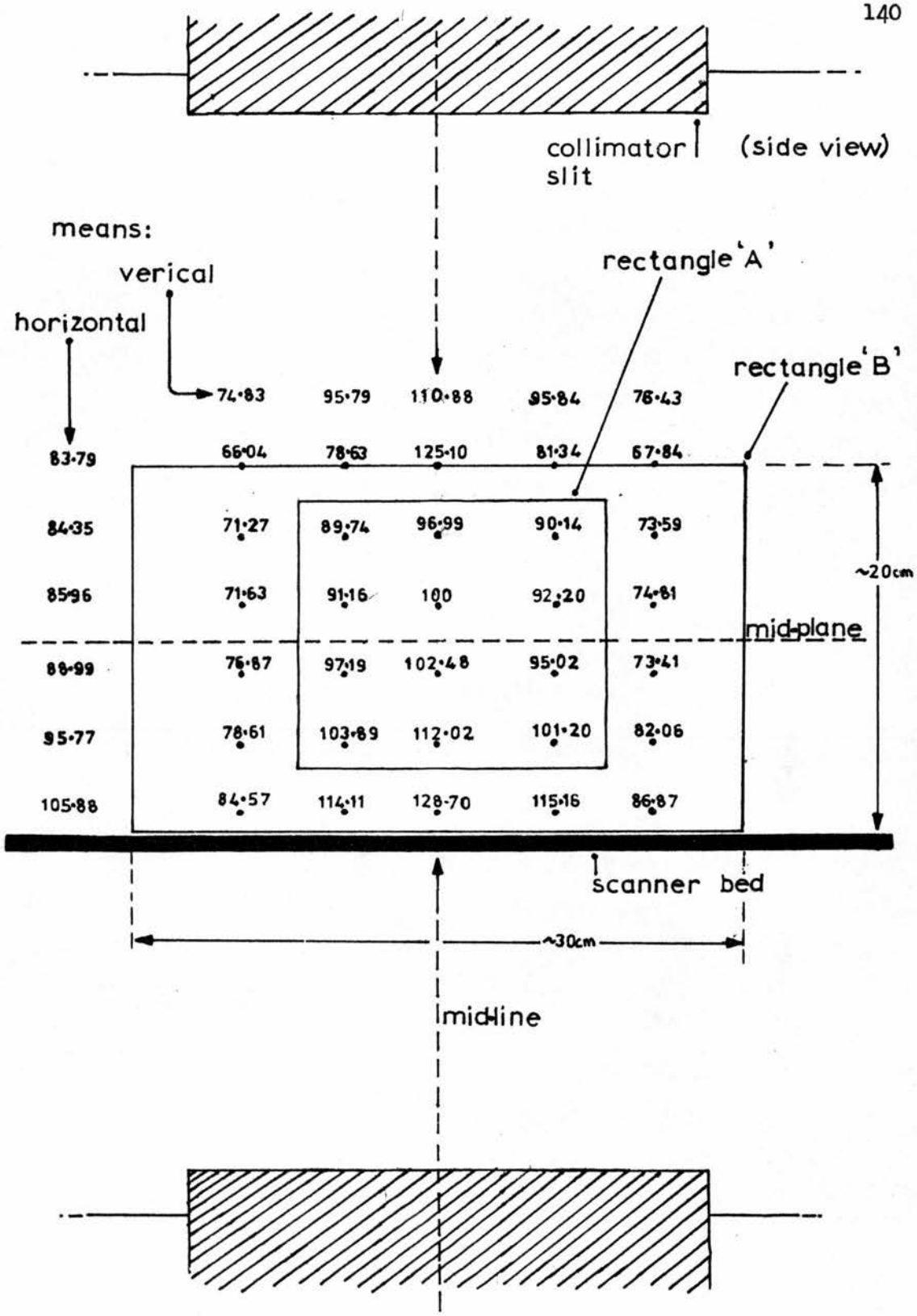

Figure 3.3.9: Spatial response of profile scanner.

observed. However,it should be appreciated that such variations would only be of any consequence when the initial spatial distribution of radioactivity differed significantly from that of of the final. The fraction of initial radioactive lung burden which was retained in the lungs would be measured with the same overall sensitivity throughout all profile scans, other factors being equal, if the spatial distribution was constant throughout. This would not be the case with the total lung burden, as this would include that fraction to be later cleared from the lungs, which would be unlikely to have the same spatial distribution as the retained fraction, at any time. Quantification of the overall effect presents great difficulties owing to the variety of unknown anatomical and particle distribution factors. It should be borne in mind that it is the initial distribution of deposited particles in the lungs that is important, not their distribution during the clearance process which has no bearing on final point determination. If the particles were initially deposited in the small airways ($<$2mm diameter), their spatial distribution might be expected to closely resemble that of the fraction later retained in the lungs, which would reside wholly or mainly in the non-ciliated respiratory zone. It is therefore likely that the effect was most important at large particle sizes, where penetration to both the small airways and respiratory zone was small. In this case the initial particle distribution of the fraction to be later cleared from the lungs would tend to be more centralized than that of the retained fraction, which would therefore tend to

be more peripheral. The overall effect may be quantified in a crude worst-case manner by assuming that the fraction to be later cleared has an initial uniform distribution entirely enclosed within the rectangle A, Figure 3.3.9, while that of the retained fraction is uniformly distributed in the remaining area, B. Taking the average of all percentage values in each area gives roughly 86% and 98%, for areas B and A, respectively. The radioactivity in area A is therefore 'overestimated' by approximately 12% relative to that in area B, which is considerably less than the maximum point to point variation. In practice it is probable that even at large particle sizes there is a finite degree of overlap between the initial distribution of retained and, later, cleared fractions, hence the overestimate of the latter compared to the former would be lower than 12%. It should also be noted that this figure is a percentage of the cleared deposition fraction, not of the amount of inhaled aerosol, I.

Using the profile scanner it was uniquely possible to obtain direct evidence of the magnitude of the combined effects of variations in detector spatial response and tissue attenuation, not over the thoracic cage alone, but over the entire body. This was accomplished by plotting the total detector counts over the whole of each profile scan, corrected for radiation background and isotope decay, over the whole series of scans obtained for each subject. Fixed radiation detectors which measure a selected part of the body cannot readily be used for this purpose. Variations in the measuring sensitivity of the cleared fraction due to its

movement from the chest to the abdomen might be expected to be comparable if not actually greater than those arising from differences in the spatial distribution of radioactivity within the thoracic cage, owing to its initial concentration into the regions bounded by the stomach and small intestines. The results for all subjects are shown in Figure 3.3.10. It has been assumed that no faecal clearance of radioactivity occurred during the first five hours after aerosol administration. The percentage variation in total detector counts was shown to normally be within $\pm$ 5%, rarely exceeding $\pm$ 10%, of the initial value, indicating that the percentage error in the estimation of the clearance and retention fractions, fC(C + R) and fR(C + R), would be comparably small, and still smaller in terms of the amount of aerosol inhaled by a subject, I.

It should be noted that some of the variation shown in Figure 3.3.10 would undoubtedly have arisen as a result of errors in the positioning of the subject on the scanner trolley. As far as possible the subject was always centralized on the same horizontal line relative to the detectors, but subject movement during a scan (duration = 200 seconds) could never be entirely eliminated. Intrinsic variation and drift in the detectors and associated electronics could be accurately monitored by scanning several standard radioactive samples throughout the measuring period, under conditions of constant geometry. Detector drift rarely exceeded $\pm$ 5% of the initial value from first to final scan, which was approximately double the percentage variation from scan

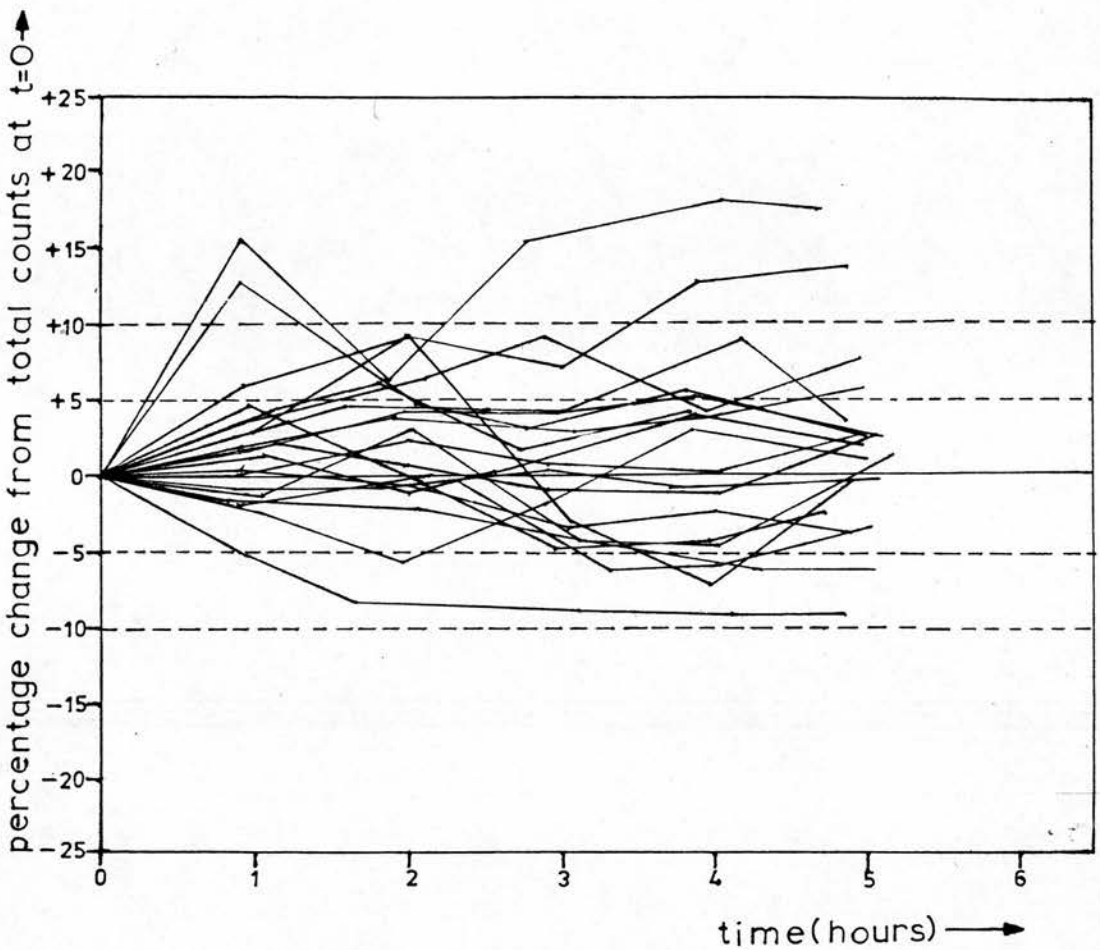

Figure 3.3.10: Variation in total count rate over first five hours for all subjects.

to scan. Further details are given below. The results shown in Figure 3.3.10 therefore indicate that the variation in detector spatial response and tissue attenuation were not serious limiting factors in the accuracy of the determination of the regional deposition fractions, using the profile scanner. This, coupled with the other advantages of profile scanning over fixed detector methods, makes the method the most appropiate one for lung clearance studies.

Radioactive decay is a random process and there is therefore a degree of uncertainty in the accuracy of any measured value that is dependent on the number of recorded detector counts per unit time, the number of repeat measurements, and whether or not the final value has been obtained from measurement of additional quantities, e.g. background radiation, in which there is also a random variation.

The standard error or standard deviation, σ_N, of individual values about their mean may be estimated, by assuming a Poisson distribution, using,

$$\sigma_N = \sqrt{\bar{N}} \simeq \sqrt{N}, \quad \text{if} \quad \text{is small} \quad \ldots\ldots\ldots \text{ equation 3.3.13}$$

where, N = number of detector counts

$\bar{N}$ = average number of detector counts over an infinite series of measurements each of which were obtained over equal periods of time

The standard error of the mean of m independent measurements,

$\sigma_{\bar{N}m}$, is given by,

$$\sigma_{\bar{N}m} = \frac{\sigma N}{\sqrt{m}} \qquad \text{..... equation 3.3.14}$$

Expressed in terms of the relative standard error, $\nu\bar{N}$, or coefficient of variation, about the mean of m measurements this becomes,

$$\nu\bar{N}m = 100\,\frac{\sigma\bar{N}m}{\bar{N}m} = \frac{100}{\bar{N}m}\left[\frac{\bar{N}m}{m}\right]^{\frac{1}{2}} \% \qquad \text{..... equation 3.3.15}$$

where, $\bar{N}m$ is the average value of N over m measurements

The standard error, σ_{1-2} , of the sum or difference of two independent measurements is given by (TOPPING, 1965),

$$\sigma_{1-2} = (\sigma_1^2 + \sigma_2^2)^{\frac{1}{2}} \qquad \text{..... equation 3.3.16}$$

where, σ_1 , σ_2 , are the standard errors of each measurement.

Using the above equations to determine $\sigma_{\overline{1-2}m}$, the standard error of the difference of two measurements over m independent observations, gives,

$$\sigma_{\overline{1-2}m} = \left[\frac{N_{\overline{1+2}m}}{m}\right]^{\frac{1}{2}} \qquad \text{..... equation 3.3.17}$$

and from equation 3.3.15,

$$\nu_{\overline{I-2}m} = \frac{100}{N_{\overline{I-2}m}} \left[\frac{N_{\overline{I+2}m}}{m}\right]^{\frac{1}{2}}\% \quad \text{..... equation 3.3.18}$$

where, $N_{\overline{I+2}m}$, $N_{\overline{I-2}m}$ = the average sum or difference of detector counts over m independent measurements, each of which were obtained over equal periods of time.

Calculated from equation 3.3.18, values of $N_{\overline{I-2}m}$ needed to be in the region of 3,500 detector counts, equivalent to approximately 29 KBq (0·78 μ Ci) of whole body radioactivity at the time of the final scan, or about 444 KBq (12 μCi) at the time of aerosol administration, to ensure that $\nu_{\overline{I-2}m}$ was within $\pm$ 2% of the mean value that would be obtained from an infinite series of measurements, with a probability of 0·683 that the average value over 3 observations, (m = 3), would fall within this range, or a probability of 0·955 that it would fall within twice this range. These were considered to be the acceptable levels of uncertainty. In some cases $\nu_{\overline{I-2}m}$ exceeded 2%, the highest value being 3%, the average being 1·8%, owing to a certain degree of unpredictability in the aerosol delivery efficiency of the aerosol administration apparatus and in the value of total deposition, fD(I), for any subject.

3.3(ii)e Use of profile scanner in the measurement of radioactive samples and detection of in vivo leaching

All radioactive samples were positioned at a standard vertical

and horizontal position relative to the scanner detectors, for radioassay. The aerosol collection bags (see part 2(iii) of the present chapter), were folded into almost flat, geometrically identical, cardboard envelopes, such that the entire sample was scanned at a constant height.

Radioactive attenuation through the walls of each sample container was small, estimated to be less than 6%, and in any case approximately equal for each sample. For samples containing liquids (mouthwash), a calibration factor was derived in a separate experiment involving reference sources. Three independent measurements of each sample were taken and one sample, the inspiratory collection bag, was scanned repeatedly throughout the measuring period (20 - 22 hours) as a check on the stability of the profile scanner electronics. The drift in the latter only occasionally exceeded $\pm$ 5% from first to final scan, which was approximately double the typical percentage variation in sample counts, from scan to scan. A correction factor for amplifier drift was applied on the basis of the mean percentage change over three scans of the inspiratory collection bag, performed at the beginning and end of the measuring period.

By means of a standard reference source of known absolute radioactivity, it was possible to calculate the radiation dose administered to a subject. Calculation of total deposition and its subdivisions did not depend on a knowledge of absolute radioactivity, because all samples were measured with the same counting efficiency, or detector sensitivity, and only relative counts for

each needed to be determined.

The inaccuracy in the measurement of the radioactive samples due to random statistical variations in emitted radiation was negligibly small, because these were measured shortly after aerosol administration when only a small amount of radioactive decay had occurred. The exception to this was when the radioactivity of a sample was extremely small in relation to that of the aerosol inhaled by the subject, I. In this case although the coefficient of variation $\nu_{\overline{I-2m}}$, calculated from equation 3.3.18, might be relatively high, it was still negligibly small in relation to I.

Profile scanning is of considerable advantage in the detection of possible *in vivo* leaching of radioactivity from labelled particles, since if radioactivity is removed from one zone it inevitably appears in another. According to HARPER *et al.* (1966), the physiological behaviour of pertechnetate compounds is similar to that of iodine, which is selectively concentrated in the thyroid and salivary glands and the stomach, transferal occurring via the bloodstream. With the exception of the stomach, such concentrations would be readily discernible on the scan profiles if of at all significant magnitude. Moreover, any radioactive content in the bloodstream would be apparent as an excess of counts above background over those channels on the scan profile corresponding to the position of the subject's legs on the scanner trolley. Such concentrations or excesses of radioactivity were not observed for any subject. Nevertheless, the possibility of an urinary excretion of leached radioactivity was investigated in one subject (AR), by

collecting the total urinary output for eight hours after aerosol administration. The urinary sample was measured for possible radioactive content, using the profile scanner, but the detector counts were found to be at the background level.

3.3(iii) Observation of tracheal and laryngeal clearance

The origin of these observations was described in part 3(ii)c above. A single detector was used in the first instance in an attempt to observe ciliary clearance in the throat of one subject (Figure 3.3.8(ii)). However, this detector was insufficiently well collimated to guarantee effective exclusion of the uppermost section of lung, that nearest the first rib of the subject, which extends typically to a line approximately four centimetres above the manubrium sterni, at the chest mid-line, as observed on randomly selected chest radiographs (Figure 3.3.13). Consideration was given to the origin of the clearance pulses and the possibility that they arose as a consequence of a periodic accumulation and emptying of ciliary transport fluid, within the larynx, was investigated. A fixed, double, radiation detector apparatus was constructed: one detector was positioned over the subject's larynx (Ta); while the other was situated over a region just below the cricoid cartilage of the larynx (Tb), such that a short section of the trachea would be included in its field of view and the upper lung lobes would ideally be wholly excluded (Figure 3.3.11(i) and (ii)). If the clearance pulses were arising as a consequence of a periodic accumulation and emptying of ciliary clearance fluid within the larynx in an otherwise 'smooth' clearance process, two

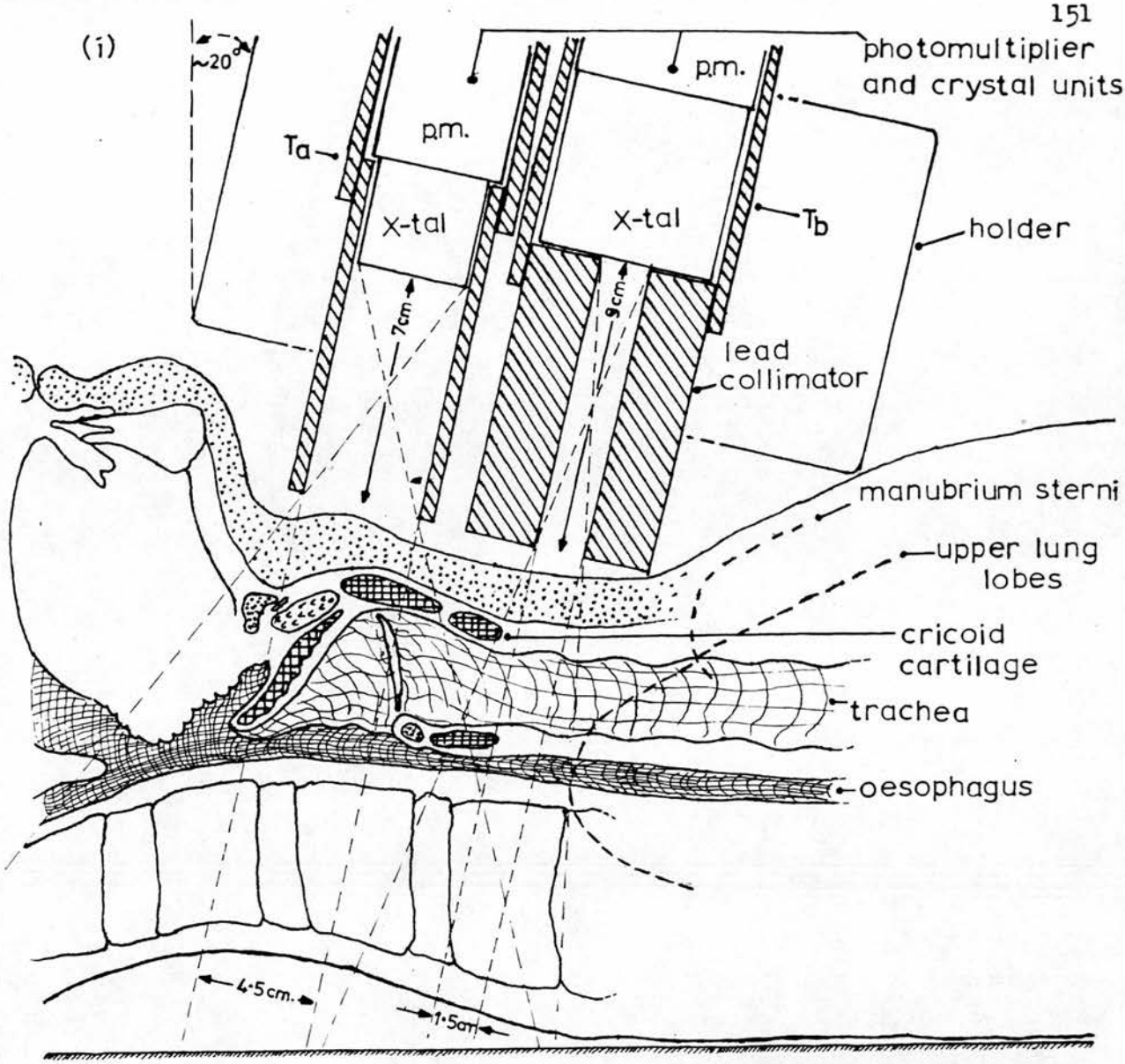

(ii)

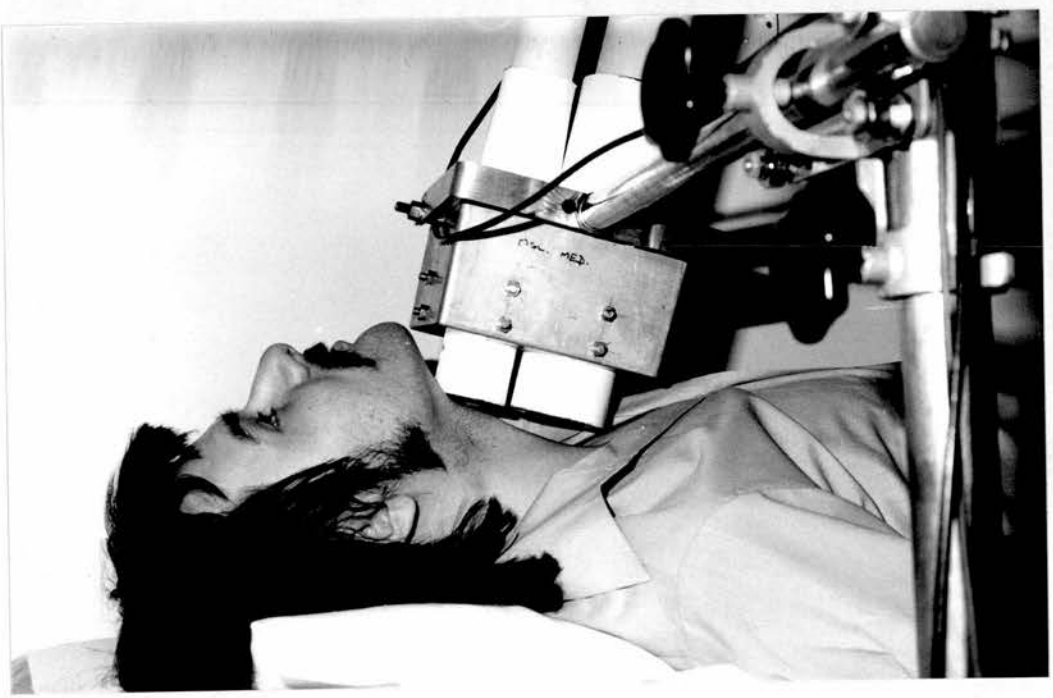

Figure 3.3.11: Throat clearance detectors.
Sectional view (i); Photograph of subject (ii).

distinct clearance curves would be obtained: one characteristic of genuine variations in the amount of radioactivity entering the larynx; the other characteristic of some other process occurring within the larynx itself. If, on the other hand, the clearance pulses were reflected in genuine variations in the distribution of radioactive particles entering the larynx, the larynx itself playing only a minor modifying role, two similarly pulsatile clearance curves would be obtained which were out of phase by the time of ciliary transit between the two detectors. Figure 3.3.12 shows the first result (subject AD) using the double detectors, which is highly consistent with the latter hypothesis.

The same detector configuration was used for all subjects studied subsequently to subject AD, Figure 3.3.12, and similar results were obtained in some cases (see Chapter 5). Owing to intersubject anatomical variations, an apparatus designed for a supposedly average subject could never be completely effective in all cases. The collimator design and dimensions were selected following examination of a number of chest radiographs, both lateral and frontal (N.C.B., medical survey unit). From these a typical value of 4 centimetres for the distance of vertical separation between the upper lung lobes and top of the manubrium sterni, at the chest mid-line, was determined. This leaves very little room for the placing of a detector between the cricoid cartilage of the larynx and the uppermost part of the lungs. Advantage had therefore to be taken of the area of tissue between the right and left upper lung lobes, by placing a slit-collimated

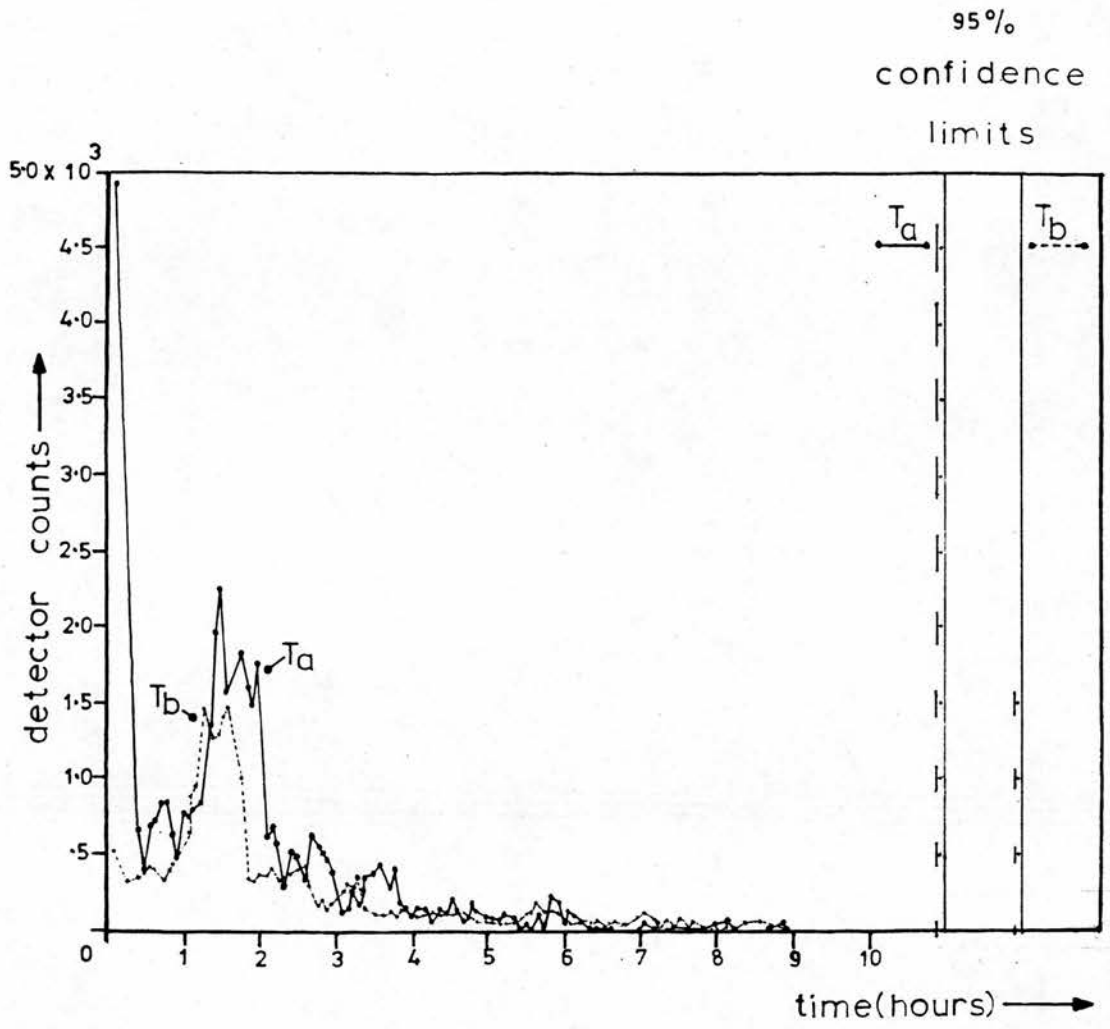

Figure 3.3.12: Throat clearance curves. Subject: AD; $\bar{d} = 13\ \mu m$.

detector at a slight inclination ($\sim 20°$) over this region, in order to detect tracheal clearance (Figure 3.3.13). Collimator design and positioning of the purely laryngeal detector was more straightforward (Figure 3.3.11(i)). In many cases, particularly at large particle sizes, the bulk of material was cleared within the first few hours after aerosol administration, as measured by the profile scanner. The tracheal and laryngeal detectors confirmed these rapid clearances and moreover their detector count rate was often later observed to fall to the background level, thus confiming that there had been no inclusion of radioactivity in the upper lung lobes.

Inevitably, because such a small area of the respiratory tract was observed during any measurement, radiation counting statistics were often poor, particularly towards the end of the clearance period. The 95% confidence limits have been indicated on all throat clearance figures. It should also be noted that the clearance pulses cannot be explained in terms of the passage of single or small groups of particles beneath the detectors. There were normally fewer than two detector counts per particle through the measuring period, which is distinct from and considerably lower than, the number of photon emissions per particle per unit time ($\leq$ 4 per second), as estimated from:

$$Nc = \sum_{n=1}^{x} \frac{Cn}{\overline{Nn}} = \frac{\sum_{n=1}^{x} Cn.tm}{fC(I).Ni.x.td} \quad \text{..... equation 3.3.19}$$

where, Nc = the number of detector counts for one particle present beneath the detectors for time td.

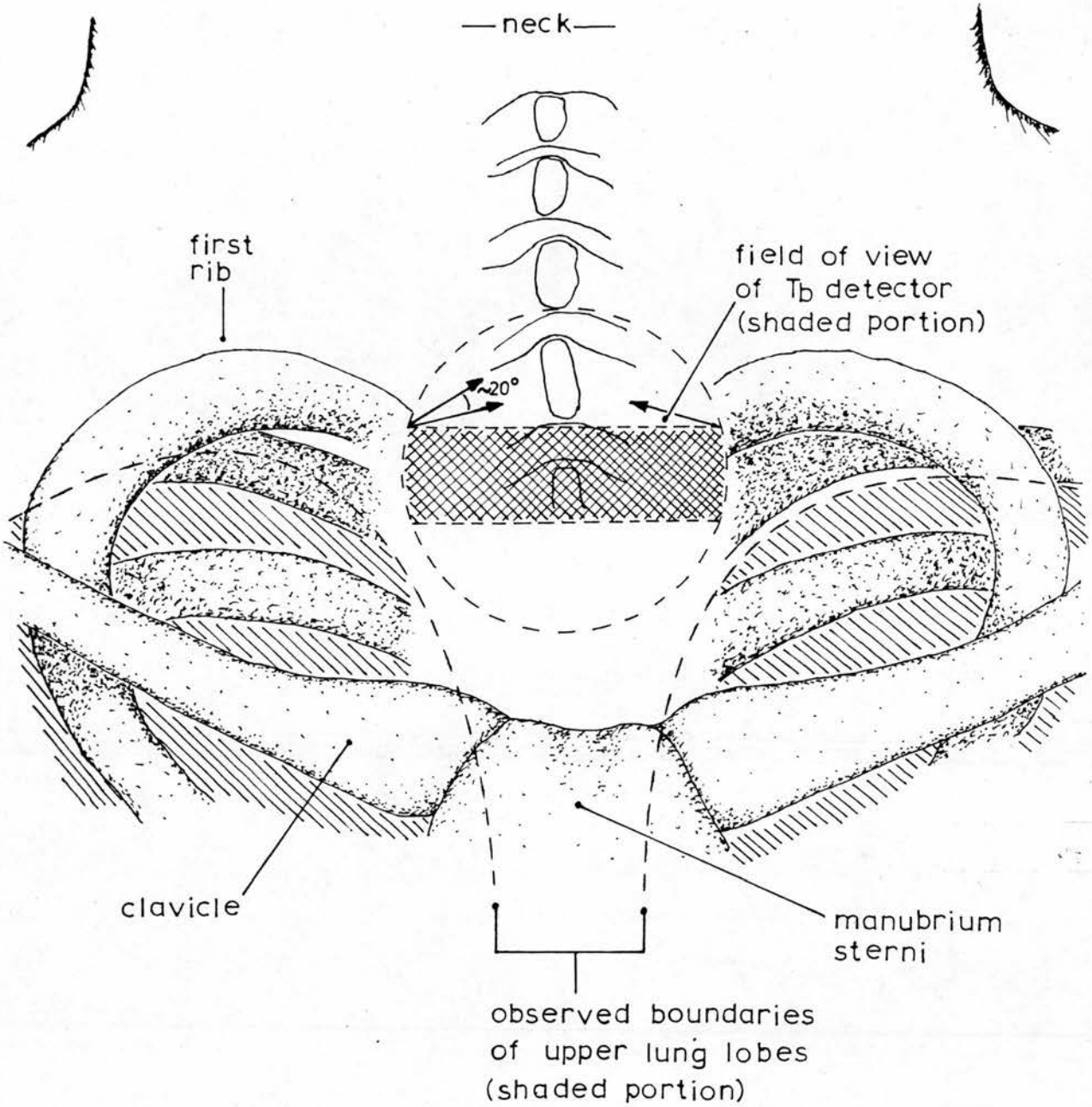

Figure 3.3.13: Shaded tracing from a chest X-ray (1:1 scale) illustrating difficulty of positioning the T_b detector over trachea.

td = time of detector measurement ($\sim 0{\cdot}033$ hour)

tm = time of total measuring period (~ 9 hours continuously)

x = number of measurements over period tm

N_i = number of particles inhaled by the subject

Nn = number of particles present beneath the detectors during the summed period of all measurements, (td.x)

Cn = total detector counts over measurement, n, corrected for radiation background and isotope decay; $1 \leq n \leq x$

$\sum_{n=1}^{x} Cn$ = total detector counts of each measurement, Cn, summed over all measurements, x.

Being single detectors, there was a greater variation in throat detector response with source depth than for the profile scanner. The hypothetical range of vertical movement for a source within the trachea or larynx would be in the region of two centimetres. If a point source moved this distance from an initial position ten centimetres from the detector crystal, the response would vary by some 30%, expressed as a percentage of the maximum. However, it is improbable that such a range of movement, in a vertical direction, would occur in the trachea (assumed horizontal) from one measurement to the next. In the larynx the situation is less certain, but the close matching, both temporal and in terms of relative magnitudes, obtained between the laryngeal and tracheal clearance curves for subject AD, suggests that the effect of any depth response variation was not large.

As the purpose of making the observations was essentially qualitative, no attempt was made to determine absolute or relative

magnitudes of radioactivity being cleared at different times. The rates of rise and fall of the clearance pulses and their degree of matching in the larynx and trachea, were considered to be of most interest. For this reason as many observations per unit time as possible were conducted for each subject. Four consecutive throat detector measurements, each of two minutes duration, were interspersed with a single profile scan, giving an interval of 8 - 10 minutes between each set of four. Before either type of clearance measurement the subject swallowed a mouthful of drinking water to assist in the clearance of material lodged in the pharynx. Clearance measurements of one form or the other were therefore conducted continuously for a long period, normally 8 - 9 hours after aerosol administration.

The throat clearance results are presented and discussed in Chapter 5, section 2, part (ii).

3.4 Subjects and experimental procedures

Consent to perform the experiments was obtained from the M.R.C. Isotope Advisory Panel (at the time of writing now under the auspices of the D.H.S.S.) and the local ethical committee of the hospital in which the experiments were conducted. The radiation doses administered to the subjects (average ~ 50 μSv or ~ 5 m.rem to any organ) were considerably less than that given in a typical chest X-ray. A total of eighteen male volunteer subjects participated in a total of twenty experiments and the nature of the work was fully described to each. Their physiological and lung function data are listed in Table 3.4.1. Only a few subjects reported symptoms of respiratory infection on the day of an experiment and those concerned have been indicated in the table.

Each smoker subject was requested not to smoke on the day before, or on the day of, an experiment. Instructions to subjects as regards swallowing and coughing, during and shortly after aerosol administration, were described in part 3(ii) above. No special instructions were given as regards coughing after the second profile scan since if this were an important factor in the natural clearance process of a subject it was considered desirable to allow it. However, only one subject (VC), a smoker, was observed to find it necessary to occasionally cough throughout the continuous part clearance measuring period (8 - 9 hours). During the latter period the subjects spent approximately half their time in a supine position. The possibility of a gravitational influence on ciliary clearance cannot be excluded. However, because of the relatively large number of clearance measurements necessary

subject	age years	height m.	weight kg.	FEV^1 l. *	FVC l. *	VC l. *	ERV l. *	A.	B.	C.
DCFM	45	1·86	71	4·32	5·70	nd	nd	110·8	NS	N
AM	29	1·71	67	4·75	5·75	6·02	2·17	121·8	NS	N
AR	26	1·67	68	3·07	3·55	3·60	1·30	80·8	NS	Y
gp.av.	33·3	1·74	68·7	4·04	5·00	4·81	1·74	104·5		
HG	30	1·86	94	4·50	6·07	5·94	1·48	102·3	NS	N
RB	26	1·83	81	4·85	5·88	6·33	1·95	110·2	NS	Y
PCE	26	1·80	78	4·80	6·28	6·02	nd	111·6	NS	N
gp.av.	27·3	1·83	84·3	4·72	6·08	6·10	1·72	108·0		
PT	55	1·72	67	3·20	4·60	4·84	1·65	94·1	NS	N
PH	25	1·78	57	5·07	2·48	5·24	2·10	117·9	LS	N
KD	28	1·76	70	4·28	5·10	5·32	2·20	104·4	NS	N
gp.av.	36·0	1·75	64·7	4·18	4·06	5·13	1·98	105·5		
TDW	46	1·80	84	3·65	4·96	nd	1·42	98·6	PS	N
JH	31	1·70	63	3·95	4·70	4·75	1·90	103·9	NS	N
AD	25	1·72	64	4·25	5·85	5·76	2·52	106·3	NS	N
gp.av.	34·0	1·74	70·2	3·95	5·17	5·26	1·95	102·9		
ATM	33	1·86	68	5·34	6·50	6·70	2·32	124·2	NS	N
FH	28	1·89	72	5·42	7·00	6·89	3·14	117·8	NS	Y
RH	33	1·87	81	5·37	6·30	6·65	1·76	124·9	NS	N
gp.av.	31·3	1·87	73·7	5·37	6·60	6·75	2·41	122·3		
VC	54	1·80	76	4·00	5·30	5·56	2·78	117·6	PS	N
MS	38	n.d.	n.d.	4·90	5·40	5·40	2·00	n.d.	NS	N
JV	38	1·78	79	3·78	5·48	5·00	1·27	96·9	LS	N
gp.av.	43·3	1·79	77·5	4·23	5·39	5·32	2·02	107·3		
pop.av.	34·2	1·79	72·9	4·42	5·38	5·63	2·00	108·5		
(σ s.d.)	9·7	0·07	9·1	0·71	1·08	0·85	0·53	11·9		

A. = % of predicted FEV^1 N = no NS = non smoker
B. = smoking history Y = yes LS = light smoker
C. = respiratory infection PS = pipe smoker
* = b.t.p.s. nd = not determined

Table 3.4.1: Physiological data. Predicted values taken from 'Lung Function' by J.E.Cotes, 1968.

(~100), in order to observe the rapid clearance fluctuations, this was considered to be an unavoidable situation.

Aerosol administration was normally initiated at about the same time of day (11.30 a.m. - 1.30 p.m.) for each subject and the clearance measurements were performed continuously for a period normally in the range 8 - 9 hours, with a final measurement (3 profile scans) at 20 - 22 hours after aerosol administration. The aerosol was normally administered for a period of 1 - 1·5 minutes, over about ten breaths. All mouthpieces were thoroughly cleaned with disinfectant before an experiment, in the interests of hygiene.

Addendum to discussion

It may be noted from Table 3.4.1 that neither the few subjects who reported respiratory infection on the day of an experiment, nor the one subject with a low value of FEV_1 were excluded from the study. This was considered to be acceptable since if significant differences between the deposition values of these individuals and the larger 'normal' group resulted, this would be of interest in its own right.

More generally, it should be clearly understood that no attempt was made in the present work to employ a population which represented the whole, however that might be defined. The aim was simply to employ male volunteers in an arbitrary age and lung function range, who represented nobody but themselves. If any significant differences in the observed deposition patterns resulted, the measurements listed in Table 3.4.1 might then be of assistance in a speculative consideration of the causes. However, a rigorous investigation of the myriad of individual factors which might influence deposition would require much larger population samples, and was therefore considered to be well beyond the scope of the present work.

CHAPTER FOUR

TREATMENT OF RESULTS AND DESCRIPTION OF LUNG MODEL

4.1 Calculation and organization of results

As was described in Chapter 3, part 2(iv)b, in some cases the proportion of satellite particles inhaled by a subject exceeded 2% by mass, or radioactivity. At the largest particle sizes, owing to the small levels of lung retention measured, it was considered desirable to attempt to express the results for two subjects (KD and TDW) in terms of those which would be obtained if primary particles alone had been inhaled. In both cases the procedure demonstrated that the corrections were always a small fraction of I ($<5\%$; Table 4.1.1).

The total deposition of an aerosol containing both primary and satellite particles is given by,

$$fD(I) = \frac{(Ip + Is) - (Ep + Es)}{(Ip + Is)} \quad \text{..... equation 4.1.1}$$

where, Ip or Is, denotes the amount of primary or satellite particles inhaled, respectively

Ep or Es, denotes the amount of primary or satellite particles expired, respectively

$$fD(I) = \frac{(Ip - Ep) + (Is - Es)}{(Ip + Is)}$$

subject	particles	$f_{D(I)}$	$f_{W(I)}$	$f_{S(I)}$	$f_{C(I)}$	$f_{R(I)}$
KD.	P+S	·9417	·0946	·4195	·2950	·1326
	P	·9644	·1047	·4605	·3057	·0936
TDW.	P+S	·9299	·0589	·4059	·3906	·0744
	P	·9428	·0636	·4365	·3992	·0434

P = primaries

S = satellites

Table 4.1.1: Satellite corrections.

since, $$fD(I) = \frac{I - E}{I}$$

$$\therefore fD(I) = \frac{(fD(I)p.Ip + fD(I)s.Is)}{(Ip + Is)}$$

where, fD(I)p or fD(I)s, denotes the values of fD(I) for primary or satellite particles, respectively.

$$fD(I) = \frac{(fD(I)p + fD(I)s.\frac{Is}{Ip})}{(1 + \frac{Is}{Ip})}$$

which rearranging leads to,

$$fD(I)p = fD(I) + \frac{Is}{Ip}.(fD(I) - fD(I)s) \quad \ldots \text{ equation } 4.1.2$$

Therefore, if the difference between fD(I) and fD(I)s, as estimated from the lower size range of the measured total deposition curve (Figure 5.2.1), is small, the difference between fD(I)p and fD(I) is also small. This was found to be the case for subjects KD and TDW (Table 4.1.1). The quantity Is/Ip was determined from the slide samples placed on the floor of the main apparatus during aerosol administration, after allowing for the effects of differential settling in the manner already described (see Chapter 3 part 2(iv)b, note that $\frac{Is}{Ip} \equiv \frac{Ns_2}{Np_2}$).

The regional deposition fraction of an aerosol containing both primary and satellite particles in region, X, say, is

given by,

$$fX(I) = \frac{(Xp + Xs)}{(Ip + Is)} \qquad \text{..... equation 4.1.3}$$

where, Xp or Xs, denotes the amount of primary or satellite particles deposited in region X, respectively.

since, $fX(I) = \frac{X}{I}$

$$\therefore fX(I) = \frac{(fX(I)p.Ip + fX(I)s.Is)}{(Ip + Is)}$$

which dividing and re-arranging as above, gives,

$$fX(I)p = fX(I) + \frac{Is}{Ip}(fX(I) - fX(I)s) \qquad \text{equation 4.1.4}$$

where, fX(I)p or fX(I)s, denotes the values of fX(I) for primary or satellite particles, respectively.

If the difference between fX(I)p and fX(I)s, as estimated from the lower size range of the measured regional deposition curves (Figures 5.1.2, 5.1.3, 5.1.4, 5.1.5)is small, according to equation 4.1.4, the difference between fX(I)p and fX(I) is also small. The largest correction to any deposition fraction was ~4% of I (Table 4.1.1) for subjects KD and TDW. The amended values for these subjects have been plotted in the figures.

The deposition fractions, fD(I), fW(I), fS(I), fC(I) and fR(I),

were measured firstly at a constant breathing pattern (tidal volume, V_T = 1·0 litre (BTPS); breathing rate = 10 breaths minute^{-1}) over a range of particle diameters (4·5 – 13·0 μm). Three subjects were studied at each particle size, making a total of twelve subjects participating in the variable particle size study. Two subjects (DCFM and PCE) were not measured at about one day after aerosol administration. In their case, the lowest point on the clearance curve was used to calculate the final level of retention. In two other cases (KD and TDW), circumstances did not permit more than one final profile scan at 20 – 22 hours after aerosol administration, and it was necessary to use only this one value in calculating their final retention. The results are presented and discussed in section 1 of the next chapter. In addition, the effects of varying the breathing pattern at a constant particle diameter (4·5 μm) were investigated in nine subjects, three at each pattern, three being in common with the variable particle size study, making a total of eighteen subjects participating in the research. The results of the variable breathing pattern study are presented and discussed in part 1(iv) of the next chapter. The number of subjects who were willing or able to participate in repeat studies, and the number of repeat studies possible, was necessarily limited by the extensive time required for each experiment. Two subjects (PT and MS) participated in the reproducibility study, two experiments being performed in each case. The results of the reproducibility study are presented and discussed in part 1(v) of the next chapter.

For all subjects a lung clearance curve was derived from the series of profile scans. Four studies were performed without any throat clearance measurements, before the relevance of the clearance pulses was fully considered (see Chapter 3, part 3(iii)). Six studies were performed using a single detector, to measure laryngeal clearance, which was described in Chapter 3, part 3(ii)c. Ten studies were performed using the double detector apparatus, which was described in Chapter 3, part 3(iii). The throat clearance results are presented, and their origin and significance is discussed, in section 2 of the next chapter.

4.2 Definition and description of lung model

For reasons discussed later, in Chapter 5, it was considered desirable to employ the measured values of regional deposition in an attempt to estimate the aerosol deposition efficiencies, as opposed to fractions, in the various regions of the respiratory tract. Four regional deposition fractions have been measured in the present work: fW(I), fS(I), fC(I), fR(I). For the purpose of the following analysis it will be assumed that each such fraction represents the fractional deposition value in a particular region, i.e. W, S, C, R, corresponding to the mouth, larynx/pharynx, dead space airways, and the respiratory zone, respectively. The validity of the assumptions will be considered in the next chapter.

In performing such an analysis it cannot be assumed that the aerosol deposition efficiencies are equal in both directions of flow, for any region, without prior consideration of the physics of the deposition mechanisms and possible variations in the

anatomy of a particular region between inspiration and expiration. For example, it is known that the glottal opening tends to be more constricted during an expiration than an inspiration (see Chapter 1, part 1(i)), which might therefore lead to a correspondingly higher aerosol deposition efficiency in the larynx during an expiration. Similarly, as a consequence of the dichotomous branching geometry of the airways, there might be a greater inertial impaction of particles in the dead space region (C) during an inspiration, than an expiration. Effectively, therefore, each deposition region, with the exception of the respiratory zone, should be considered to behave as two filters assumed to possess unequal aerosol deposition efficiencies. In the present analysis these filters are denoted by the subscript, i, for an inspiration: W_i, S_i, C_i; and e, for an expiration: W_e, S_e, C_e.

In addition, it must be considered that not the entire tidal volume of aerosol traverses the filters W, S, and C, during an inspiration. For the mouth and laryngeal/pharyngeal regions the volume of tidal air not making the complete traverse is relatively small ($\sim$50 ml) and the error introduced by ignoring this volume is likely to be negligible. However, in the case of dead space airways the proportion of tidal air not making the complete traverse may be significant and must therefore be taken into account. According to WEIBEL (1963), the volume of dead space airways (generations 0 - 16) at about $\frac{3}{4}$ of maximum lung inflation ($\sim$ normal inflation level) is 175 ml. This implies that up to about 18% of the inhaled air would fail to reach the

respiratory zone at a tidal volume of 1·0 litre (BTPS), assuming plug-type flow. The question of the degree of penetrance to the respiratory zone is complicated by the likelihood that the gas-flow in the smaller airways is of the Poisseuille type (i.e. the plot in two dimensions of the forward flow velocity over an air-way cross section possesses a parabolic profile). The consequence of this is that the respiratory zone may be reached by a volume of inspired air that may sometimes be only some half of the dead space volume (BRISCOE et al. 1954). This does not mean that the volume of inhaled air which fails to penetrate to the respiratory zone is always about half the dead space volume, since it is probable that at tidal volumes several times greater than the dead space volume the fraction approaches, $\left[\frac{Vd}{V_T}\right]$, where Vd is the dead space volume and V_T is the tidal volume.

In the formulation of a lung model it must also be remembered that a proportion of the inspired air, respiratory gas exchange notwithstanding, will become inextricably mixed with the expiratory reserve and residual 'air' already in the lungs (see Chapter 1, part 1(i)). However, experiments using 1 μm diameter particles as tracers of gas flow in the lungs have demonstrated that the amount of such mixing is negligibly small (DAVIES et al. 1972).

The journey of the inhaled aerosol into and out of the respiratory tract may therefore be closely represented by the lung model shown in Figure 4.2.1. The regions, W and S are represented by four discrete in-series filters : W_i, W_e, S_i and S_e, to allow for possible differences in the unidirectional aerosol deposition efficiencies. Alternatively, these may be represented

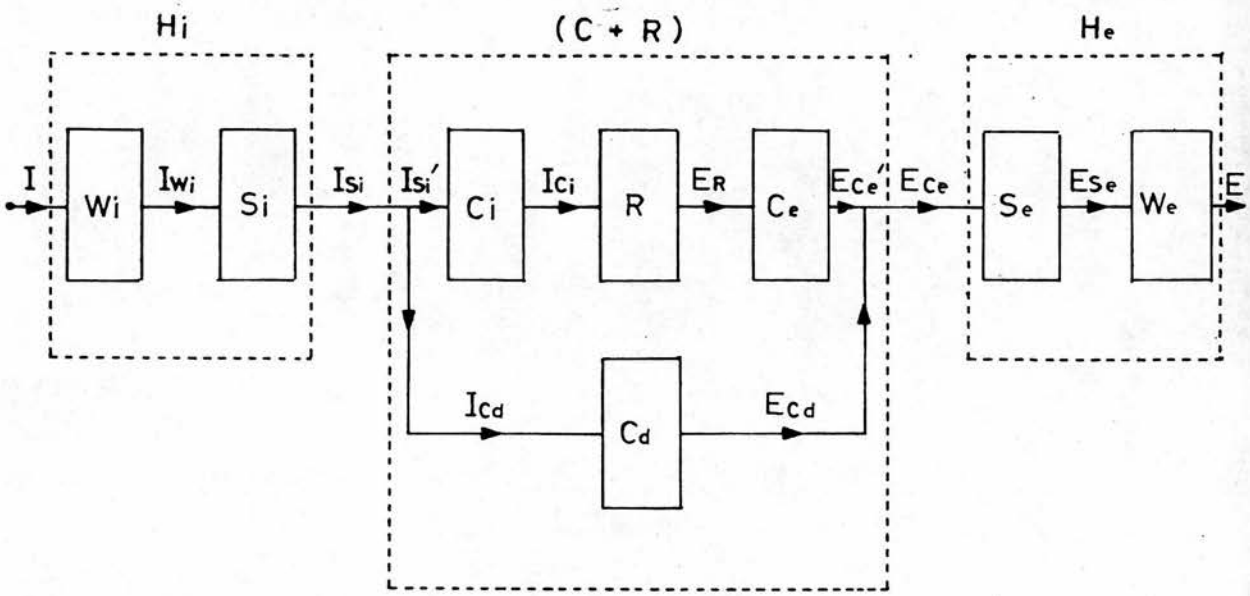

Figure 4.2.1 : Lung model.

together as a single 'head' filter, H, where $(W_i + S_i) = H_i$, and $(W_e + S_e) = H_e$. The dead space airways are represented as three filters: two in-series, representing the unidirectional aerosol deposition; and one in parallel with these, representing the deposition of the portion of the inhaled aerosol which just fails to penetrate to the respiratory zone. The respiratory zone itself is represented by a single in-series filter, R. The filters, Ci, R, Ce, Cd, may also be represented by a single filter, (C + R), for convenience, in some calculations.

Referring to Figure 4.2.1, the algebraic relationships are as given below,

$$W = (W_i + W_e) \quad \text{..... equation 4.2.1}$$

$$S = (S_i + S_e) \quad \text{..... equation 4.2.2}$$

$$H = (W + S) = H_i + H_e \quad \text{..... equation 4.2.3}$$

$$H_i = (W_i + S_i) \quad \text{..... equation 4.2.4}$$

$$H_e = (W_e + S_e) \quad \text{..... equation 4.2.5}$$

$$C = (C_i + C_d + C_e) \quad \text{..... equation 4.2.6}$$

$$(C + R) = (C_i + C_d + C_e + R) \quad \text{..... equation 4.2.7}$$

$$W_i = (I - I_{wi}) \quad \text{..... equation 4.2.8}$$

$$S_i = (I_{wi} - I_{si}) \quad \text{..... equation 4.2.9}$$

$$C_i = (I_{si}' - I_{ci}) \quad \text{..... equation 4.2.10}$$

$$C_d = (I_{cd} - E_{cd}) \quad \text{..... equation 4.2.11}$$

$$R = (I_{ci} - E_R) \quad \text{..... equation 4.2.12}$$

$$C_e = (E_R - E_{ce}') \quad \text{..... equation 4.2.13}$$

$$S_e = (E_{ce} - E_{se}) \quad \text{..... equation 4.2.14}$$

$$W_e = (E_{se} - E) \quad \text{..... equation 4.2.15}$$

$$D = (I - E) = W_i + S_i + C_i + C_d + C_e + R + S_e + W_e \quad \text{.....}$$

..... equation 4.2.16

$$I_{cd} = Y.I_{si} \quad \text{..... equation 4.2.17}$$

$$I_{si}' = (1 - Y).I_{si} = Y'.I_{si} \quad \text{..... equation 4.2.18}$$

$$I_{si} = I_{si}' + I_{cd} \quad \text{..... equation 4.2.19}$$

$$Y = \left[P.\frac{V_d}{V_T}\right] \quad \text{..... equation 4.2.20}$$

where, $0 < P < 1$, and P is the factor which determines the proportion of the dead space volume, V_d, occupied by the inspired air.

A deposition efficiency is defined here as the aerosol deposition in a region divided by the total aerosol flux into that region, i.e.,

$$\epsilon_{Wi} = \frac{W_i}{I} \quad \text{..... equation 4.2.21}$$

$$\epsilon_{Si} = \frac{S_i}{I_{Wi}} \quad \text{..... equation 4.2.22}$$

$$\epsilon_{Hi} = \frac{H_i}{I} \quad \text{..... equation 4.2.23}$$

$$\epsilon_{Ci} = \frac{C_i}{I_{Si}} \quad \text{..... equation 4.2.24}$$

$$\epsilon_{Cd} = \frac{C_d}{I_{Cd}} \quad \text{..... equation 4.2.25}$$

$$\epsilon_{R} = \frac{R}{I_{Ci}} \quad \text{..... equation 4.2.26}$$

$$\epsilon_{Ce} = \frac{C_e}{E_R} \quad \text{..... equation 4.2.27}$$

$$\epsilon_{He} = \frac{H_e}{E_{Ce}} \quad \text{..... equation 4.2.28}$$

$$\epsilon_{Se} = \frac{S_e}{E_{Ce}} \quad \text{..... equation 4.2.29}$$

$$\epsilon_{We} = \frac{W_e}{E_{Se}} \quad \text{..... equation 4.2.30}$$

The relationship between the inspiratory and expiratory aerosol deposition efficiencies of certain regions, and that between ϵ_{Cd} and ϵ_{Ci} , or ϵ_{C} , are defined by 'q-values', i.e.,

$$\epsilon_{Cd} = q_1 . \epsilon_{C} \quad \text{..... equation 4.2.31}$$

$$\epsilon_{He} = q_2 . \epsilon_{Hi} \quad \text{..... equation 4.2.32}$$

$$\epsilon_{Ce} = q_3 . \epsilon_{Ci} \quad \text{..... equation 4.2.33}$$

$$\epsilon_{Cd} = q_4 . \epsilon_{Ci} \quad \text{..... equation 4.2.34}$$

As the measured values of fW(I) were generally small at all particle sizes it was considered not to warrant a separate analysis in the case of $\epsilon_{Wi} \neq \epsilon_{We}$

When the 'q-values' are unity, the aerosol deposition efficiencies reduce to,

$$\epsilon_{Wi} = \epsilon_{We} = \epsilon_{W}$$

$$\epsilon_{Si} = \epsilon_{Se} = \epsilon_{S}$$

$$\epsilon_{Hi} = \epsilon_{He} = \epsilon_{H}$$

$$\epsilon_{Ci} = \epsilon_{Ce} = \epsilon_{C}$$

The 'q-values', q_2 and q_3, are of more importance in determining the magnitude of the aerosol deposition efficiencies than q_1 or q_4. It may be shown that the permissible values of q_1 lie in the range, $0 < q_1 < \sim 2$, for small values of ϵ_{Cd}, and $q_4 \simeq \frac{q_1 + q_4}{2}$ .... equation 4.2.35, which is intended as a simple approximation only (Appendix 1).

Considering now the various cases in which the 'q-values' are non-unity, it may be shown that ϵ_{Hi} and ϵ_{He} , may be determined from a knowledge of fH(I), and fC + R(I), for a range of possible values of q_2 .

Case A; $\epsilon_{Hi} \neq \epsilon_{He}$, $q_2 \neq 1$

now, $H = Hi + He = \epsilon_{Hi}.I + \epsilon_{He}.E_{Ce}$

$$\therefore H = \epsilon_{Hi}\left[I + q_2(I_{Si} - (C + R))\right]$$

dividing by I, substituting $I_{Si} = I(1 - \epsilon_{Hi})$ and re-arranging gives,

$$fH(I) = \epsilon_{Hi}\left[1 + q_2(1 - \epsilon_{Hi}) - q_2.fC + R(I)\right]$$

$$\therefore 0 = \epsilon_{Hi} + q_2(\epsilon_{Hi} - \epsilon_{Hi}^2) - \epsilon_{Hi}.q_2.fC + R(I) - fH(I)$$

$$\therefore 0 = a\epsilon_{Hi}^2 - b\epsilon_{Hi} + c \qquad \text{..... equation 4.2.36}$$

where, $a = q_2$

$b = \left[1 + q_2(1 - fC + R(I))\right]$

$c = fH(I)$

Solving the quadratic equation 4.2.36 for ϵ_{Hi}, in the normal manner, leads to,

$$\epsilon_{Hi} = \frac{b \pm (b^2 - 4ac)^{\frac{1}{2}}}{2a} \quad \text{..... equation 4.2.37}$$

Case B: $\epsilon_{Ci} \neq \epsilon_{Ce}$, $q_3 \neq 1$

Now, $C = C_i + C_e + C_d$

$$\therefore C = \epsilon_{Ci} . I_{Si}' + \epsilon_{Ce} . E_R + \epsilon_{Cd} . I_{Cd}$$

putting, $I_{Si}' = Y' . I_{Si}$, $E_R = (I_{Ci} - R)$, $I_{Cd} = Y . I_{Si}$,

gives, $$C = \epsilon_{Ci}\left[Y' . I_{Si} + q_3(I_{Ci} - R)\right] + q_4 . \epsilon_{Ci} . Y . I_{Si}$$

putting, $I_{Si} = I(1 - \epsilon_{Hi})$; $I_{Ci} = I_{Si}' . (1 - \epsilon_{Ci})$,

gives, $$C = \epsilon_{Ci}\left[Y' . I(1 - \epsilon_{Hi}) + q_3(I_{Si}' . (1 - \epsilon_{Ci}) - R)\right] + q_4 . \epsilon_{Ci} . YI(1 - \epsilon_{Hi})$$

dividing by I and making similar substitutions and re-arranging gives,

$$fC(I) = \epsilon_{Ci}\left[Y' . (1 - \epsilon_{Hi}) + q_3 . Y' (1 - \epsilon_{Hi})(1 - \epsilon_{Ci}) - q_3 fR(I)\right] + q_4 . \epsilon_{Ci} . Y(1 - \epsilon_{Hi})$$

$$\therefore fC(I) = -\epsilon_{Ci}^2\left[q_3.Y'.(1-\epsilon_{Hi})\right]$$

$$+\ \epsilon_{Ci}\left[Y'(1-\epsilon_{Hi})(1+q_3+\frac{q_4.Y}{Y'})-q_3.fR(I)\right]$$

$$\therefore 0 = a'.\epsilon_{Ci}^2 - b'.\epsilon_{Ci} + c' \quad \text{.... equation 4.2.38}$$

where, $a' = \left[q_3.Y'.(1-\epsilon_{Hi})\right]$

$$b' = \left[(1-\epsilon_{Hi})(Y'+q_3.Y'+q_4.Y)-q_3.fR(I)\right]$$

or putting $Y' = (1-Y)$,

$$b' = \left[(1-\epsilon_{Hi})(1+q_3+Y(q_4-1-q_3))-q_3.fR(I)\right]$$

$$c' = fC(I)$$

Solving the quadratic equation 4.2.38 as above, for ϵ_{Ci}, gives,

$$\epsilon_{Ci} = \frac{b' \pm (b'^2 - 4a'c')^{\frac{1}{2}}}{2a'} \quad \text{..... equation 4.2.39}$$

When $q_3 = 1$, b' reduces to,

$$b' = \left[(1-\epsilon_{Hi})(2+Y(q_4-2))-fR(I)\right]$$

Having calculated values of ϵ_{Hi}, ϵ_{Ci}, for the desired values of q_1, q_2, q_3, it is then possible to determine ϵ_R,

Now, $\epsilon_R = \frac{R}{Ici}$

$$\text{and,}\quad I_{Ci} = I_{Si}' - C_i = I_{Si}'.(1 - \epsilon_{Ci})$$

$$\text{and,}\quad I_{Si}' = I_{Si}.Y' = Y'.I(1 - \epsilon_{Hi})$$

$$\therefore\ \epsilon_R = \frac{R}{I.Y'(1 - \epsilon_{Hi})(1 - \epsilon_{Ci})}$$

$$\therefore\ \epsilon_R = \frac{fR(I)}{Y'.(1 - \epsilon_{Hi})(1 - \epsilon_{Ci})} \qquad \text{..... equation 4.2.40}$$

When $q_2 = 1$, ϵ_{Hi} may be replaced by ϵ_H, and when $q_3 = 1$, ϵ_{Ci} may be replaced by ϵ_C, in equation 4.2.40.

It should be noted from equation 4.2.40 that ϵ_R values have their maximum when ϵ_{Hi} and ϵ_{Ci} are also a maximum. In the case when all losses in regions H and C occur during inspiration only, the values of ϵ_{Hi} and ϵ_{Ci}, may be calculated as follows,

$$\epsilon_H = \frac{H}{I} = fH(I) \qquad \text{..... equation 4.2.41 (case } q_2 = 0)$$

- which is intended as an approximate solution in the case $H_i \gg H_e$, as might occur for the large particle sizes.

As Ce must now equal 0, Ci becomes a much greater fraction of C than in the cases already mentioned. Considering the relatively large values of fE(I) measured at the large particle sizes, for which this part of the analysis is intended, the output from the filter Cd (i.e. E_{cd}) would need to be a substantial contributor to this, if E_{ce}' was not allowed to be other than zero. In this

case it would therefore appear that ϵ_{Ci} increases more rapidly with particle size than ϵ_{Cd}, and Ci $\gg$ Cd. Putting Ci $\simeq$ C, therefore gives,

$$\epsilon_{Ci} = \frac{C}{I_{Si'}} = \frac{C}{Y'.I(1 - \epsilon_{Hi})} = \frac{fC(I)}{Y'(1 - \epsilon_{Hi})}$$

..... equation 4.2.42
(case $q_3 = 0$)

Case C: $\epsilon_{Si} = \epsilon_{Se} = \epsilon_S$: $\epsilon_{Wi} = \epsilon_{We} = \epsilon_W$; $q_2 = 1$

Although values of fW(I) were considered too trivial to warrant an analysis of the case $\epsilon_{Wi} \neq \epsilon_{We}$, it was considered desirable to at least express ϵ_W and ϵ_S, separately, in one case ($q_2 = 1$).

Now, $W = Wi + We = \epsilon_W(I + E_{SE})$

and, $E_{Se} = E_{Ce} - S_e = E_{Ce}(1 - \epsilon_S)$

$$\therefore fW(I) = \epsilon_W\left[1 + fE_{Ce}(I)(1 - \epsilon_S)\right]$$

$$\therefore \epsilon_W = \frac{fW(I)}{\left[1 + fE_{Ce}(I).(1 - \epsilon_S)\right]}$$ ..... equation 4.2.43

now, $E = E_{Ce} - H_e = E_{Ce}(1 - \epsilon_H)$

(Values of ϵ_H are more convenient to use here, and if $(\epsilon_{Si} + \epsilon_{Wi}) = (\epsilon_{Se} + \epsilon_{We})$, then $\epsilon_{Hi} = \epsilon_{He} = \epsilon_H$).

$$\therefore Ece = \frac{E}{(1 - \epsilon_H)}$$

$$\therefore fEce(I) = \frac{fE(I)}{(1 - \epsilon_H)} = \frac{(1 - fD(I))}{(1 - \epsilon_H)} \quad \ldots\ldots \text{equation 4.2.44}$$

Now, $S = S_i + S_e = \epsilon_s(I_{wi} + Ece)$

and, $I_{wi} = I(1 - \epsilon_w)$

$$\therefore fS(I) = \epsilon_s[(1 - \epsilon_w) + fEce(I)]$$

substituting for ϵ_w using equation 4.2.43 gives,

$$fS(I) = \epsilon_s\left[\left(1 - \frac{fW(I)}{[1 + fEce(I)(1 - \epsilon_s)]}\right) + fEce(I)\right]$$

$$\therefore fS(I).[1 + fEce(I)(1 - \epsilon_s)] = \epsilon_s[1 + fEce(I).(1 - \epsilon_s)]$$
$$- fW(I).\epsilon_s + fEce(I).\epsilon_s[1 + fEce(I).(1 - \epsilon_s)]$$

$$\therefore 0 = -fS(I) - fS(I).fEce(I) + fS(I).fEce(I).\epsilon_s + \epsilon_s$$
$$+ fEce(I).\epsilon_s - fEce(I).\epsilon_s^2 - fW(I).\epsilon_s$$
$$+ fEce(I).\epsilon_s + fEce(I)^2.\epsilon_s - fEce(I)^2.\epsilon_s^2$$

$$\therefore 0 = -\epsilon_s^2[fEce(I) + fEce(I)^2] + \epsilon_s[1 + fS(I).fEce(I)$$
$$+ fEce(I) + fEce(I) - fW(I) + fEce(I)^2]$$
$$- [fS(I) + fS(I).fEce(I)]$$

$$\therefore\ 0 = a''.\epsilon_s^2 - b''.\epsilon_s + c'' \quad \ldots\ldots\ldots \text{ equation 4.2.45}$$

where, $a'' = \left[fEc_e(I)(1 + fEc_e(I))\right]$

$b'' = \left[1 - fW(I) + fEc_e(I)(2 + fS(I) + fEc_e(I))\right]$

$c'' = \left[fS(I).(1 + fEc_e(I))\right]$

Solving for ϵ_s in the quadratic equation 4.2.45 gives,

$$\epsilon_s = \frac{b'' \pm (b''^2 - 4a''.c'')^{\frac{1}{2}}}{2a''} \quad \ldots\ldots\ldots \text{ equation 4.2.46}$$

It was considered necessary to adopt some means of independently checking the accuracy of the calculated aerosol deposition efficiencies for each subject.

Now, $D = H_i + C_i + C_d + R + C_e + H_e$

$$\therefore\ fD(I) = \frac{1}{I}\Big[\ \epsilon_{Hi}.I + \epsilon_{Ci}.Y'.I(1 - \epsilon_{Hi}) + q_4.\epsilon_{Ci}.YI(1 - \epsilon_{Hi})$$
$$+ \epsilon_R(Y'.I(1 - \epsilon_{Hi}) - \epsilon_{Ci}.Y'.I(1 - \epsilon_{Hi}))$$
$$\frac{}{+ \epsilon_{Ce}(Y'.I(1 - \epsilon_{Hi}) - \epsilon_{Ci}.Y'.I(1 - \epsilon_{Hi})}$$
$$- \epsilon_R(Y'.I(1 - \epsilon_{Hi}) - \epsilon_{Ci}.Y'.I(1 - \epsilon_{Hi})))$$
$$\frac{}{+ \epsilon_{He}(Y'.I(1 - \epsilon_{Hi}) - \epsilon_{Ci}.Y'.I(1 - \epsilon_{Hi})}$$
$$- \epsilon_R(Y'.I(1 - \epsilon_{Hi}) - \epsilon_{Ci}.Y'.I(1 - \epsilon_{Hi}))$$
$$- \epsilon_{Ce}(Y'.I(1 - \epsilon_{Hi}) - \epsilon_{Ci}.Y'.I(1 - \epsilon_{Hi})$$
$$- \epsilon_R(Y'.I(1 - \epsilon_{Hi}) - \epsilon_{Ci}.Y'.I(1 - \epsilon_{Hi}))))$$
$$\frac{}{+ \epsilon_{He}(YI(1 - \epsilon_{Hi}) - q_4.\epsilon_{Ci}.YI(1 - \epsilon_{Hi}))}\Big]$$

Cancelling I and simplifying gives,

$$fD(I) = \Big[\epsilon_{Hi} + \epsilon_{Ci}.Y'(1 - \epsilon_{Hi}) + q_4 . \epsilon_{Ci}.Y(1 - \epsilon_{Hi}) + \epsilon_R(Y'(1 - \epsilon_{Hi})(1 - \epsilon_{Ci})) + \epsilon_{Ce}(Y'(1 - \epsilon_{Hi})(1 - \epsilon_{Ci})(1 - \epsilon_R)) + \epsilon_{He}(Y'(1 - \epsilon_{Hi})(1 - \epsilon_{Ci})(1 - \epsilon_R)(1 - \epsilon_{Ce})) + \epsilon_{He}(Y(1 - \epsilon_{Hi})(1 - q_4 . \epsilon_{Ci}))\Big]$$

putting, $P_1 = Y'(1 - \epsilon_{Hi})$

$P_2 = P_1(1 - \epsilon_{Ci})$

$P_3 = P_2(1 - \epsilon_R)$

$P_4 = P_3(1 - \epsilon_{Ce}) = P_3(1 - q_4 . \epsilon_{Ci})$

$P_1' = Y(1 - \epsilon_{HI})$

$P_2' = P_1'(1 - q_4 . \epsilon_{Ci})$

Where in the above notation Px, say, represents the aerosol penetrance to region, X.

$$\therefore fD(I) = \epsilon_{Hi} + P_1 . \epsilon_{Ci} + P_1' . q_4 . \epsilon_{Ci} + P_2 . \epsilon_R + P_3 . \epsilon_{Ce} + P_4 . \epsilon_{He} + P_2' . \epsilon_{He}$$

$$\therefore fD(I) = \epsilon_{HI}\left[1 + q_2(P_4 + P_2')\right] + \epsilon_{Ci}\left[P_1 + q_4 . P_1' + q_3 . P_3\right] + \epsilon_R . P_2$$

..... equation 4.2.47

where, $fH(I) = \epsilon_{Hi}\left[1 + q_2(P_4 + P_2')\right]$

$fC(I) = \epsilon_{Ci}\left[P_1 + q_4 . P_1' + q_3 . P_3\right]$

$fR(I) = \epsilon_R . P_2$

When $q_2 = 1$, ϵ_{Hi} may be replaced by ϵ_H in equation 4.2.47; when $q_3 = 1$, ϵ_{Ci} may be replaced by ϵ_C, and q_4 by q_1.

Using the above equations it is therefore possible to determine whether the predicted values of fractional deposition tally with the actual.

By an essentially similar process of calculaution it may be shown that to include the terms, ϵ_w and ϵ_s, $fD(I)$ should be written (Appendix 2),

$$fD(I) = \epsilon_w\left[1 + P_5 + P_3'\right] + \epsilon_s\left[1 - \epsilon_w + P_4 + P_2'\right] + \epsilon_{Ci}\left[P_1 + q_4 . P_1' + q_3 . P_3\right] + \epsilon_R . P_2$$

..... equation 4.2.48

where, $fW(I) = \epsilon_w(1 + P_5 + P_3')$

$fS(I) = \epsilon_s(1 - \epsilon_w + P_4 + P_2')$

$fC(I) = \epsilon_{Ci}(P_1 + q_4 . P_1 + q_3 . P_3)$

$fR(I) = \epsilon_R . P_2$

and, $P_1 = Y'(1 - \epsilon_w)(1 - \epsilon_s)$

$P_2 = P_1(1 - \epsilon_{Ci})$

$P_3 = P_2(1 - \epsilon_R)$

$P_4 = P_3(1 - \epsilon_{Ce}) = P_3(1 - q_3 . \epsilon_{Ci})$

$$P_5 = P_4(1 - \epsilon_s)$$

$$P_1' = Y(1 - \epsilon_w)(1 - \epsilon_s)$$

$$P_2' = P_1'(1 - q_4 \cdot \epsilon_{ci})$$

$$P_3' = P_2'(1 - \epsilon_s)$$

CHAPTER FIVE

RESULTS AND DISCUSSION

The following text presents and discusses the results obtained by the methods described in Chapter 3, treated subsequently in the manner described in Chapter 4. Although the same terms and symbols that were defined in these chapters are used in the present chapter, the glossary given below may serve as a useful reminder. Only loose definitions are listed, the definitive ones having been given earlier in the thesis.

Fractions:	fD(I)	.....	total deposition fraction
	fW(I)	.....	mouth deposition fraction
	fS(I)	.....	throat deposition fraction
	fC(I)	.....	cleared fraction
	fR(I)	.....	retained fraction
	fE(I)	.....	exhaled fraction
	fH(I)	.....	'head' deposition fraction
	fC + R(I)	.....	deposition fraction below larynx

where, $fH(I) = fW(I) + fS(I)$

$fC + R(I) = fC(I) + fR(I)$

All fractions being expressed relative to I, the inhaled aerosol.

Efficiencies:

The symbol $\in_x$ has been used throughout to signify the aerosol deposition efficiency in region x, say, where the subscript x may may be replaced by W, S, C, R, H, or C+R, and further subscripted by i or e, denoting inspiration or expiration, respectively.

5.1 Aerosol deposition at variable particle size and breathing pattern

(i) Preliminary discussion

The deposition fractions obtained for the twelve subjects of the variable particle size study are listed in Table 5.1.1 and their individual breathing conditions during aerosol administration in Table 5.1.2. It should be noted that deposition fractions to four decimal places have been quoted in these tables because this is helpful when confirming the accuracy of certain equations, described in the preceding chapter. The 95% confidence limits shown on some figures have been calculated using 'Student's t-test'.

The total deposition results, $f_D(I)$ versus particle size, are plotted in Figure 5.1.1. These have three notable features: (1) the increase in $f_D(I)$ with increasing particle size is small; (2) a large amount of aerosol is exhaled, particularly towards the larger sizes, compared to the results of some other workers (see Figure 5.1.9); (3) there are finite differences between subjects. The most important source of inter-subject variability would appear to be $f_S(I)$ (Figure 5.1.3). This is somewhat predictable as the laryngeal/pharyngeal region has a variable geometry and flow rates are high (see Chapter 1, part 1(i)). The first two

features may indicate the importance of the relatively large volume of anatomical dead space in the mouth, pharynx, larynx, and large airways. Since much of these zones contains a significant vertical volume element and aerosol which enters last, leaves first, residing for only a short period, it appears that the total deposition 'saturates' at or below about 4·5 μm particle diameter, increasing only gradually thereafter.

The deposition fractions, fW(I) and fS(I), show clear upward trends with increasing particle size (Figures 5.1.2 and 5.1.3). At this point it should be noted that no attempt is made in the present work to plot the deposition fractions as a unique function of an impaction parameter, e.g. particle density x particle diameter^2 x mean flow rate, as some other workers have attempted (LIPPMANN, 1977). Such an approach may well be erroneous because the amount of aerosol depositing in a given region is dependent on the amount which enters, from either direction of flow, as well as its intrinsic aerosol filtration efficiency. It is first necessary to express, if possible, the measured values of deposition in terms of efficiencies, as opposed to fractions, which may require a detailed preliminary analysis. Moreover, since aerosol deposition is never a unique function of an impaction parameter (for example, a sedimentation parameter might also vary directly with particle density and diameter , but inversely with flow), it must be borne in mind that the combination of variables of flow and residence times in the respiratory tract is critical in this respect. In the present work, respired flow rates have been held nearly constant

which is therefore not conducive to any attempt at distinguishing the relative importance of sedimentation and impaction. Other approaches have been attempted however (see part 1(iv) of the present chapter).

While the curve of fC(I) (Figure 5.1.4) also shows a generally increasing trend with increasing particle size, this appears to falter at the largest particle sizes. However, it must be remembered that aerosol exposure below the larynx will be considerably reduced owing to the increase in fW(I) and fS(I) (Figure 5.1.8). In this instance, it would be helpful to attempt to express the deposition of the cleared fraction, fC(I), in terms of the absolute aerosol deposition efficiency in the region concerned. Considering the plot of fR(I) versus particle diameter it appears that the larger sizes are able to penetrate and deposit in the respiratory zone in relatively large numbers (Figure 5.1.5). This is a most unusual result when the relative magnitudes of the other deposition fractions are considered (Figure 5.1.6). If fC(I) is reduced at the larger particle sizes because of greatly decreased aerosol penetrance below the larynx, it might be expected that, owing to the fact that the deposition efficiency in the dead space airways is certain to increase greatly at the larger particle sizes, the measured values of fC(I) would be much greater in comparison to fR(I) than actually turns out to be the case (Figure 5.1.7). At both 10·4 μm and 13 μm particle diameter, fR(I) is a significant fraction of fC(I). However, the complicated interactions between aerosol exposure and deposition efficiency makes such intuitive analysis

uncertain. To analyse this and other questions more rigorously, it is first necessary to formulate a descriptive model of the lung, as a series of discrete filters, which may enable the regional deposition efficiencies (as opposed to fractions) to be estimated, within reasonable limits. Such a lung model was described in section 2 of the preceding chapter. The results of this analysis are discussed below.

5.1(ii) Discussion of calculated regional deposition and efficiencies in variable particle size study

Taking an assumed value of P = 1 (see equation 4.2.20), giving Y = 0·18, Y′ = 0·82, values of ϵ_C have been calculated for a range of values of q_1, when $q_2 = q_3 = 1$, using equations 4.2.37 and 4.2.38. The individual and group average values of ϵ_H are plotted in Figure 5.1.10. Average values only for ϵ_C are plotted in Figure 5.1.11 with error bars at the 95% confidence limit, for a range of values of q_1, i.e. 0·5, 1, and 2, the latter being an extreme. This demonstrates that the influence of q_1 on ϵ_C values is not large. Putting a reasonable estimate of $q_1 = 1$ throughout subsequent derivations of ϵ_C and ϵ_{Ci}, for a range of values of q_2 and q_3, will not therefore introduce a significant error. Individual and group-average values of ϵ_C for $q_1 = 1$ and $q_3 = q_2 = 1$, are plotted in Figure 5.1.12.

The trend in ϵ_H and ϵ_C, (Figures 5.1.10 and 5.1.12) is generally upwards with increasing particle size, as might be expected. At 10·4 μm particle diameter there appears to be a disproportionate increase in the curve for ϵ_H, but this falls within the observed range of values taken over the whole curve.

The values of ϵ_H may be further subdivided into values of ϵ_W and ϵ_S (this is not to imply that $\epsilon_H = \epsilon_W + \epsilon_S$, in fact $\epsilon_H = 1 - (1 - \epsilon_W)(1 - \epsilon_S)$), calculated using equations 4.2.43 and 4.2.46. The individual and group-average values for ϵ_W and ϵ_S are plotted in Figures 5.1.13 and 5.1.14, respectively. ϵ_W manifests a clear upward trend with increasing particle size, as did $fW(I)$, and ϵ_S , while also showing a generally upwards trend, possesses a similar scatter of points to $fS(I)$ and gives an obvious clue as to the main source of intersubject variability in $fD(I)$.

Values of ϵ_R for various values of ϵ_{Ci} and ϵ_{Hi} , or ϵ_C and ϵ_H , may now be calculated from equation 4.2.40. The individual and group-average values of ϵ_R for $q_3 = q_2 = 1$ are plotted in Figure 5.1.15. This curve shows an obvious downwards trend with increasing particle size. However, the result is somewhat remarkable in the light of an assumed dominance of aerosol sedimentation in the respiratory zone. Before other factors are considered it is first necessary to examine the possibility that the downwards trend in ϵ_R , shown in figure 5.1.15, is being caused by incorrect assumptions in the values of q_3 and q_2 . Figure 5.1.16 is a plot of group-average ϵ_R values for a wide range of combinations of values of q_3 and q_2 . Whichever values, or combination of values, is selected, the trend in ϵ_R is always generally downwards with increasing particle size.

The bizarre nature of the trend in ϵ_R may be exemplified by considering intuitively the relationship between the particle falling speed, lung morphology, and mean particle residence times,

in the airways, at the largest particle diameter: 13 μm. According to Stokes' Law, a spherical 13 μm particle of density $10^3 Kg.m^{-3}$ falls in still air at a rate of approximately 5·4 mm every second. The diameter of the largest respiratory bronchiole in the Weibel Model is approximately 540 μm. Neglecting airway orientation influences, airborne particles entering the respiratory zone therefore need only to reside about a tenth of a second before depositing. When the mean respired flow rate, f_o, say, is 333 cc $sec.^{-1}$, as in the variable particle size study, the average time taken for particles to traverse the dead space, volume V_d, is given by $\sim\left[\frac{V_d}{f_o}\right]$, or 0·55 seconds. Therefore, for a 6 second breathing cycle, the residence time of particles in the respiratory zone would lie in the range 0 – 4·9 seconds, averaging approximately 2·5 seconds. It may therefore be safely concluded that the overwhelming majority of 13 μm particles resided in the respiratory zone for a time far greater than that actually required for deposition to be assured. Yet according to the results plotted in Figures 5.1.15 and 5.1.16 well over half such particles are able to enter and leave the respiratory zone without depositing. It seems only possible to conclude that the measured deposition fractions are incorrect.

Besides possible errors arising in the experimental technique, discussed in Chapter 3, section 3, there are two central assumptions that have been made in the derivation of the regional deposition fractions, fR(I) and fC(I) : (1) that an insignificant amount of material which initially deposited in the respiratory zone was cleared from the lungs in the first day after aerosol administration;

(2) that an insignificant amount of material which initially deposited on the dead space airways remained there the first day after aerosol administration. Put more simply, if either one of these assumptions is incorrect, it implies either that: (1) C was overestimated at the expense of R; or, (2) R was overestimated at the expense of C, respectively. The third possibility, that neither assumption is correct, cannot be excluded. Although in that case the errors resulting from each incorrect assumption would be partly, or wholly, compensatory.

In Chapter 1, part 1(ii), it was concluded that on the basis of recent evidence (GORE and PATRICK, 1978) it was quite possible that assumption (2) above was incorrect, but probably not assumption (1) (STAHLHOFEN et al., 1979). If, however, some of the retained fraction at 13 μm particle diameter was actually retained outside the respiratory zone, this would have the effect of lowering $\epsilon_R (= \left[\frac{R}{I_{Ci}}\right])$ still further. Only if the whole of the measured retained fraction was actually retained outside the respiratory zone, i.e. if there was actually negligible penetrance to the respiratory zone at this size could the ϵ_R values be explained in terms of assumption (2) being incorrect. Before discussing this possibility further the validity of assumption (1) will be considered.

It would superficially appear plausible to explain the 'low' ϵ_R values, in part, in terms of a short-term clearance of particles which initially deposited in the respiratory zone. If the majority of particles which initially deposited in the respiratory zone were to be cleared from the lungs, within the first day after

aerosol administration, the resultant clearance curve would have a fairly predictable shape. In the first few hours after aerosol administration the material which initially deposited in the dead space airways would be cleared (let it be assumed). When the material which initially deposited in the respiratory zone was cleared, probably after a delay, both the profile scanner and throat clearance detectors would register its transit. It is apparent from examination of the profile scanner clearance curves in Figure 5.2.4, that most material which is ultimately cleared, is cleared within a short time after aerosol administration; the same result is even more apparent on examination of most of the corresponding throat clearance curves (Figures 5.2.10 – 5.2.13 and 5.2.17, 5.2.18). In the latter, there is in some cases no clearance whatever registered by the throat detectors, from several to nine hours after aerosol administration (Figure 5.2.12). Taking this most obvious example, it does not seem reasonable to suggest that for subject PT (who produced the same result on two occasions), all the material which initially deposited on the entire area of the dead space airways was cleared in only 2 – 3 hours after aerosol administration. If it is accepted that the ciliary clearance rates for this subject were not simply exceptionally rapid, then it must be concluded that the absence of any cleared material from several to nine hours after aerosol administration is evidence for no significant aerosol penetrance to the smaller ciliated airways and, therefore, also evidence for no significant penetrance to the respiratory zone. Yet for the same subject there is clear evidence

from the profile scans (see Figure 3.3.3) of a finite retention, somewhere in the lungs, about one day after aerosol administration. Accepting the above axiom, it seems only possible to conclude that the retention observed for this subject at this time was actually caused by a one-day retention of dust which initially deposited on the dead space airways.

It should be noted that although for some other subjects at large sizes (e.g. JH, $\bar{d}$ = 13 μm, Figure 5.2.11) there is a finite amount being cleared at 8 - 9 hours, this does not necessarily imply a finite penetrance to the smaller ciliated airways and respiratory zone, and may well be caused by a 'delayed' clearance from the large airways. If some subjects retain dust on the ciliated airways for periods greater than about one day, it might be anticipated that others would exhibit a delayed clearance of 8 - 9 hours of dust which initially deposited on the larger ciliated airways.

The obvious inconsistency between the throat clearance curves and profile scans observed for subject PT, is a good indication that there was also an incomplete one-day ciliary clearance in the other subjects of this study for whom this inconsistency was a little less obvious. Seen in isolation, it might be possible to argue that the one obvious result obtained for this subject was merely a rare case: seen with regard to the similar, rapidly declining, throat clearance curves obtained for certain other subjects (e.g. subject AD, Figure 5.2.13), also at large particle sizes, this seems a dubious proposition; seen, moreover, in

conjunction with the other more bizarre inconsistencies in the calculated regional deposition efficiencies, brought to light by the above analysis, it seems more reasonable to conclude that the measured levels of retention at the larger particle sizes were actually caused by an incomplete ciliary clearance at about one-day after aerosol administration, for all subjects concerned.

This considerably complicates the interpretation of the measured deposition fractions. Considering the situation at 13 μm, if the above conclusion is correct, it may be predicted that ϵ_{CI} should become unity when the 'real' value of fC(I), fC(I) real, say, is substituted into the equations, where,

$$fC(I)\ \text{real} = fC(I) + fR(I) = 0{\cdot}426 \text{ at } 13\ \mu\text{m particle diameter}$$

This then serves as a rough test of the mutual consistency of the analysis and the conclusion. Equations 4.2.41 and 4.2.42 are the most appropiate ones to use here since most material will be lost in the upper airways during inspiration if the above conclusion is correct.

$$\epsilon_{CI}\ \text{real} = \frac{fC(I)\ \text{real}}{Y'(1 - fH(I))} = 0{\cdot}955, \text{ which is close to unity}$$

At a certain particle diameter, between 4·5 - 13 μm, it is possible that there was a finite penetrance to the respiratory zone. However, without a foreknowledge of retention due to purely respiratory zone deposition, which is likely to depend on particle size, it is

impossible to further advance the present analysis of these results. The present curve for fR(I) may therefore only be regarded as an upper limit to respiratory zone aerosol deposition.

Before discussing the wider implications of the results of the present work, and their comparability to those of other groups, it may be worth considering one, perhaps, less likely explanation for the phenomena described above. An interesting incidental effect sometimes observed by experienced bronchographers is that the radio-opaque bronchographic medium can be re-distributed in patterns interpreted as alveolar filling (LEITH, 1977). This raises the possibility of a transfer of deposited particles from the dead space airways to the respiratory zone and should certainly be borne in mind as a possible factor in interpreting the results of the present work. However, considering the averaged profile scan clearance curves shown in Figure 5.2.5, if a total re-distribution of deposited particles were to occur, it may be reasoned that these curves would be similar at all particle sizes and, moreover, that similar proportions of particles would be retained and cleared at any size. Alternatively, it might also be reasonable to postulate that only a partial internal re-distribtion occurs, one which merely serves to slightly modify existing clearance trends and to give the false impression that the large particle sizes were able to penetrate and be retained in the respiratory zone. However, although such a possibility is hard to entirely discount for the majority of subjects, in a few cases the evidence of the throat clearance curves, again, most notably those of subject PT, does not support this hypothesis. If an internal re-distribution of

deposited particles were to occur, such that a finite and significant portion of these were transferred into the respiratory zone (~15% for subject PT), then a finite and significant portion of the same must also have been transferred into the fine-calibre ciliated airways. It is very doubtful whether the clearance of particles from these airways could be completed in only 2 - 3 hours after aerosol administration.

Overall then, it is reasonable to suppose that the single causative factor of an ineffective one-day ciliary clearance is the important one in the interpretation of the results of the present work.

5.1(iii) Comparison of deposition data of variable particle size study with published work of other groups

Comparing these results to those of other workers (Figure 5.1.9), it is apparent that there is reasonable agreement in fR(I) and fC(I) with the results obtained for one subject by STAHLHOFEN et al.(1979), and in fR(C + R) with FOORD et al, (1978), in a limited region of particle size overlap and conditions of aerosol administration, but the results for fR(I) of LIPPMANN and ALBERT (1969) are in much closer agreement with existing respirable dust sampling curves, although there appears to be more scatter of observations in the results of the latter.

The influence of particle shape, as well as size, should be borne in mind however (see Chapter 3, part 1(iii)a). All the above mentioned groups used similar particle production techniques to those of the present study and their data may well be comparable, but caution should be exercised until more information is available

concerning particle shape factors.

Aerosol losses in the mouth (fW(I)) are lower in the present work than those reported by FOORD et al. (1978), who used a one centimetre diameter mouthpiece, and LIPPMANN and ALBERT (1969), whose subjects clamped their teeth onto tabs at the centre-line of the mouthpiece in some tests and closed their teeth and lips around the external rim of the mouthpiece (diameter not specified) in others. The results for fH(I) (= fW(I) + fS(I)) are reasonably close to those of STAHLHOFEN et al. (1979), who used a two centimetre diameter mouthpiece (c.f. 2·5 centimetres in the present work). While it is therefore possible that mouthpiece diameter is an important factor in determining the magnitude of aerosol losses in the mouth it is more likely that the method employed to remove the mouth deposit is more critical in this respect. FOORD et al. (1978) and LIPPMANN and ALBERT (1969) both employed a gargling method, which would almost certainly include some of the throat deposit.

Of all four groups, the observations of LIPPMANN and ALBERT (1969) exhibit the most scatter in any deposition fraction. In the light of the experience obtained in the present work, the following explanatory comments may be helpful:

A. fD(I): The inhaled aerosol was not measured directly by LIPPMANN and ALBERT (1969), fD(I) being obtained indirectly by measurement of D (I = D + E). This requires careful measurement of the radioactive content of the lungs using whole body

(Continued from opposite P.199.)

It may therefore be impossible ever to definitively answer the question as to how the present results would differ from those obtained under 'natural' conditions. One way out of this dilemma has recently been pioneered by Heyder et al (1979). In their work fourteen male and female subjects were asked to breathe 'spontaneously', i.e. as normally as possible in the circumstances, while their total deposition values were obtained. The mean values of several basic physiological parameters were measured simultaneously. A group of three additional volunteer subjects then breathed aerosols at the same values of physiological parameter, but under standardized conditions. No significant differences between the mean total deposition values of the two groups were observed. However, the group which had breathed under non-standardized conditions exhibited considerably greater scatter of results. This result suggests that extrapolation from artificial to 'natural' conditions is justified and that differences, for example, in peak inspiratory flows are not very important.

Ample justification for the artificial conditions of aerosol administration employed in the present work is borne in the observation of only small differences in the deposition fractions (below the larynx) between subjects. With this observation it is possible to conclude that the influence of the respiratory infections and range of lung function parameters reported in Table 3.4.1 (P.159) was only small. Changes induced in the small peripheral airways would probably not be important, because of the short particle residence times in these airways in which gravitational deposition is believed to be dominant (see P.19). The present results also suggest that the filtration efficiency of the large airways, which would account for the bulk of the losses ascribed to the cleared fraction (fC(I)), does not vary much with the resistance these airways present to gas-flow (as estimated by FEV^{1} and FVC measurements). At any particle size studied it is unlikely on theoretical grounds that the small ciliated airways would account for more than a small fraction of total losses (TAULBEE and YU, 1975).

(or whole lung) counting systems (EHRET et al. 1964). While the variation in point to point counting sensitivity of their detectors has been described by ALBERT et al. 1967, the details of how the arbitrary detector count rate was converted into a measure of the radioactive content of the whole thoracic cage, in absolute units, are too vaguely described to form a sound basis for judging the overall accuracy of the method.

B. fW(I): The mouthpiece design favoured high mouth losses and changed during their experiments, and the mouthwash technique would be likely to include some of the throat deposit.

C. fS(I) The difficulties encountered when attempting to measure this fraction were described in Chapter 3, section 3. In the method of LIPPMANN and ALBERT (1969), the collimator design was such as to be unlikely to be capable of separately resolving the laryngeal/pharyngeal region from the upper lung lobes (see Figure 3.3.11). Some of the high values shown on Figure 5.1.9 (iii) may therefore be caused by the inclusion of some lung radioactivity in the throat counts, while on the other hand some of the low values may be caused by a failure to prevent swallowing between the end of aerosol administration and the time of measurement of the laryngeal/pharyngeal deposit (when the lung deposit was not included in the throat counts). It is possible to argue this point both ways because of possible inter-subject differences in anatomy and positioning.

D. Clearance: The rapid fall-off in retention often observed by LIPPMANN and ALBERT (1969) and ALBERT et al. (1973), in

Addendum to follow discussion on P.199.

In considering the comparability of the published results of other research groups with the present results, it must be remembered that some groups have imposed the strict artificial breathing conditions of the present work (Stahlhofen et al, 1979) while others have not (Lippmann and Albert, 1969). This is not to imply that the latter employed 'natural' patterns. The more appropriate distinction to be perceived is not that between natural and artificial, but that between standardized and non-standardized breathing patterns. Since, by definition, a standardized pattern cannot be other than artificial, it is impossible to employ a standardized 'natural' pattern. Therefore, the only purpose served by failing to control even basic physiological parameters such as tidal volume, while partially controlling others (Lippmann and Albert, 1969), is to ensure that the results are one-off, non-reproducible and not strictly comparable with anything. It is worth noting here that the deposition fractions below the larynx measured by workers who controlled the conditions of aerosol administration, exhibit considerably less scatter than the fractions measured by those who did not.

Having established the degree of difference between subjects under standard conditions, differences caused mainly by intrinsic lung factors such as airway morphology, it is then reasonable to ask how the results would differ under 'natural' conditions. What are 'natural' conditions? In one sense 'natural' conditions of breathing can never exist since the agent of subconscious or conscious control of respiration is always the human being. Aside from this semantic caveat, it must also be remembered that a myriad of factors constitute the 'natural' condition, many of which change considerably with time and effort. If an attempt were to be made to observe or measure the influence of even one of these factors, the interference which resulted would, by definition, make the conditions artificial.

contrast to the results of many other studies (BOOKER et al, 1967; CAMNER and PHILIPSON, 1978; PAVIA and THOMSON, 1976; STAHLHOFEN et al, 1979), indicates that the initial laryngeal/ pharyngeal deposit may have been included in their initial values of lung retention. This would be consistent with the possibilities discussed in point C above.

The results for total deposition fD(I), in the present work, are lower than those of both FOORD et al. (1978) and LIPPMANN and ALBERT (1969), but agree better at the smaller particle sizes with those of STAHLHOFEN et al. (1979). Although the results for fD(I) in the present work show a generally increasing trend with increasing particle size, the relative amount of aerosol exhaled at the larger sizes are quite high for some subjects. The aerosol which occupies the mouth, pharynx, trachea, and main bronchi (total volume ~100 cc), may be a significant contributor in this respect, It should also be borne in mind that aerosols in the respiratory tract obey a 'last in, first out' principle (MUIR, 1967). The residence time of particles which fail to penetrate even to the intrathoracic dead space airways is therefore the smallest of any part of the respiratory tract. Moreover because of the nature of flows in a typical breathing cycle, and to only a slightly lesser extent in an artificial one, these particles are also carried in the slowest flows of any part of the cycle duration, which must also lower the probability of deposition by inertial impaction.

5.1(iv) Discussion of results of variable breathing pattern study

In the generally accepted understanding of the deposition of aerosols in the particle size range of the present study, there are two main deposition mechanisms: inertial impaction and sedimentation. Other factors being equal, the former is velocity dependent, the latter, time dependent. In investigating the relative importance of each mechanism it would be desirable to hold the effects of one constant while the other was allowed to vary. Variations of the physiological parameters which define breathing pattern: tidal volume and breathing frequency, are of little use in this respect since both residence time and respired flow rates change together when there is a change in either physiological parameter. It is not possible to vary the residence time of particles in a lung airway without a simultaneous variation in the mean air flow velocity through it.

However, by adopting breathing patterns 1 and 2, shown in Figure 5.1.17, it is at least possible to investigate the importance of the time-dependent deposition mechanisms in the respiratory zone. This is accomplished by using the same breathing flow rates in both patterns. The aerosol deposition efficiency in the dead space airways during an inspiration and expiration, which depends on breathing flow rate, is therefore constant in both cases. The aerosol penetrance to the respiratory zone (I_{Ci}) is consequently a constant fraction of I and the effects of varying the particle residence times (by varying tidal volume) in the respiratory zone, on ϵ_R, may be examined. (It should be noted that in the calculation of ϵ_R,

ϵ_{Ci} must also be determined. This depends on C, which may not be exactly equal in the results of both patterns because of a difference in C_e (not ϵ_{Ce}). However, since C_e makes about an order of magnitude smaller contribution to C, than C_i, even at the smallest particle diameter, the error in ϵ_{Ci}, and hence ϵ_R, is probably neglible. It should also be noted that although the fraction, C_d, is a different fraction of C, between the two patterns, this is allowed for in the calculation of ϵ_R by using the appropiate values of Y'). Pattern 3 is another variation which allows the effects of a change in breathing flow rate to be examined by a comparison between the values of ϵ_{Ci} and ϵ_{Ce}, obtained from the results of pattern 2.

Three subjects were studied for each pattern, all at 4·5 μm particle diameter, which was considered to be about the highest size that could be employed in a study of the time-dependency of aerosol deposition in the respiratory zone. The deposition fractions obtained are listed in Table 5.1.3 and plotted in Figure 5.1.18. The individual and group-average breathing conditions are listed in Table 5.1.4. The calculated regional deposition efficiencies, ϵ_H, ϵ_c and ϵ_R, for values of $q_2 = q_3 = 1$, are plotted in Figures 5.1.19, 5.1.20, and 5.1.22, respectively.

Values of ϵ_R show no obvious increase between patterns 1 and 2, despite the fact that the mean particle residence time was some 50% higher in pattern 1, than 2. Values of ϵ_R in pattern 3 also show no obvious differences over those of pattern 1, although it should be borne in mind that the relative aerosol exposure to the respiratory zone is slightly different to that of patterns 1 and 2.

In view of the strong possibility of a finite retention of particles in the dead space airways, about one day after aerosol administration, the results of the breathing pattern study must be treated with some caution. In particular, it is possible, for example, that there are differences in ϵ_R between patterns 1 and 2, being masked by a large proportional contribution of dead space retention. Whatever the cause, the analysis of the preceding section has demonstrated that the deposition fractions, and therefore efficiencies, cannot be correct. It is therefore doubtful if any useful information can be derived from this aspect of the present work.

5.1.(v) Reproducibility of aerosol deposition fractions

Owing to the considerable time spent by each subject who participated in the study, it was not possible to obtain consent to perform repeat observations in more than a strictly limited number of subjects (MS and PT). Nonetheless, agreement between the two repeat runs was generally good in both cases (Table 5.1.5). Values of fD(I) are almost exactly equal, as are all the other deposition fractions for subject, MS. For subject, PT, there appears to be an increase in fS(I) at the expense of fC(I). This again indicates the importance of the larynx as a source of variability in a subject.

group mean $\bar{d}_{\mu m}$	subject	$f_{D(I)}$	$f_{W(I)}$	$f_{S(I)}$	$f_{C(I)}$	$f_{R(I)}$
	DCFM	7020	·0088	0	·2579	·4353
	AM	7945	·0087	·0265	·2331	·5262
	AR	·8776	·0116	·2555	·2210	·3895
4.5	group av.	·7914	·0097	·0940	·2373	·4503
	HG	·7882	·0105	·1362	·3528	·2887
	RB	·8946	·0215	·1460	·3468	·3803
	PCE	·7490	0	0	·3745	·3745
6.7	group av.	·8106	·0107	·0941	·3580	·3478
	PT *	·9050	·0352	·4526	·3562	·0611
	PH	·9281	·0367	·3565	·4386	·0963
	KD	·9644	·1047	·4605	·3057	·0936
10.4	group av.	·9325	·0589	·4232	·3658	·0837
	TDW	·9428	·0636	·4365	·3992	·0434
	JH	·8647	·1682	·2870	·3276	·0819
	AD	·8382	·0492	·3636	·3573	·0681
13·0	group av.	·8819	·0937	·3624	·3613	·0646

* = average of 2 results

Table 5.1.1: Deposition fractions in variable particle size study.

group mean $\bar{d}_{\mu m}$	subject	breaths min^{-1} f_b	sec. t_{p1}	inh : exh	litres (b.t.p.s.) e.r.v. + V_T
	DCFM	9·17	·70	1:2·20	n.d.
	AM	10·09	·62	1:2·50	3·17
	AR	10·15	·31	1:0·96	2·30
4·5	group av.	9·80	·54	1:1·89	2·74
	HG	10·27	·25	1:1·19	2·48
	RB	10·07	·34	1:1·71	2·95
	PCE	10·12	·25	1:0·94	n.d.
6·7	group av.	10·15	·28	1:1·28	2·72
	PT *	10·21	·32	1:0·98	2·65
	PH	10·03	·30	1:1·00	3·10
	KD	10·60	·24	1:1·29	3.20
10·4	group av.	10·28	·29	1:1·09	2·98
	TDW	9·81	·49	1:0·67	2·42
	JH	9·94	·27	1:0·95	2·90
	AD	9·90	·26	1:1·09	3·52
13·0	group av.	9·88	·34	1:0·90	2·95

n.d. = not determined

* = average of 2 results

Table 5.1.2: Individual breathing conditions (f_b = 10 breaths $min.^{-1}$, V_T = 1·0 l.) in variable particle size study.

pattern	subject	$f_D(I)$	$f_W(I)$	$f_S(I)$	$f_C(I)$	$f_R(I)$
1. V_T = 1·0 l f_b = 10 b.min.$^{-1}$	DCFM	·7020	·0088	0	·2579	·4353
	AM	·7945	·0087	·0265	·2331	·5262
	AR	·8776	·0116	·2555	·2210	·3895
	group av.	·7914	·0097	·0940	·2373	·4503
2. V_T = 1·5 l f_b = 6·67 b.min.$^{-1}$	ATM	·8356	·0027	·0774	·1239	·6316
	FH	·7566	·0005	·0371	·1869	·5321
	RH	·8292	0	·1780	·2084	·4428
	group av.	·8071	·0011	·0976	·1731	·5355
3. V_T = 1·0 l f_b = 6·67 b.min.$^{-1}$	VC	·8372	·0034	0	·3335	·5003
	MS *	·7308	·0044	·0639	·1623	·5002
	JV	·8466	·0010	·0204	·4456	·3796
	group av.	·8049	·0029	·0281	·3138	·4600

* average of 2 results

Table 5.1.3: Deposition fractions in variable breathing pattern study.

pattern	subject	breaths $min.^{-1}$ f_b	sec. t_{p1}	inh: exh	litres (b.t.p.s) V_T	litres (b.t.p.s) e.r.v.+ V_T
1.	DCFM	9·17	·70	1 : 2·20	1·0	n.d.
	AM	10·09	·62	1 : 2·50	1·0	3·17
	AR	10·15	·31	1 : 0·96	1·0	2·30
	group av.	9·80	·54	1 : 1·89	1·0	2·74
2.	ATM	6·77	·44	1 : 1·14	1·5	3·82
	FH	6·58	·35	1 : 1·18	1·5	4·54
	RH	6·57	·27	1 : 1·13	1·5	3·26
	group av.	6·64	·35	1 : 1·15	1·5	3·91
3.	VC	6·95	·66	1 : 1·48	1·0	3·78
	MS *	6·71	·37	1 : 1·05	1·0	3·00
	JV	6·67	·37	1 : 1·56	1·0	2·27
	group av.	6·78	·47	1 : 1·39	1·0	3·02

n.d. = not determined

* = average of 2 results

Table 5.1.4: Individual breathing conditions in variable breathing pattern study.

subject	$\bar{d}_{\mu m}$	$f_{D(I)}$	$f_{W(I)}$	$f_{S(I)}$	$f_{C(I)}$	$f_{R(I)}$
MS 1	4·5	·7312	·0045	·0873	·1471	·4923
MS 2	4·7	·7304	·0042	·0405	·1783	·5074
MS av.	4·6	·7308	·0044	·0639	·1623	·5002
PT 1	10·2	·8920	·0269	·3358	·4605	·0688
PT 2	10·6	·9180	·0434	·5693	·2519	·0534
PT av.	10·4	·9050	·0352	·4526	·3562	·0611

A. Deposition fractions.

subject	breaths min^{-1} f_b	sec. t_{p1}	inh:exh	litres (b.t.p.s.) V_T	litres (b.t.p.s.) erv + V_T
MS 1	6·70	·29	1:1·09	1·0	3·00
MS 2	6·72	·44	1:1·01	1·0	3·00
MS av	6·71	·37	1:1·05	1·0	3·00
PT 1	10·20	·34	1:0·91	1·0	2·65
PT 2	10·22	·30	1:1·05	1·0	2·65
PT av	10·21	·32	1:0·98	1·0	2·65

B. Breathing conditions.

Table 5.1.5: Reproducibility of results.

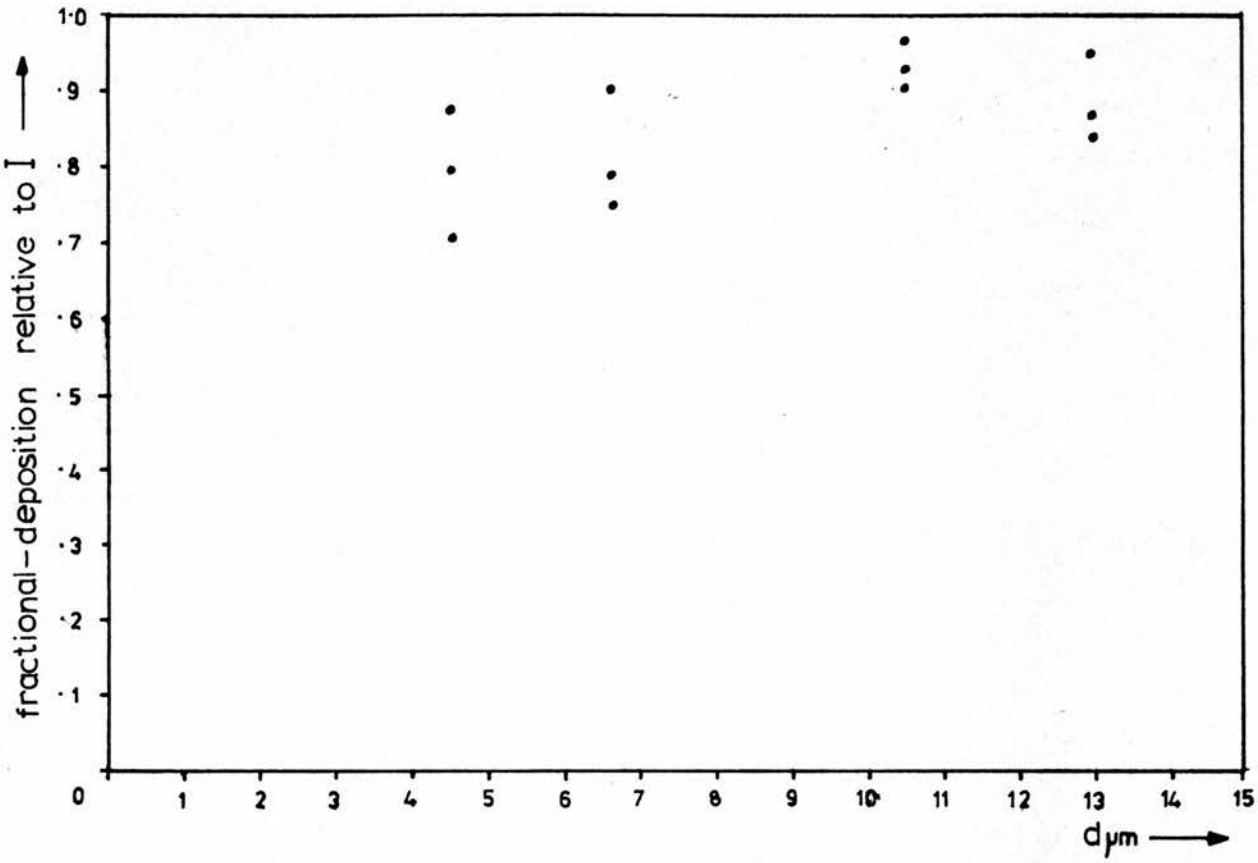

Figure 5.1.1: Total deposition fraction fD(I) vs. particle diameter (μ m).

N.B. On figures 5.1.2 - 5.1.6 which follow, the average values of the total deposition fraction (fD(I)) appear for purposes of comparison with each regional sub-division of this fraction.

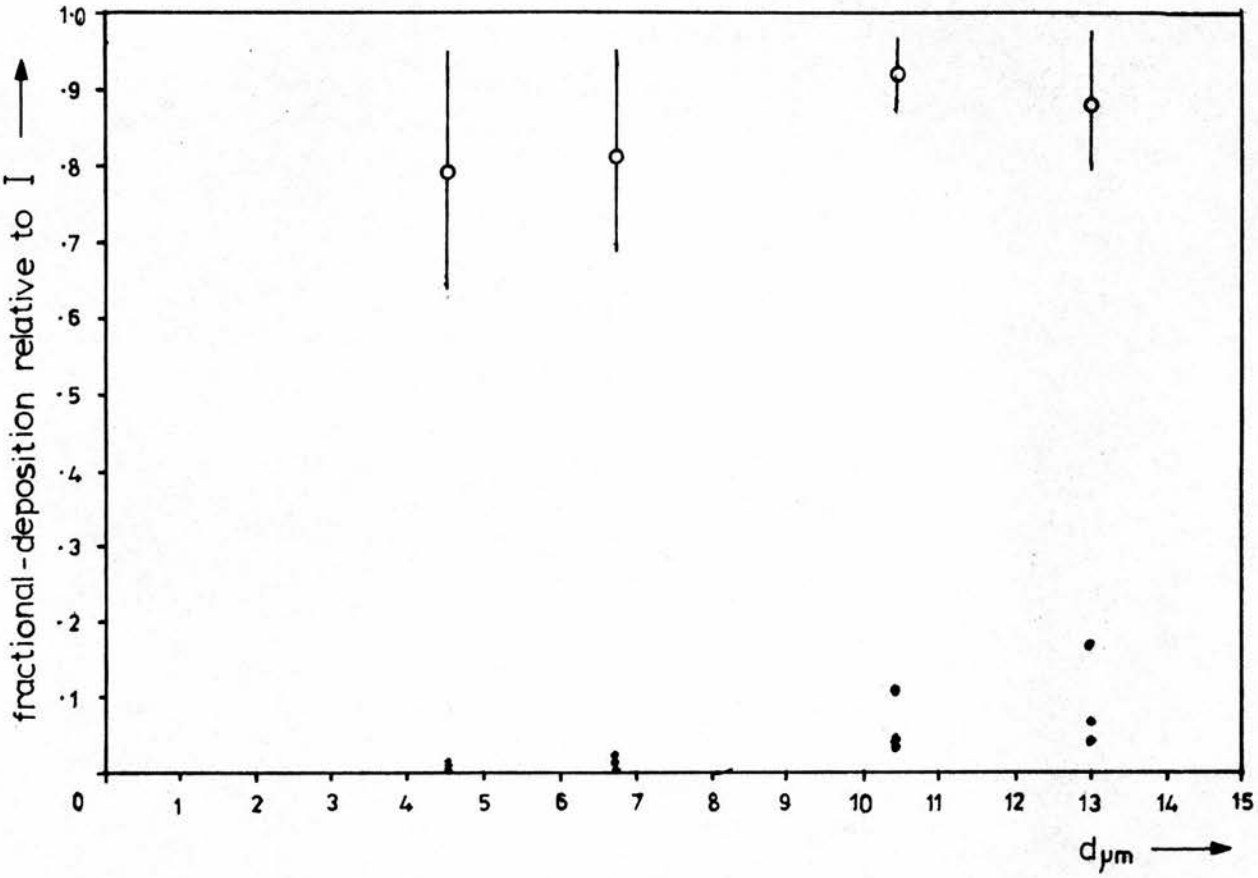

Figure 5.1.2: Mouth deposition fraction (fW(I)) vs. particle diameter (μm). Bars on fD(I) indicate 95% confidence limits about mean.

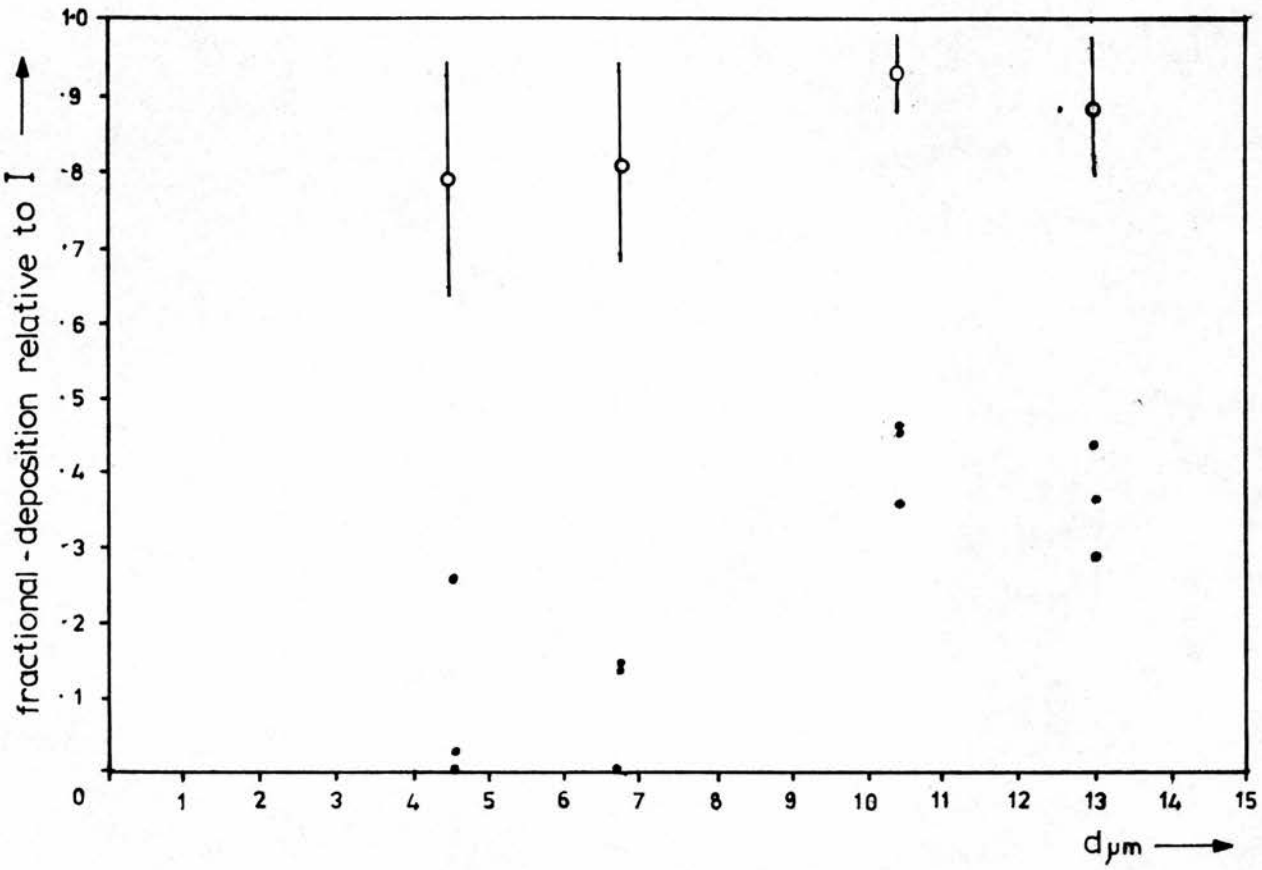

Figure 5.1.3: Throat deposition fraction (fS(I)) vs. particle diameter (μm). Bars on fD(I) indicate 95% confidence limits about mean.

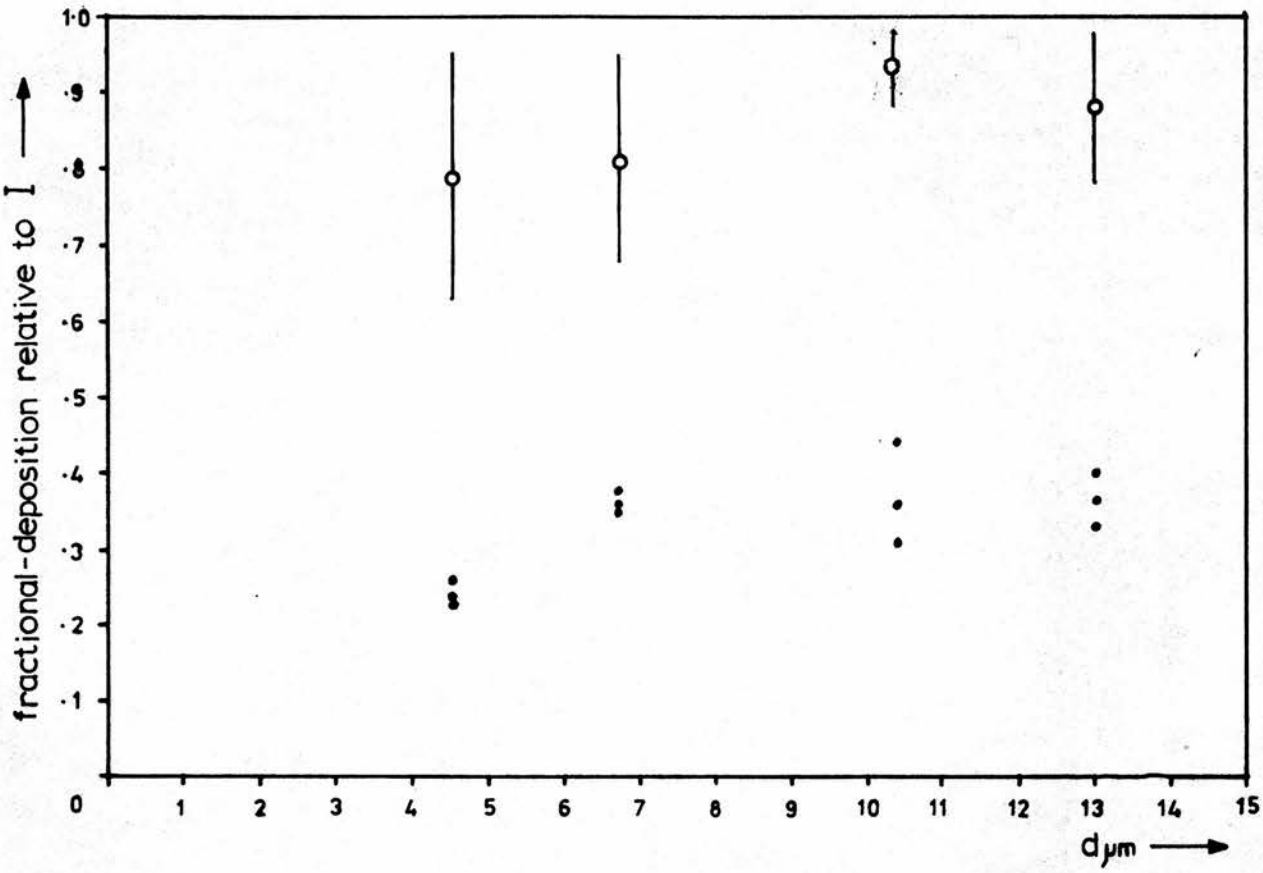

Figure 5.1.4: Cleared fraction (fC(I)) vs. particle diameter (μm). Bars on fD(I) indicate 95% confidence limits about mean.

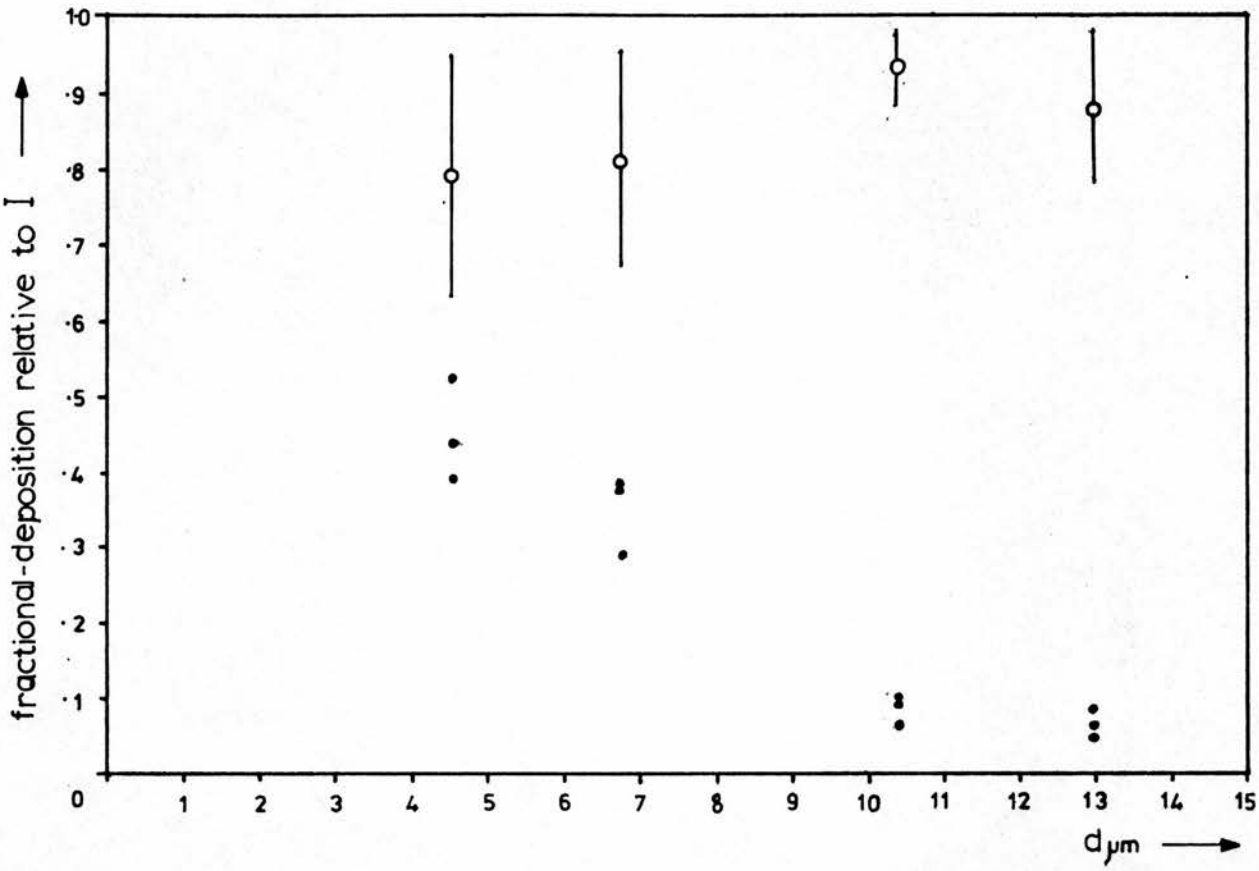

Figure 5.1.5: Retained fraction (fR(I)) vs. particle diameter (μm). Bars on fD(I) indicate 95% confidence limits about mean.

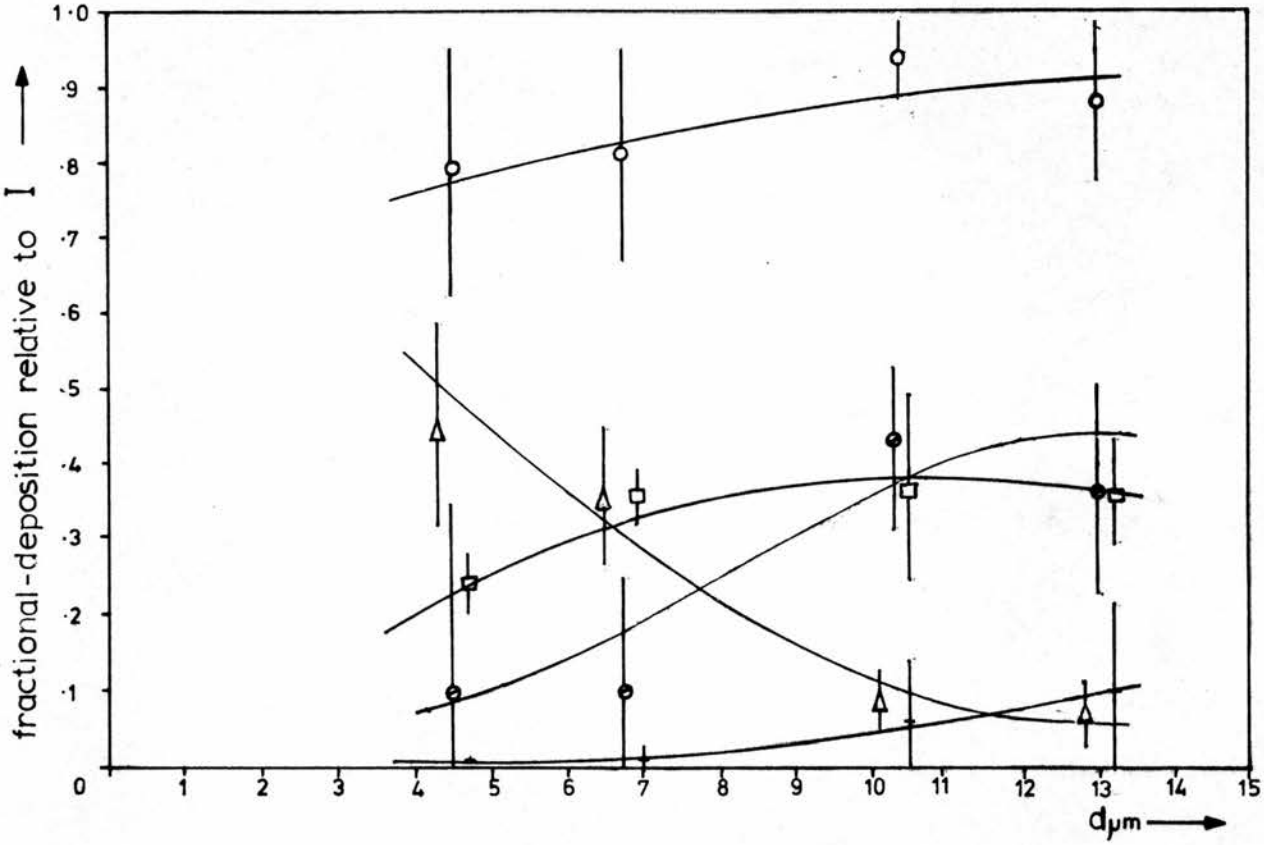

fW(I)

fS(I)

fC(I)

fR(I)

fD(I)

Figure 5.1.6(A): Average values of mouth deposition fraction (fW(I)), throat deposition fraction (fS(I), cleared fraction (fC(I)), retained fraction (fR(I)), and total deposition fraction (fD(I)), vs. particle diameter (μm). Bars indicate 95 % confidence limits about mean.

Lines drawn by eye-fit.

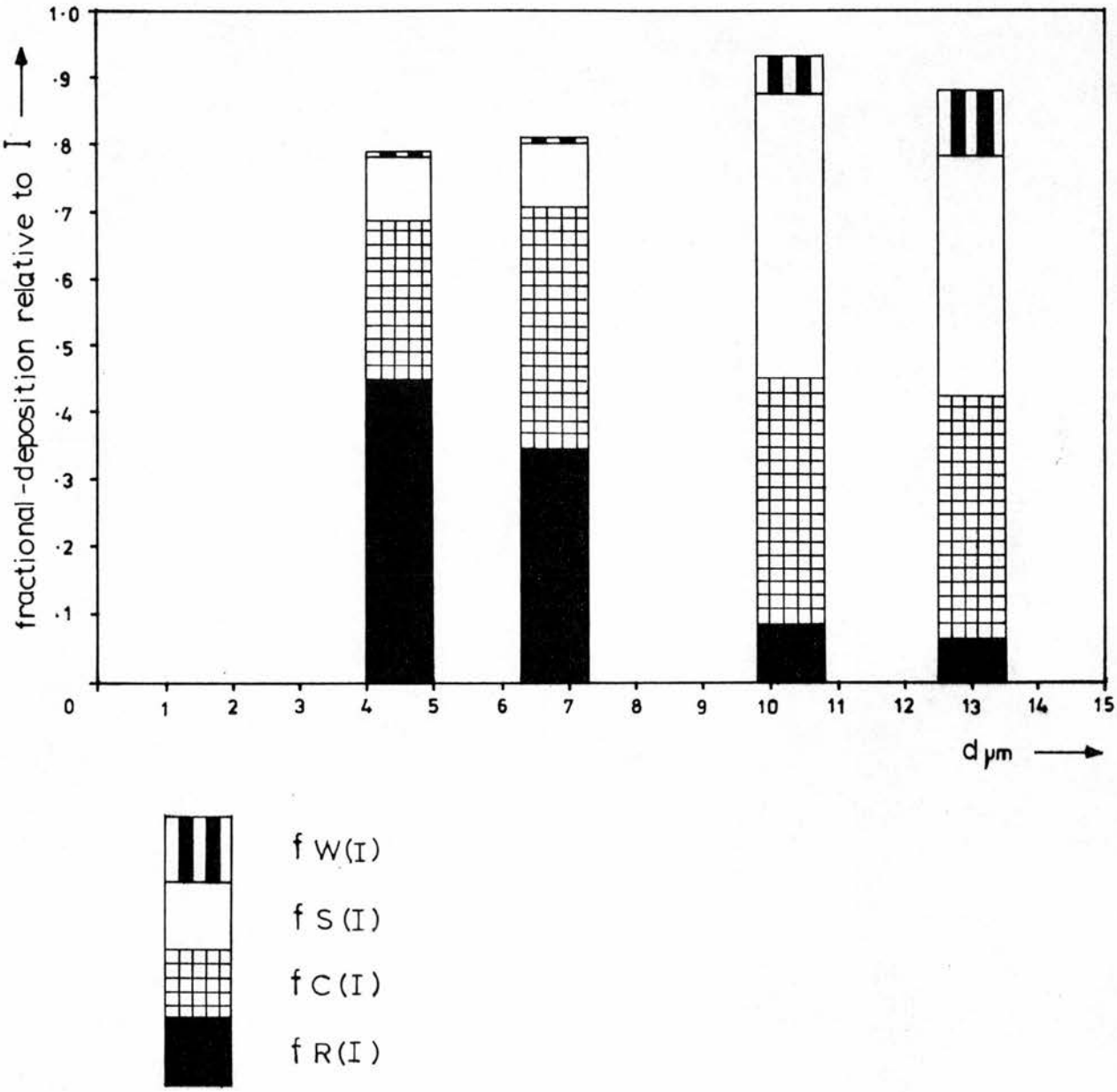

Figure 5.1.6(B): Average values of mouth deposition fraction (fW(I)), throat deposition fraction (fS(I)), cleared fraction (fC(I)), retained fraction (fR(I)), and total deposition fraction (fD(I)), vs. particle diameter (μm), expressed in histogram form.

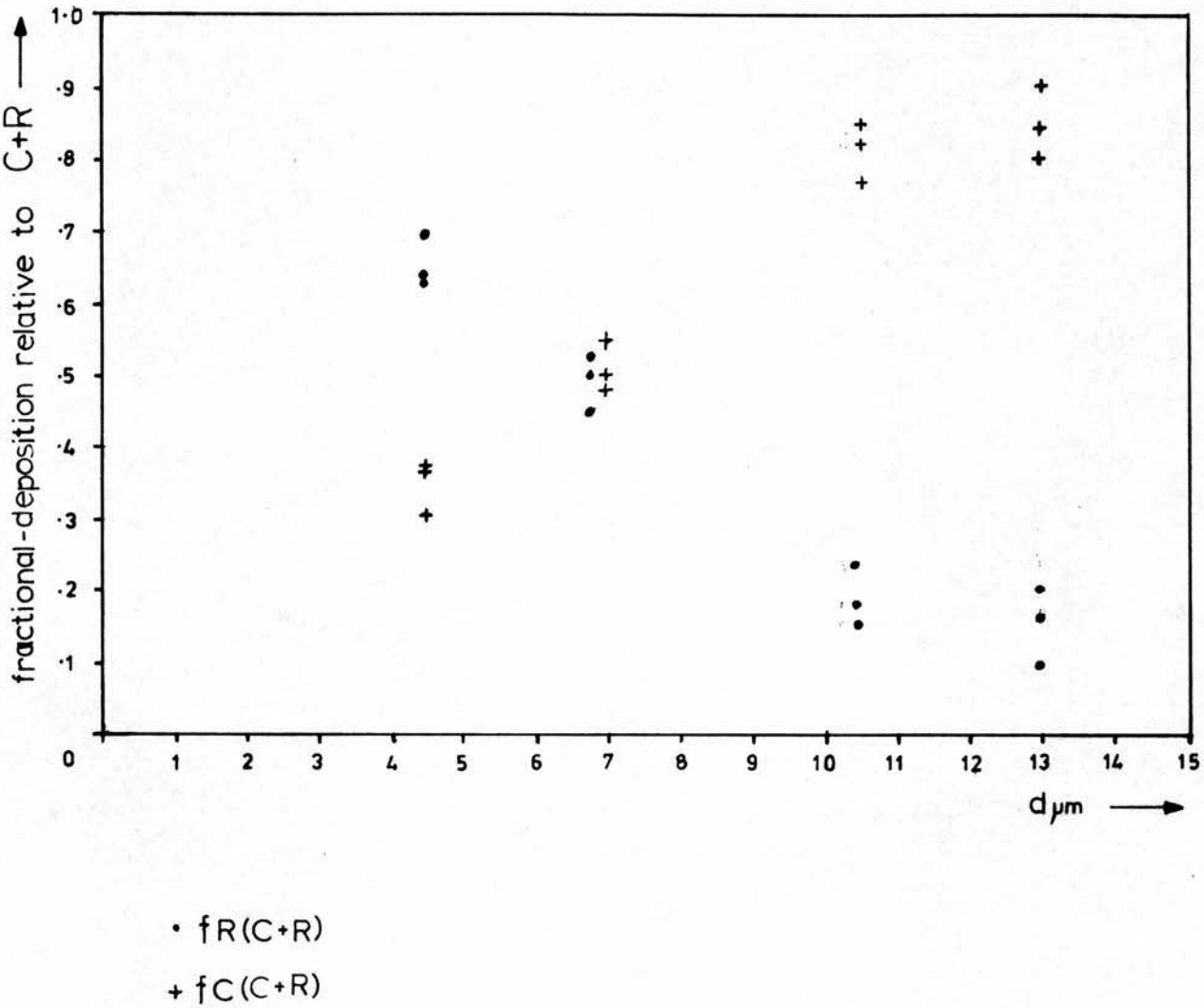

Figure 5.1.7: Cleared (fC(C + R)) and retained (fR(C + R)) material expressed as fractions of deposition below larynx (C + R) vs. particle diameter (μm).

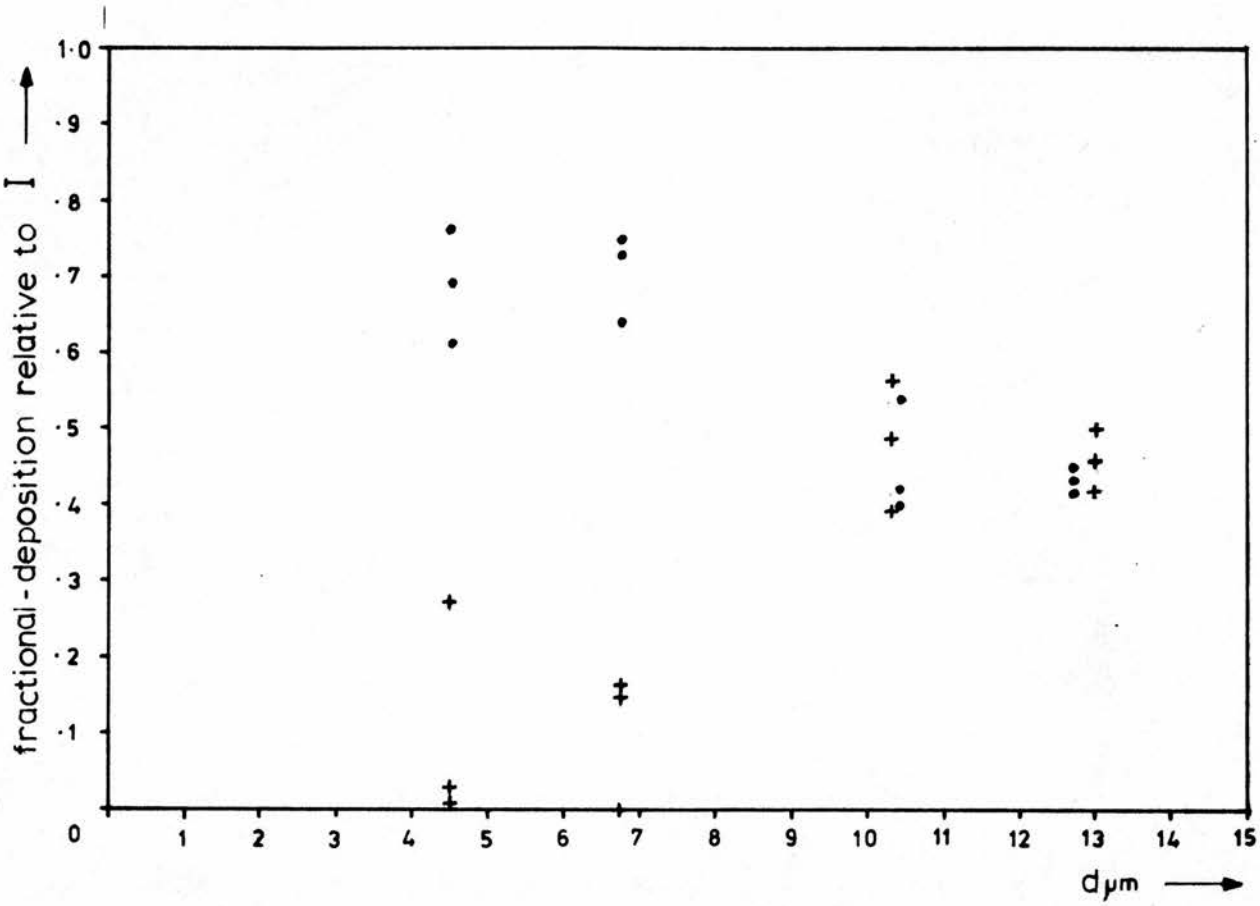

• fC+R(I)

+ fW+S(I) = f H(I)

Figure 5.1.8: Deposition fractions above (fW + S(I)) and below (fC + R(I)) larynx, expressed as fractions of the inhaled aerosol (I), vs. particle diameter (μm).

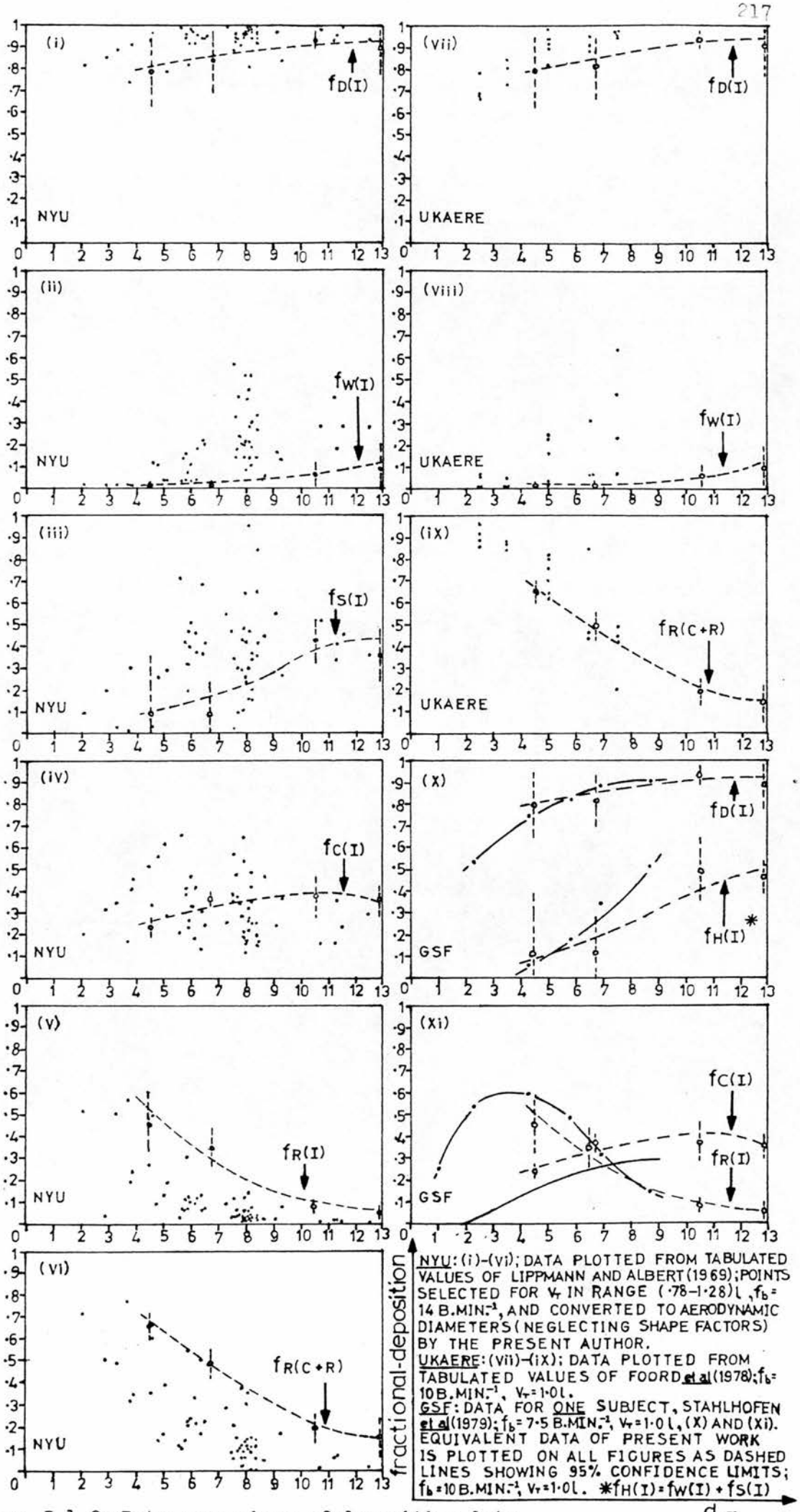

NYU: (i)-(vi); DATA PLOTTED FROM TABULATED VALUES OF LIPPMANN AND ALBERT (1969); POINTS SELECTED FOR V_T IN RANGE (·78–1·28) l, f_b = 14 B.MIN.$^{-1}$, AND CONVERTED TO AERODYNAMIC DIAMETERS (NEGLECTING SHAPE FACTORS) BY THE PRESENT AUTHOR.
UKAERE: (vii)-(ix); DATA PLOTTED FROM TABULATED VALUES OF FOORD et al (1978); f_b = 10 B.MIN.$^{-1}$, V_T = 1·0 l.
GSF: DATA FOR ONE SUBJECT, STAHLHOFEN et al (1979); f_b = 7·5 B.MIN.$^{-1}$, V_T = 1·0 l, (X) AND (Xi). EQUIVALENT DATA OF PRESENT WORK IS PLOTTED ON ALL FIGURES AS DASHED LINES SHOWING 95% CONFIDENCE LIMITS; f_b = 10 B.MIN.$^{-1}$, V_T = 1·0 l. * $f_{H(I)} = f_{W(I)} + f_{S(I)}$

Figure 5.1.9: Intercomparison of deposition data.

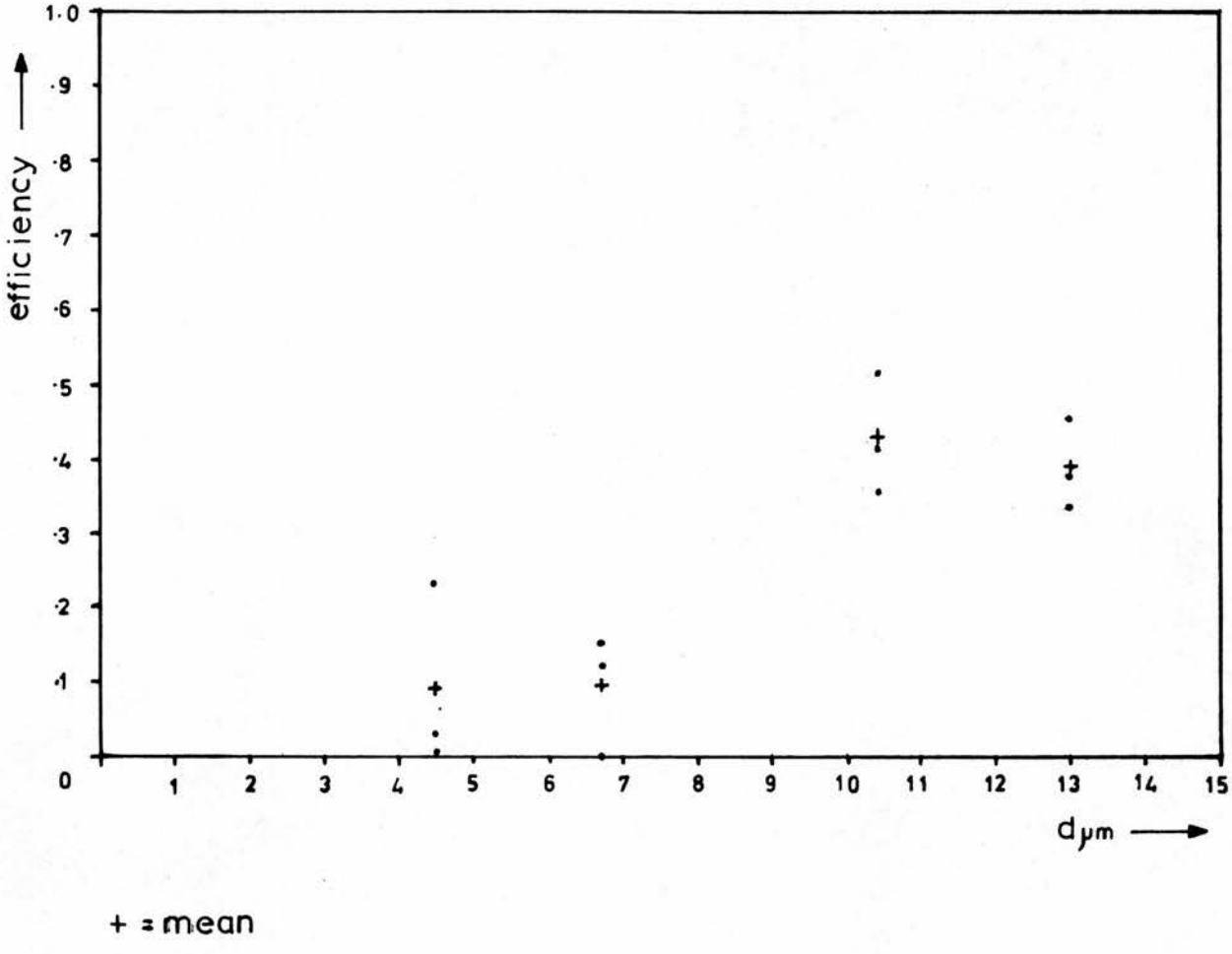

Figure 5.1.10: Estimated deposition efficiency (ϵ_H) in 'head filter' (H), vs. particle diameter (μm).

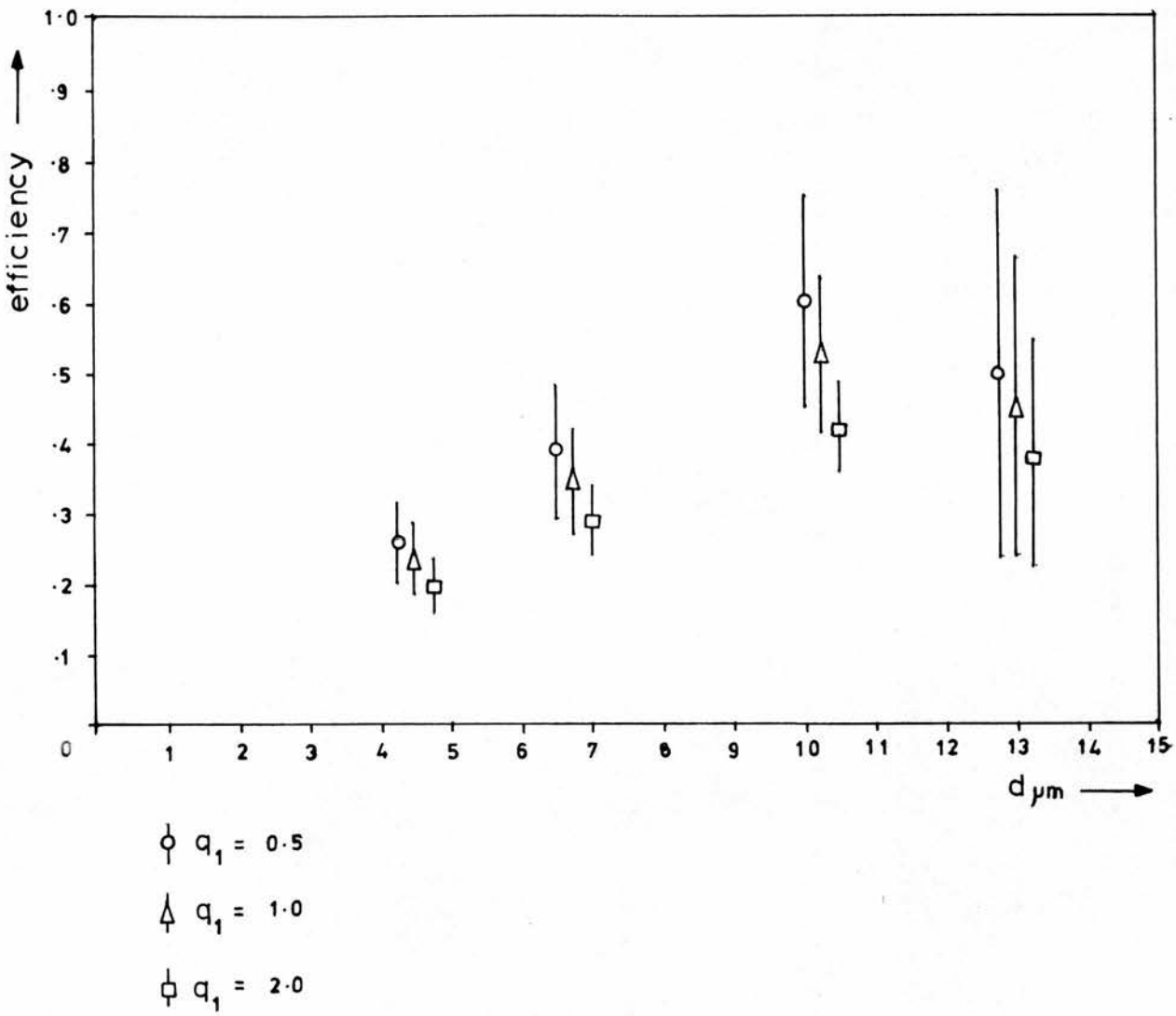

Figure 5.1.11: Estimated deposition efficiency (ϵ_c) in 'clearance filter' (C), vs. particle diameter (μm), for a range of q_1 values. Bars indicate 95% confidence limits about mean.

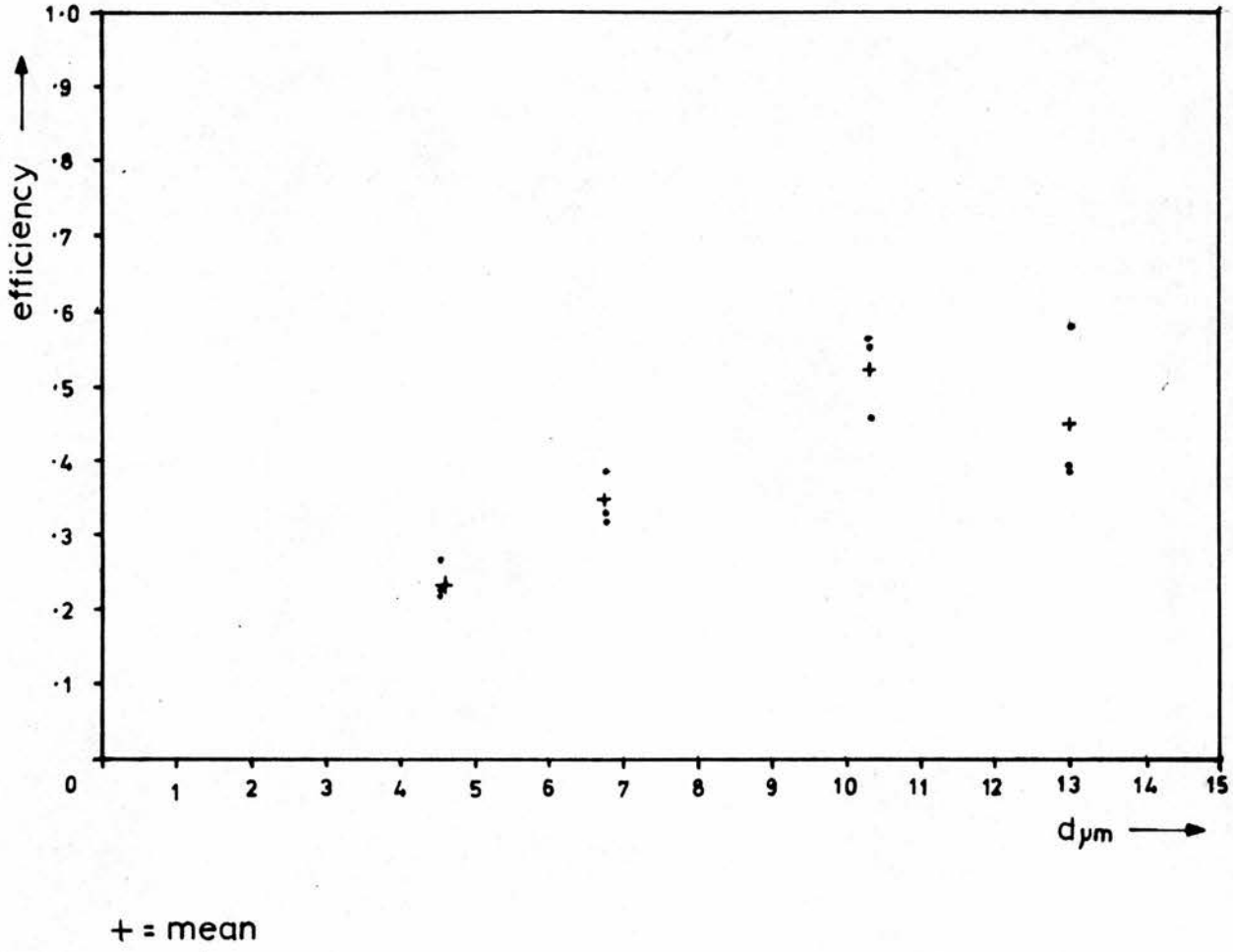

Figure 5.1.12: Estimated deposition efficiency (ϵ_c) in 'clearance filter' (C), vs. particle diameter (μm) for $q_3 = q_2 = q_1 = 1$

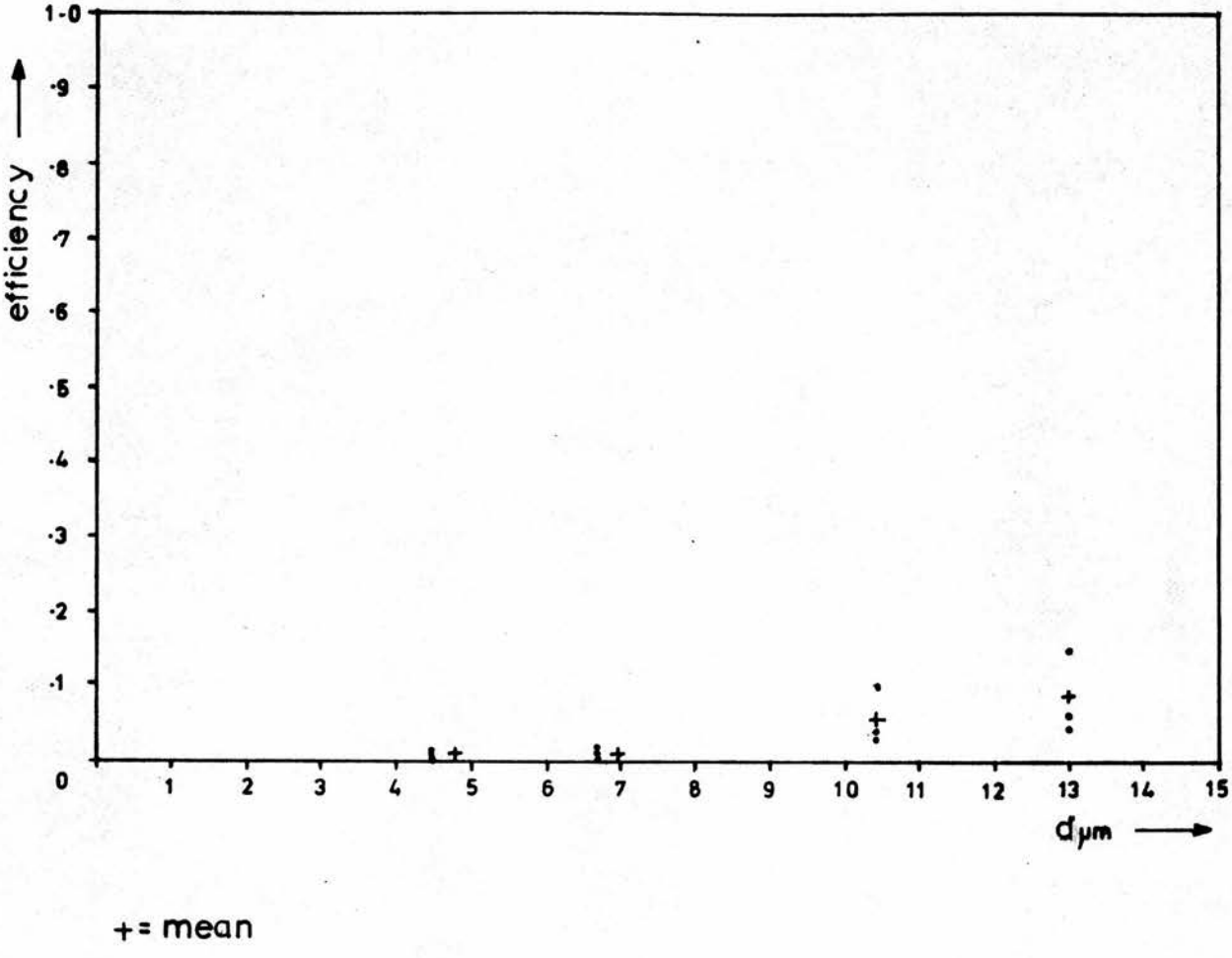

Figure 5.1.13: Estimated deposition efficiency (ϵ_W) in 'mouth filter' (W), vs. particle diameter (μm), for $q_3 = q_2 = q_1 = 1$.

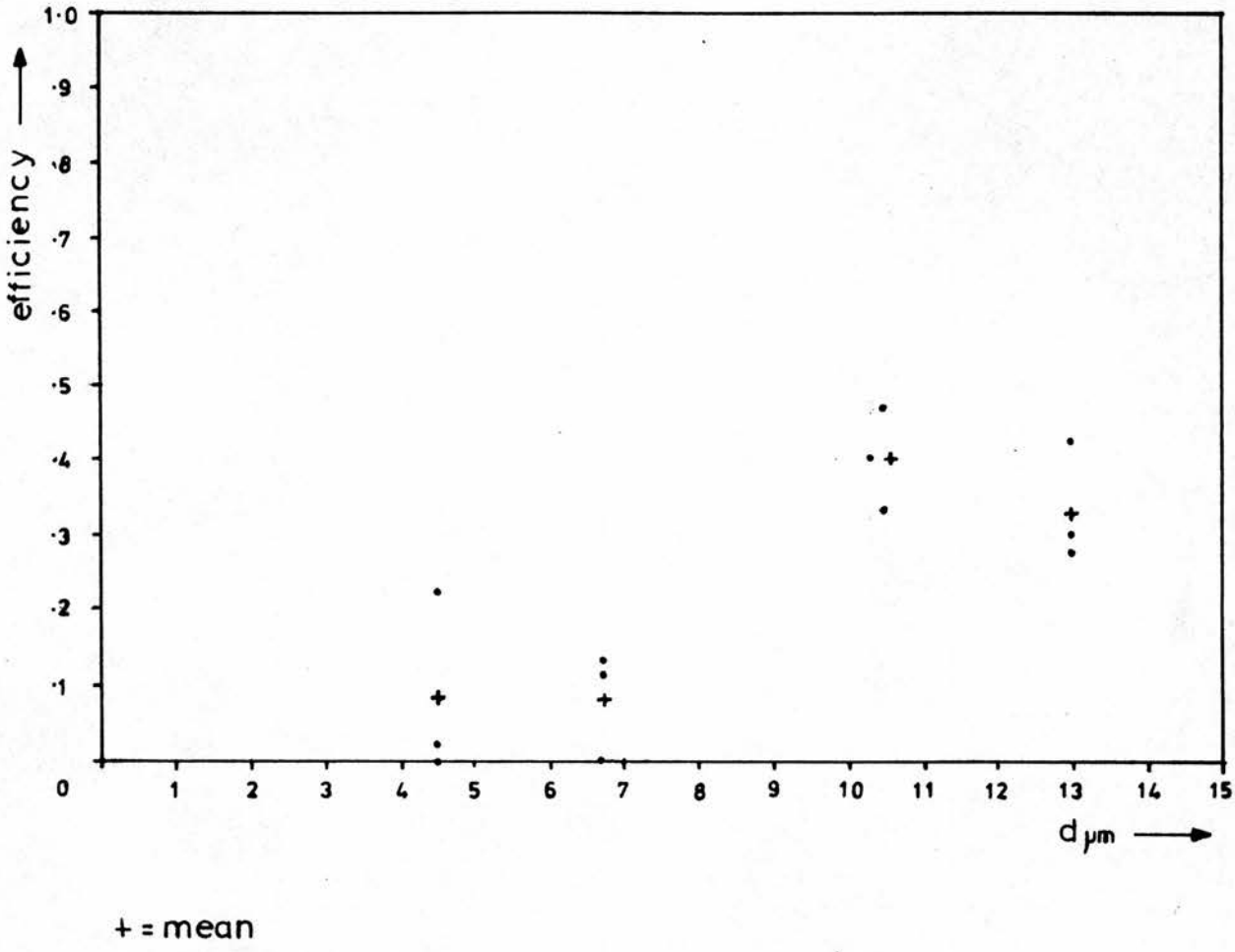

Figure 5.1.14: Estimated deposition efficiency (ϵ_S) in 'throat filter' (S), vs. particle diameter (μm), for $q_3 = q_2 = q_1 = 1$.

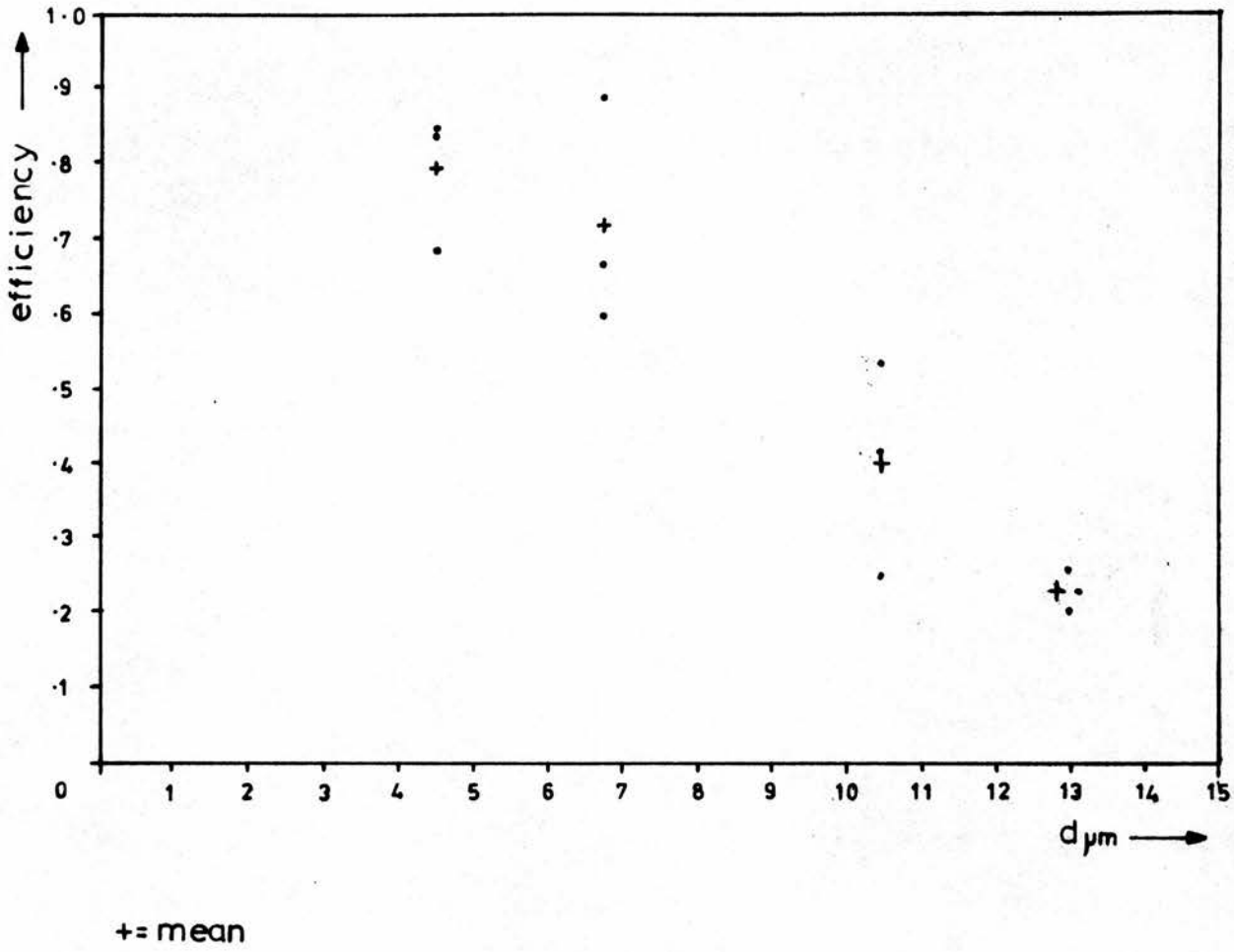

Figure 5.1.15: Estimated deposition efficiency (ϵ_R) in 'respiratory zone filter' (R), vs. particle diameter (μm), for $q_3 = q_2 = q_1 = 1$.

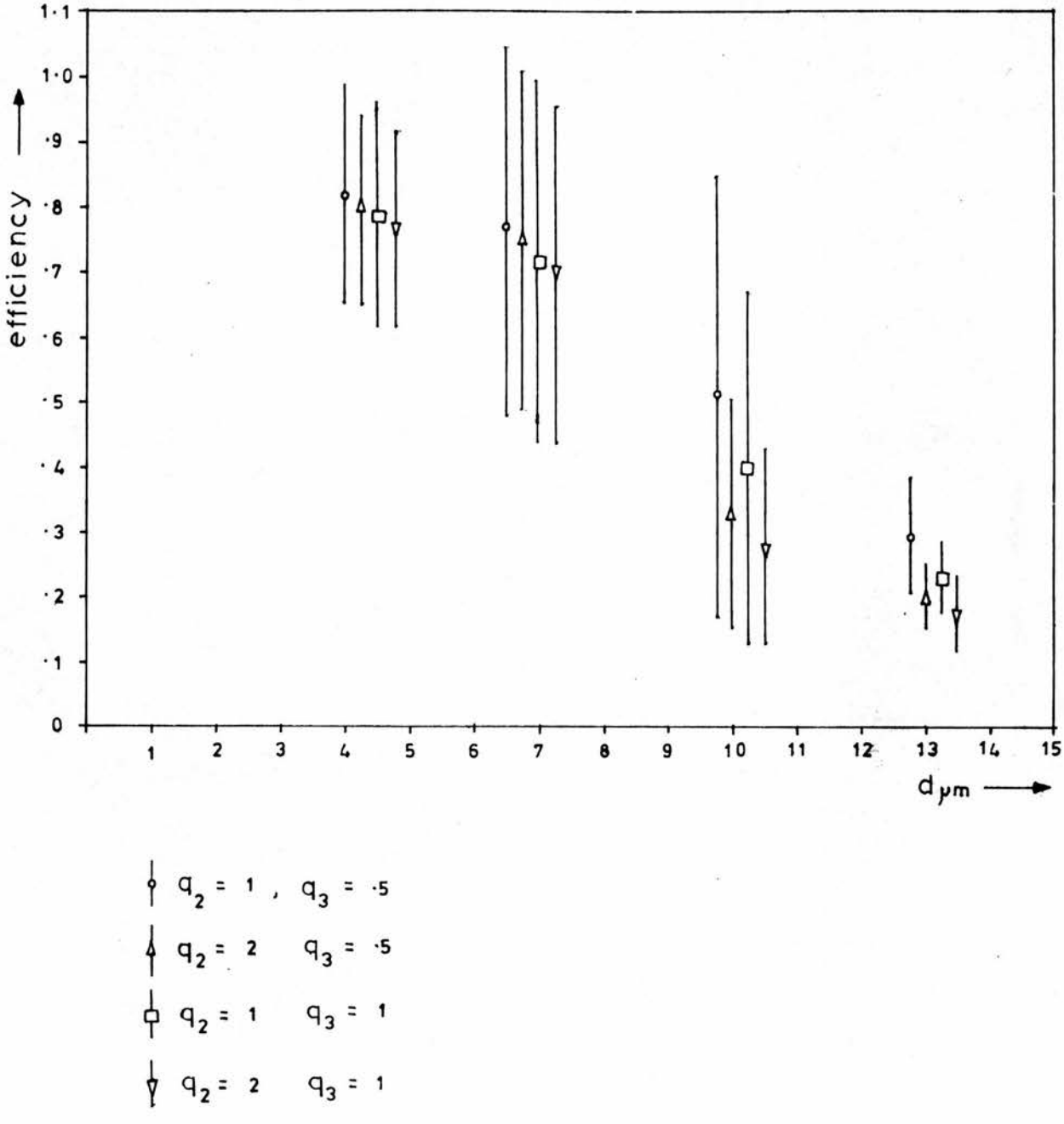

Figure 5.1.16: Estimated deposition efficiency (ϵ_R) in 'respiratory zone filter' (R), vs. particle diameter (μm), for a wide range of assumptions. Bars indicate 95% confidence limits about mean.

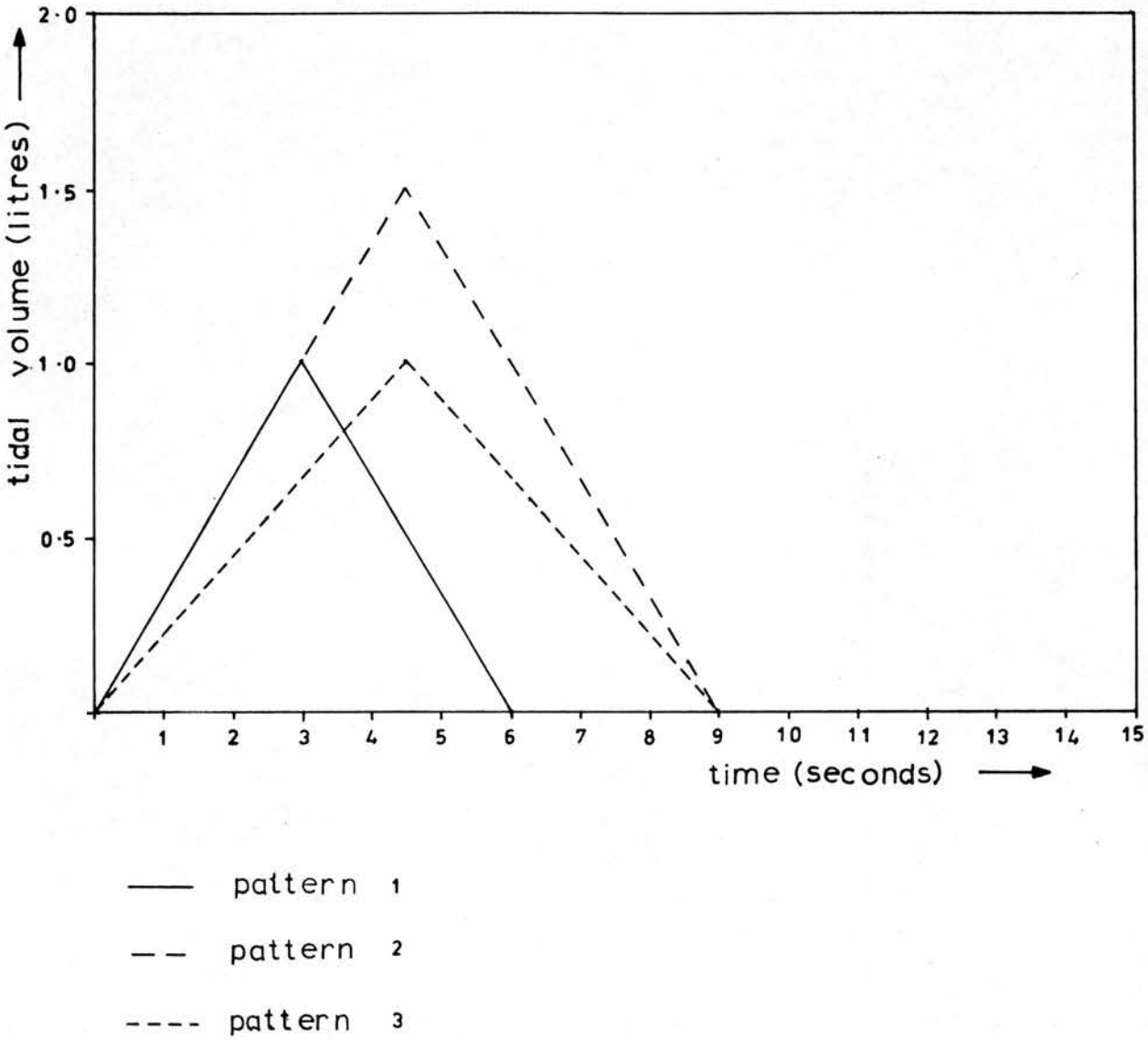

Figure 5.1.17: Breathing pattern study.

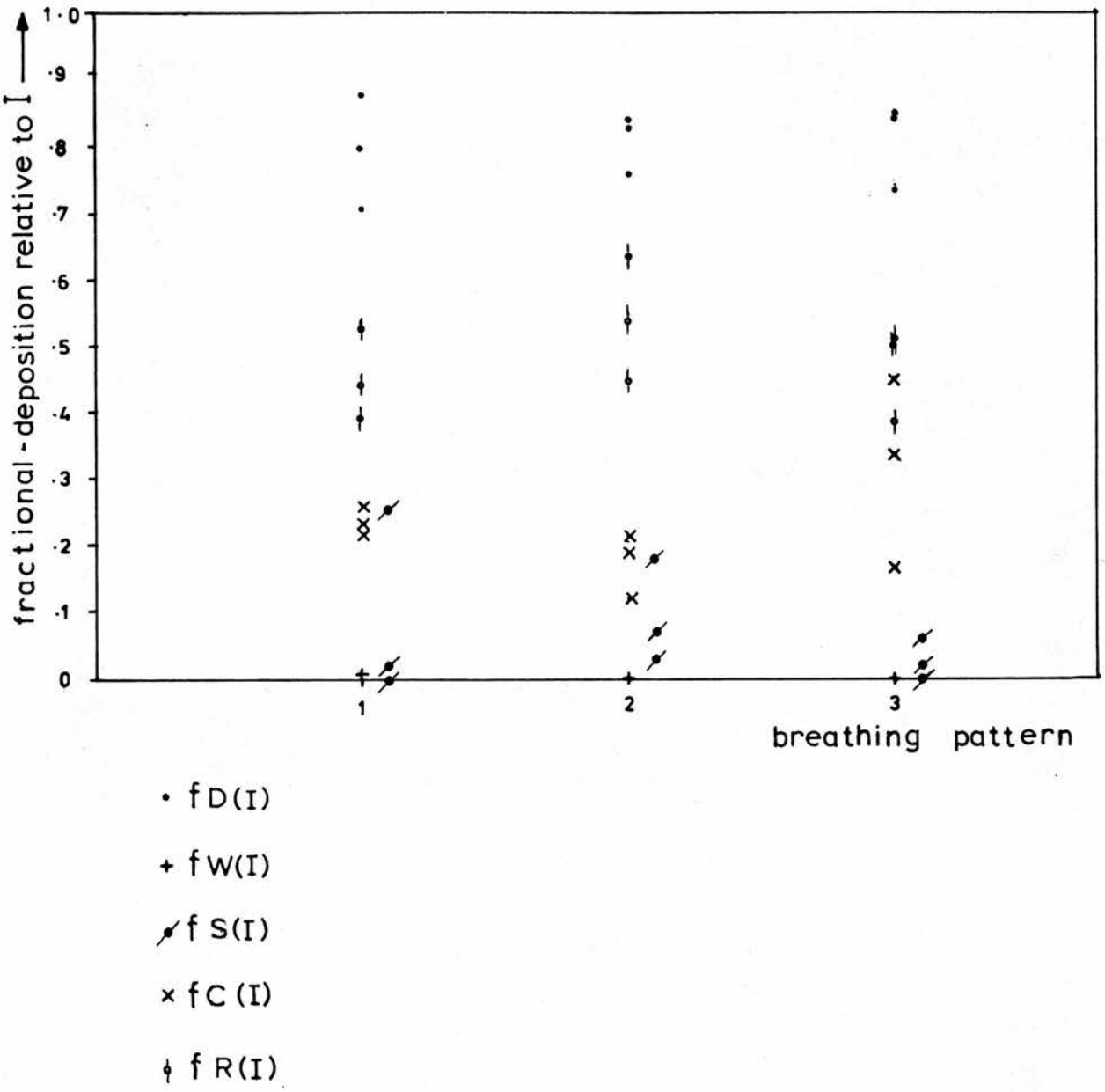

Figure 5.1.18: Breathing pattern results.

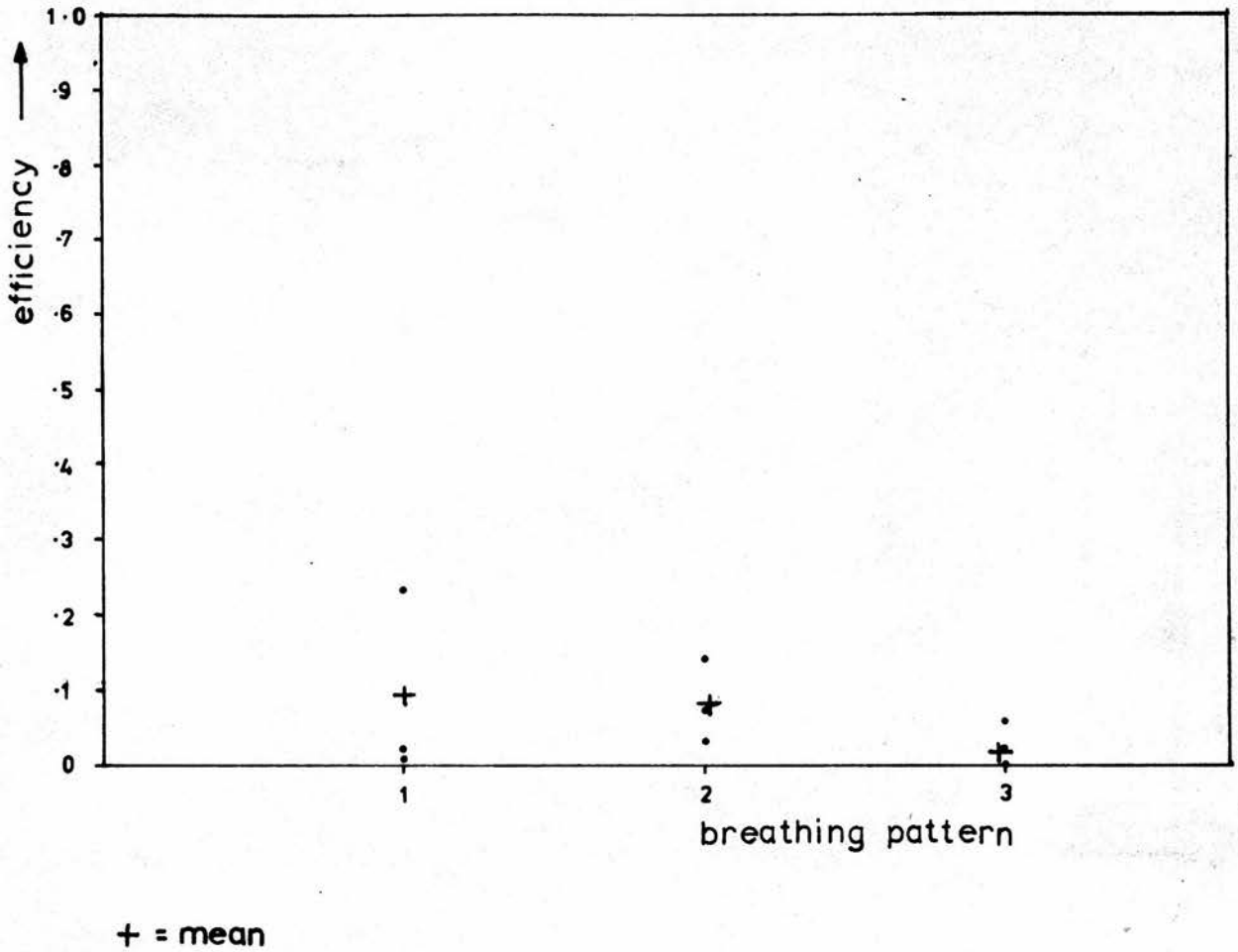

Figure 5.1.19: Estimated deposition efficiency (ϵ_H) in 'head filter' (H) in breathing pattern study, vs. particle diameter (μm), for $q_2 = q_1 = 1$.

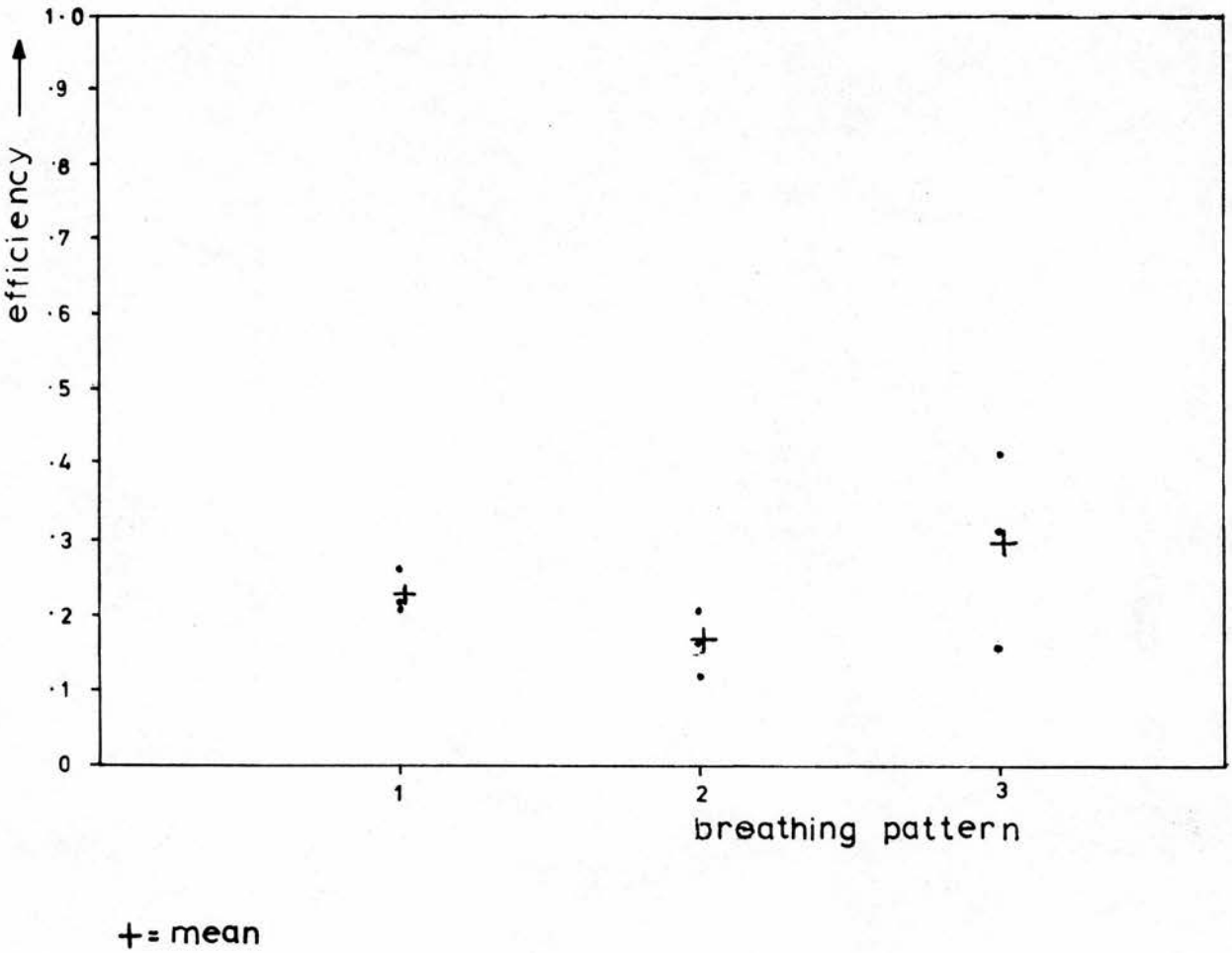

Figure 5.1.20: Estimated deposition efficiency (ϵ_c) in 'clearance filter' (C) in breathing pattern study, vs. particle diameter (μm), for $q_3 = q_2 = q_1 = 1$.

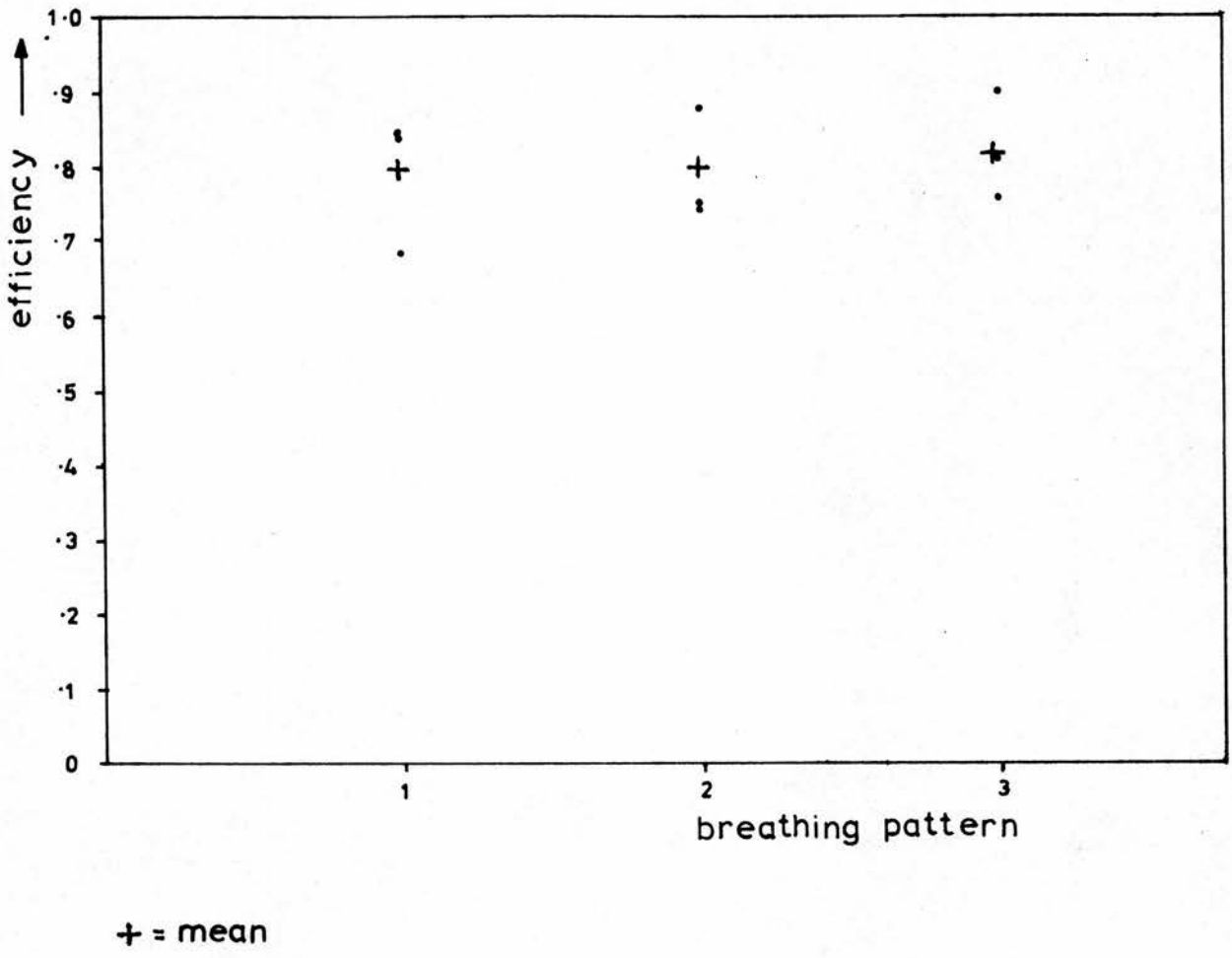

Figure 5.1.21: Estimated deposition efficiency (ϵ_R) in 'respiratory zone filter' (R) in breathing pattern study, vs. particle diameter (μm), for $q_3 = q_2 = q_1 = 1$.

5.2 Short-term clearance results

(i) Profile scanner clearance curves

The individual profile scanner clearance curves are plotted in Figures 5.2.1 - 5.2.4. The averages alone are shown in Figure 5.2.5 (averages calculated at hourly intervals). By means of the vertical scale shown in the latter figure, the times taken to clear specific percentages of the initial deposit below the larynx have been calculated, and are plotted in Figure 5.2.6. Although all individual clearance curves exhibit a marked scatter of points, whose possible origin is discussed below, all manifest a clear downwards trend with increasing time and a virtual levelling-off after several hours, particularly at large particle sizes.

This indicates that the larger particle sizes tend to deposit in the upper airways, to be cleared quickly, while the smaller particles penetrate more deeply into the lungs and are cleared more slowly. The results shown in Figure 5.2.6 indicate that the percentage of the initial deposit cleared is a reasonably constant fraction of the final amount cleared, at any particle size, for the early part of the clearance period. This might imply that the relative amount of aerosol depositing in very large airways at successively greater depths, tends to be a reasonably constant fraction of the total deposit below the larynx, at any size. However, the picture is complicated by the liklihood of a finite dead space retention, which might vary in an unknown manner with particle size.

There is no obvious evidence in these curves of a 'delayed' short-term clearance from the respiratory zone. The final point determination at 20 - 22 hours after aerosol administration is generally close to the levels of retention measured the previous night (on the individual curves), indicating only a small degree of clearance in the intervening period.

The observation of a very rapid fall-off in retention in the first few minutes after aerosol administration by ALBERT et al. (1973), is not supported by the present data, which are more consistent with the results of BOOKER et al. (1967) and STAHLHOFEN et al. (1979). It is possible that full account was not taken by ALBERT and LIPPMANN (1973) of the material which initially deposits in the laryngeal/pharyngeal region, as was discussed above. This is shown in the present work to be a significant deposit at all particle sizes employed and, also, to be rapidly translocated to the stomach.

5.2(ii) Throat clearance curves

The origin and purpose of the throat clearance measurements was described in Chapter 3, part 3(iii). As many measurements per unit time as possible were made in order to resolve the very rapid clearance fluctuations. The throat clearance curves for those subjects with only a single detector placed over the larynx are presented in Figures 5.2.7 - 5.2.12, and those for subjects with the double detector arrangement, in Figures 5.2.13 - 5.2.22. In the figures showing the double detector results, Tα refers to the laryngeal measurements, Tb , to the tracheal. Two sets of curves are presented in each case: (i) a plot of total counts obtained in

a two-minute counting period (after allowing for radiation background and isotope decay); (ii) a plot of the average recorded counts over four successive two-minute counting periods. The latter enables the slower phase changes to be more rapidly discerned.

The throat clearance curves obtained at the large particle sizes (PT1, Figure 5.2.12; PT2, Figure 5.2.17; AD, Figure 5.2.13; KD, Figure 5.2.18), with the possible exceptions of subjects JH, Figure 5.2.11, and PH, Figure 5.2.10 (a smoker), manifest a rapid fall-off in count rate after only several hours, as might be expected. The throat clearance curves for subject, PT, obtained at different dates (c.f. Figures 5.2.12 and 5.2.17(i), Tα curve), are markedly alike. In the case of subject, MS, the Tα and Tb , curves (Figures 5.2.20 and 5.2.21) obtained at different dates and averaged over four consecutive measurements (ii) show only poor agreement, which is not any more obviouly apparent in the non-averaged curves (i). In Figure 5.2.20(i), (MS1), any agreement between the Tα/Tb, curves obtained on the same date is somewhat obscured by the rapidity of the clearance fluctuations, but is apparent on the averaged curves(ii).

The double detector curves for subject, AD, manifest the most obvious temporal phase-lag agreement between the Tα and Tb curves (Figure 5.2.13(i) and (ii)), while those for subjects ATM, RH, and KD, (Figures 5.2.14, 5.2.16, and 5.2.18, respectively), are uncertain over both curves (i) and (ii). Subjects, FH, VC, and JV, (Figures 5,2.15, 5.2.19, 5.2.22, respectively) show no obvious signs of matching between Tα and Tb . Subject JV in particular exhibits the worst disagreement between the Ta and Tb curves for any subject.

His was also the only case when it became necessary to employ a wholly inexperienced operator of the throat detectors and it seems likely that the Tα detector was wrongly positioned over the throat, perhaps missing most of the larynx.

However, all these clearance curves exhibit temporal variations that are often non-random, indicating they are of systematic origin. The absence of phasic matching in the Tα and Tb curves of some subjects indicates that changes in the distribution of particles whilst they reside in the tracheal/laryngeal region may be of importance in some cases, while the phasic matching in other cases is good evidence for the existence of large variations in the distribution of particles over the airway walls, before they are cleared into the trachea. This would be consistent with the limited observations of MORROW (1967), who placed a single detector above the carinal ridge of the trachea and observed a single clearance 'oscillation', having a period of about one hour. Some non-random clearance fluctuations were also observed by ALBERT *et al* (1967).

It therefore seems justifiable to consider the origin of the fluctuations in relation to the deposition and clearance processes of the human respiratory tract. However, it is pointed out that the following discussion is intended only as helpful speculation.

Although there will undoubtedly be a local variation in the initial distribution of inhaled particles over the airways, particularly at the bifurcations, it would seem improbable that such local variations could persist during the ciliary transport

process and arrive at the trachea 'intact'. YEATES et al. (1975) have observed the tracheal transit of several impaction 'boli', shortly after dust insufflation, so it is just possible that some of the early peaks observed in the present work have such an origin. Despite this, the observation of non-random clearance fluctuations, even up to nine hours after aerosol administration, makes it highly unlikely that their sole origin lies in the initial particle distribution. It is generally accepted that sedimentation is the dominant deposition mechanism in the smaller airways (TAULBEE and YU, 1975), which would tend to leave a fairly uniform deposit over the airway walls. The possibility of a local variation in the sedimentation deposit is hard to predict, but even if such deposits existed they would be unlikely to persist during the long ciliary transport process. Moreover, the slower phase clearance fluctuations observed in the present work must also be considered. In many subjects there is a slow but large rise in count rate, followed by a slow fall, followed by another rise. It would seem improbable that the intervening period of low count rate between peaks represents a specific region of the airways in which neglible particle deposition occurred. Presumably, the ciliary transport fluid entering the trachea at any given time has its origin over a wide range of different airway paths. It seems inconceivable that each of these different paths, at a given point, experience a simultaneous failure in the particle deposition mechanisms. It may therefore be more reasonable to consider the possibility of a biological modification to the inhaled particle distribution.

A number of biological factors may exert a possible influence on the relative amounts of inhaled particles clearing into the trachea at different times. Perhaps the most obvious is the liklihood that the thickness of the ciliary transport fluid increases as it 'ascends' the airways (HILDING, 1965). This arises because material is being cleared from a large area ($\sim 0{\cdot}5\ m^2$; see Table 1.1.1) into the comparatively small area of the trachea. It has even been postulated that a fluid 're-sorption' must occur in the larger airways in order to accommodate this large volume of cleared fluid (KILBURN, 1968). A degree of mixing and overlapping of fluid layers from daughter airways is therefore likely to occur at the bifurcations. This would have the effect of raising the specific radioactivity per unit area of an inhaled radioactive aeroaol. However, since such changes would be necessarily slow in character they may, perhaps, only account for the more gradual changes observed in the present work. Although, before this mechanism is entirely discounted,it should be remembered that airway morphometry is highly asymmetrical and, in reality, quite unlike the classical mathematical descriptions frequently employed (WEIBEL, 1963). It is therefore likely that material which is inhaled at a particular time and enters the trachea, at any time, has its origin, in part, over the large airways, and, in part, over the smaller airways having shorter total clearance paths to the trachea. Assuming that the ciliary transport fluid thickens as it 'ascends' the airways, the material which initially deposited over the small airways,and was concentrated, would therefore arrive

at the trachea simultaneously with material which initially deposited on the large airways, and was not. Since a few areas of the radioactive deposit in the small airways must clear quite quickly, relative to other deposits in the large airways, both the early and later peaks observed might be explained in these terms.

Another possible biological modifying influence on the inhaled particle distribution is that of the secretion of mucus from the mucous glands that are found most frequently in the large airways. Such an influence would depend on there being an irregularity in the mucus emissions as well as a subsequent delaying effect on the clearance process.

Finally, there is the more direct possible influence of the cilia themselves. If their beat frequency were to undergo large temporal variations in the large airways or trachea, clearance fluctuations might result. However, aside from the slow diurnal changes, more rapid fluctuations have never been reported by those involved in the direct measurement of clearance rates in the trachea and elsewhere (SACKNER et al, 1973; BATEMAN et al. 1978), as far as can be ascertained from the literature.

In conclusion, no definitive explanation of the observed clearance fluctuations can be offered, but the balance of arguments would seem to favour a mainly biological cause.

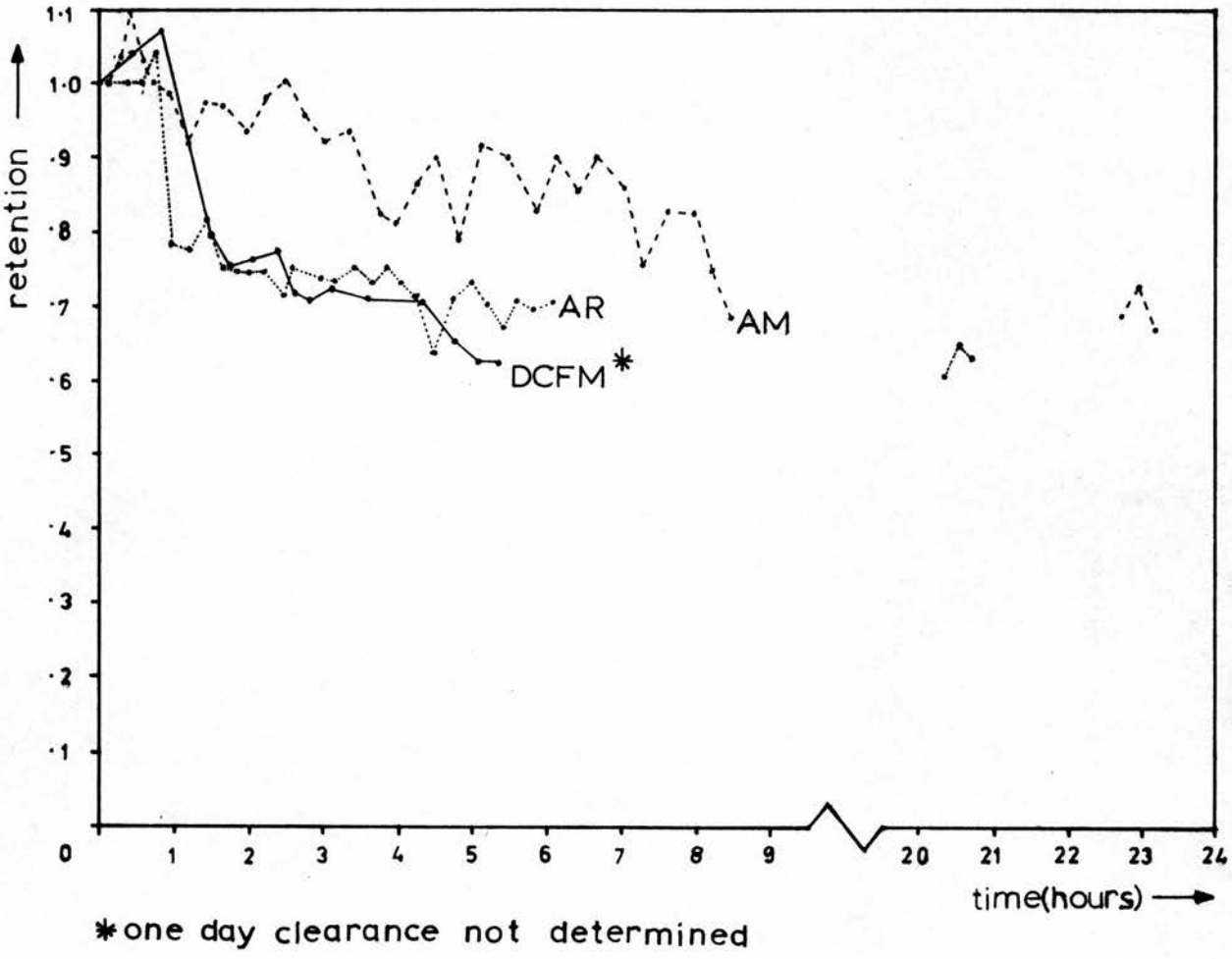

Figure 5.2.1: Clearance curves at a group-mean particle diameter of 4·5 μm

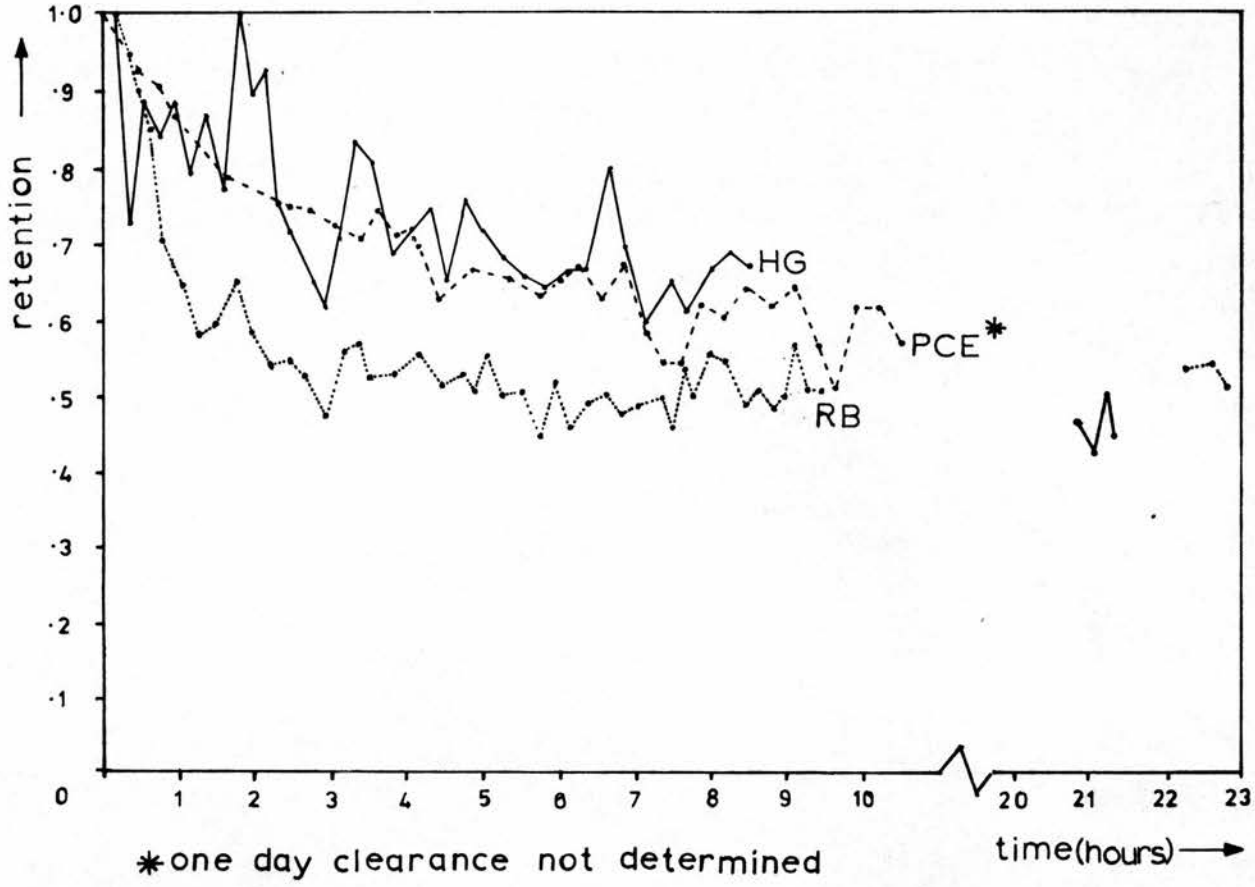

Figure 5.2.2: Clearance curves at a group-mean particle diameter of 6·7 μm.

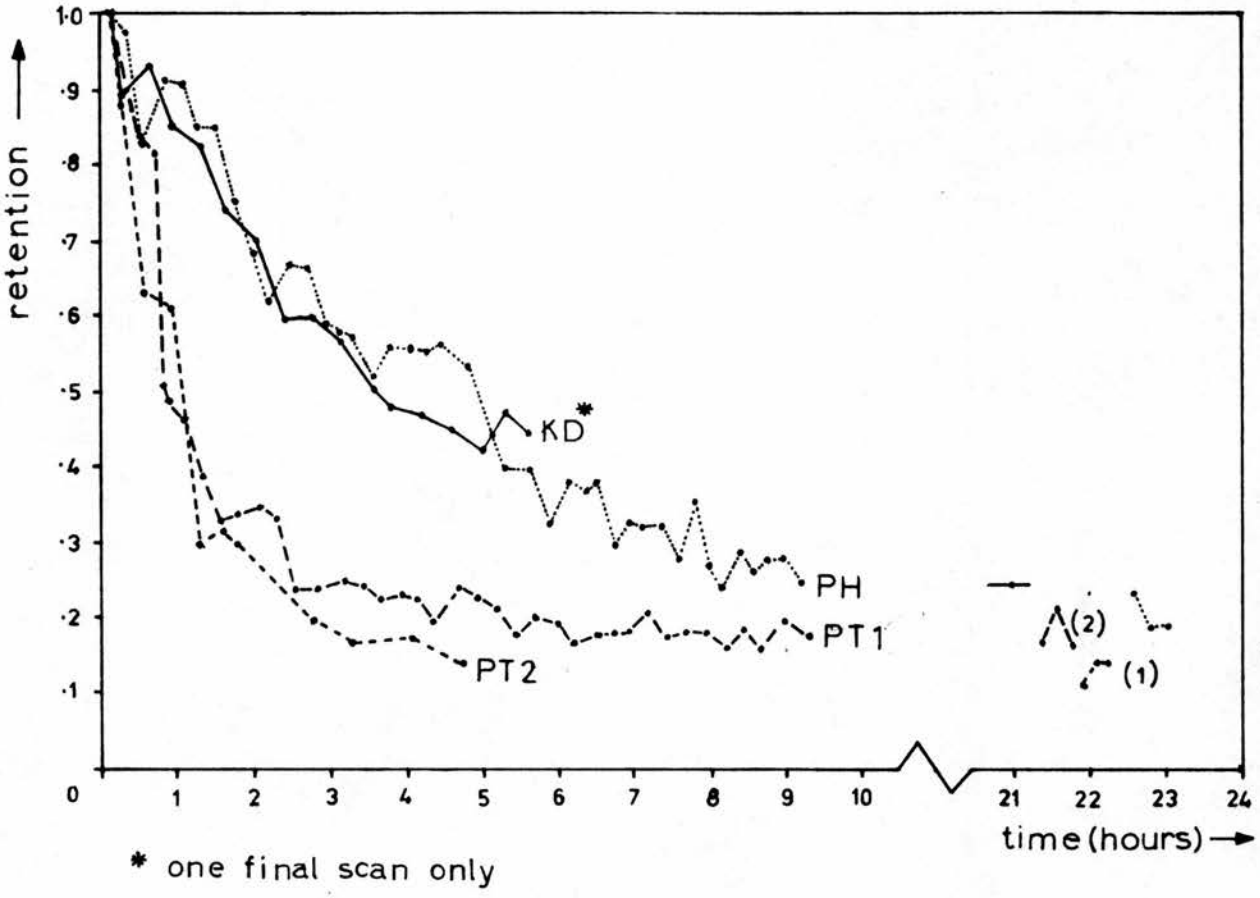

Figure 5.2.3: Clearance curves at a group-mean particle diameter of 10·4 μm

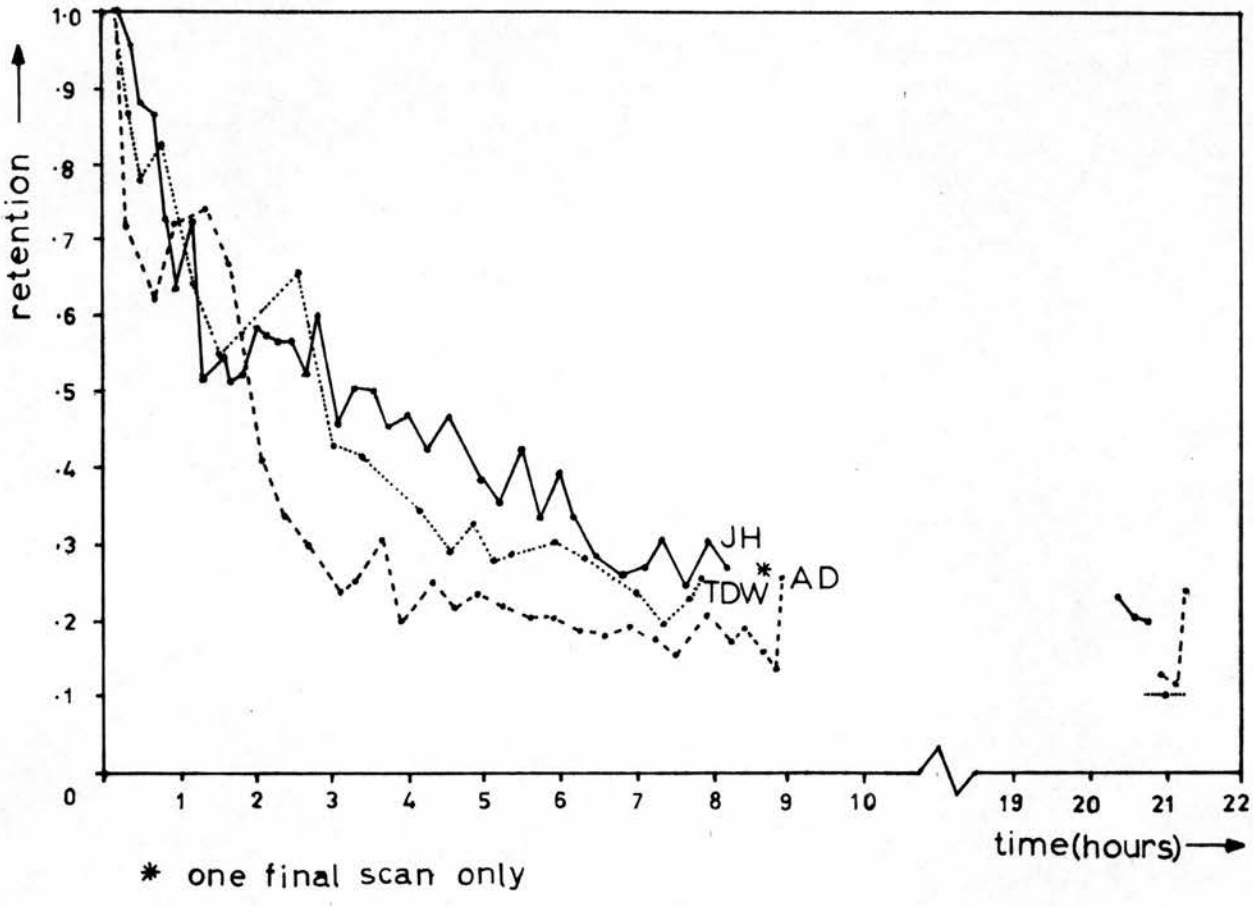

Figure 5.2.4: Clearance curves at a group-mean particle diameter of 13 μm.

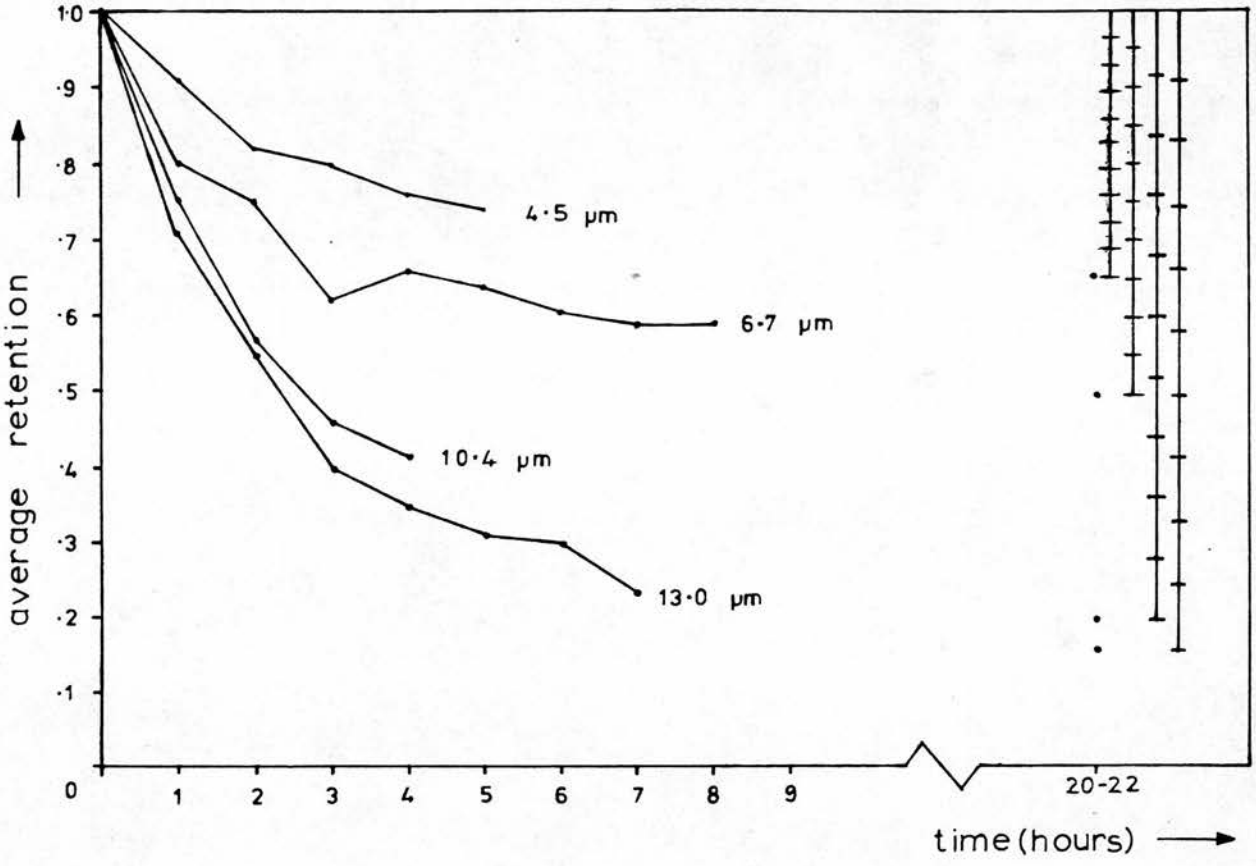

Figure 5.2.5: Averaged clearance curves, all sizes.

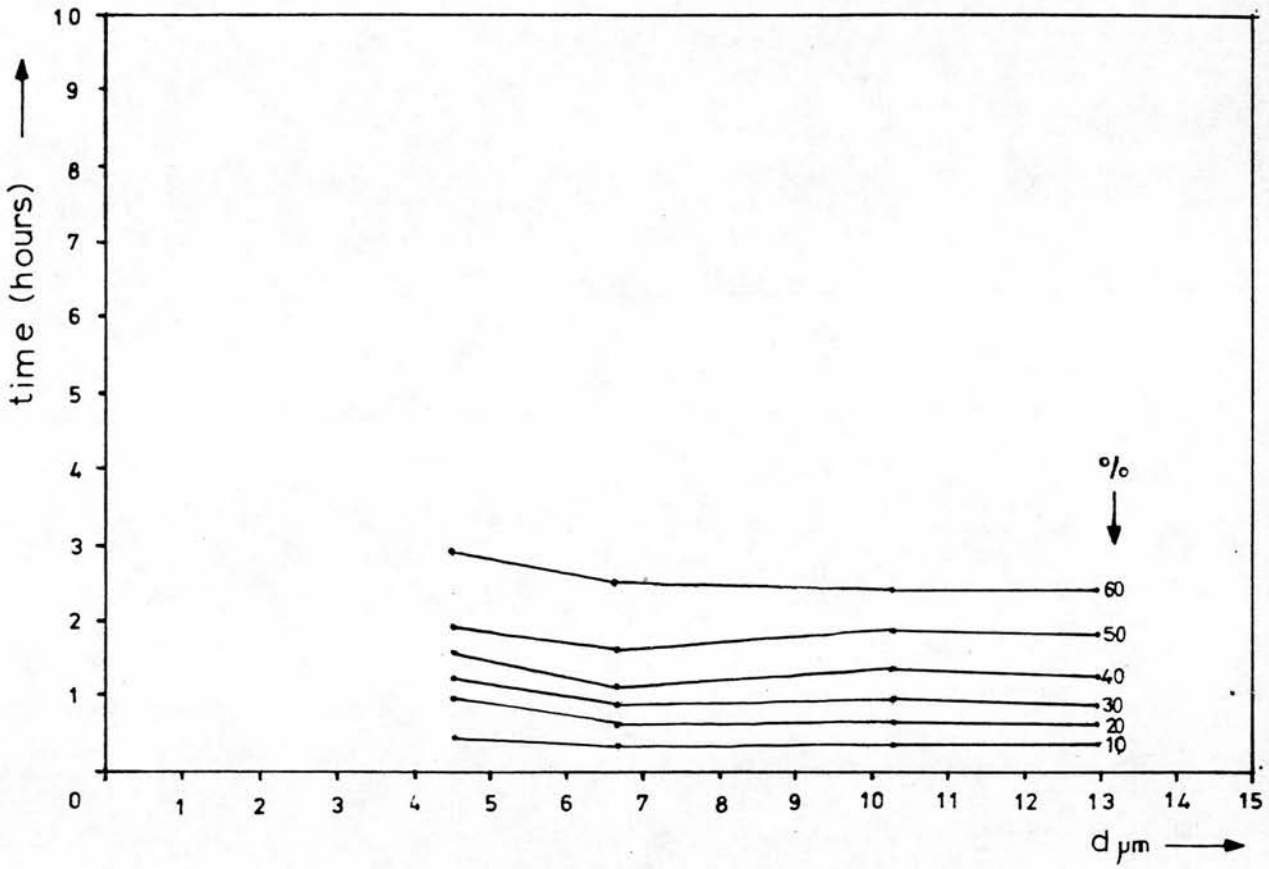

Figure 5.2.6: Time to clear particular percentages of initial deposit below larynx, 10 - 60%.

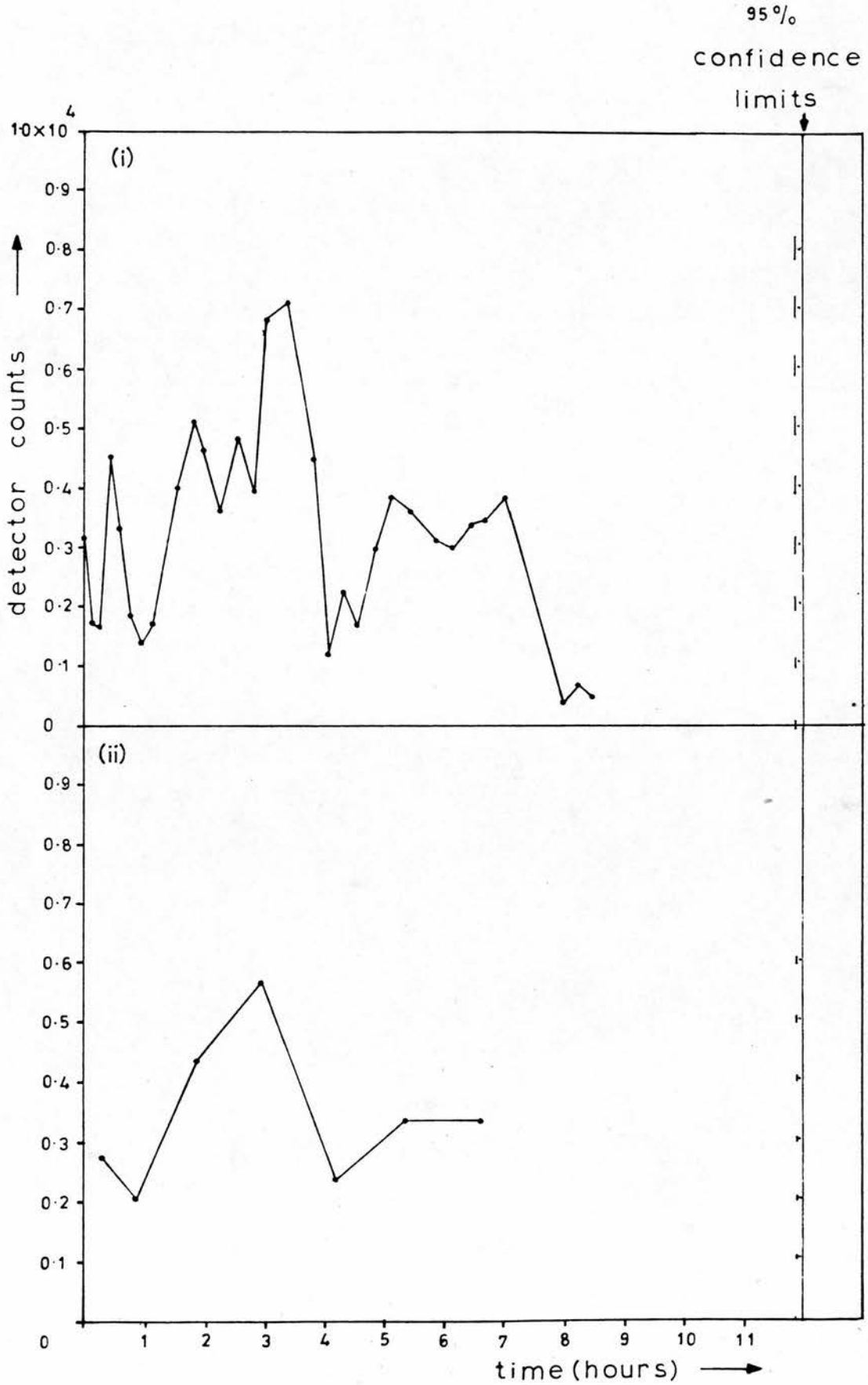

Figure 5.2.7: Single detector throat clearance curves.
Subject AM, $\bar{d}$ = 4·6 μm.

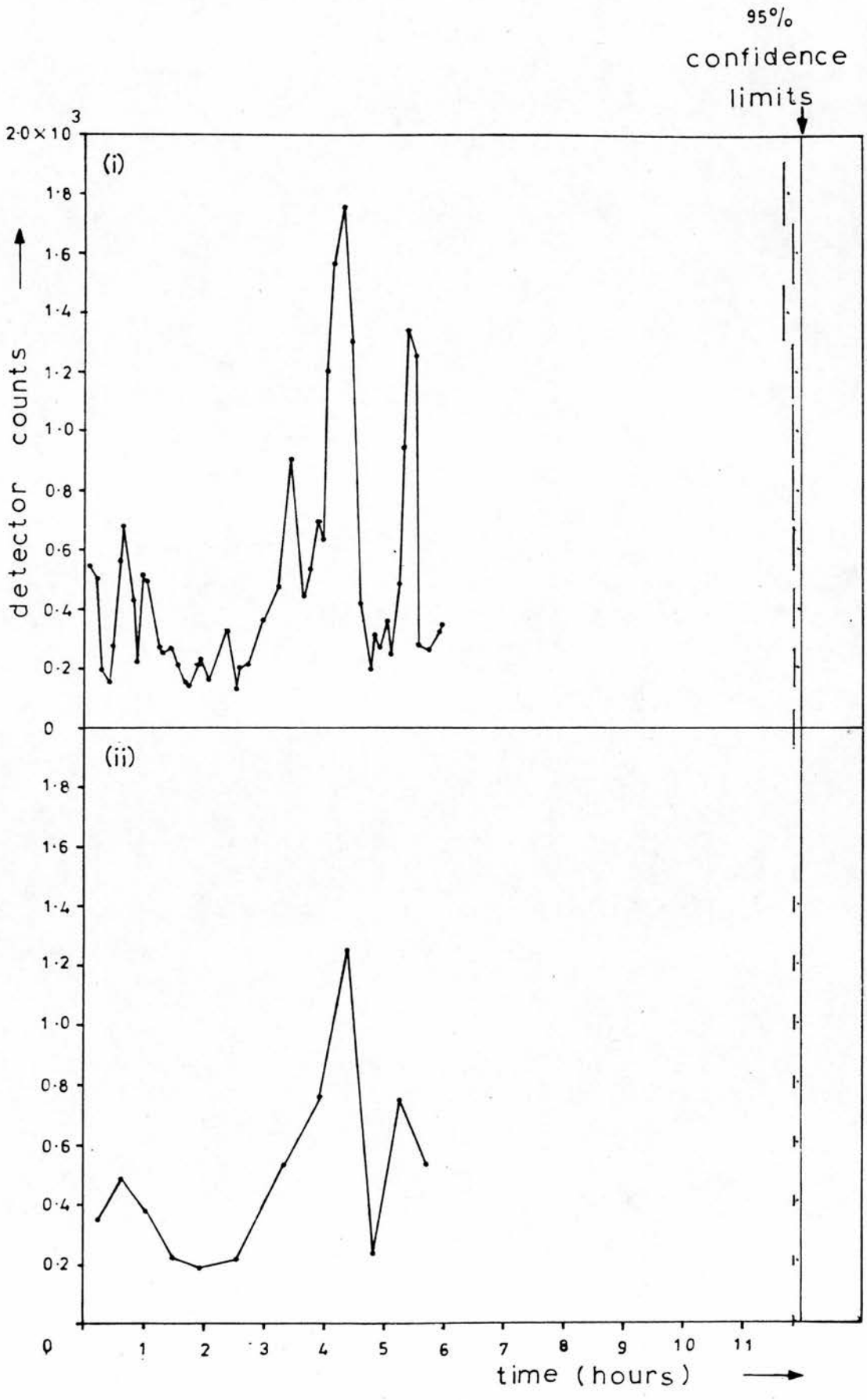

Figure 5.2.8: Single detector throat clearance curves.
Subject AR, $\bar{d} = 4{\cdot}5$ μm.

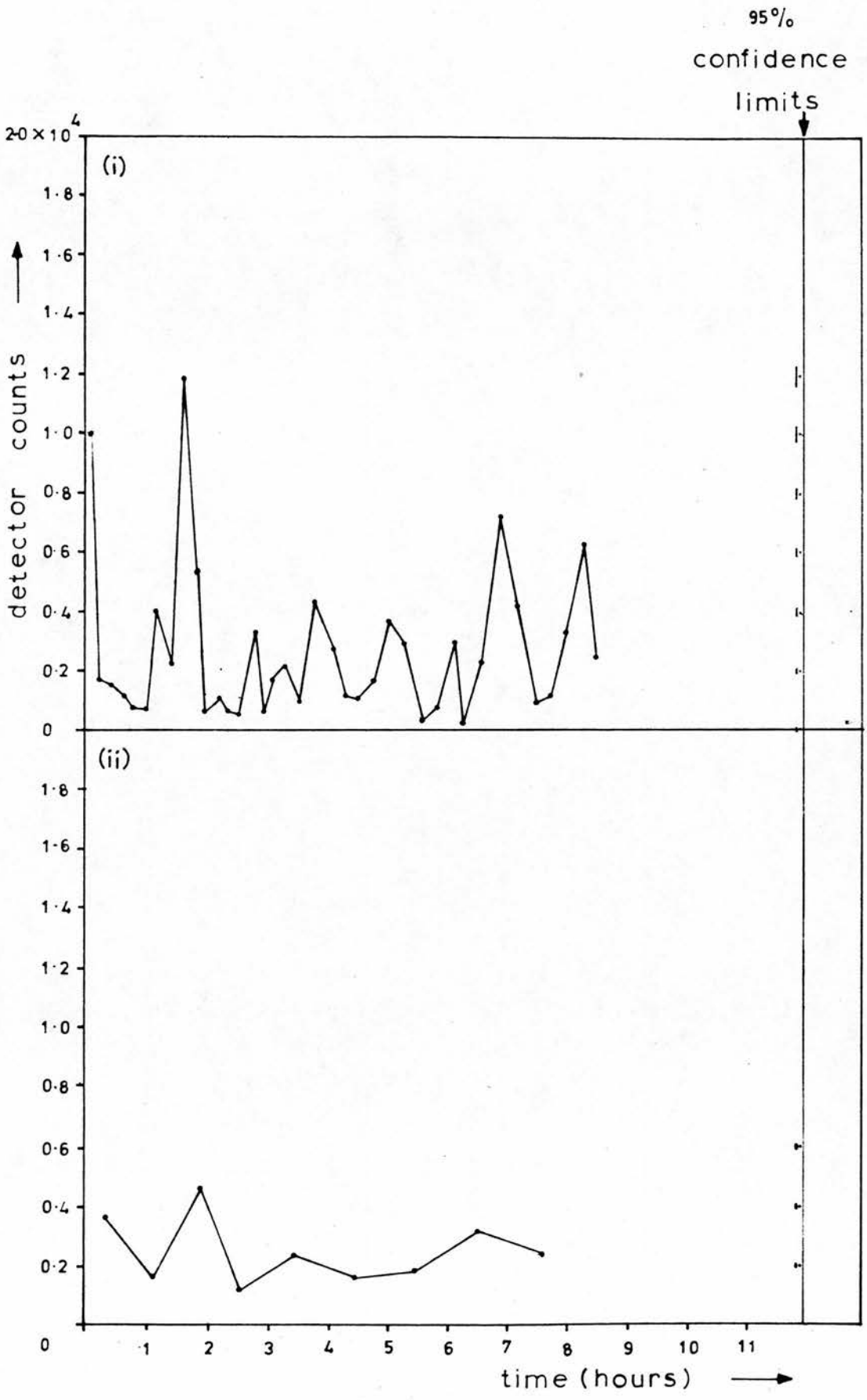

Figure 5.2.9: Single detector throat clearance curves. Subject HG, $\bar{d} = 7{\cdot}0\ \mu m$.

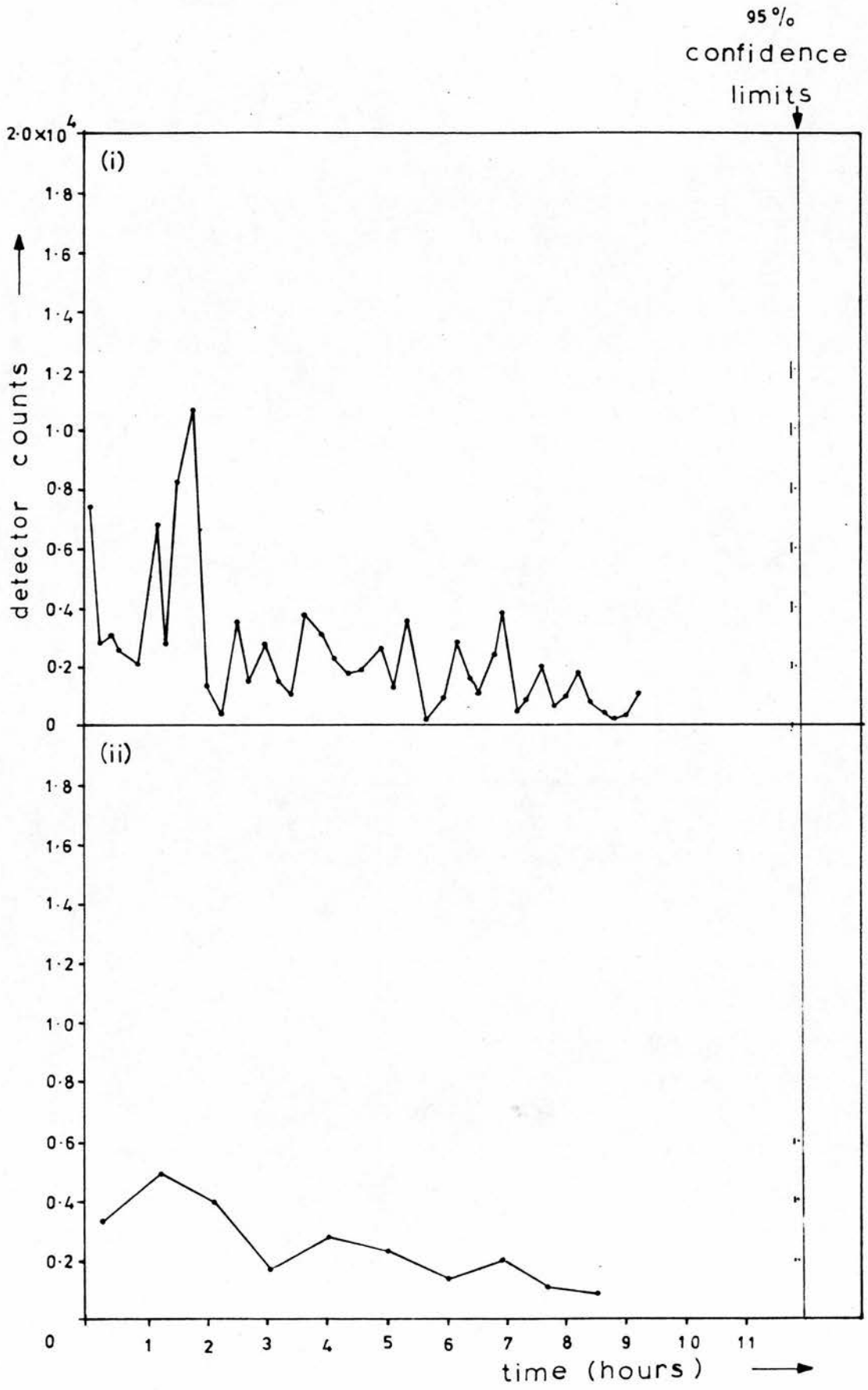

Figure 5.2.10: Single detector throat clearance curves.
Subject PH, $\bar{d}$ = 10·4 μm.

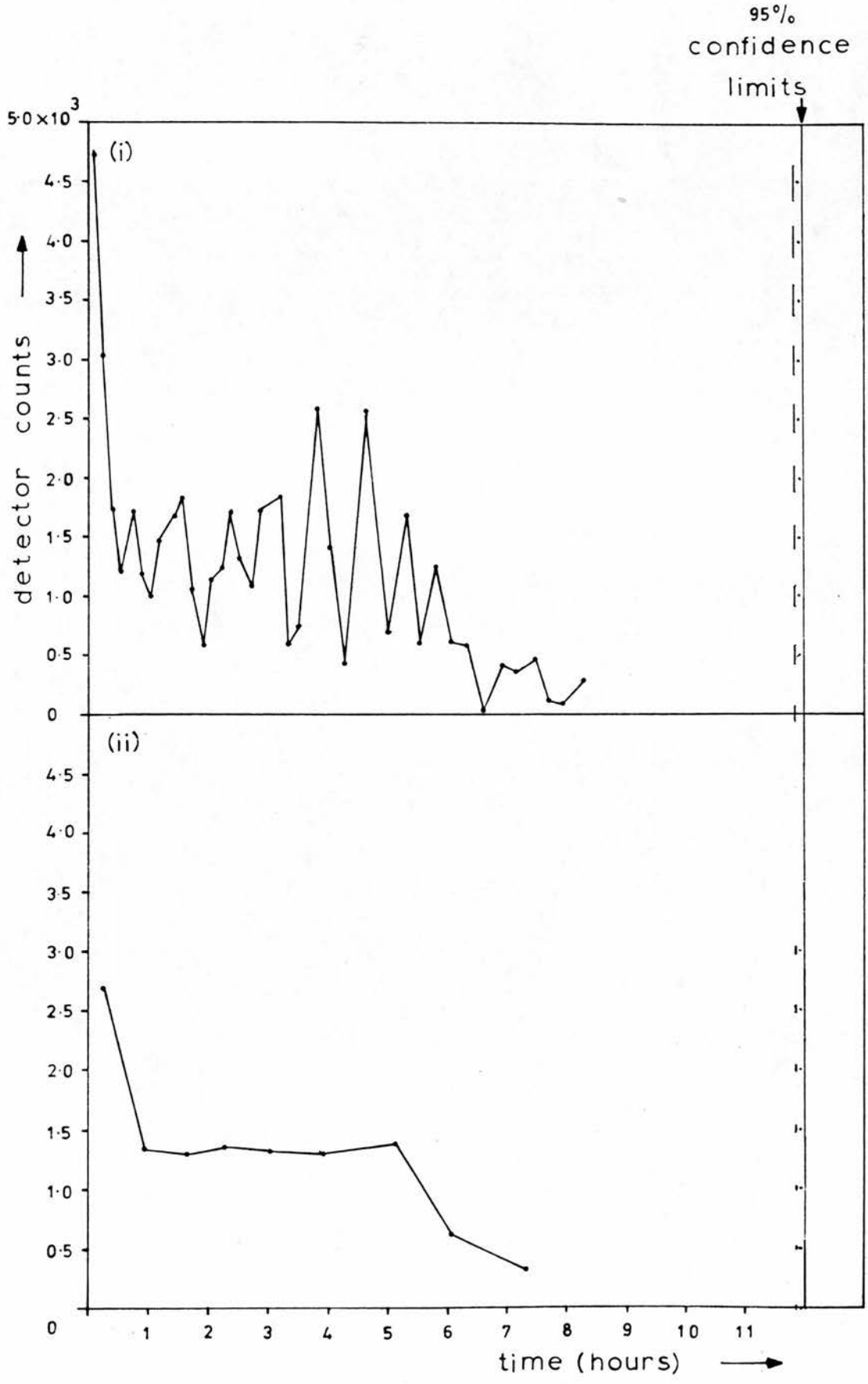

Figure 5.2.11: Single detector throat clearance curves. Subject JH, $\bar{d}$ = 13·0 μm.

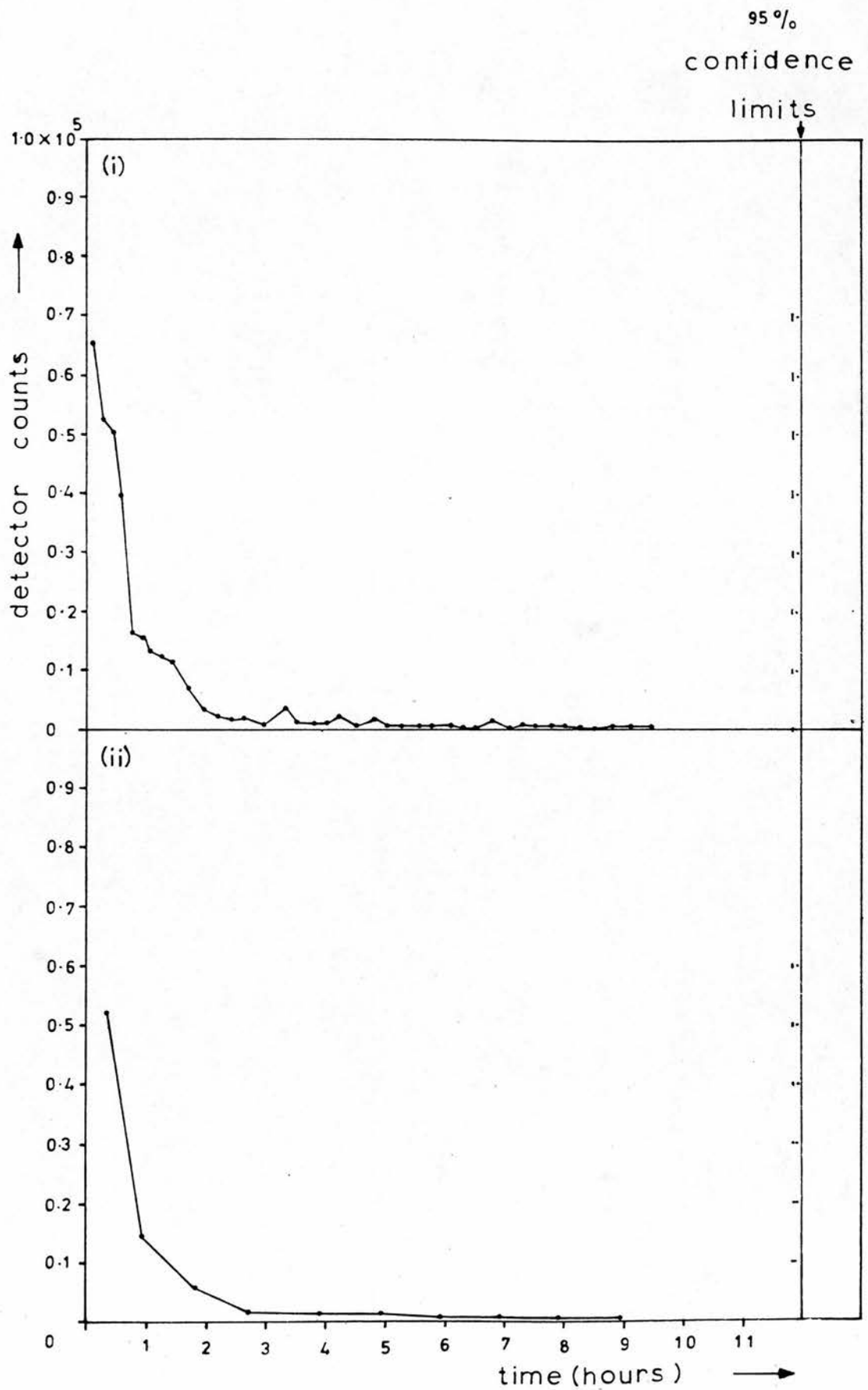

Figure 5.2.12: Single detector throat clearance curves.
Subject PT1, $\bar{d}$ = 10·2 μm.

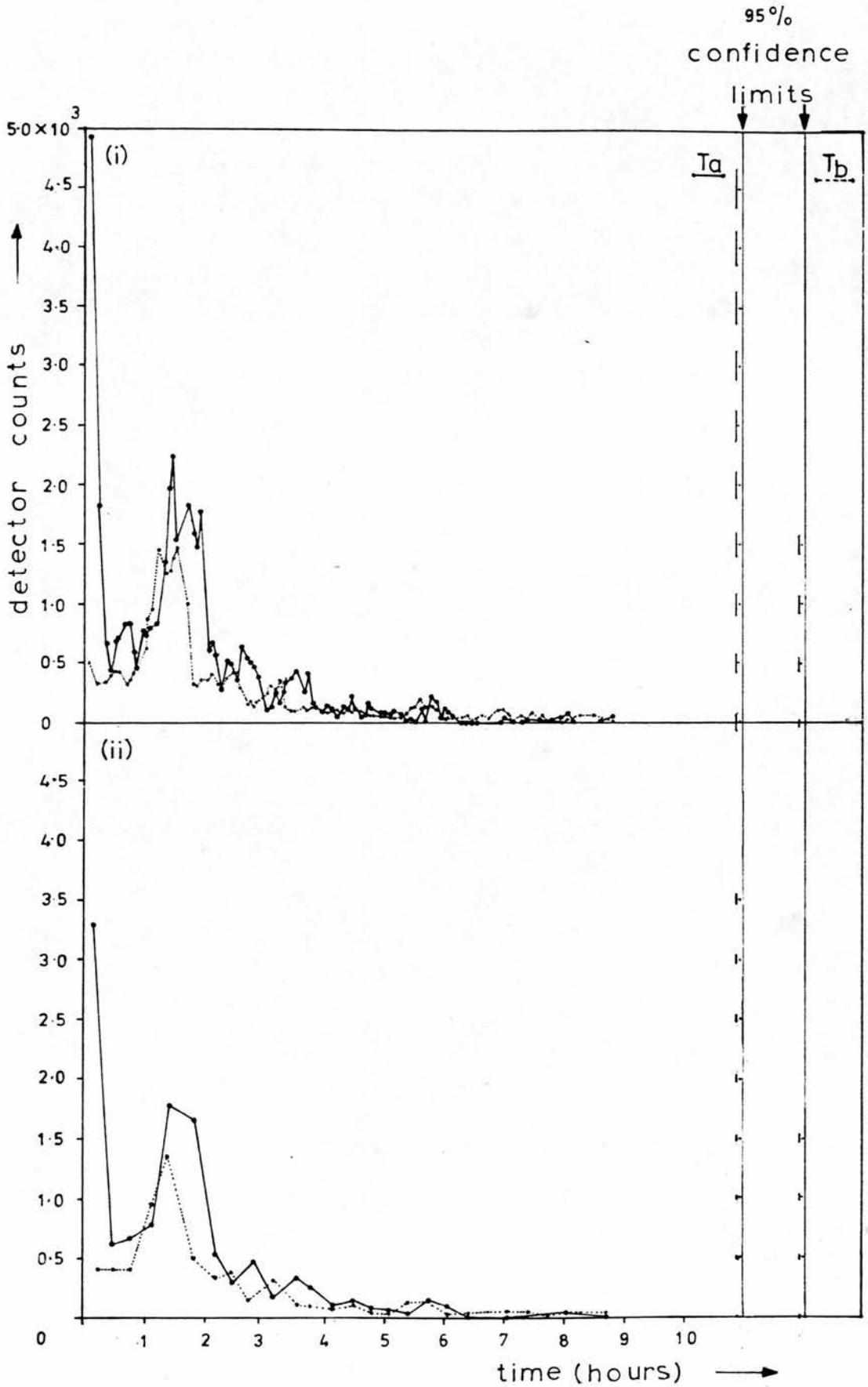

Figure 5.2.13: Double detector throat clearance curves.
Subject AD, $\bar{d}$ = 13·2 μm.

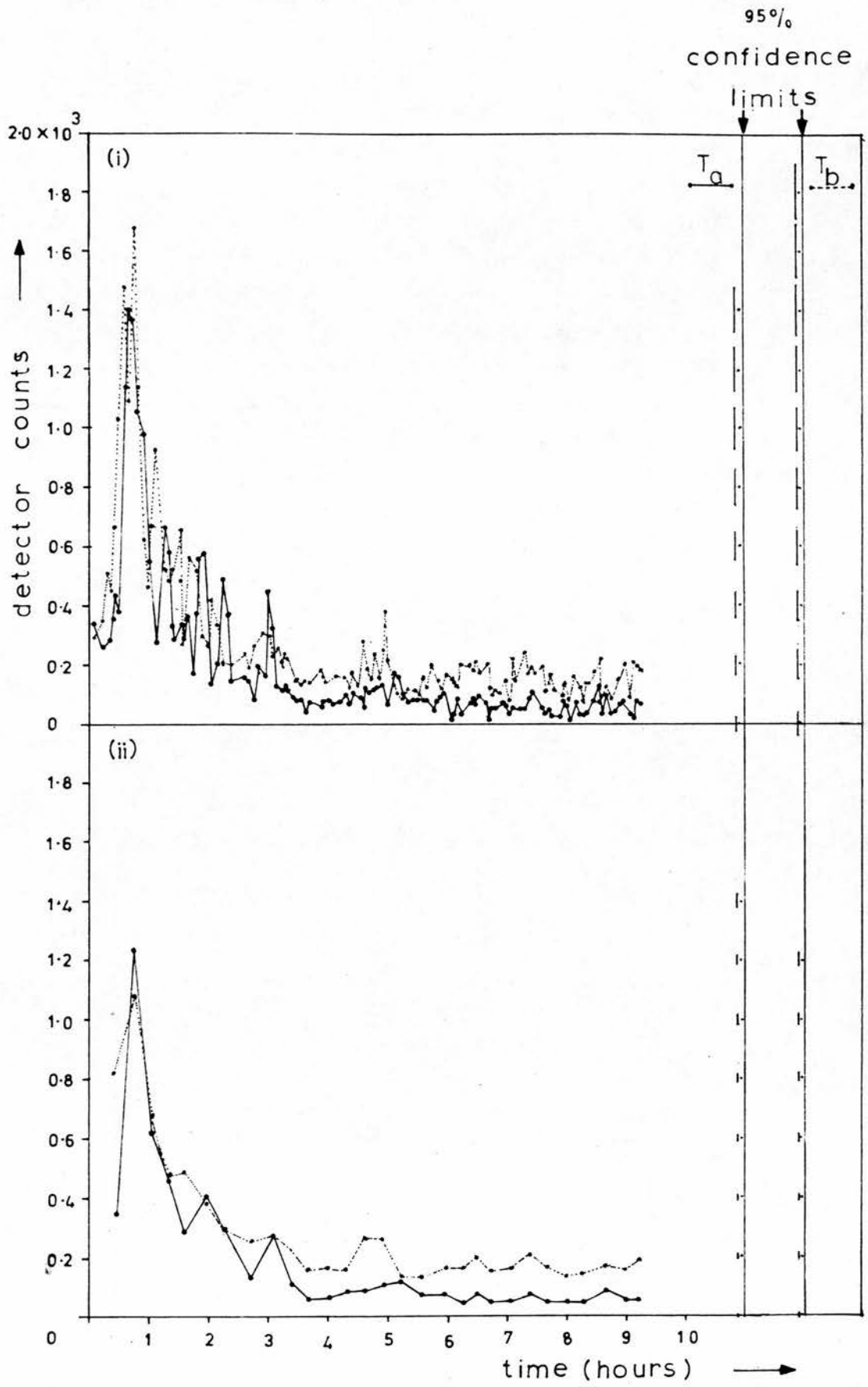

Figure 5.2.14: Double detector throat clearance curves.
Subject ATM, $\bar{d}$ = 4·5 μm.

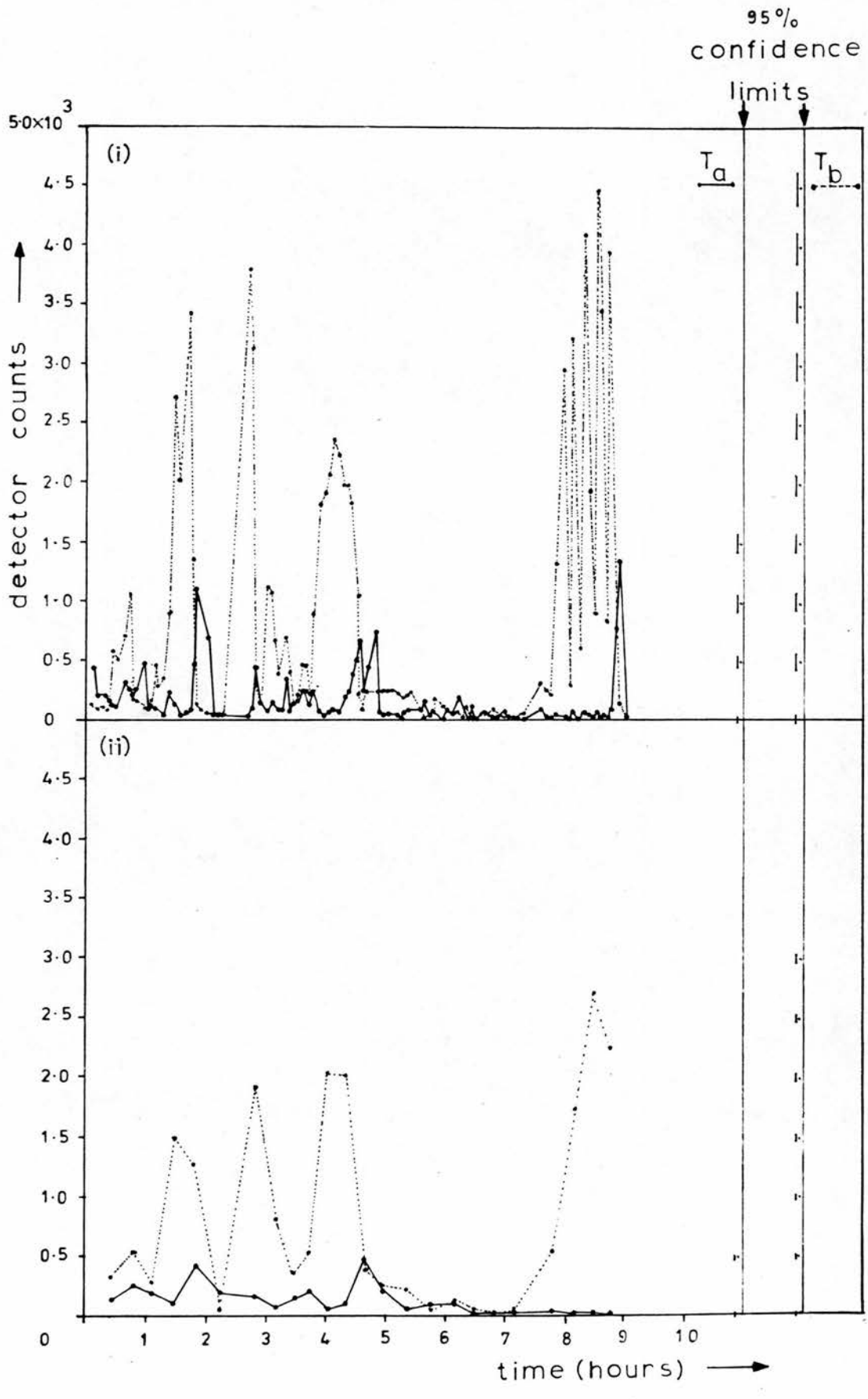

Figure 5.2.15: **Double detector throat clearance curves.**
Subject FH, $\bar{d} = 4 \cdot 5$ μm.

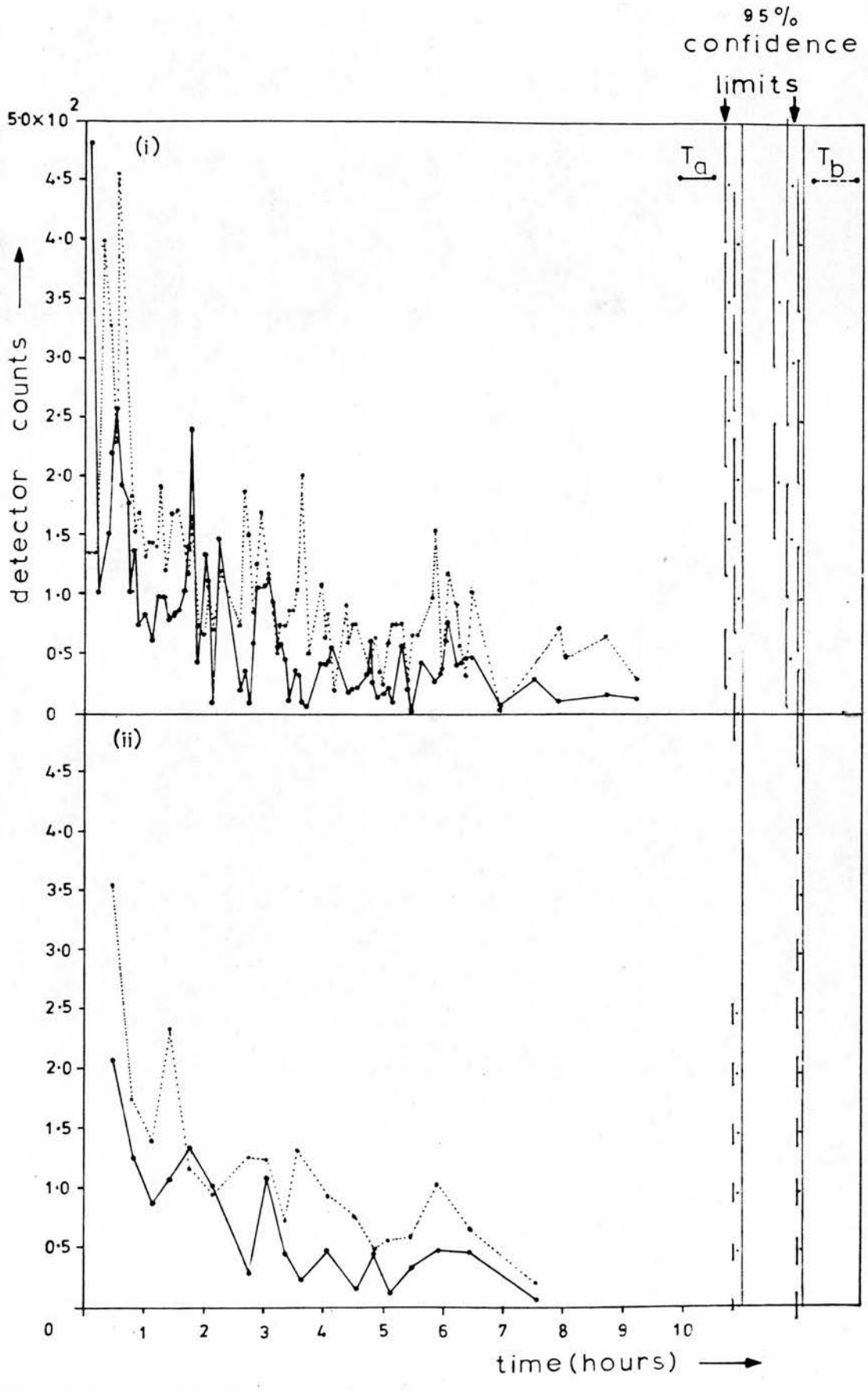

Figure 5.2.16: Double detector throat clearance curves.
Subject RH, $\bar{d}$=4·5 μm.

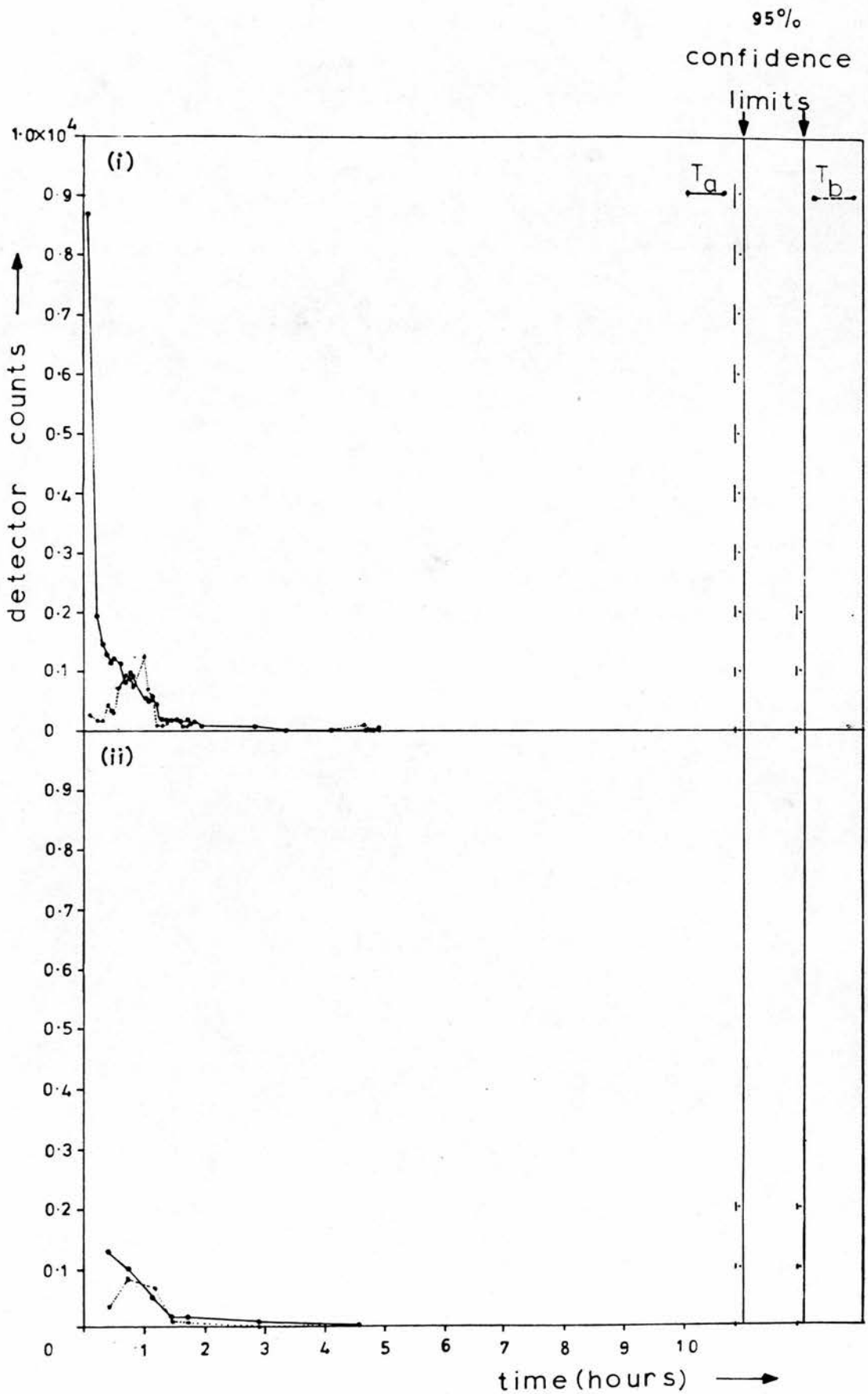

Figure 5.2.17: Double detector throat clearance curves.
Subject PT2, $\bar{d} = 10{\cdot}5\ \mu m$.

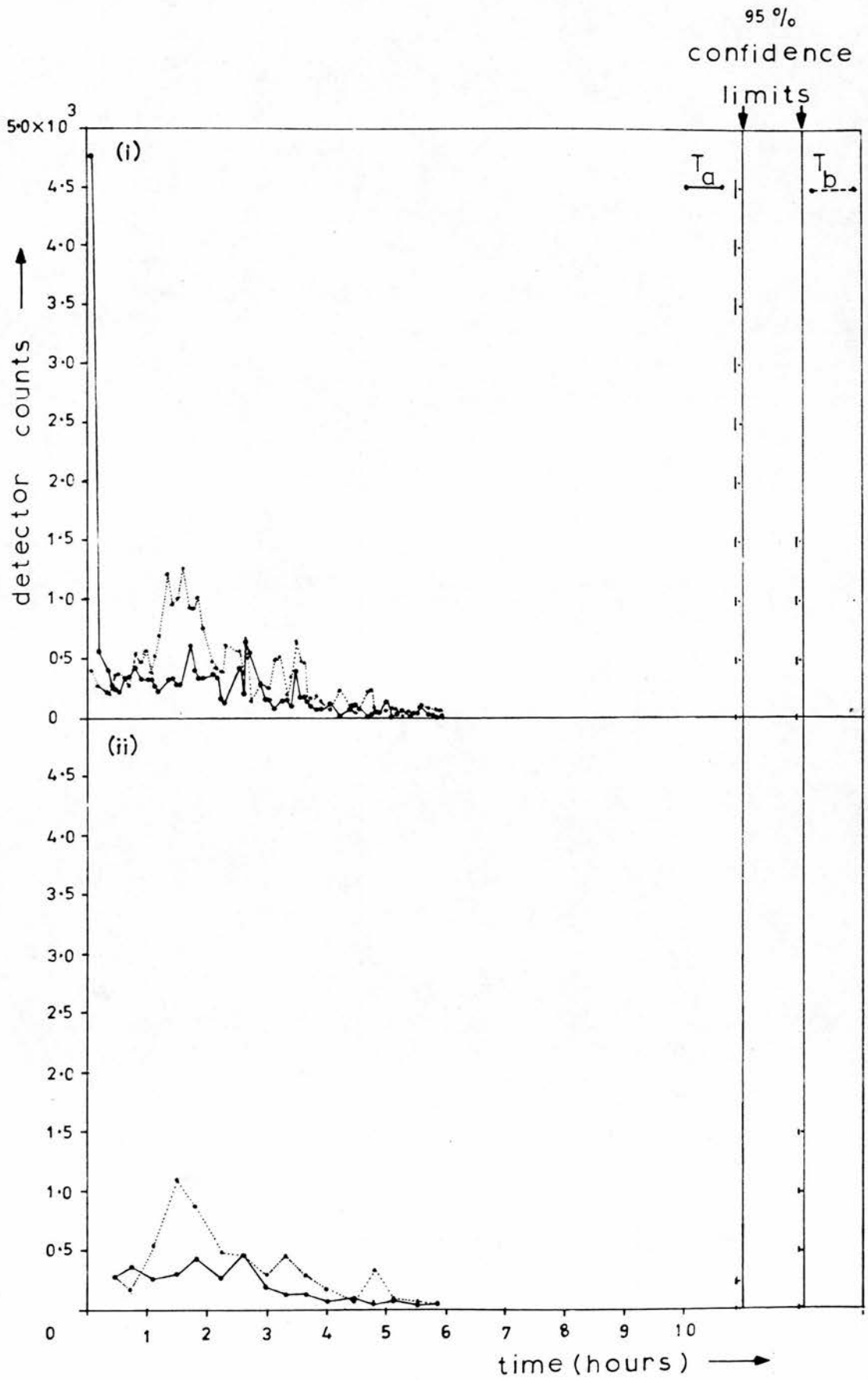

Figure 5.2.18: **Double detector throat clearance curves.**
Subject KD, $\bar{d}$ = 10·5 μm.

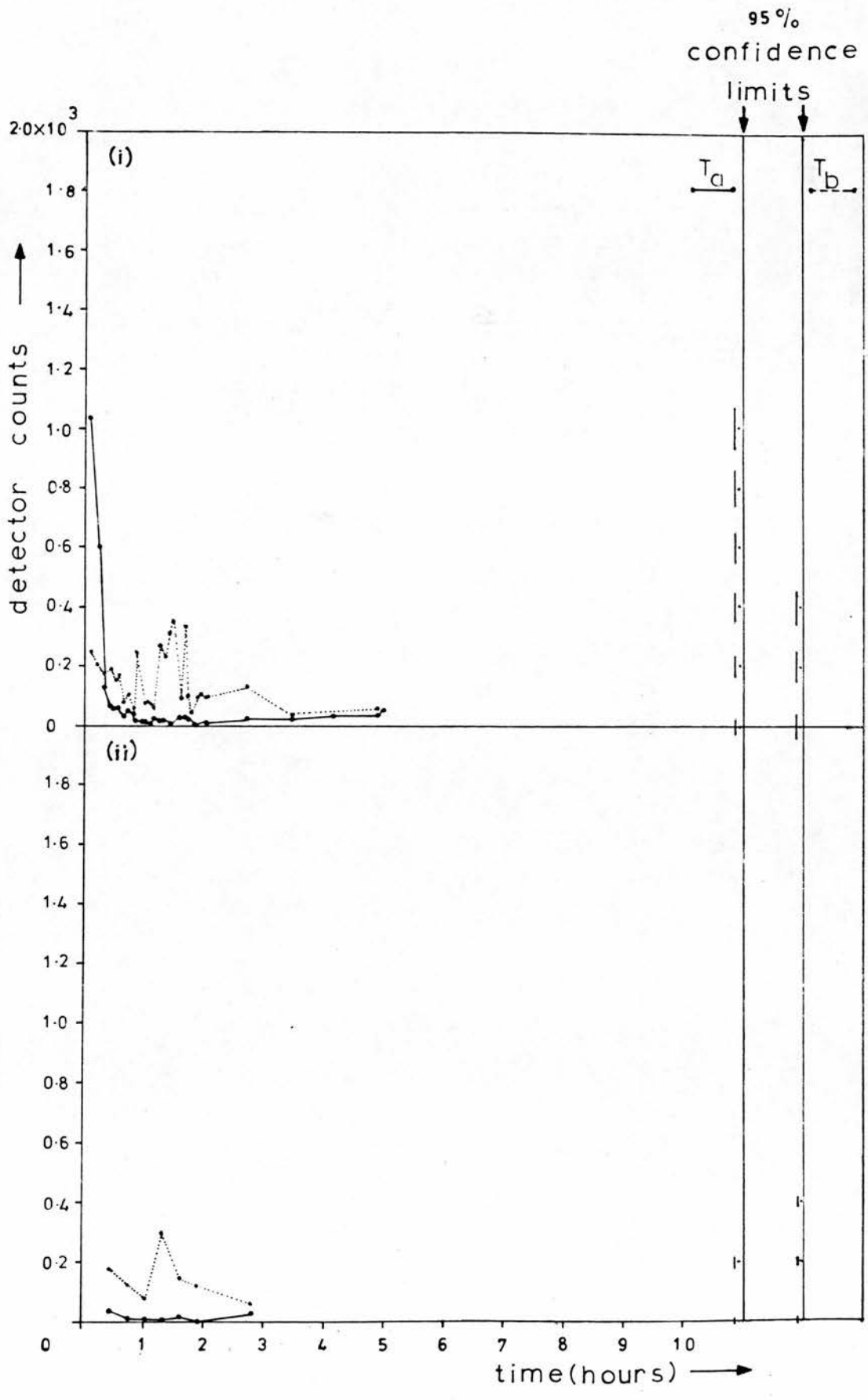

Figure 5.2.19: Double detector throat clearance curves.
Subject VC, $\bar{d}$ = 4·6 μm.

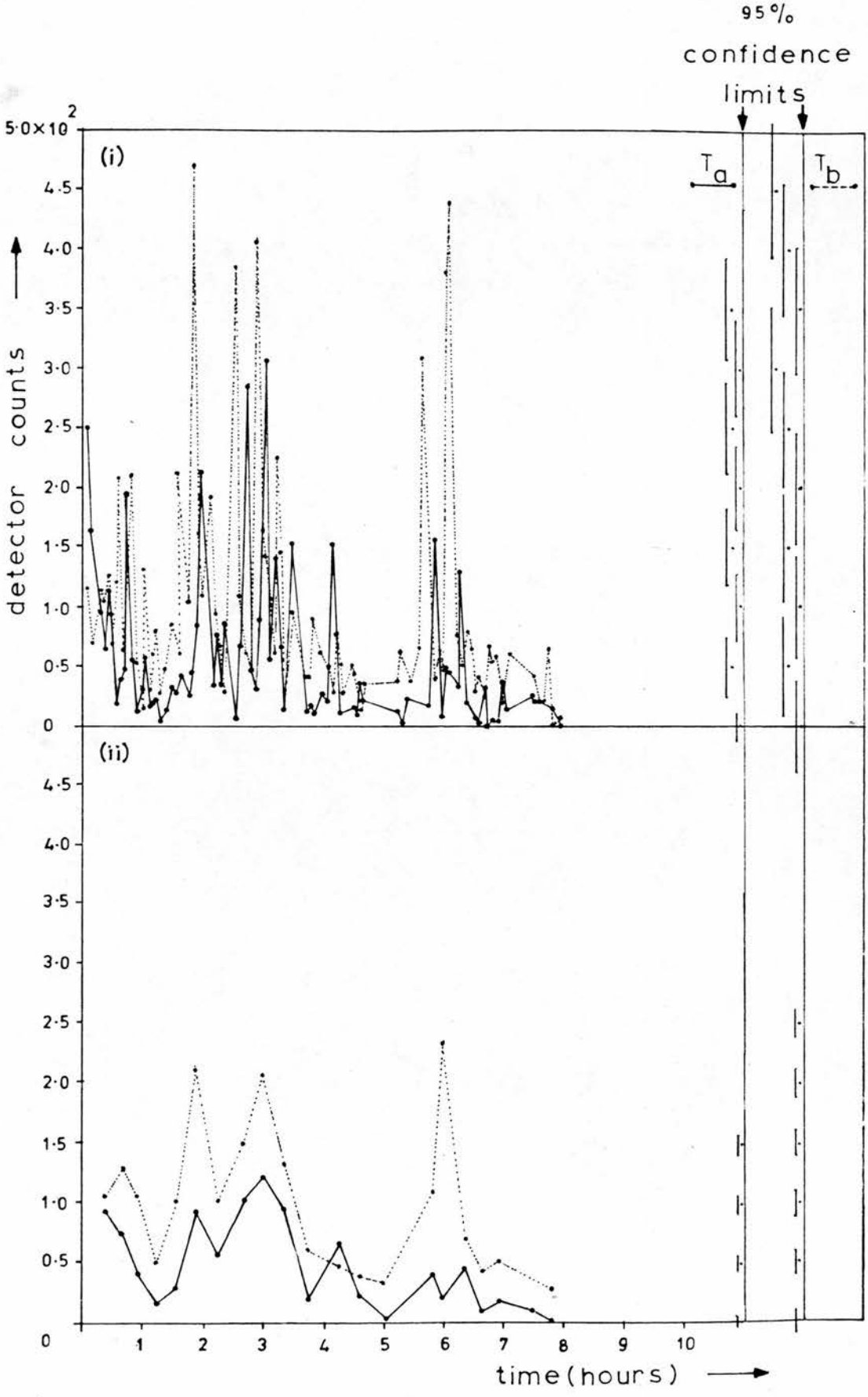

Figure 5.2.20: Double detector throat clearance curves.
Subject MS1, $\bar{d}$ = 4·5 μm.

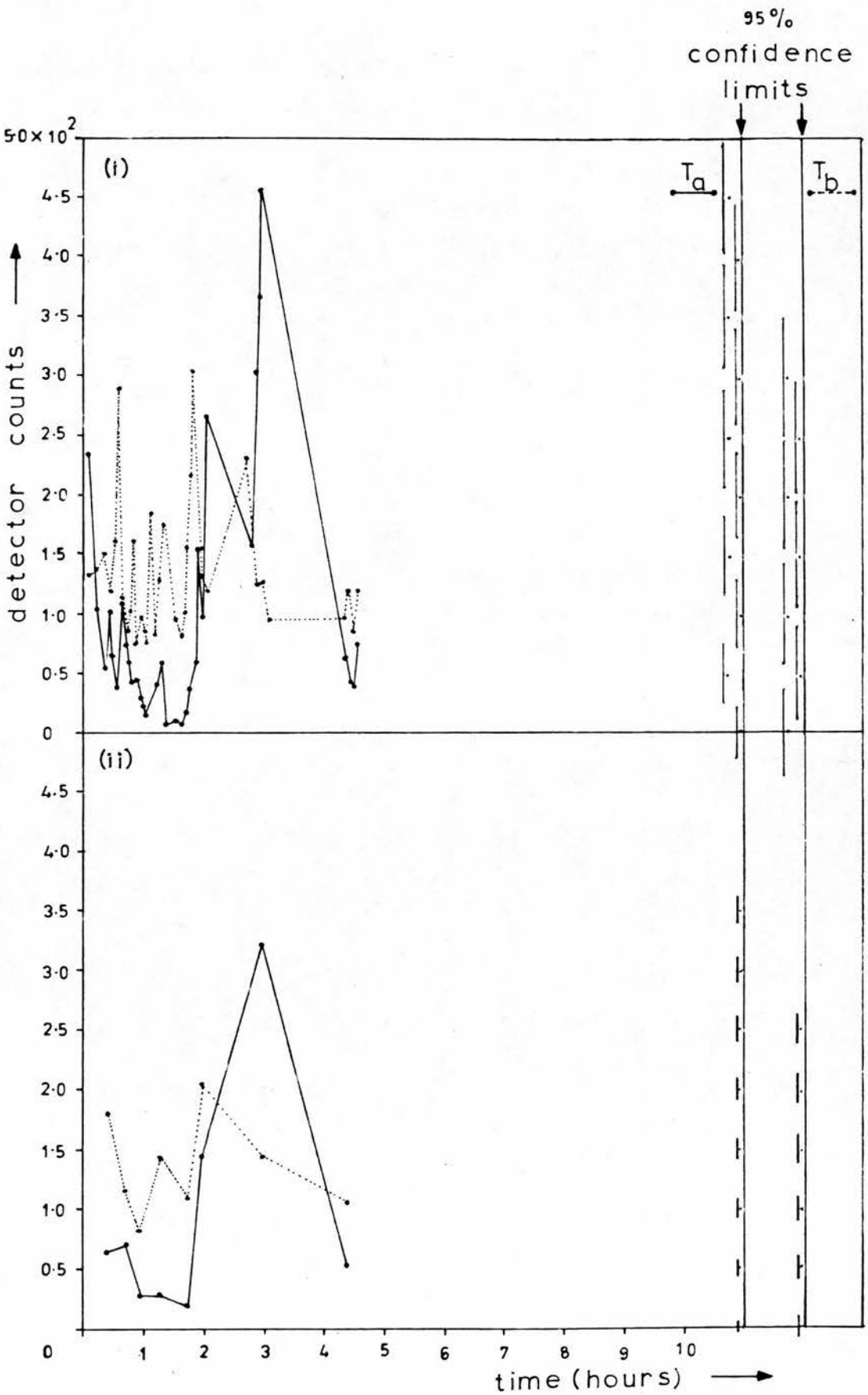

Figure 5.2.21: Double detector throat clearance curves.
Subject MS2, $\bar{d}$ = 4·7 μm.

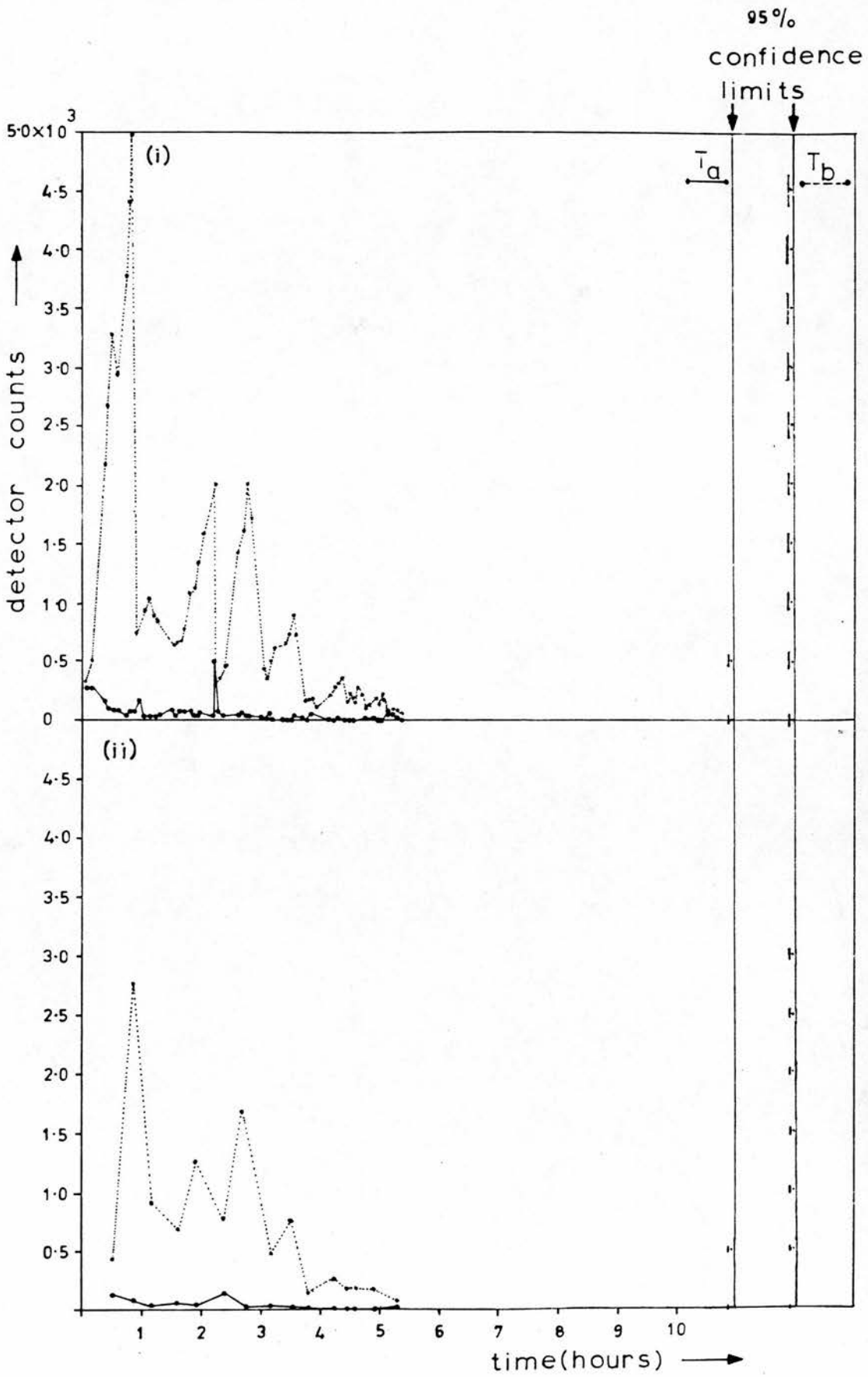

Figure 5.2.22: Double detector throat clearance curves. Subject JV, $\bar{d}$ = 4·6 μm.

CHAPTER SIX

CONCLUSIONS AND FINAL COMMENTS

The main findings of the present work are listed below. Unless otherwise stated the percentage deposition values quoted are expressed relative to the inhaled aerosol and are close to averages obtained using three subjects at each particle size (range = 4·5 μm - 13 μm diameter):

(i) The total deposition results are lower than those reported by LIPPMANN and ALBERT (1969) and FOORD et al. (1978), but agree well with the values obtained for one subject by STAHLHOFEN et al. (1979). The mean values ranged from about 80% at a particle diameter of 4·5 μm, rising only slowly to about 88% at 13 μm. It is suggested that the vertical volume elements of the dead space airways and the significant dead volume of the oral and laryngeal/pharyngeal regions may be causing this 'saturation' effect.

(ii) Mouthwash recovery rose steadily from 1% to just over 9% in the particle size range studied. These values are lower than those obtained by some other workers and it is suggested that the gargling methods employed by LIPPMANN and ALBERT (1969) and FOORD et al. (1978), have caused an over-high mouth deposition estimation owing to the inclusion of some of the initial throat deposit in this fraction.

(iii) Aerosol losses in the laryngeal/pharyngeal region exhibit the largest scatter of observations of any region studied; the mean deposition values ranging from about 9% to about 42% over the particle size range studied. These values are lower than those reported by LIPPMANN and ALBERT (1969), whose results exhibited considerably greater scatter. Considering the rapidly increasing trend in these losses with increasing particle size, it seems unlikely that particles more than several microns above 13 μm diameter are able to penetrate below the larynx in significant amounts. However, the cautionary rider must be added that at higher levels of exercise the glottal opening becomes more dilated (see Chapter 1, section 1), and the aerosol deposition efficiency of this region might well be reduced. Otherwise, the larynx/pharynx has been shown to be an important defence mechanism against inhaled matter, rivalled only by the human nose in terms of absolute filtration efficiency (HEYDER and RUDOLF, 1977).

(iv) Estimated percentage deposition on the dead space airways maintains a fairly constant level throughout most of the particle size range studied, rising from about 24% at 4·5 μm to about 36% at 6·7 μm and remaining at this level up to and including a 13 μm particle diameter. These estimates agree well with those of STAHLHOFEN et al (1979) and to a lesser extent with those of LIPPMANN and ALBERT (1969), whose results exhibited greater scatter. The estimated levels of one-day retention are higher than those of LIPPMANN and ALBERT (1969), particularly at the larger

particle sizes, but agree well with those of STAHLHOFEN et al. (1979). Good agreement was also obtained with the fractional retention estimates i.e. the deposition in the respiratory zone as a fraction of the total deposit below the larynx, of FOORD et al.(1978), in a limited region of particle size overlap. However, it is concluded that all these estimates for the regional distribution of the deposit below the larynx are incorrect, owing to the fallacy of one of the underlying assumptions, i.e. that small particles deposited on the dead space airways are removed by ciliary action within about one day after aerosol administration, because:

a. The trend in some of the independently obtained throat clearance curves suggests, obviously in one subject, less obviously in some others, that nearly all the inhaled aerosol at the two large particle sizes studied actually deposited in the first few airway generations, never reaching the respiratory zone.

b. An analysis of the data using a simple filter model of the respiratory tract demonstrates that the observed apparent behaviour of the large particles in the respiratory zone is wholly inconsistent with that which might be expected on the basis of well established physical principles.

(v) Short-term clearance usually proceeds in an apparently irregular fashion, the clearance curves exhibiting distinct peaks and troughs whose origin has been shown in the present work to be mainly below the larynx, the larynx itself normally playing only

a minor modifying role. No definitive explanation of the phenomenon can be offered, but the balance of arguments favours a mainly biological cause.

Final comments: Besides being of value in resolving questions concerning the experimental accuracy of the present results, there are other important reasons why the effectiveness of short-term clearance in the dead space airways merits further investigation. For example, if the residence time of dust on the dead space airways is longer than presently assumed, then the calculated radiation dose due to inhaled radionuclides may well be seriously underestimated. Such assumptions are also often involved in the determination of what is, ostensibly, long-term alveolar clearance in experimental animals (HATCH and GROSS, 1964).

The purely qualitative observations on the nature of clearance patterns in the present work also merit further investigation. The relevance of this phenomenon, besides possibly underlying some basic physical or biological mechanism, lies in the concentration of dust deposits at selected points in the lungs. Complications might arise, for example, in the interpretation of the regional deposition and clearance patterns of inhaled radioactive aerosols, obtained using scintillation cameras (LOURENÇO et al. 1971).

The reliable definition of the fractional dust penetration below the larynx should find useful application in the contemporary debate as to what constitutes 'inhalable' dust. However, it is doubtful whether much useful information may be obtained from the present results concerning the size fraction of dust which deposits

in the respiratory zone, so called respirable dust, or that size fraction which deposits on the dead space airways. Agreement between the regional deposition results of the present work and those of two other groups is good, in a limited range of comparison, suggesting that reasonable 'accuracy' has been obtained in each case. Whether or not the same comments should apply in the case of total deposition must ultimately depend on a subjective evaluation of the techniques employed by each group. However, it is the regional deposition that is of most practical significance, and until the advent of new techniques of measurement the results of all these groups should be regarded only as an upper deposition limit, in the case of respirable dust, and a lower deposition limit, in the case of that dust fraction which deposits on the dead space airways. Although certain respirable dust sampling criteria (BMRC and ACGIH)* fall within this limit and may seem reasonable, while those recommended by the TASK GROUP ON LUNG DYNAMICS (1966) may seem too high, on this basis of comparison, the cautionary warnings given in Chapter 1 concerning the applicability of laboratory-derived data to the workplace are repeated: such results should only be applied with intelligent regard to the particular conditions pertaining in each situation.

* BMRC = British Medical Research Council

ACGIH = American Conference of Governmental Industrial Hygenists

ACKNOWLEDGEMENTS

I would like to gratefully acknowledge the helpful advice and criticisms rendered to me in the pursuit of this research by my supervisors, Dr. D.C.F.Muir, Dr. M. Sudlow and Dr. P. Tothill. I would also like to thank: Mr. W.H. Walton, who conceived a method of performing the inhalation sampling, using a single spirometer, quite independently of a knowledge of the double spirometer configuration; Mr. G. Lynch and the IOM workshop who did a splendid constructional job on the total deposition apparatus; Dr. J. Hannan, whose advice and direct assistance in the development of the radioactive scanning techniques, computing and many other aspects of the research was most helpful; Mr. R.J. Aitken, whose considerable efforts in the development of techniques and during the long period of obtaining results were invaluable; Dr. R.G.Love for his helpful comments and advice on the physiological aspects of the study, Drs. N. Foord, of AERE, Harwell, and W. Stahlhofen, of GSF, Frankfurt, for their free exchange of unpublished data and their encouragement.

I would like to pay special thanks to my wife for the ungrateful task of deciphering my manuscript and to my daughter, Helen, for her mature forbearance during its preparation.

I thank the European Coal and Steel Community and the National Coal Board for their generous financial support and co-operation, particularly when it became necessary to allow extra time for completion of the research. I also thank Professor J.R. Greening of the Department of Medical Physics, The Royal Infirmary, Edinburgh,

for permission to store my apparatus, over a long period, and also for the use of the resources of the department.

Finally, I would like to thank my eighteen subjects for their considerable time and efforts, for whom the experience of participating in the research was always an ordeal.

REFERENCES

ALBERT, R.E. and ARNETT, L.C.(1955) A.M.A. Arch. Ind. Health, 12, 99.

ALBERT, R.E., LIPPMANN, M., PETERSON, H.T., BERGER, J., SANBORN, K., and BOHNING, E. (1973) Arch. intern. med., 131, 115.

ALBERT, R.E., LIPPMANN, M., SPIEGELMAN, J., STREHLOW, W., BRISCOE, P., WOLFSON, P. and NELSON, N. (1967) In: Inhaled Particles 11, pp 361 - 378. (edited by Davies, C.N.), Pergamon Press, Oxford.

ALLEN, T.(1974) In: 'Particle Size Measurement', Ch. 4. Published by Chapman and Hall.

ALTSHULER, B. (1959) Bull. Math. Biophys., 21, 257.

ALTSHULER, B., YARMUS, L., PALMES, E.D. and NELSON, N. (1957) A.M.A. Arch. Ind. health, 15, 293.

ANDERSON, I.B., LUNDQUVIST, G.R., PROCTOR, D.F. and SWIFT, D.L. (1979) Am. Rev. Resp. Dis., 119, 619.

ASSMUNDSSON, T. and KILBURN, K. (1970) Am. Rev. Resp. Dis., 102,388.

BATEMEN, J.R.M., CLARKE, S.W., PAVIA, D. and SHEAHAN, N.F. (1978) J. of Physiol., 284, 55.

BATEMAN, J.R.M., NEWMAN, S.P., DAUNT, K.M., PAVIA, D. and CLARKE, S.W. (1979) Lancet, i, 294.

BAUMBERGER, J.P. (1923) J. Pharmacol. Exptl. Therap., 21, 47.

BLACK, A. and WALSH, M. (1970) Ann. Occ. Hyg. 13, 87.

BOLTON, R. (1979) Private communication.

BOOKER, D.V., CHAMBERLAIN, A.C., RUNDO, J., MUIR, D.C.F., and THOMSON, M.L. (1967) Nature (Lond.), 215, 30.

BRICARD, J. and PRADEL, J. (1966) In: 'Aerosol Science', Ch. 4, P.89. Published by Academic Press, New York.

BRISCOE, W.A., FORSTER, R.E. and COMROE, J.H.(Jr.)(1954) J. Appl. Physiol. 7, 27.

BROWN, C.E. (1931) J. Ind. Hyg. Toxicol., 13, 285.

BROWN, J.H., COOK, K.M., NEY, F.G. and HATCH, T. (1950) Am. J. Public Health, 40, 450.

CAMNER, P. (1971) Environ. Physiol., 1, 137.

CAMNER, P. and PHILIPSON, K. (1978) Arch. Env. Hlth, 33, 181.

COMROE, J.H., FORSTER, R.E., DUBOIS, A.B., BRISCOE, W.A. and CARLSEN, E. (1955) In: 'The Lung', P.28, Year Book Med. Pub.U.S.A.

COTES, J.E. (1968) In: 'Lung Function', 2nd ed., Blackwell, Oxford.

DALHAM, T. (1956) Acta. Physiol. Scanda., 36 (Supplement 123, P.89).

DAUTREBANDE, L. (1962) In: 'Microaerosols', P.34. Published by Academic Press, New York.

DAUTREBANDE, L., BECKMANN, H. and WALKENHORST, W. (1957) A.M.A. Arch. Ind. Health, 16, 179.

DAUTREBANDE, L., CARTRY, D., VAN KERKOM, J. and CEREGHETTI, A. (1954) In: 'Essai de Prevention de la Silicose', Union Minière du Haut, Katanga.

DAVIES, C.N. (1964) Annal. Occ. Hyg., 7, 169.

DAVIES, C.N. (1974) Chemistry and Industry (June 1st), 441.

DAVIES, C.N., HEYDER, J. and SUBBA RAMU, M.C. (1972) J. Appl. Physiol., 32, 591.

DAVIES, C.N., LEVER, M.J. and ROTHENBERG, J.S. (1977) In: Inhaled Particles IV, pp. 151 - 162, (Edited by Walton, W.H.). Published by Pergamon Press, Oxford.

DENNIS, R. (1976) In: 'Handbook on Aerosols', P.113. Published by E.R.D.A. Technical Information Centre, USA.

DENNIS W.L. (1950) J. Sci. Instrum., 27, 1,950.

DENNIS, W.L. (1971) In: Inhaled Particles 111, (Edited by Walton, W.H.), pp.91 - 103. Published by Unwin Bros., London.

DRINKER, P., THOMSON, R.M. and FINN, J.L. (1928) J. Ind. Hyg. Toxicol., 10, 13.

EHRET, R., KIEFER, H., MAUSHART, R. and MÖHRLE, G. (1964) In: 'Assessment of Radioactivity in Man', 1, 141. Published by I.A.E.A., Vienna.

EMMETT, P.C., AITKEN, R.J. and MUIR, D.C.F. (1979) J. Aerosol Sci., 10, 123.

FEW, J.D., SHORT, M.D. and THOMSON, M.L. (1970) Radiochem. Radional. Lett., 5, 275.

FOORD, N., BLACK, A., WALSH, M. (1977) In: Inhaled Particles 1V, pp.137 - 148, (Edited by Walton, W.H.). Published by Pergamon Press, Oxford.

FOORD, N., BLACK, A. and WALSH, M. (1978) J. Aerosol Sci., 9, 343.

FRY, F.A. (1970) J. Aerosol Sci., 1, 135.

FUCHS, N. and SUTUGIN, A.G. (1966) In: 'Aerosol Science', (Edited by Davies, C.N.). Ch.1, P.2.

GALEN, (between 129 - 199 AD) In: 'On the Usefulness of Parts of the Body', translated by M.T. May, Ithaca, N.Y., Cornell Univ. Press, 1968, Vol. 11, P.525.

GOODMAN, R.M., YERGIN, B.M., LANDA, J.F., GOLINVAUX, M.H. and SACKNER, M.A. (1978) Am. Rev. Resp. Dis., 117, 205.

GORE, D.J. and PATRICK, G. (1978) Phys. Med. Biol., 23, 730.

GREEN, H. and LANE, W. (1957), In: 'Particulate Clouds ', P.6. Published by Spon, London.

GUNN, R. (1954) J. Meterol., 11, 339.

GUNN, R. (1955), J. Colloid Sci., 10, 107.

HAMILL, P. (1979) Hlth Phys., 36, 355.

HANNAN, J. (1978) Private communication.

HARPER, P.V., LATHROP, K.A. and GOTTSCHALK, A. (1966). In: 'Pharmacodynamics of some Technetium-99m Preparations', P.335, USAEC Report CONF-651111.

HATCH, T.F. and GROSS, P. (1964) In: 'Pulmonary Deposition and Retention of Inhaled Aerosols'. Published by Academic Press, New York.

HEYDER, J. (1971) Staub-Reinhalt Luft, 31, 11. (English Edition).

HEYDER, J., ARMBRUSTER, L., GEBHART, J., GREIN, E. and STAHLHOFEN, W. (1975) J. Aerosol Sci., 6, 311.

HEYDER, J. and DAVIES, C.N. (1971) J. Aerosol Sci., 2, 437.

HEYDER, J., GEBHART, J., HEIGNER, G., ROTH, C. and STAHLHOFEN, W. (1973). J. Aerosol Sci., 4, 191.

*1 HEYDER, J. and RUDOLF, G. (1977) In: Inhaled Particles IV, pp. 107 - 126, (Edited by Walton, W.H.). Published by Pergamon Press, Oxford.

HIDY, G.M. and BROCK, J.R. (1969) Environ. Sci. Tech., 3, 563.

HILDING, A.C. (1965) Med. Thorac., 22, 329.

HOLMA, B. (1967) In: Inhaled Particles II, pp. 189 - 201, (Edited by Davies, C.N.)Published by Pergamon Press, Oxford.

HORSFIELD, K. and CUMMING, G. (1967) Bull. Math. Biophys., 29, 245.

JACOBSEN, M., RAE, S., WALTON, W.H. and ROGAN, J.M. (1971) In: Inhaled Particles III, pp. 903 - 920, (Edited by Walton, W.H.). Published by Unwin Bros., London.

* 1 HEYDER, J., GEBHART, J. and STAHLHOFEN, W. (1979), Paper presented before Division of Environmental Chemistry, American Chemical Conference, Hawaii.

KILBURN, K.H. (1968) Am. Rev. Resp. Dis., 98, 449.

KOPS, J., DIBBETS, L., HERMANS, L. and VAN DE VATE, J.F. (1975) J. Aerosol Sci., 6, 329.

LANDAHL, H.D. (1950) Bull. Math. Biophys., 12, 43.

LANDAHL, H.D. and BLACK, S. (1947) J. Ind. Hyg. Toxicol., 29, 269.

LANDAHL, H.D. and HERRMANN, R.G. (1948) J. Ind. Hyg. Toxicol., 30, 181.

LANDAHL, H.D., TRACEWELL, T.N. and LASSEN, W.H. (1951) A.M.A. Arch Ind. Hyg. Occup. Med., 3, 359.

LANDAHL, H.D., TRACEWELL, T.N. and LASSEN, W.H. (1952), A.M.A. Arch. Ind. Hyg. Occup. Med., 6, 508.

LEITH, D.E. (1977) In: 'Respiratory Defense Mechanisms', Part 11, Vol. 5 of 'Lung Biology in Health and Disease', P. 575. Published by Marcel Dekker INC., New York.

LIPPMANN, M. (1977) In: Handbook of Physiology, Section on Environmental Physiology, (Edited by Lee, D.H.K. and Murphy, S.). Published by Am. Physiol. Soc.

LIPPMANN, M. and ALBERT, R.E. (1969) Am. Ind. Hyg. Ass. J., 30, 257.

LIPPMANN, M. and ALTSHULER, B. (1976) In: 'Air Pollution and the Lung', P. 43. Published by J. Wiley & Sons, New York.

LISTER, J. (1868) Brit. Med. J., 2, 53.

LOURENÇO, R., KLIMEK, M.F. and BOROWSKI, C.J. (1971) J. Clin. Invest., 50, 1411.

LUCAS, A.M. and DOUGLAS, L.C. (1934) Arch. Otolaryngol., 20, 518.

MACKLEM, P.T. and MEAD, J. (1967) J. Appl. Physiol., 22, 395.

MAY, K.R. (1949) J. Appl. Phys., 20, 932.

MELANDRI, C., PRODI, V., TARRONI, G., FORMIGNANI, M., DE ZAIACOMO, T., BOMPANE, C.F. and MAESTRI, G. (1977) In: Inhaled Particles 1V, pp. 193 - 201, (Edited by Walton, W.H.). Published by Pergamon Press, Oxford.

MERCER, T.T. (1973) In: 'Aerosol Technology in Hazard Evaluation', P.287 (re. Ch. 2), P. 358 (re. Ch. 3). Published by Academic Press, New York.

MITCHELL, R.I. (1977) In: Inhaled Particles 1V, pp. 163 - 170, (Edited by Walton, W.H.). Published by Pergamon Press, Oxford.

MORROW, P.E. (1977) In: 'Lung Biology in Health and Disease', Vol. 5, Part 11.

MORROW, P.E., GIBB, F.R. and GAZIOYLU, K. (1967) In: Inhaled Particles 11, pp. 351 - 359, (Edited by Davies, C.N.). Published by Pergamon Press, Oxford.

MORSY, S.M., ECKHARDT, B., STAHLHOFEN, W., and POHLIT, W., (1978) Hlth Phys., 35, 325.

MUIR, D.C.F. (1967) J. Appl. Physiol., 23, 210.

MUIR, D.C.F. and DAVIES, C.N. (1967) Ann. Occup. Hyg., 10, 161.

MUIR, D.C.F., SWEETLAND, K. and LOVE, R.G. (1971) In: Inhaled Particles 111, pp. 81 - 90, (Edited by Walton, W.H.). Published by Unwin Bros., London.

OGDEN, T.L. and BIRKETT, J.L. (1977) In: Inhaled Particles 1V, pp. 93 - 105, (Edited by Walton, W.H.). Published by Pergamon Press, Oxford.

ORENSTEIN, A.J., (Ed.) (1960) Proc. Pneumoconiosis Conf., Johannesburg, 1959. Published by A. Churchill Ltd., London.

OWENS, J.S. (1923) Trans. Med. Soc., London, 45, 79.

PAVIA, D. and THOMSON, M.L. (1976) Ann. Occ. Hyg., 19, 109.

PHILIPSON, K. (1973) J. Aerosol Sci., 4, 51.

PORSTENDÖRFER, J., GEBHART, J. and ROBIG, G. (1977), J. Aerosol Sci., 8, 371.

PROCTOR, D.F. (1964) In: Handbook of Physiology, Respiration, Vol. 1, Ch. 8, (Edited by Fenn, W. and Rahn, H.). Published by Am. Physiol. Soc., Washington. D.C.

PROCTOR, D.F. and SWIFT, D.L. (1971) In: Inhaled Particles III, pp. 59 - 69, (Edited by Walton, W.H.). Published by Unwin Bros., London.

PROTECTION OF THE PATIENT IN RADIONUCLIDE INVESTIGATIONS (1971) ICRP PUBLICATION 17, Pergamon Press, Oxford.

ROGAN, J.M., ATTFIELD, M.D., JACOBSEN, M., RAE, S., WALKER, D.D. and WALTON, W.H.(1973) Br. J. Ind. Med., 30, 217.

RYLEY, D.J. (1959) Brit.J. of Appl. Phys., 10, 93.

SACKNER, M.A., ROSEN, M.J. and WARNER, A. (1973) J. Appl. Physiol., 34, 495.

SAITO, Y. (1912) Arch. Hyg. Bacteriol., 75, 134.

SAYERS, R.R., FIELDNER, A.C., YANT, W.P., THOMAS, B.G.H. and McCONNELL, W.J. (1924) Bur. Mines, Rept. Invest., No. 2661. USA.

SCHLESINGER, R.B., BOHNING, D.E., CHAN, T.L. and LIPPMANN, M. (1977) J.Aerosol Sci., 8, 429.

SCHLESINGER, R.B. and LIPPMANN, M. (1972) Am. Ind. Hyg. Ass. J., 33, 237.

SCHOENBERG, M.D., GILMAN, P.A., MUMAW, V.R. and MOORE, R.D. (1961) Brit. J. Exp. Path., 42, 486.

SILVERMAN, L., LEE, G., PLOTKIN, T., SAWYERS, L.A. and YANCY, A.R. (1951), A.M.A. Arch. Ind. Hyg. Occup. Med., 3, 461.

SLEIGH, M.A. (1977) In: 'Respiratory Defense Mechanisms' Vol. 5, Part 1, of 'Lung Biology in Health and Disease', P. 251. Published by Marcel Dekker, INC., New York.

STAHLHOFEN, W., ECKHARDT, B., GEBHART, J., HEYDER, J. and STUCK, B. (1979) J. Aerosol Sci., 10, 222.

STANESCU, D.C., PATTIJN, J., CLEMENT, J. and VAN DE WOESTIJNE, K.P. (1972) J. Appl. Physiol., 32, 460.

STÖBER, W. (1972) In: 'Assessment of Airborne Particles', P. 249, (Edited by Mercer, T.T., Morrow, P. and Stöber, W.). Published by C.C. Thomas, Springfield, USA.

STUART, B.O. (1973) Arch. Intern. Med., 131, 60.

STURGESS, J. (1977) Am. Rev. Resp. Dis., 115, 819.

TAKAHASHI, K. and KUDO, A. (1973) J. Aerosol Sci., 4, 209.

TASK GROUP ON LUNG DYNAMICS (1966) Hlth, Phys., 12, 173. Report of Committee 11 of a Task Group of the ICRP, 1965.

TAULBEE, D.B. and YU, C.P. (1975) J. Appl. Physiol., 38, 77.

TOPPING, J. (1965) In: 'Errors of Observation and their Treatment', P. 79. Published by Chapman and Hall Ltd., London.

TOTHILL, P. (1974) In: 'Instrumentation in Nuclear Medicine', Vol. 2, Ch. 11. Published by Academic Press INC., New York.

TOTHILL, P. and GALT, J.M. (1971) Phys. Med. Biol., 16, 625.

TYNDALL, J. (1870) Proc. Roy. Inst. of Gt. Brit., 6, 1.

VAN AS, A. (1977) Am. Rev. Resp. Dis., 115, 721.

VAN WIJK, A.M. and PATTERSON, H.S. (1940) J. Ind. Hyg. Toxicol., 22, 31.

WALKER, J.E.C., WELLS, R.E. and MERRILL, W. (1961) Am. J. Med., 30, 259.

WALSH, M., BLACK, A. and FOORD, N,(1977) J. Aerosol Sci., 8, 83.

WEIBEL, E.R. (1963) In: 'Morphometry of the Human Lung'. Published by Springer Press, Berlin.

WHITBY, K.T. and LIU, B.Y.H. (1966) In: 'Aerosol Science', Ch. 3. (Edited by Davies, C.N.). Published by Pergamon Press, Oxford.

WHITBY, K.T., LUNDGREN, D.A. and PETERSON, C.M. (1965) Int. J. Air Wat. Poll., 9, 263.

WILSON, I.B. and LA MER, V.K. (1948) J. Ind. Hyg. Toxicol., 30, 265.

YEATES, D.B., ASPIN, N., LEVISON, H., JONES, M.T. and BRYAN, A.C. (1975) J. Appl. Physiol., 39, 487.

YU, C.P. (1977) J. Aerosol Sci., 8, 237.

YU, C.P. and CHANDRA, K. (1978) J. Aerosol Sci., 9, 175.

APPENDICES

APPENDIX 1: Analysis of filter, C_d

The filter C_d is in effect comprised of two in-series filters, C_{di} and C_{de}, say, each possessing an aerosol deposition efficiency, ϵ_{Cdi} and ϵ_{Cde}, denoting inspiration and expiration, respectively.

Referring to Figure A.1,

$$\epsilon_{Cd} = \frac{I_{Cd} - E_{Cd}}{I_{Cd}} = \left[1 - \frac{E_{Cd}}{I_{Cd}}\right]$$

for simplicity suppose that,

$$\epsilon_{Cde} = \frac{C_{de}}{I_{Cd}'} = \epsilon_{Cdi} = \frac{C_{di}}{I_{Cd}} = \epsilon_{Cd}'$$

$$\therefore E_{Cd} = I_{Cd}'(1 - \epsilon_{Cd}')$$

and, $$I_{Cd}' = I_{Cd}(1 - \epsilon_{Cd}')$$

$$\therefore \epsilon_{Cd} = \left[1 - \frac{I_{Cd}(1 - \epsilon_{Cd}')^2}{I_{Cd}}\right]$$

$$\therefore \epsilon_{Cd} = 2\epsilon_{Cd}' - \epsilon_{Cd}'^2 \sim 2\epsilon_{Cd}', \quad \text{for small values of } \epsilon_{Cd}$$

Since, assuming equal efficiencies in both directions of flow, it is necessary that,

$$\epsilon_{Cd}' < \epsilon_C$$

$$\therefore \epsilon_{Cd} < \sim 2\epsilon_C$$

$$\therefore 0 < q_1 < \sim 2$$

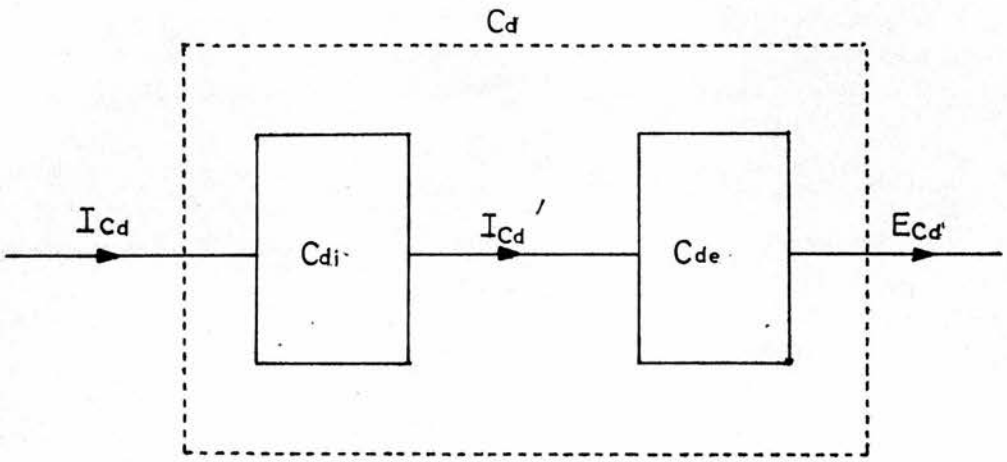

figure A.1 : filter Cd

When, $q_3 \neq 1$, ϵ_{cd} cannot be related directly to ϵ_c, only to ϵ_{ci} or ϵ_{ce}. When $\epsilon_{ci} > \epsilon_{ce}$, $q_1 > q_4$; when $\epsilon_{ci} < \epsilon_{ce}$, $q_1 < q_4$; when $q_3 = 1$, $\epsilon_{ci} = \epsilon_{ce} = \epsilon_c$, $q_1 = q_4$; conditions which are satisfied by the equation below, intended as a simple approximation only.

$$q_4 = \frac{q_1 + q_3}{2} \qquad \text{..... equation 4.2.35}$$

APPENDIX 2: Proof of equation 4.2.48

Now,

$$D = W_i + S_i + C_i + C_d + R + C_e + S_e + W_e$$

therefore,

$$\begin{aligned}
fD(I) = \frac{1}{I}\Big[& \epsilon_w . I + \epsilon_s . I(1-\epsilon_w) + \epsilon_{ci} . Y'.I(1-\epsilon_w)(1-\epsilon_s) \\
& + q_4 . \epsilon_{ci} . Y.I(1-\epsilon_w)(1-\epsilon_s) \\
& + \epsilon_R\Big(Y'.I(1-\epsilon_w)(1-\epsilon_s) - \epsilon_{ci}.Y'.I(1-\epsilon_w)(1-\epsilon_s)\Big) \\
& + \epsilon_{Ce}\Big(Y'.I(1-\epsilon_w)(1-\epsilon_s) - \epsilon_{ci}.Y'.I(1-\epsilon_w)(1-\epsilon_s) \\
& \quad - \epsilon_R\Big(Y'.I(1-\epsilon_w)(1-\epsilon_s) - \epsilon_{ci}.Y'.I(1-\epsilon_w)(1-\epsilon_s)\Big)\Big) \\
& + \epsilon_s\Big(Y'.I(1-\epsilon_w)(1-\epsilon_s) - \epsilon_{ci}.Y'.I(1-\epsilon_w)(1-\epsilon_s) \\
& \quad - \epsilon_R\Big(Y'.I(1-\epsilon_w)(1-\epsilon_s) - \epsilon_{ci}.Y'.I(1-\epsilon_w)(1-\epsilon_s)\Big) \\
& \quad - \epsilon_{Ce}\Big(Y'.I(1-\epsilon_w)(1-\epsilon_s) - \epsilon_{ci}.Y'.I(1-\epsilon_w)(1-\epsilon_s) \\
& \quad - \epsilon_R\Big(Y'.I(1-\epsilon_w)(1-\epsilon_s) - \epsilon_{ci}.Y'.I(1-\epsilon_w)(1-\epsilon_s)\Big)\Big)\Big) \\
& + \epsilon_w\Big(Y'.I(1-\epsilon_w)(1-\epsilon_s) - \epsilon_{ci}.Y'.I(1-\epsilon_w)(1-\epsilon_s) \\
& \quad - \epsilon_R\Big(Y'.I(1-\epsilon_w)(1-\epsilon_s) - \epsilon_{ci}.Y'.I(1-\epsilon_w)(1-\epsilon_s)\Big) \\
& \quad - \epsilon_{Ce}\Big(Y'.I(1-\epsilon_w)(1-\epsilon_s) - \epsilon_{ci}.Y'.I(1-\epsilon_w)(1-\epsilon_s) \\
& \quad - \epsilon_R\Big(Y'.I(1-\epsilon_w)(1-\epsilon_s) - \epsilon_{ci}.Y'.I(1-\epsilon_w)(1-\epsilon_s)\Big)\Big) \\
& \quad - \epsilon_s\Big(Y'.I(1-\epsilon_w)(1-\epsilon_s) - \epsilon_{ci}.Y'.I(1-\epsilon_w)(1-\epsilon_s) \\
& \quad - \epsilon_R\Big(Y'.I(1-\epsilon_w)(1-\epsilon_s) - \epsilon_{ci}.Y'.I(1-\epsilon_w)(1-\epsilon_s)\Big) \\
& \quad - \epsilon_{Ce}\Big(Y'.I(1-\epsilon_w)(1-\epsilon_s) - \epsilon_{ci}.Y'.I(1-\epsilon_w)(1-\epsilon_s) \\
& \quad - \epsilon_R\Big(Y'.I(1-\epsilon_w)(1-\epsilon_s) - \epsilon_{ci}.Y'.I(1-\epsilon_w)(1-\epsilon_s)\Big)\Big)\Big)\Big)
\end{aligned}$$

$$+ \epsilon_s\Big(YI(1-\epsilon_w)(1-\epsilon_s) - q_4 \cdot \epsilon_{ci} \cdot Y \cdot I(1-\epsilon_w)(1-\epsilon_s)\Big)$$

$$+ \epsilon_w\Big(YI(1-\epsilon_w)(1-\epsilon_s) - q_4 \cdot \epsilon_{ci} \cdot Y\, I(1-\epsilon_w)(1-\epsilon_s)$$

$$- \epsilon_s\Big(YI(1-\epsilon_w)(1-\epsilon_s) - q_4 \cdot \epsilon_{ci} \cdot Y \cdot I(1-\epsilon_w)(1-\epsilon_s)\Big)\Big)\Big]$$

Cancelling I and simplyfying gives,

$$fD(I) = \Big[\epsilon_w + \epsilon_s(1-\epsilon_w) + \epsilon_{ci} \cdot Y'(1-\epsilon_w)(1-\epsilon_s)$$

$$+ q_4 \cdot \epsilon_{ci} \cdot Y(1-\epsilon_w)(1-\epsilon_s)$$

$$+ \epsilon_R\Big(Y'(1-\epsilon_w)(1-\epsilon_s)(1-\epsilon_{ci})\Big)$$

$$+ \epsilon_{ce}\Big(Y'(1-\epsilon_w)(1-\epsilon_s)(1-\epsilon_{ci})(1-\epsilon_R)\Big)$$

$$+ \epsilon_s\Big(Y'(1-\epsilon_w)(1-\epsilon_s)(1-\epsilon_{ci})(1-\epsilon_R)(1-\epsilon_{ce})\Big)$$

$$+ \epsilon_w\Big(Y'(1-\epsilon_w)(1-\epsilon_s)(1-\epsilon_{ci})(1-\epsilon_R)(1-\epsilon_{ce})(1-\epsilon_s)\Big)$$

$$+ \epsilon_s\Big(Y(1-\epsilon_w)(1-\epsilon_s)(1-q_4 \cdot \epsilon_{ci})\Big)$$

$$+ \epsilon_w\Big(Y(1-\epsilon_w)(1-\epsilon_s)(1-q_4 \cdot \epsilon_{ci})(1-\epsilon_s)\Big)\Big]$$

putting,

$$P_1 = Y'(1-\epsilon_w)(1-\epsilon_s)$$

$$P_2 = P_1(1-\epsilon_{ci})$$

$$P_3 = P_2(1-\epsilon_R)$$

$$P_4 = P_3(1-\epsilon_{ce})$$

$$P_5 = P_4(1 - \epsilon_S)$$

$$P_1' = Y(1 - \epsilon_W)(1 - \epsilon_S)$$

$$P_2' = P_1' (1 - q_4 \cdot \epsilon_{Ci})$$

$$P_3' = P_2' (1 - \epsilon_S)$$

fD(I) becomes,

$$fD(I) = \epsilon_W + \epsilon_S(1 - \epsilon_W) + \epsilon_{Ci}\left[P_1 + q_4 \cdot P_1' + q_3 \cdot P_3\right] + \epsilon_R \cdot P_2 + \epsilon_S \cdot P_4 + \epsilon_W \cdot P_5 + \epsilon_S \cdot P_2' + \epsilon_W \cdot P_3'$$

therefore,

$$fD(I) = \epsilon_W\left[1 + P_5 + P_3'\right] + \epsilon_S\left[1 - \epsilon_W + P_4 + P_2'\right] + \epsilon_{Ci}\left[P_1 + q_4 \cdot P_1' + q_3 \cdot P_3\right] + \epsilon_R \cdot P_2 \quad \text{... equation 4.2.48}$$

APPENDIX 3: Published paper

:ol Sci., Vol. 10, pp. 123 to 131.
amon Press Ltd. 1979. Printed in Great Britain.

0021-8502/79/0301-0123 $02.00/0

A NEW APPARATUS FOR USE IN STUDIES OF THE TOTAL AND REGIONAL DEPOSITION OF AEROSOL PARTICLES IN THE HUMAN RESPIRATORY TRACT DURING STEADY BREATHING

P. C. EMMETT, R. J. AITKEN and D. C. F. MUIR*
Institute of Occupational Medicine, 8 Roxburgh Place, Edinburgh EH8 9SU, Scotland, U.K.

(*Received* 17 *August* 1978)

Abstract – A new apparatus for use in combined studies of total and regional deposition has been constructed, which accurately samples the aerosol to be inhaled by means of a simple mechanical servomechanism and precision aerosol flow divider. Reversal of operation during expiration enables measurements to be taken during steady breathing. The sampling accuracy has been tested using a bag-in-a-box breathing simulator, which collects the "inhaled" aerosol for comparison with the predicted figure. The result of nine observations was a predicted figure of 100·02 ± 0·8% of the "inhaled" aerosol.

The exhaled aerosol particles are automatically separated for collection by means of two in-series valves controlled by a combination of volume limit switches and pressure changes near the mouth. Tidal volumes can, thus, be set to a predetermined value, enabling the subject to concentrate more effectively on the control of his respiratory flowrates and on minimizing his period of breath-holding.

NOMENCLATURE

T	total deposition
AI	amount of aerosol inhaled
AE	amount of aerosol exhaled
Ic	amount of aerosol in sampling bag, I
Ec	amount of aerosol in collection bag, E
Dc	amount of aerosol in collection bag, D
DS	amount of aerosol lost in mouthpiece
DS^1	amount of aerosol lost in sampling tube
Kn	amount of aerosol which occupies mouthpiece or sampling tube at the end of an inspiration, summed over n breaths
li	amount of aerosol lost in sampling tube or mouthpiece during inspiration
le	amount of aerosol lost in sampling tube or mouthpiece during expiration
Tv	tidal volume
f	breathing rate
ti	average period of inspiration
te	average period of expiration
FRC	functional residual capacity
d	particle diameter
$\bar{d}$	mean particle diameter

1. INTRODUCTION

definition of a safe or acceptable level of dust exposure requires some knowledge of the unt and site of deposition of dust in the human respiratory tract, under a variety of ditions, and its subsequent rate of clearance. Calculation of the dust filtration acteristics of the human respiratory tract is complicated and consensus has not yet been olished (Taulbee and Yu, 1975). If possible, therefore, these characteristics are best rmined experimentally. While useful information may be obtained by the use of models, ollow casts, of the upper respiratory tract, the technique would be difficult to apply to the e intricate lower respiratory tract (Schlesinger and Lippmann, 1972). The use of icially ventilated excised-lungs is also limited, for reasons of availability and technique chell, 1975).

Present address: Health Sciences Centre, McMaster University, 1200 Main Street West, Hamilton, Ontario, 4J9, Canada.

Accurate assessment of the degree of a dust hazard, therefore, requires experimental using live human subjects. Such experimental work is often concerned with the measure of the total amount of dust which deposits in the respiratory tract relative to that inh called total deposition. It is also possible to combine this with the measurement of the re amount of dust which deposits within an area of the respiratory tract, called reg deposition, often by the use of radioactive aerosols (Lippmann and Albert, 1969).

Although many experiments have been performed to measure total deposition, v various techniques, the scatter of observations has been considerable (Davies, 1974). Be individual variations, such scatter may be due in part to poor aerosol sampling techniqu in part to a failure to define or control those factors, such as breathing pattern, v determine the rate of aerosol loss in the subject. It is the purpose of the present paper to attention to some of the more fundamental experimental difficulties which ma encountered when attempting to measure total deposition and to describe a new ty apparatus designed to overcome them.

2. EXPERIMENTAL BACKGROUND

2.1 *Measurement of inhaled and exhaled aerosol*

Total deposition may be defined by the equation:

$$T = \frac{AI - AE}{AI}.$$

For practical purposes, therefore, the measurement of total deposition requires an accu method of sampling the aerosol to be inhaled, a method of distinguishing or separatin exhaled aerosol for collection or sampling, and effective control of the conditions u which the aerosol is breathed.

Representative aspiration sampling of an aerosol from a pulsatile bidirectional flow difficult problem and one which becomes progressively more difficult with increasing par size. Ideally, the aerosol to be inhaled, in a total deposition experiment, should be sam close to the point of entry into the subject. Yet most of the early experimenters in the fie total deposition, with the notable exception of Landahl (1948), sampled the aerosol t inhaled at a point remote from the subject, thus, allowing the possibility of aerosol loss the connecting pipework (Drinker *et al.*, 1928; Brown, 1931; Wilson and La Mer, 1948 these early experiments sampling of the exhaled aerosol was not required as, give effective means of separation, it could be collected. The means of separation were often cr however, and the use of flap valves may have resulted in inefficient collection and large space errors. Dennis (1950) introduced a valve, sensitive to pressure, by which the separa of the exhaled aerosol could be accomplished automatically. An improved version of thi recently been developed (Walsh *et al.*, 1977).

Altshuler *et al.* (1957) describe an optical scatter technique by which the aer concentration is measured, as a function of time, close to the point of entry into the sub By relating this measurement to simultaneous recordings of respiratory flowrates volumes, the relative amounts of inhaled and exhaled aerosol are calculated. Measureme the exhaled aerosol is more difficult than measurement of that inhaled, in the optical sc method, since the concentration of aerosol falls rapidly from the beginning of an expira and the estimation of the true average is difficult (Davies, 1974). This is the converse o aspiration sampling problem when it is, in general, harder to obtain accurate estimates o total inhaled aerosol than total exhaled. Total deposition measurements based on the r complicated optical scatter method have been performed by only a few other workers (I and Davies, 1967; Davies *et al.*, 1972; Giacomelli-Maltoni *et al.*, 1972; Heyder *et al.*, 1 1975).

The present paper describes a new and simpler approach to the sampling proble which the apparatus samples the aerosol to be inhaled, close to the point of entry int subject, and automatically separates and collects the exhaled aerosol. Due to the inhe

ıetry of the system, aerosol losses during inspiration in the mouthpiece, are cancelled by l losses in the sampling tube.

'ontrol of breathing pattern

e objective of determining deposition when the subject breathes naturally, possibly at a in level of exercise, must be distinguished from the objective of understanding the .ion characteristics of the human respiratory tract under artificial breathing conditions. ıst also be borne in mind that when a subject breathes from an apparatus respiration become more conscious than would normally be the case and some form of artificial ol may in any case be required.

he factors which determine the rate of aerosol loss in the human respiratory tract are to ıderstood, it is necessary that they are standardized in each experiment. If standardi- n cannot be satisfactorily achieved in practice, then deviations from the standard ld, at least, be recorded. Tidal volume and breathing rate do not entirely define these rs since it is possible for the ratio of the duration of inspiration to expiration to vary from h to breath (Heyder *et al.*, 1973).

ime dependent factors: diffusion and sedimentation, and velocity dependent factors: al impaction and mechanical mixing, are to be standardized, it is desirable that ratory flowrates should be constant, during constant, but not necessarily equal, periods piration and expiration. Such a pattern also implies standardization of tidal volume, yet been stated by both Davies *et al.* (1972) and Heyder *et al.* (1973) that even experienced cts cannot ensure that inhaled and exhaled volumes are equal in every breath. While it be the case that the effect on deposition averages out over a number of breaths, to the ɔrs' knowledge, this has never been demonstrated experimentally. The effect on regional sition also remains obscure.

:yder *et al.* (1975) discuss the influence of lung volume on deposition and suggest the lardization of lung volume from which aerosol inhalation is initiated, at *FRC*. For such lardization to be effective, again, it is essential that inhaled and exhaled volumes are l.

rt of the problem of breathing control may be that the subject is often obliged to attempt ltaneous control and co-ordination of different variables. The present paper describes a ıique by which tidal volumes are automatically and precisely controlled on every breath, enabling the subject to concentrate more effectively on controlling his respiratory ates and on minimizing the duration of his breath-holding. The method has the further ntage that a signal is derived at the end of each inspiration and expiration, which ipates changes in direction of respiratory excursion by the subject. By means of this .l, the collection of exhaled aerosol can be accomplished with little possibility of the n of the initial portion of exhaled aerosol into the breathing apparatus at the beginning expiration or the re-inhalation of the end portion of the same at the beginning of an ration.

3. DESCRIPTION OF APPARATUS

Sampling and reset

ıe principle of operation is illustrated in Fig. 1a. In a sealed 90 l. perspex box radioactive cles are dispersed to form an aerosol. The subject breathes from one side of a Y-piece, h is incorporated within the respiratory valve, V1. Inspired volumes are detected by ɔmeter A, which is attached to a pulley wheel on a freely rotatable shaft. The latter, is nted on the rear wall of the box by means of a low-friction, air-tight bearing. A second ɔmeter, B is attached in a similar fashion to the opposite end of the shaft and is identical irometer A in all respects. Therefore, both spirometers are equally balanced out of water movement in one induces equal and opposite movement in the other.

ıe base of spirometer B is connected to a 12 l. perspex box in which there is situated a -walled neoprene rubber bag, I, attached to the sampling side of the Y-piece in V1. When ubject inspires, an amount of aerosol equal to that inhaled, is drawn into the sampling

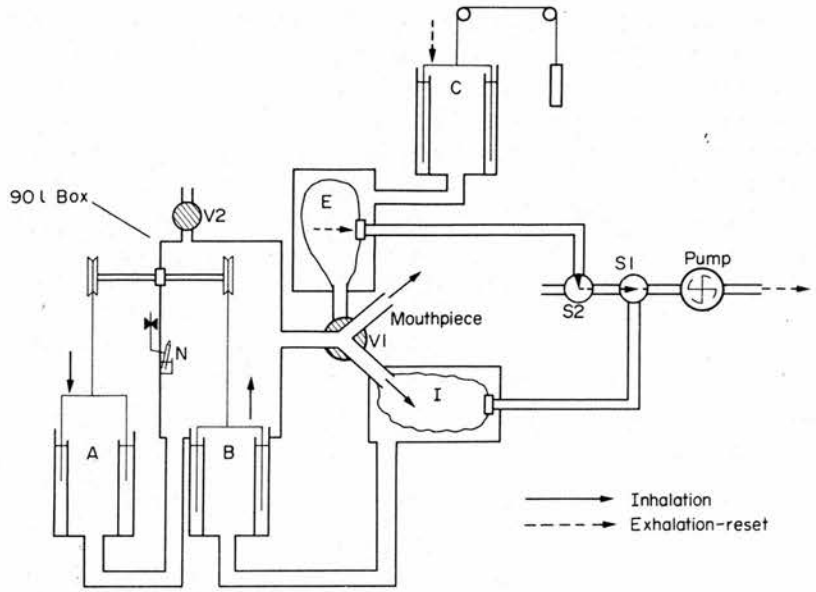

Fig. 1a. Apparatus during inspiration.

bag, I, as a result of the action of spirometer B and the flow division within V1. Spirometer therefore, serves to redistribute a fixed quantity of aerosol around a closed volume.

It is necessary to return the spirometers to an initial starting point for each inspiration expiration so, at the end of an inspiration and the beginning of an expiration, the follo mechanisms are actuated (Fig. 1b):

(i) V1 isolates the subject from the main system and allows him to exhale freely in second rubber bag, E, in which the exhaled aerosol is collected. V1 also seals the out V1 of the sampling bag, I.

(ii) A filter contained within the sampling bag, I, is automatically connected to a suc pump via the solenoid valve, S1.

(iii) A second valve, V2 opens the 90 l. box to atmosphere (with no danger of external lea of radioactive particles).

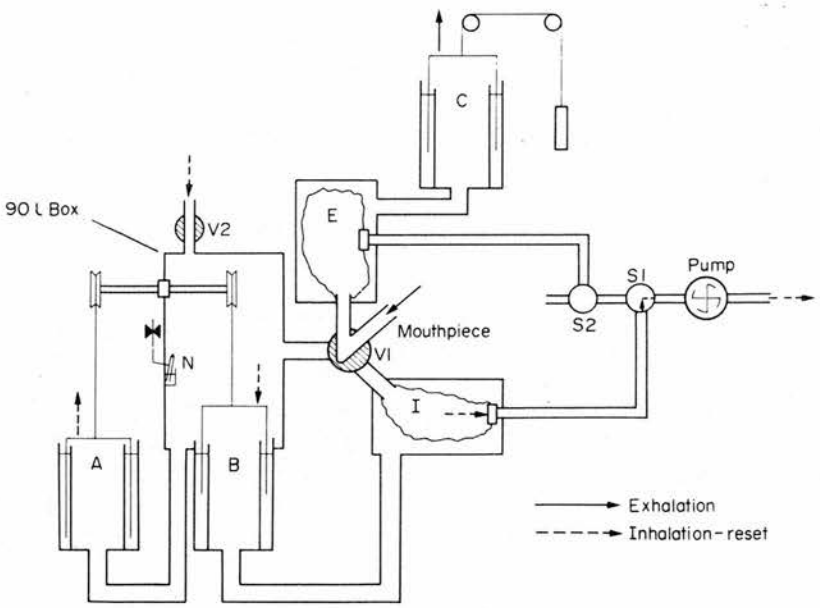

Fig. 1b. Apparatus during expiration.

e net effect of these steps is to put the entire system into reverse. When the sampling bag, ıtracts, spirometer B falls, since the surrounding pressure is atmospheric, due to the ing of V2. Thus, spirometer B now leads the movement of the two and spirometer A s air into the box to replace that which has been removed during an inspiration.
haled volumes are detected by spirometer C via rubber bag, E. At the beginning of an ration the filter contained within the collection bag E is automatically connected to the on pump, via solenoid valves S1 and S2, thus, resetting the position of spirometer C. th inspiration and expiration resetting processes are halted at a given point by means of roximity limit switches, RI and RE, respectively (Fig. 2). It is essential that the speed of esetting process is greater than that of inspiration or expiration in any breath. The nt apparatus employs a 160 l. min^{-1} pump, which results in a resetting rate of about sec^{-1} and, hence, a useful range of possible breathing patterns.

Breathing control and valve actuation

ferring to Fig. 2 A and C are the spirometers used for the detection of inspired and ed volumes, respectively. Spirometer C is maintained at a constant 37°C. LI and LE are sion proximity limit switches, whose position is adjusted relative to RI and RE to obtain desired tidal volume. Inhaled and exhaled volumes are equalized by adjusting LI, ving for gas expansion in the lungs (assumed to be at 37°C and 100% R.H.) from ambient erature and humidity. A change in thoracic volume due to unequal exchange of carbon de and oxygen is small over a few breaths and can be ignored.
tached to the pulley wheels of spirometers A and C are magnets, which perform the dual of actuating the limit switches and of counterbalancing any floatation forces on the meters. V1 is the main respiratory valve whose position, up for an expiration and down n inspiration, is determined by the position of the limit switches LE and LI, respectively. subject inspires until the magnet actuator of spirometer A reaches LI, when V1 moves the expiration position. When the subject expires V1 does not return to the inspiration ion until the magnet actuator of spirometer C reaches LE.
is an open/close valve under the combined control of volume limit switches, LI and LE pressure changes near the mouth. At the end of an inspiration or expiration, as mined by the position of LI and LE, respectively, V3 closes and V1 moves into the opriate position. It is this rapid closing of V3, in anticipation of a change in direction of ratory excursion by the subject, which ensures that none of the exhaled aerosol is passed through the inspiratory port of V1 at the beginning of an expiration and that the led aerosol is not partly re-inhaled at the beginning of an inspiration.

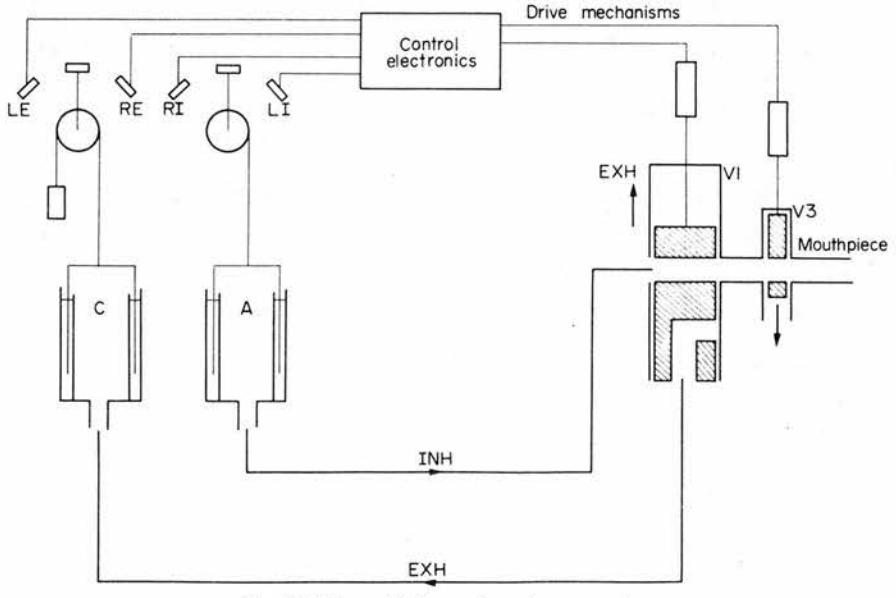

Fig. 2. Volume limits and respiratory valves.

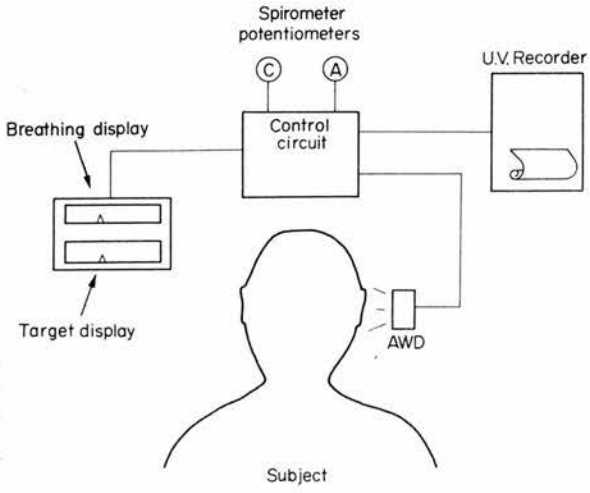

Fig. 3. Respiratory flowrate control.

At the instant of the closing of V3, at the end of an inspiration or expiration, the su receives a signal to change from expiration to inspiration or vice versa. Referring to F this signal is applied by an audible warning device (AWD), which emits a high-pitched w close to the subject's right ear and sounds for as long as it takes the subject to respond t command. When, at the end of an inspiration or expiration, with V3 closed and the A operative, the subject responds by expiring or inspiring, respectively, micromanon probes placed close to the subject's mouth, but which do not interfere with aerosol flow i mouthpiece, detect the positive or negative pressure change which results. This pres signal is then converted to voltage and passed into the control of electronics. The latter opens V3, switches off the AWD, and initiates the spirometer resetting process describe Section 3.1, when the pressure signal exceeds a threshold of ± 0.2 mm H_2O. In the event o subject mistakenly inspiring or expiring before LI or LE is reached by the magnet actuat small pressure of ± 0.05 mm H_2O is sufficient to close V3 and operate the AWD, unti correct pressure is reapplied (Table 1).

In addition to minimizing the duration of the audible warning, i.e. of breath holding subject is asked to observe a miniature edge-level meter, called the breathing display, w indicator follows the movements of spirometers A and C, in each half cycle, adjustabl scale. Immediately below the breathing display is an identical meter, called the target dis whose indicator moves according to a sawtooth waveform of adjustable frequency symmetry. The majority of subjects have little difficulty in ensuring that the indicator o breathing display oscillates in-phase with that of the target display, during a total deposi

Table 1. Operating sequences on one breathing cycle

Subject	V1 position	V3 position	Reset	AWD
begin inspiration	down	open	begin spiro. C reset	off
if mistaken expiration	down	closed	—	on
end of inspiration	up	closed	—	on
begin expiration	up	open	begin spiro. A reset	off
if mistaken inspiration	up	closed	—	on
end of expiration	down	closed	—	on

Table 2. Total dead space losses
Tv = 1.0 l. (BTPS), f = 10 breaths min^{-1}

d μm	$\frac{(DS + DS^1)}{AI}$ %*
4.5	1.1
7.0	1.2
10.5	4.0
13.0	14.2

* Each figure is the mean of either two or three observations.

nent. With a target rate of $f = 10$ breaths min^{-1} at a fixed tidal volume of 1.01. (BTPS), rage rate for the six subjects studied, at the time of writing, was 10.03 ± 0.004 breaths ; the mean period of breath holding when changing from an inspiration to an ion was only 0.3 ± 0.05 sec, as measured on the u.v. recorder paper trace.

rosol generation and tagging

present study employs monodisperse polystyrene particles (coefficient of variation), produced by an air-driven spinning top (Walton and Prewett, 1949; May, 1949) and d with ^{99m}Tc by the method of Few *et al.* (1970). The tagged particles are collected in l and ultrasonified prior to redispersion by an air jet atomizer (N) in the breathing tus.

he end of a total deposition experiment the dead space regions of the apparatus are ly swabbed and the sampling bag, I, and the collection bag, E, are folded into trically identical cardboard containers, for radioassay. Care is taken to ensure that ng efficiencies for the different samples are not affected by geometrical differences in nd positioning within the detectors. Differences in counting efficiencies due to ation of radiation through the thin-walled rubber bags, can be neglected when using which is a γ-emitter and has a photopeak energy of 140 KeV.

eatment of dead space errors

ors due to dead space losses become important above about d = 10 μm (Table 2) and herefore, be taken into account. Two types of dead space error are distinguished in the ent; those due to particle losses in the dead space (Fig. 4) and those due to particles remain airborne long enough in the dead space to be included in the sampling bag, I or llection bag, E. The latter can be calculated from the known volume of dead space, in this case is 25 ml., in both the mouthpiece and sampling tube, equation (5). Aerosol in the mouthpiece during exhalation are estimated by assuming equal loss efficiencies h directions of flow; hence, the losses in each direction depend only on aerosol

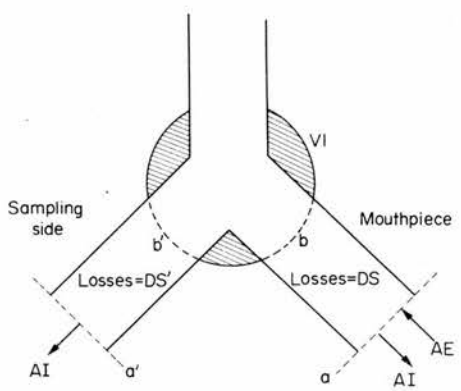

Fig. 4. Mouthpiece and sampling tube dead space.

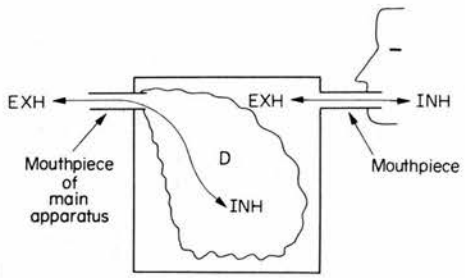

Fig. 5. Testing of sampling accuracy.

concentrations and average times of inspiration and expiration, equations (3) and (4 space errors due to the finite wall thickness of spirometer B are negligibly small.

The equation for the calculation of total deposition becomes:

$$T = 1 - \frac{(Ic - Kn + DS^1 - li)}{(Ec - Kn + le)},$$

where:

$$li \simeq \frac{Ic}{(Ic + Ec)} \frac{ti}{(ti + te)} DS,$$

$$le = (DS - li),$$

$$Kn \simeq \frac{0.025}{Tv(L)} (Ic + DS^1).$$

3.5 *Testing of sampling accuracy and delivery efficiency*

The apparatus illustrated in Fig. 5 is used to test the accuracy of the aerosol sampli a number of breaths and also serves to determine the delivery efficiency. The aerosol w "inhaled" into the bag, D, either settles out or is passed into the collection bag, E, expiration. The actual quantity of "inhaled" aerosol can, therefore, be derive measurements of the radioactive contents of bags, E and D, taking into account deac losses as below, equations (6) and (7).

$$AI = (Ec - Kn + le + Dc).$$

The quantity, AI, is then compared to the predicted figure which is given by;

$$AI \text{ predicted} = (Ic - Kn + DS^1 - li).$$

The result of nine observations at $Tv = 1.0$ l., $f = 10$ breaths min^{-1}, and $\bar{d} = 6.4$ μm predicted figure of $100.02 \pm 0.8\%$, expressed as a percentage of AI, calculated from eq (6). In the particle size range studied ($d = 4.5 - 13.0$ μm) the magnitude of each err unaffected by particle size.

Acknowledgements – The authors would like to thank Mr. W. H. Walton for his assistance in the formulati basic concept and Mr. G. Lynch for his skilled constructional work on the apparatus. This appara constructed for a project financed by the European Coal and Steel Community, whom we thank for their g support.

REFERENCES

Altshuler, B., Yarmus, L., Palmes, D. D. and Nelson, N. (1957) *A.M.A. Archs ind. Hlth* **15,** 293.
Brown, C. E. (1931) *J. ind. Hyg. Toxicol.* **13,** 293.
Davies, C. N., Heyder, J. and Subba Ramu, M. C. (1972) *J. appl. Physiol* **32,** 591.
Davies, C. N. (1974) *Chemistry in Industry* (June 1st), 441.
Dennis, W. L. (1950) *J. Sci. Instrum* **27,** 1950.
Drinker, P., Thomson, R. M. and Finn, J. L. (1928) *J. ind. Hyg. Toxicol.* **10,** 13.
Few, J. D., Short, M. D. and Thomson, M. L. (1970) *Radiochem. Radioanal. Letts* **5,** 275.
Giacomelli-Maltoni, G., Melandri, C., Prodi, V. and Tarroni, G. (1972) *Am. ind. Hyg. Ass. J.* **33,** 603.

J., Gebhart, J., Heigner, G., Roth, C. and Stahlhoffen, W. (1973) *J. Aerosol Sci.* **4,** 191.
J., Armbruster, L., Gebhart, J., Grein, E. and Stahlhoffen, W. (1975) *J. Aerosol Sci.* **6,** 311.
l, H. D. and Herrmann, R. G. (1948) *J. ind. Hyg. Toxicol.* **30,** 181.
nn, M. and Albert, R. E. (1969) *Am. ind. Hyg. Ass. J.* **30,** 257.
. R. (1949) *J. appl. Physiol.* **20,** 932.
l, R. I. (1975) *Inhaled Particles and Vapours* IV, (Edited by Walton, W. H.), p. 163, Pergamon Press, Oxford.
). C. F. and Davies, C. N. (1967) *Ann. occup. Hyg.* **10,** 161.
-ger, R. B. and Lippmann, M. (1972) *Am. ind. Hyg. Ass. J.* **33,** 237.
, D. B. and Yu, C. P. (1975) *J. appl. Physiol.* **38,** 77.
M., Black, A. and Foord, N. (1977) *J. Aerosol Sci.* **8,** 83.
, W. H. and Prewett, W. C. (1949) *Proc. phys. Soc.* **62,** 341.
I. B. and La Mer, V. K. (1948) *J. ind. Hyg. Toxicol.* **30,** 265.

APPENDIX 4: Worked example of method of profile scan analysis for subject PT1 (also alluded to in figure 3.3.3).

(i) Derivation of throat deposit, fS(I).

Now the amount of radioactivity which remains in the subject at the time of the first profile scan and after mouthwashing, must must equal the total deposition fraction, fD(I), less the mouthwash fraction, fW(I).

i.e. The initial lung deposit (C + R) and throat deposit (S) expressed as fractions of the inhaled aerosol (I) are given by the equation,

$$fC + R + S(I) = fD(I) - fW(I) \qquad \text{..... equation A.4.1}$$

From the first two profile scans (figures A.4.1(i) and (ii)), the fraction that the initial throat deposit constituted of the whole body deposit, i.e. fS(C + R + S), could be determined. This was accomplished by summing all counts to the right of channel C2 (the point of convergence mentioned on P.128) on both these profiles, and subtracting the counts of profile (ii) from those of profile (i).

i.e., $\int_{C2}^{200} \text{Scan 1 } (=32{,}557) - \int_{C2}^{200} \text{Scan 2 } (=9{,}239) = S \ (=23{,}318)$

The total body count $(=C+R+S)$ averaged over the first five profile scans was then derived, allowing fS(C + R + S) to be calculated.

i.e., $$fS(C+R+S) = \frac{S}{C+R+S} = \frac{23{,}318}{60{,}065} = 0{\cdot}3882$$

From equation A.4.1, fC + R + S(I) was then calculated, where

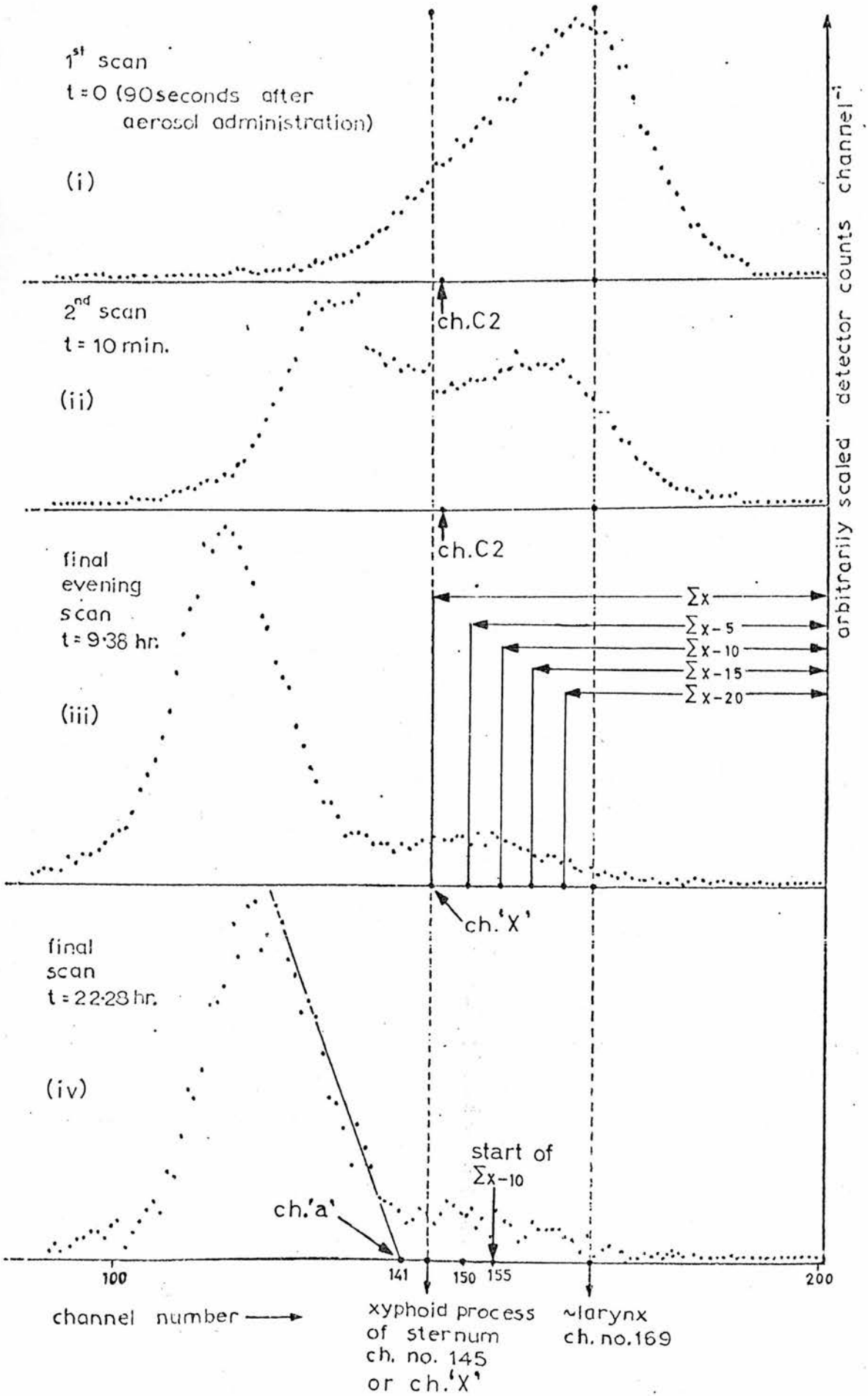

Figure A.4.1: Example of profile scan analysis

in this case,

$$fC + R + S(I) = 0{\cdot}8920 - 0{\cdot}0269 = 0{\cdot}8651$$

Finally fS(I) was calculated using equation 3.3.7 (P.111),

i.e., $$fS(I) = fS(C + R + S).fC + R + S(I)$$

..... equation 3.3.7

$$fS(I) = 0{\cdot}3882 \times 0{\cdot}8651 = \underline{0{\cdot}3358}$$

(ii) Derivation of fractions below larynx, fC(I) and fR(I).

The initial value of the lung counts for a clearance curve were obtained from scan 2 (figure A.4.1(ii)), which was performed after gargling and swallowing to remove the throat deposit. Each scan profile was analysed as shown in figure A.4.1(iii). The profiles were sectionalized to the right of the anatomical reference point 'X', as already described on pages 133 and 134. Five possible summations (Σx; $\Sigma x - 5$; $\Sigma x - 10$; $\Sigma x - 15$; $\Sigma x - 20$) could be executed and five possible clearance curves derived from each series of such summations; i.e. each point on the clearance curves was obtained by expressing the counts derived for one summation section on one profile as a fraction of the same summation section on scan 2.

An example of such a clearance curve, in this case obtained from the series of $\Sigma x - 10$ counts for subject PT1, is shown in figure A.4.2.

e.g., The point at t = 9·38 hr. was obtained from the scan shown in figure A.4.1(iii) by summing all counts to the right of channel number 155 (@ $\Sigma x - 10$, 10 channels from channel 'X'), and expressing this as a fraction of those counts obtained by summing over channels $\Sigma x - 10$ on scan 2 (figure A.4.1(ii)).

i.e., retention value at t = 9·38hr. = $\dfrac{\Sigma x - 10 \text{ of scan at } 9{\cdot}38\text{hr}}{\Sigma x - 10 \text{ of scan at 10 min.}}$

giving, $\dfrac{3{,}296}{18{,}763} = 0{\cdot}1757$

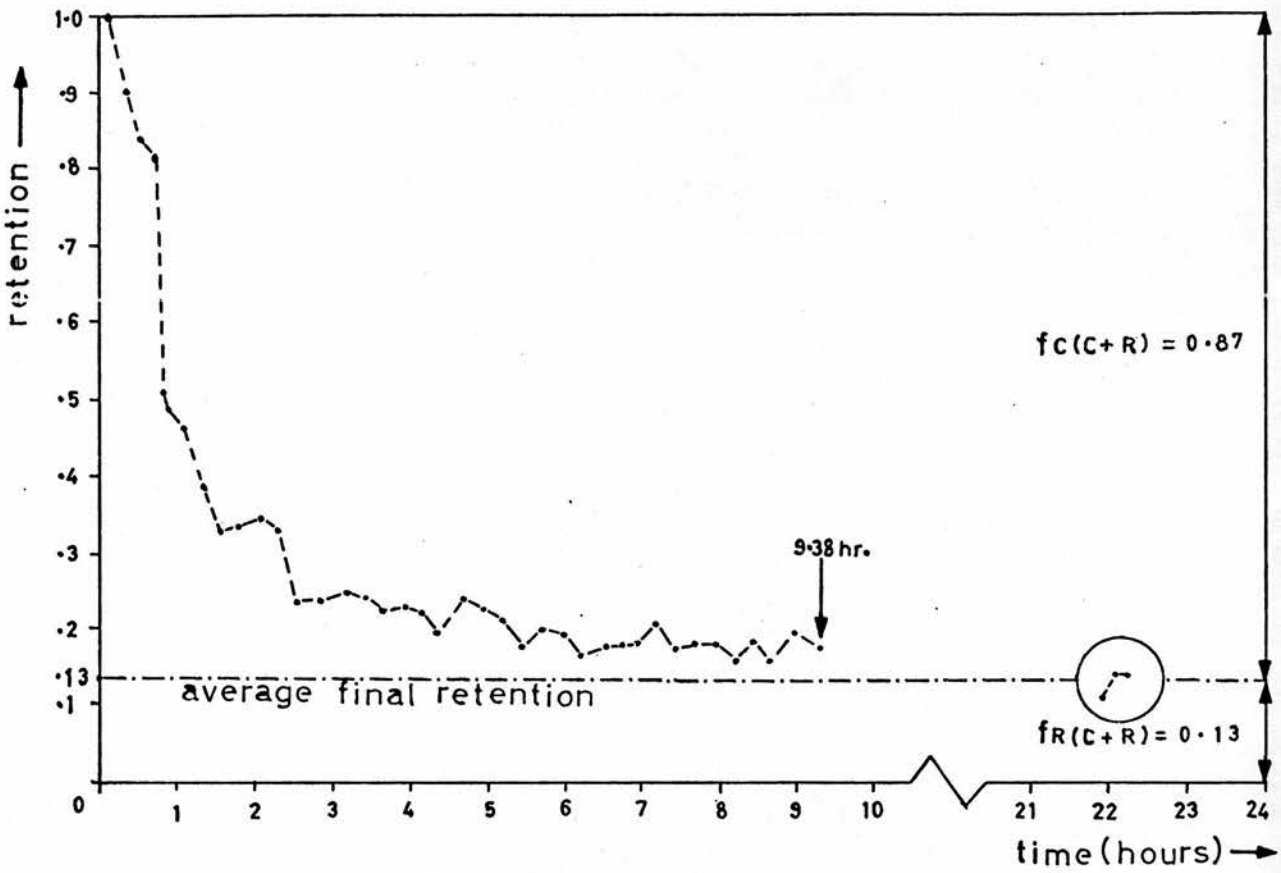

Figure A.4.2: Clearance curve for subject PT1.

In order to ensure the exclusion of abdominal activity in the lung counts, an objective criterion was devised for the selection of the clearance curves to be employed in the derivation of fC(I) and fR(I). Referring to figure A.4.1(iv), this was accomplished by projecting the right hand side of the abdominal peak to the baseline of the scan profile at 'a', and choosing that summation section which was greater than 10 channels distant from this point. In this particular example, since 'a' was at channel 141, and the summation section $\Sigma x - 10$ was more than 10 channels distant from this, the clearance curve derived from the series of counts for section $\Sigma x - 10$ was employed for the calculation of final retention values.

The final value of retention (fR(C + R)) was obtained by calculating the average figure over the three final scans performed at about one day after aerosol administration.

i.e., In this case, $fR(C + R) = 0{\cdot}13$

and, $fC(C + R) = 0{\cdot}87$

Now, $fR(I) = fR(C + R) \times fC + R(I)$

where, $fC + R(I)$ is the fraction of the inhaled aerosol (I) deposited below the larynx; i.e. excluding the throat deposit (fS(I)) and the mouth deposit (fW(I)).

hence, $fC + R(I) = fD(I) - fS(I) - fW(I)$

which in this case gives,

$$fC + R(I) = 0{\cdot}892 - 0{\cdot}0269 - 0{\cdot}3358$$

$$\therefore fC + R(I) = 0{\cdot}5293$$

$$\therefore fR(I) = 0{\cdot}5293 \times 0{\cdot}13 = \underline{0{\cdot}0688}$$

and similarly, since $fC(I) = fC(C + R).fC + R(I)$

$$\therefore fC(I) = 0{\cdot}5293 \times 0{\cdot}87 = \underline{0{\cdot}4605}$$